LATE EOCENE SEA COWS (MAMMALIA , SIRENIA) FROM WADI AL HITAN IN THE FAYUM BASIN, EGYPT

by

IYAD SALEH ZALMOUT

A dissertation submitted in partial fulfillment
of the requirements for the degree of
Doctor of Philosophy
(Geology)
in The University of Michigan
2008

Doctoral Committee:

Professor Philip D. Gingerich, Chair
Professor Daniel C. Fisher
Professor Philip D. Myers
Associate Research Scientist Gregg F. Gunnell
Assistant Research Scientist William J. Sanders

TO MY FAMILY

ACKNOWLEDGMENTS

I am indebted to my committee members: to Philip D. Gingerich for his unwavering support, insight, enthusiasm, and generosity; for allowing me to describe the best sirenian specimens collected from the Tethys Sea; and for his considerable time and attention devoted to my training in the field of vertebrate paleontology. I thank Daniel C. Fisher for long insightful conversations, guidance, and helpful suggestions; Philip Myers for his experience in studying mammalian evolution and taxonomy ; William J. Sanders, whose interests and substantial contribution to this work are much appreciated; and Gregg F. Gunnell for his many helpful comments and for his help with the identification and management of specimens. I am also grateful to Daryl P. Domning of Howard University and the National Museum of Natural History for his guidance, valued discussion, and access to Eocene Sirenia of Jamaica as well as comparative material at the Smithsonian Institution.

This work could not been achieved without the Egyptian government collaborations; thanks are due to the director and staff of Egyptian Environment Affairs Agency Dr. Mustafa Fouda, Mohammad S. A. Abdulhamid, Mohammed Talaat El-Hennawy; Mohammad Al Hakeem, Yusri Attia, Majdi Zakaria, Ehab El-Sady, and Medhat Al Said of the Geological Museum of Egypt. I also thank the field crew members who carried out several expeditions to Wadi Al Hitan with Philip D. Gingerich when many fossil sirenians were collected and recorded: B. Holly Smith, William J. Sanders, Ali Barakat, William C. Clyde, Amin Strougo, Alex van Nievelt, M. Hilal, A. A. Abdul Latif, Jeffrey A. Wilson, David J. Ward, Chris King, Shannon Peters, Martin Sander, Carole Gee, T. M. Bown, and Elwyn L. Simons.

William J. Sanders, Joseph R. Groenke, and John Graf did fabulous work in preparing, molding and casting the sirenian material studied here. I am also deeply thankful to Museum of Paleontology illustrator Bonnie J. Miljour for many of the illustrations included here. Timothy P. Utter and Karl E. Longstreth from the Map Library of the University of Michigan were very helpful and supportive during my research. In addition, I thank Gerald R. Smith, Bruce Wilkinson, Catherine E. Badgley, Jeffrey A. Wilson, Kyger Lohmann, Samuel Mukasa, Abdulmajid Al Nubhani, Daniel j. Miller, Miriam L. Zelditch, John A. Whitlock, Jacques LeBlanc, Aaron A. Wood, Adam Rountrey, Ross Secord, Takehito Ikejiri, Ryan M. Bebej, Kathlyn M. Smith, John I. Bloch, Brian Beatty, and Doug M. Boyer for their help and support during my graduate studies at the University of Michigan.

Finally, this research was funded by grants from the U. S. National Science Foundation (EAR 0517773, OISE 0513544), the National Geographic Society (most recently 09-1035), and the University of Michigan.

TABLE OF CONTENTS

LIST OF TABLES

LIST OF FIGURES

ABSTRACT

Sea cows from the Eocene of Egypt were first described from the Lutetian of the Mokattam Limestone of Cairo. These include the type species of two genera: *Protosiren fraasi* (Abel, 1907) and *Eotheroides aegyptiacum* (Owen, 1875). The first sea cow specimens described from Fayum Province, Egypt, are from the late Eocene (Priabonian) of the Qasr El-Sagha Formation in northern Fayum and include the type species of a third genus and species: *Eosiren libyca* (Andrews, 1902).

The richly fossiliferous marine mammal bone-bearing beds of middle and late Eocene sediments of the Wadi Al Hitan in the Western Desert of Egypt are important for understanding the morphology and evolution of Eocene sirenians in Africa. The sirenian-bearing beds are mostly siliciclastic nearshore deposits of the Gehannam, Birket Qarun, and Qasr El Sagha formations, deposited in Tethys. *Protosiren*, *Eotheroides*, and *Eosiren* are all known from the Fayum Basin, and all are represented by exceptionally complete skulls and axial skeletons with pectoral and pelvic girdles. The skeletal remain of *Protosiren* and *Eotheroides* of the Birket Qarun Formation in Wadi Al Hitan are of special interest because they represent an intermediate stage of evolution and an intermediate stage of secondary adaptation to life in water.

Protosiren smithae of Domning and Gingerich (1994) appears to be a direct descendant of *Protosiren fraasi*, and these species differ from contemporary sirenians (*Eotheroides* spp.) in being larger and in having slight rostral deflection; osteosclerotic postcranial elements lacking pachyostosis; thoracic through lumber vertebrae with spinous processes higher than those of any other sirenian, thoracic vertebrae with a keyhole-shaped vertebral canal; and having rib heads with a cartilaginous rather than fully-ossified articular surface. *Protosiren* retained larger hind limbs than contemporaneous sirenians, although these were reduced compared to hind limbs of land mammals and they were incapable of supporting the weight of the body on land.

Eotheroides (Dugongidae, Halitheriinae) is described for the first time from the Priabonian of the Wadi Al Hitan. The two Wadi Al Hitan species *Eotheroides clavigerum* sp. nov. and *Eotheroides sandersi* sp. nov. are most similar to *Eotheroides aegyptiacum* (Owen, 1875) from the Lutetian nummulitic limestone beds of Cairo. They share the following derived characteristics: prominent falx cerebri and bony tentorium in the roof of the braincase; nasals long and in contact along the midline; palate broad with its posterior border posterior to the toothrow; and anterior ribs pachyosteosclerotic. Wadi Al Hitan *Eotheroides* were medium to large dugongs, ranging in length from 1.5 to 2.5 m; the skull is robust and heavy; the rostrum is deflected and bears medium to diminutive tusks; the trunk is widest between the ninth and eleventh thoracics; the end of the tail was fluked; the pelvis is greatly reduced with a shallow acetabulum, but retains an expanded club-like ilium; and the femur is short and slender. There cannot have been any substantial lower leg or foot. Of all cranial and postcranial elements, extensively pachyosteosclerotic anterior ribs and club-like ilia are central in diagnosis of the genus and its species. *Eotheroides*, like *Eosiren*, had more reduced hind limbs compared to those of *Protosiren*, and both were fully aquatic.

Eosiren libyca Andrews (1902) and *Eosiren stromeri* (Sickenberg, 1934) are limited to the Qasr el Sagha Formation and neither of these species is found in older units. Both species of *Eosiren* are similar to species of *Eotheroides*. However, in *Eosiren* the ribs are gracile and osteosclerotic but not pachyostotic, and the ilium is narrow and rod-like. In *Eosiren stromeri* M^2 is always larger than M^3, a consistent difference from *Eosiren libyca*.

Protosiren, *Eotheroides*, and *Eosiren* all exhibit secondary sexual dimorphism of the bony pelvis. As in modern dugongs, males of the Eocene species consistently have the distal thickness of the ischium about twice as that of the ramus, where females ischia and rami have approximately equal thickness.

The coexistence of *Protosiren smithae*, *Eotheroides clavigerum*, and *Eotheroides sandersi* in the same biotope reflects the diversity of this group in early Priabonian Tethys. The observed morphological diversity reflects dietary and environmental specialization and niche partitioning. Seagrass preserved as leaf impressions in Priabonian marine mammal beds is a direct indicator of the shallowness of Tethyan waters in the Fayum Basin. This corner of Africa was a special environment that supported sirenian faunas for more than 13 million years (middle to late Eocene), and sea cows are known to have survived here through at least the early Oligocene.

CHAPTER ONE

INTRODUCTION

Sirenia or sea cows, including dugongs and manatees, are relatively large herbivorous marine mammals that are fully aquatic, have fore limbs modified as flippers, and lack external hind limbs. Sirenians make their first appearance in the fossil record in the early middle Eocene. The earliest representatives were not fully aquatic but amphibious or semiaquatic, and they retain well developed fore- and hind limbs like terrestrial mammals (Domning, 2001).

Sirenia are interesting from an evolutionary point of view because they represent one of two replicated experiments involving land mammals that became fully aquatic. Sirenians parallel whales in crossing the boundary between terrestrial and aquatic adaptive zones. Sirenia are herbivorous and most closely related to Proboscidea today (Gill, 1870; Schlosser, 1923; Simpson, 1945; McKenna, 1975, Shoshani, 1986) , while Cetacea are piscivorous and planktivorous and most closely related to Artiodactyla (Gingerich et al., 2001). Both groups made the transition from land to sea independently in the early and middle Eocene, and fossils described here show that sirenians were fully aquatic and marine by the late Eocene.

Most living sirenians today inhabit tropical near-shore marine habitats, but there are exceptions. Manatees are restricted to fresh and brackish water of rivers, deltas, and keys, and the recently-extinct 10-meter long Steller's sea cow, a dugongid, lived in shallow marine habitats at higher latitudes (Steller, 1751). Sea cows eat sea grass, which is dependent on light for energy and thus restricted to relatively clear, shallow water. This was seemingly true for sirenians throughout their evolutionary history, and sirenians are thus important paleoenvironmental indicators.

The following introductory paragraphs provide an overview of sirenian evolution, the history of study of fossil sirenians in Egypt, new sirenian specimens from Egypt described here, methods used to study these, and objectives of this study. Following chapters will consider the geology and stratigraphy of sirenian-bearing deposits in Egypt, a general overview of sirenian evolution in Africa, description of important new specimens, and a consideration of their sexual dimorphism, paleoenvironments, paleoecology, and paleobiology.

Sirenian Evolution

Sirenia have a dense fossil record, and much is known about their evolution in the middle and late Cenozoic (Figure 1.1). The earlier record is less well known. The oldest sirenian represented by substantial parts of a skeleton is *Pezosiren portelli* from the early middle Eocene of Jamaica (Domning 2001). This is classified in the family Prorastomidae, and is more primitive than all other sirenians in retaining a longer neck, a fused sacrum, and well developed fore- and hind limbs capable of supporting the animal's weight on land.

Extant sirenians are fully aquatic with morphological and hydrostatic characteristics maintained as secondary adaptations to aquatic habitats. Morphological and skeletal characteristics include: the overall submarine or fusiform body shape, almost hairless and thick skin, large and mobile lips. They have short necks (short cervicals), forelimbs modified as flippers, hind limbs reduced to internal vestiges, and a tail that is modified into a horizontal caudal fin for dorsoventral spinal undulation and peddling.

Like whales, the earliest sirenians (Figure 1.1) show a gradual transition from more terrestrial ancestors with well developed hipbone and hind limbs attached to a multi-centrum sacrum (Abel, 1907; Domning and Gingerich, 1994; Domning, 2001); while the derived forms of these have their pelvic girdle reduced to a vestigial state located within the soft tissue.

Sirenia, which are the sister group to Proboscidea and Hyracoidea (McKenna, 1975: 42), made its first appearance in the Middle Eocene (Figure 1.1) and reached its highest diversity during the Miocene (Domning, 1994 and 1996). The oldest real sirenians come from the early middle Eocene of Jamaica (Table 1.1, Figure 1.2): *Prorastomus sirenoides* (Owen, 1855) and the quadrupedal *Pezosiren portelli* of Domning (2001); however indications based on the oldest sister groups from the Eocene of the Old World may support the theory of their Tethyan origin (Domning et al., 1982; Wells and Gingerich, 1983; Rose et al., 2006).

According to Domning (1994), there are over 42 species of living and fossil sirenians belonging to 24 genera included in 4 families: Prorastomidae (early middle Eocene of Jamaica), Protosirenidae (middle and late Eocene of Egypt and Pakistan), Dugongidae (Eocene to Recent), and Trichechidae (Miocene to Recent). Four species of the genera

Dugong and *Trichechus* are living today, and are distributed on the margins of southern continents and the Gulf of Mexico.

Sirenia of Egypt (Cairo and Fayum)

The global distribution of Eocene sirenians shows that Old World Tethys and eastern and southeastern coastlines of United States are the most common places where these fossils are found (Figure 1.2).

Sirenians are the first fossil vertebrates to be reported from Paleogene rocks of Africa and the first fossil marine mammals to be discovered in Egypt, based on a collection of vertebrae and rib fragments illustrated as pinniped material (de Blainville 1840: 43, 51). De Blainville's conclusion that the material he studied were those of marine mammals was close to reality, but was not related to pinnipeds. In a note four years later de Blainville corrected himself (1844:119-120) and concluded that the martial that he originally described was indeed the first fossil sirenian specimen from Africa. De Blainville was not specific about the locality where the fossils were collected, however he hinted about chalk beds on the left side of the River Nile from what is called Lower Egypt. These chalk beds from Lower Egypt on the left side of the River Nile probably refer to the Lutetian Nummulitic Limestone or the Great Pyramids Building Stones near the historic city of Giza.

Later, Sir Richard Owen (1875), described *Eotherium* (*Eotheroides*) *aegyptiacum* from the upper part of the Lower Building Stone Member of the Gebel Mokattam (Mokattam Mountain) Formation of Middle Lutetian age (Strougo et al., 1982). From the same level, which is also known as the level of *Protocetus atavus* of Fraas (1904), Abel

(1904) wrote about a new taxon of sirenian that he published as a *nomen nudum* with no illustration or diagnosis; Abel's 1904 new taxon was later published as *Protosiren fraasi* (Abel, 1907). Filhol (1878) erected *Manatus coulombi* from the Mokattam, which later was synonomized with *Protosiren fraasi* (Abel, 1907). Sickenberg (1934) revised the fossil sirenians from Egypt and the Mediterranean region and added *Eosiren abeli* (replacement of *Eotherium aegyptiacum* of Abel, 1912) to the Mokattam sirenians on the basis of very limited elements including a skull that was destroyed in World War II. *Eotherium majus* of Zdansky (1938) is the last sirenian to be named from the Mokattam Building Stones near Cairo. This taxon is also based in a single upper molar. However, the specimen is probably lost since it has not been catalogued and the locality in Zdansky's publication is confusing. Gingerich (1992) concluded that the sirenian taxa from the Lutetian of the Mokattam belong to two taxa: *Eotheroides aegyptiacum* and *Protosiren fraasi* (Figure 2.1).

Southwest of Cairo and to the left of the Nile Valley of Lower Egypt, the Fayum Basin has drawn tremendous paleontological and geological attention for its valuable fossil vertebrates from the Birket Qarun and Qasr El Sagha and Gebel Qatrani formations (Figure 1.4). The Fayum fossils have been studied for more than a century (Andrews, 1902; Beadnell and Andrews, 1904; Andrews, 1906). These unique deposits have produced many North African near shore vertebrate specimens.

During the middle and late Eocene (40-33.9 Ma) and lower Oligocene (33.9-28.4 Ma) (Figures 1.3 and 1.4) the Fayum area provided sutable environments for both shallow marine and terrestrial vertebrate faunas; these faunas are now preserved in thick sedimentary packages that are extensively exposed in wide valleys and benches in the

Fayum Basin. These faunas are part of prehistoric biotopes that include terrestrial mammals (Proboscidea, Primates, Carnivora), marine mammals (archaeocetes and sirenians), birds, reptiles (chelonians, crocodilians, and snakes), and fishes (see Simons and Rasmussen, 1990). Invertebrate fossils such as benthic and planktonic forams are very common, and floral remains, such as tropical trees and mangrove-like plants, also have been recorded from the Eocene beds of the Fayum Basin (Wing and Tiffney, 1982; Bown and Kraus, 1988; Wing et al., 1995).

Marine mammals from these beds are of special interest because they provide detailed information about their evolutionary history. Andrews (1902, 1906) described *Eosiren libyca* from Qasr El Sagha Formation. *E. libyca* is represented by a number of skulls and partial skeletons (Sickenberg, 1934). Siegfried (1967) described a femur and pelvis and some lumbar and caudal vertebrate of *E. libyca* from the Qasr El Sagha Formation near Lake Qarun, and noticed that the femur is substantially deviated from that of the Oligocene *Halitherium schinzii*, moreover he concluded that the rear limbs of these Eocene sirenians are functionless, but somehow retained a local muscle movement. From the same beds of the Qasr El Sagha Formation and from an area near the west side of the historical town of Dimeh (North of Birket Qarun), *Eosiren stromeri* was described by Sickenberg (1934, 131). Reinhart (1959) described a partial sirenian cranium and called it an *Eotheroides*. Domning et al. (1982: 55) reported a sirenian mandible from beds below the Qasr El Sagha Formation. Domning and Gingerich (1994) described *Protosiren smithae* from the Wadi AL Hitan (Zeuglodon Valley: Valley of Whales) based on a very good skull associated with vertebral column, pectoral and pelvic girdles.

Oligocene beds of the Jabal Qatrani Formation above the Qasr El Sagha Formation produced a very derived taxon named *Eosiren imenti* (Domning et al., 1994).

New Specimens

New fossil sirenians in this dissertation include virtually complete skeletons from Wadi Al Hitan (Table 1.2) collected from the western side of the Fayum Basin and from the cliffs above the north shore of Birket Qarun (Lake Moeris). These fossils provided detailed information about the evolution and systematics of Eocene sirenians in Egypt because they include cranial and postcranial elements found in association. The described sirenian fossils from the Mokattam Hills near Cairo (Owen, 1875, Andrews, 1902; Abel, 1907; Sickenberg, 1934) were found as isolated elements (skulls with no postcrania, isolated vertebrae, ribcages with no cranial or pectoral elements), which made it extremely difficult to develop a clear estimation of the overall morphology of these animals.

Table 1.2 summarizes the fossil sirenian material from the Wadi Al Hitan and the surroundings areas; some of these have been already published and the rest are either new or represent new material of formerly known taxa that added more detailed information. Locations and stratigraphic units of all studied specimens are plotted in Figures 1.5, 1.6, and 1.7.

Of all the contributions towards understanding the natural history of the Fayum sirenian fossils, only very few published reports discussed structure, systematics, habitats, and secondary adaptation of these marine mammals to life in water (Andrews, 1906; Abel, 1907; Sickenberg, 1934; Siegfried, 1967; Gingerich, 1992; Domning and

Gingerich, 1994; Domning et al., 1994). Most studies of Eocene sirenians of Egypt have barely commented on postcranial elements of the sirenian skeletons and their paleobiological value, either because little was known about postcranial elements, or because postcranial elements were neglected or underestimated.

Methods

Obtaining the material that provide the fundamental bases of this desertion required fieldwork and laboratory work. Filed work in Wadi AL Hitan between 1980 and 1993 included prospecting for fossils, field identification, fossil logging and location registry, surface collecting and excavation, plaster jacketing, geological mapping, and stratigraphic section measuring. During the last five years, the fossil localities where these skeletal materials were collected were revisited in order to place each in their geological and stratigraphic context, and to update the coordinate readings from a handheld GPS. In addition to this detailed mapping of the geological formations and structures using digital lands imagery in the field was used to track the extent of the local stratigraphic units and to find new fossil localities.

Laboratory work included first, fossil preparation and cleaning, and second, examining and identifying the fossils, measuring significant skeletal and dental dimensions, and recording significant landmarks and characters that provide the raw material for this research.

Sirenian remains that were wrapped and covered in soft paper were unwrapped and hardened by Polyvinyl Acetate (PVA) dissolved in acetone; broken pieces were glued to their origin by Duco Cement and PaleoBond, and sometimes by hot glue. Sirenian

skeletons that were excavated and removed from the field in plaster jackets were prepared carefully by using fine airscribes under magnification lenses.

Examination of Eocene sirenians here includes two major tasks. The first is identifying the sirenian skeletons and remains and assign them to a systematic position based on primitive and derived characters published by Domning (1994, 1996). The second task include measuring variable dimensions of cranial and postcranial elements to describe the morphological variation in these animals. Postcranial elements with significant variable attributes include vertebrae length and height, and lengths of pectoral and pelvic girdle elements. These were used to show variation among the different groups of the Eocene sirenians of Egypt. Pectoral and pelvic girdle elements were measured in detail for comparative purposes. Most measurements of both cranial and postcranial elements (see Appendixes) are after Domning (1978) and Furusawa (1988).

A Mitutoyo digital calipers was used for the liner dimensions. Circumferences, arc lengths, and perimeters were all measured by using a measuring tape. During all measuring events digital calipers and measuring tape have not been replaced.

Objectives

This dissertation will try to address questions concerning the Eocene Sirenia and their environments at Wadi Al Hitan of the Fayum Basin. Questions to be addressed include the following: (1) Considering the high diversity in the Priabonian Sirenia of Fayum, how many sirenian species lived in Wadi Al Hitan? What were the reasons behind such diversity? Is it biological or physical or both? (2) Exploring geological and biological data in the late Eocene of the Fayum Basin, what were the sirenian habitats? (3) Given

the structural and morphological differences in the skeletal elements preserved in these fossils what was (were) the locomotion behavior(s) in these marine mammals? How could such behavior(s) be explained? (4) The Tethyan Sea is known for its Eocene marine vertebrate communities from Asia, Europe, and North America, How similar or different are these communities from the Fayum area? (5) Since this study deals with the last chapter of the Eocene (Priabonian), what was the destiny of these marine mammals by the end of the Priabonian and how do they differ from the Rupelian sirenians in the same basin (the fauna of the Gebel Qatrani Formation)? This study includes an up to date literature review and new information about the Eocene sirenians of Wadi Al Hitan World Heritage Site and the Fayum Basin and the surrounding area (Chapter 1); geological and stratigraphic overview of the main Eocene marine mammal fossil beds in the Fayum Basin (Chapter 2); a review of the Cenozoic sirenians of Africa and their spatial and temporal distribution (Chapter 3); systematics and description of new fossil sirenians from the Fayum Basin (Chapter 4);sexual dimorphism in Eocene Sirenia (Chapter 5), paleoenvironments and paleoecology of the marine mammals bearing beds (Chapter 6); secondary adaptation in water, swimming capabilities, and feeding behavior (Chapter 7); a brief summary (Chapter 8).

In summary the three known genera (*Eotheroides*, *Eosiren*, and *Protosiren*) from the Eocene of Fayum will be reviewed and compared one to another for their anatomy, and adaptation in water based on new cranial and skeletal elements. Moreover, the Bartonian and Priabonian sirenians from Fayum will be compared to those known from the Lutetian nummulitic limestone of the Gebel Mokattam Formation near Cairo.

TABLE 1.1. The global record of Eocene sirenians (localities are plotted on the world map in Figure 1.2). Data are based on Domning et al. (1982), Paleobiology Data Base of the Smithsonian Institute, and new material at the University of Michigan. This table is organized stratigraphically, with the oldest sirenians at the bottom and youngest sirenians at the top.

Taxon	Family	Country	Age	Authorship
Sirenia indet.	Dugongidae	Libya	Priabonian-Rupelian	Savage, 1977
Eotheroides sandersi	Dugongidae	Egypt	Priabonian	This study
Eotheroides clavigerum	Dugongidae	Egypt	Priabonian	This study
"*Eotheroides*, *Halitherium*"?	Dugongidae	Romania	Priabonian	Sickenberg, 1934
Eotheroides sp.	Dugongidae	France	Priabonian	Freudenthal, 1970; Savage, 1977
Eotheroides sp.	Dugongidae	Jordan	Priabonian	Zalmout et al. 2003b
Indosiren javaensis	Dugongidae	Java	Priabonian	von Koenigswald, 1952
Prototherium veronense	Dugongidae	Italy	Priabonian	de Zigno, 1875
Prototherium intermedium	Dugongidae	Italy	Priabonian	Bizzotto, 1983, 2005
Paralitherium tarkanyense	Dugongidae	Hungary	Priabonian	Kordos, 1977
Halitherium taulannense	Dugongidae	France	Priabonian	Sagne, 2001
Eosiren libyca	Dugongidae	Egypt	Priabonian	Andrews, 1902
Sirenia indet.	Dugongidae	Mexico	Priabonian	Müllerried, 1932
Sirenia indet.	Dugongidae	USA	Priabonian (Jacksonian)	Domning et al., 1982
Sirenia indet.	Dugongidae	USA	Priabonian (Jacksonian)	Flower and Garson, 1884
Protosiren sattaensis	Protosirenidae	Pakistan	Bartonian	Gingerich et al., 1995
Protosiren fraasi	Protosirenidae	Egypt	Bartonian	Filhol, 1878; Abel, 1907
Eotheroides sp.	Dugongidae	USA	Bartonian	Domning et al., 1982
Prototherium montserratense	Dugongidae	Spain	Bartonian	Pilleri et al., 1989
Prototherium solei	Dugongidae	Spain	Bartonian	Pilleri et al., 1989
Eosiren sp.	Dugongidae	India	Bartonian	Bajpai et al., 2006
Eosiren stromeri	Dugongidae	Egypt	Bartonian	Sickenberg, 1934
Sirenia indet.	Dugongidae	Qatar	Bartonian	This study
Eotheroides sp.	Dugongidae	USA	Bartonian (Claibornian)	Domning et al., 1982
Sirenia indet.	Dugongidae	USA	Bartonian (Claibornian)	Domning et al., 1982
Sirenia indet.	Dugongidae	USA	Bartonian (Claibornian)	Arata and Jackson, 1965
Sirenia indet.	Dugongidae	USA	Bartonian (Claibornian)	Siler, 1964
Sirenia indet.	Dugongidae	USA	Bartonian (Claibornian)	Domning et al., 1982
Sirenia indet.	Dugongidae	USA	Bartonian (Claibornian)	Reinhart, 1976
Sirenia indet.	Dugongidae	USA	Bartonian (Claibornian)	Vernon, 1951, Reinhart, 1976
Sirenia indet.	Dugongidae	USA	Bartonian (Claibornian)	Domning et al., 1982
Sirenia indet.	Dugongidae	USA	Bartonian (Claibornian)	Domning et al., 1982
Sirenia indet.	Dugongidae	USA	Bartonian (Claibornian)	Domning et al., 1982
Sirenia indet.	Dugongidae	USA	Bartonian (Claibornian)	Domning et al., 1982
Sirenia indet.	Dugongidae	USA	Bartonian (Claibornian)	Domning et al., 1982
Sirenia indet.	Dugongidae	USA	Bartonian (Claibornian)	Sanders, 1974
Sirenia indet.	Dugongidae	USA	Bartonian (Claibornian)	Domning et al., 1982
Sirenia indet.	Dugongidae	USA	Bartonian (Claibornian)	Domning et al., 1982
Sirenia indet.	Dugongidae	USA	Bartonian (Claibornian)	Domning et al., 1982
Sirenia indet.	Dugongidae	USA	Bartonian (Claibornian)	Domning et al., 1982

Sirenia indet.	Dugongidae	USA	Bartonian (Claibornian)	Emmons, 1858
Sirenia indet.	Dugongidae	Egypt	Bartonian?	Gingerich et al., 2007
Protosiren smithae	Protosirenidae	Egypt	Bartonian-Priabonian	Domning and Gingerich, 1994
Sirenia indet.	Dugongidae	Madagascar	Bartonian-Priabonian	Samonds et al., 2005
Sirenia indet.	Dugongidae	Madagascar	Bartonian-Priabonian	Samonds et al., 2007
Sirenia indet.	Dugongidae	Spain	Lower Bartonian	Astibia et al., 2005
Protosiren sp.	Protosirenidae	Egypt	Lutetian	This study
Eotheroides aegyptiacum	Dugongidae	Egypt	Lutetian	Owen, 1875; Zdansky, 1938
Eosiren abeli	Dugongidae	Egypt	Lutetian	Sickenberg, 1934
Protosiren sp.	Protosirenidae	Egypt	Lutetian?	Blainville, 1840, 1844
Protosiren minima	Protosirenidae	France	Lutetian	Sickenberg, 1943; Richard, 1946
Protosiren cf. *fraasi*	Protosirenidae	Hungary	Lutetian	Kordos, 1978
Sirenavus hungaricus	Dugongidae	Hungary	Lutetian	Kretzoi, 1941
Anisosiren pannonica	Dugongidae	Hungary	Lutetian	Kordos, 1979
Eotheroides sp.	Dugongidae	Hungary	Lutetian "?"	Kordos, 1980, 2002
Protosiren fraasi	Protosirenidae	India	Lutetian	Sahni and Mishra, 1975
Protosiren sp.	Protosirenidae	India	Lutetian	Bajpai et al., 2006
Eotheroides babiae	Dugongidae	India	Lutetian	Bajpai et al., 2006
Indosiren koemgswaldi	Dugongidae	India	Lutetian	Sahni and Mishra, 1975
Sirenia indet.	Dugongidae	Jordan	Lutetian	Zalmout et al. 2003b
Libysiren sickenbergi	Protosirenidae	Libya	Lutetian	Heal, 1973
Eotheroides sp.	Dugongidae	Libya	Lutetian	Heal, 1973
Protosiren eothene	Protosirenidae	Pakistan	Lutetian	Zalmout et al., 2003a
Sirenia indet.	Dugongidae	Somalia	Lutetian	Savage, 1969
Sirenia indet.	Dugongidae	Somalia	Lutetian	Savage, 1969
Sirenia indet.	Dugongidae	Somalia	Lutetian	Savage, 1969
Halitherium sp.	Dugongidae	Spain	Lutetian - Bartonian	Bataller, J. R., 1956
Sirenia indet.	Dugongidae	Togo	Lutetian	Gingerich et al., 1992
Sirenia indet.	Dugongidae	Tunisia	Lutetian	Batik and Fejfar, 1990
Sirenia indet.	Dugongidae	Yemen	Lutetian	As-Saruri et al., 1999
Pezosiren portelli	Prorastomidae	Jamaica	Lutetian	Domning, 2001
Prorastomus sirenoides	Prorastomidae	Jamaica	Lutetian	Owen, 1855
Sirenia indet.	Dugongidae	Hungary	Ypresian?	Kretzoi, 1953

TABLE 1.2. Eocene and Oligocene sirenian specimens and their localities in the Fayum Basin. The oldest specimen, UM 101229, was collected from the top of the Medawar Formation (Bartonian), and the youngest, CGM 40210, came from the Rupelian Gebel Qatrani Formation. Abbreviations for localities: DUQ, Duke University Quarry in Gebel Qatrani; GelEsh, Garet El Esh; QS, Qasr El Sagha; WR, Wadi El Rayan Protected Area; ZV, Zeuglodon Valley (Wadi Al Hitan).

Catalogue	Taxon	Family	Locality	Longitude	Latitude	Age
CGM 40210	*Eosiren imenti*	Dugongidae	DUQO	30.5757	29.64346	Rupelian
CGM 42179	*Eosiren libyca*	Dugongidae	QS005	30.70044	29.62192	Priabonian
CGM 42180	*Eosiren libyca*	Dugongidae	QS009	30.54544	29.5705	Priabonian
CGM 42181	*Eotheroides sandersi*	Dugongidae	ZV230	30.06849	29.32138	Priabonian
CGM 42287	*Eotheroides clavigerum*	Dugongidae	ZV190	30.05552	29.2634	Priabonian
CGM 42292	*Protosiren smithae*	Protosirenidae	ZV054	30.04581	29.29639	Priabonian
CGM 42298	*Eotheroides clavigerum*	Dugongidae	ZV101	30.04472	29.26962	Priabonian
UM 50354	*Eotheroides sandersi*	Dugongidae	ZV231	30.06913	29.32319	Priabonian
UM 50355	*Eotheroides* indet	Dugongidae	ZV130	30.03498	29.27845	Priabonian
UM 50356	*Eotheroides* indet	Dugongidae	ZV124	30.04743	29.27235	Priabonian
UM 50357	*Eotheroides* indet	Dugongidae	ZV034	30.03386	29.28175	Priabonian
UM 50358	*Eotheroides* indet	Dugongidae	QS008	30.55245	29.57063	Priabonian
UM 50359	*Eotheroides* indet	Dugongidae	QS002	30.50217	29.5634	Priabonian
UM 16069	*Protosiren* indet	Protosirenidae	WR2	30.48042	29.18617	Bartonian
UM 83903	*Eotheroides clavigerum*	Dugongidae	ZV207	30.05684	29.30225	Priabonian
UM 94806	*Eotheroides clavigerum*	Dugongidae	ZV033	29.28212	30.03437	Priabonian
UM 94809	*Eotheroides sandersi*	Dugongidae	ZV079	30.02493	29.27087	Priabonian
UM 97514	*Eotheroides sandersi*	Dugongidae	ZV110	30.03139	29.27626	Priabonian
UM 97515	*Eotheroides sandersi*	Dugongidae	ZV117	30.03531	29.2769	Priabonian
UM 97520	*Eotheroides clavigerum*	Dugongidae	ZV128	30.0317	29.27729	Priabonian
UM 97523	*Protosiren smithae*	Protosirenidae	ZV144	30.05695	29.30296	Priabonian
UM 97524	*Eotheroides clavigerum*	Dugongidae	ZV145	30.05664	29.30362	Priabonian
UM 97539	*Eosiren libyca*	Dugongidae	GelEsh-1	30.56436	29.56816	Priabonian
UM 97540	*Eosiren libyca*	Dugongidae	GelEsh-1	30.56436	29.56816	Priabonian
UM 97549	*Eosiren libyca*	Dugongidae	GelEsh-1	30.56436	29.56816	Priabonian
UM 97556	*Eosiren libyca*	Dugongidae	GelEsh-1	30.56436	29.56816	Priabonian
UM 97568	*Eosiren libyca*	Dugongidae	GelEsh-1	30.56436	29.56816	Priabonian
UM 100137	*Eosiren stromeri*	Dugongidae	GelEsh-4	30.56503	29.56934	Priabonian
UM 100138	*Eotheroides sandersi*	Dugongidae	ZV180	30.04124	29.28403	Priabonian
UM 100184	*Eotheroides clavigerum*	Dugongidae	ZV200	30.06089	29.31468	Priabonian
UM 100191	*Eosiren stromeri*	Dugongidae	GelEsh-9	30.56856	29.57004	Priabonian
UM 100192	*Eosiren stromeri*	Dugongidae	GelEsh-10	30.56857	29.57004	Priabonian
UM 101219	*Eotheroides clavigerum*	Dugongidae	ZV219	30.05147	29.30901	Priabonian
UM 101220	*Eotheroides clavigerum*	Dugongidae	ZV220	30.052	29.3094	Priabonian
UM 101224	*Protosiren smithae*	Protosirenidae	ZV227	30.06853	29.32028	Priabonian
UM 101226	*Eosiren libyca*	Dugongidae	QS003	30.50982	29.56094	Priabonian
UM 101228	*Eosiren libyca*	Dugongidae	QS006	30.70333	29.6239	Priabonian
UM 101229	*Protosiren smithae*	Protosirenidae	ZV224	30.15395	29.1531	Bartonian
UM 111558	*Eotheroides sandersi*	Dugongidae	ZV174	30.04108	29.29035	Priabonian

FIGURE 1.1. Phylogeny of the Sirenia. Known stratigraphic ranges indicated by bold lines; dashed lines indicate uncertain phylogenetic relationships and sirenian family ranges. Closed black diamonds represent extinct families with very short stratigraphic ranges (modified from Gheerbrant, Domning, and Tassy, 2005).

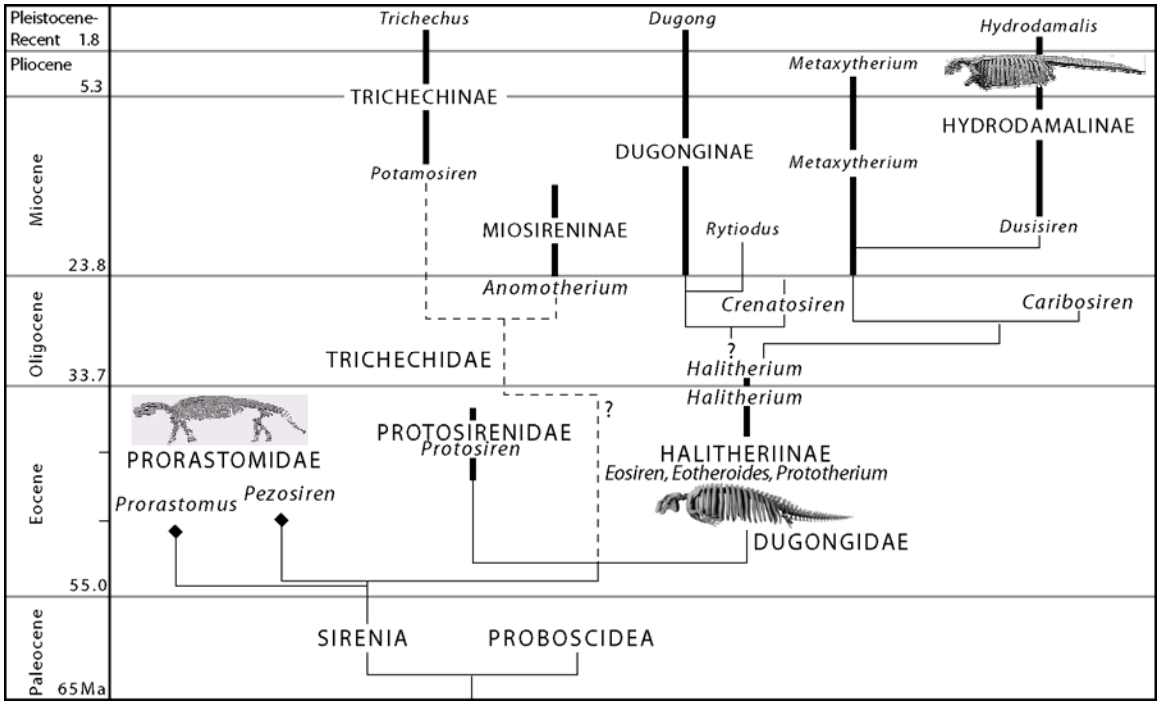

FIGURE 1.2. Global occurrences of Eocene sirenians compiled from authors listed in Table 1.2. Anthracobunid records from the Ypresian and early Lutetian of India and Pakistan (Wells and Gingerich, 1983; Rose et al., 2006) show the distribution of possible ancestors of Sirenia.

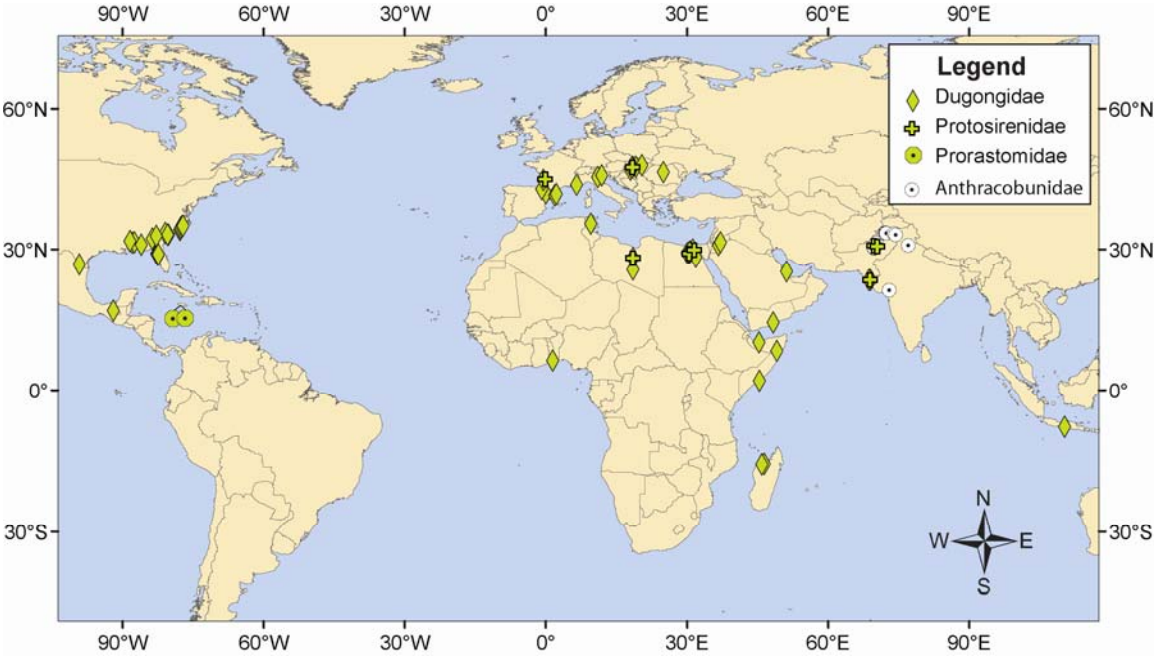

FIGURE 1.3. Political map of Egypt and the surrounding countries of northeastern Africa. The Fayum Basin is bounded by the rectangle southwest of Cairo.

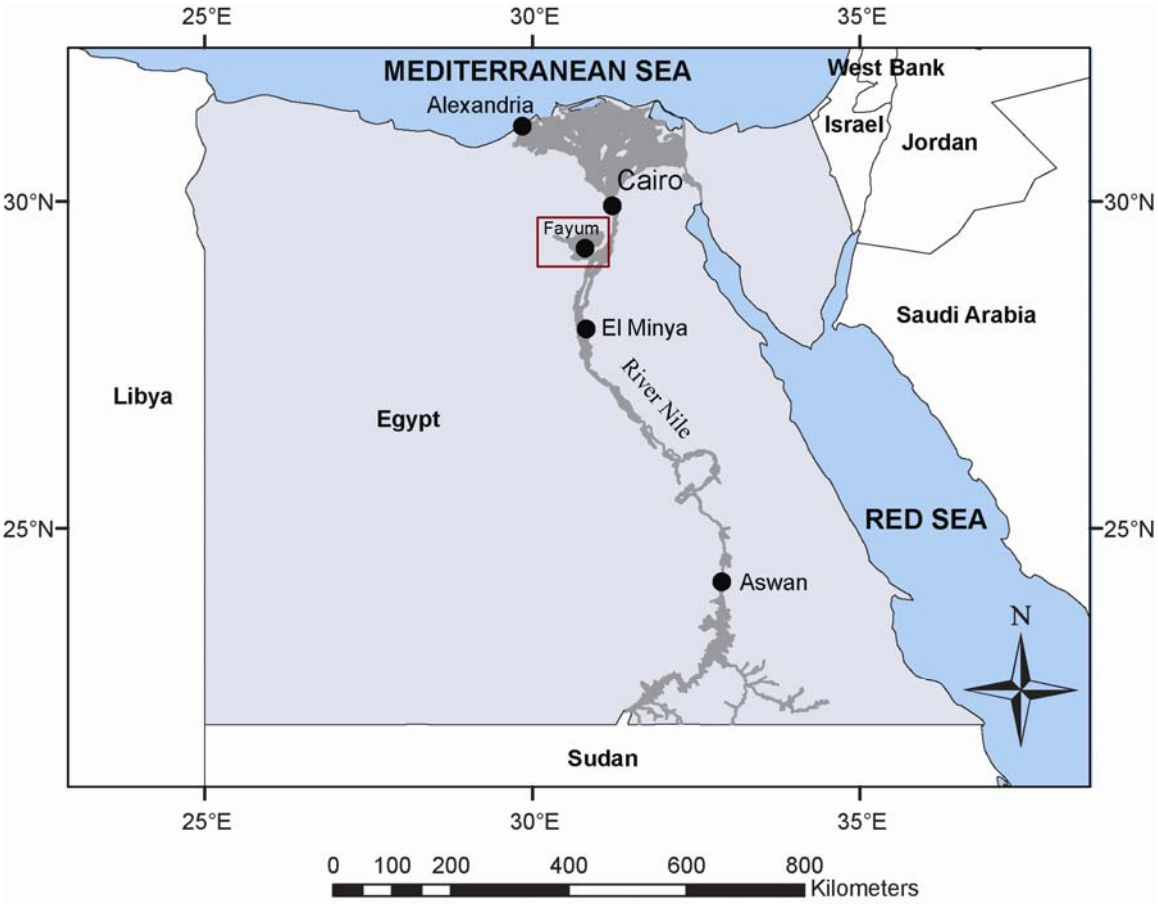

FIGURE 1.4. Geological map of the Fayum Basin and Nile River valley in northern Egypt. Shallow carbonate (nummulitic) and clastic rocks are the dominant Eocene lithologies in Cairo and Fayum. Cretaceous rocks are the oldest sedimentary strata exposed west of Cairo. Geological units and their boundaries are extracted and modified from the Conoco Oil Company 1:500.000 geological map series, including sheets for Alexandria, Baharia, Beni Suief, and Cairo. The Gehannam , Birket Qarun, Qasr El Sagha, and Gebel Qatrani formations of Beadnell (1905) were revised by Bown and Krause (1988), Gingerich (1992), and recent field mapping in Fayum. Green diamonds show the distribution of sirenian fossils in the study area (listed in Table 1-1).

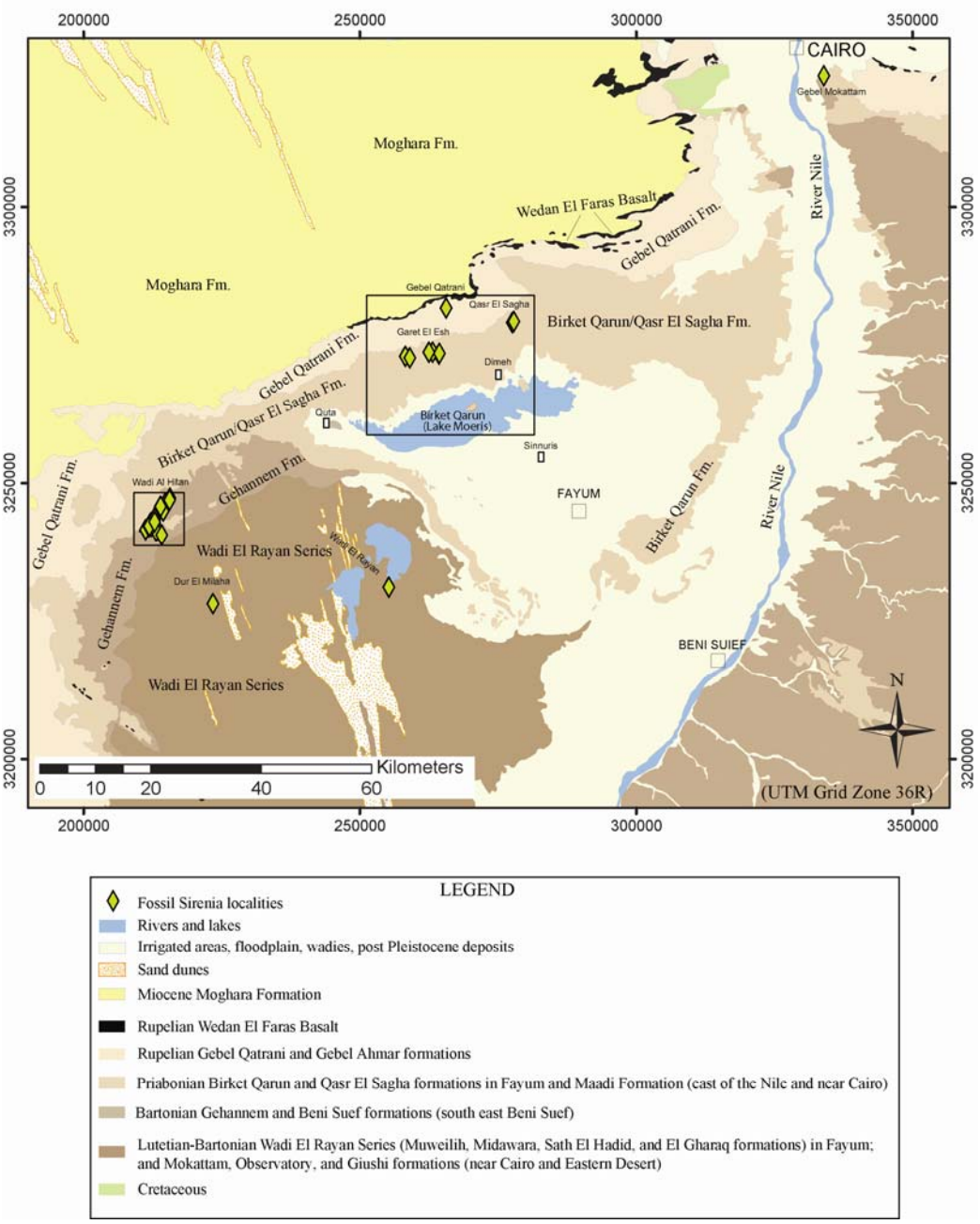

FIGURE 1.5. Sirenian fossil distribution in Wadi Al Hitan west of the Fayum Basin. Most specimens come from the Birket Qarun Formation (lower Priabonian).

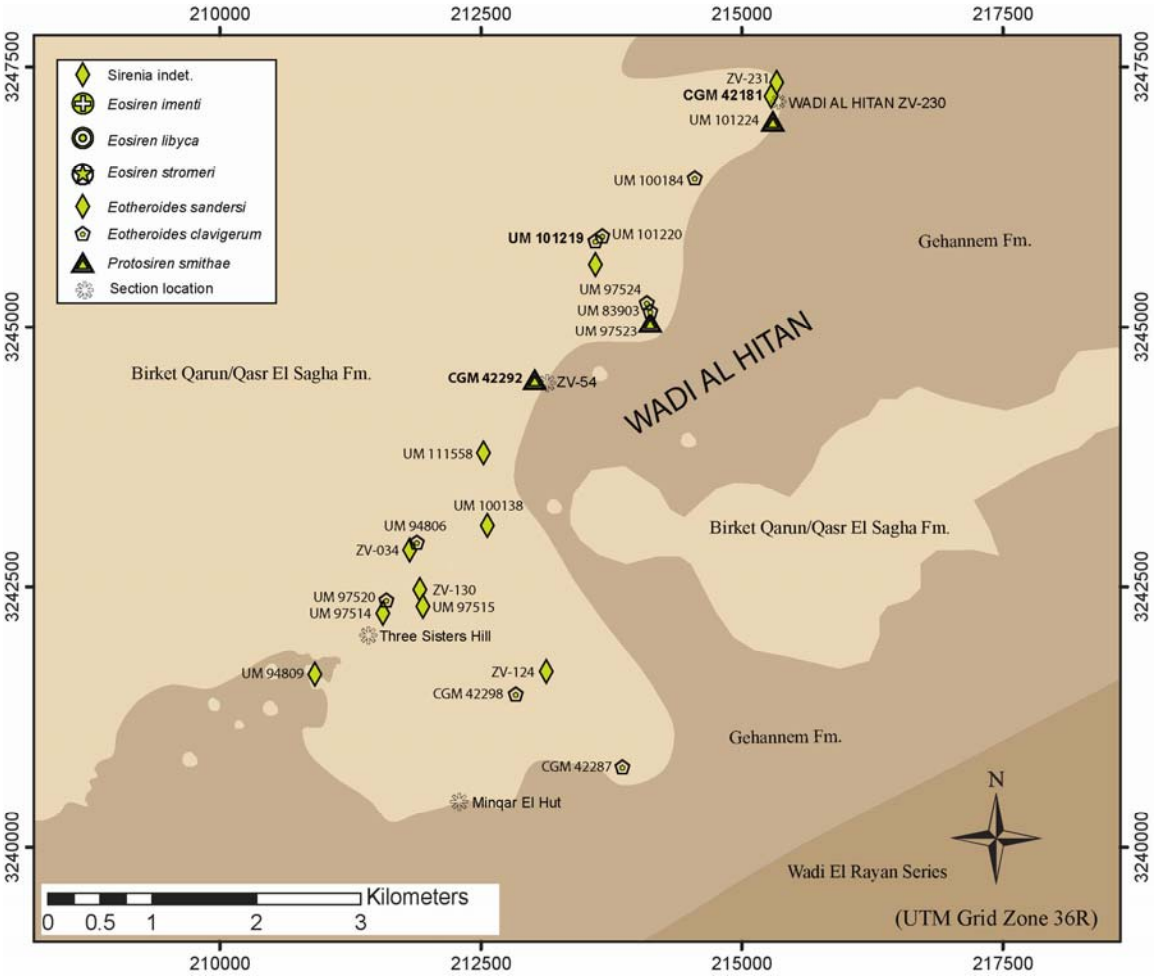

.

FIGURE 1.6. Sirenian fossil distribution in Wadi El Rayan, rocks exposed here are the Wadi El Rayan series of Lutetian and Bartonian ages. UM 101229 was collected from the top of the Medawar Formation, and UM 16069 was collected from the El Gharaq Formation.

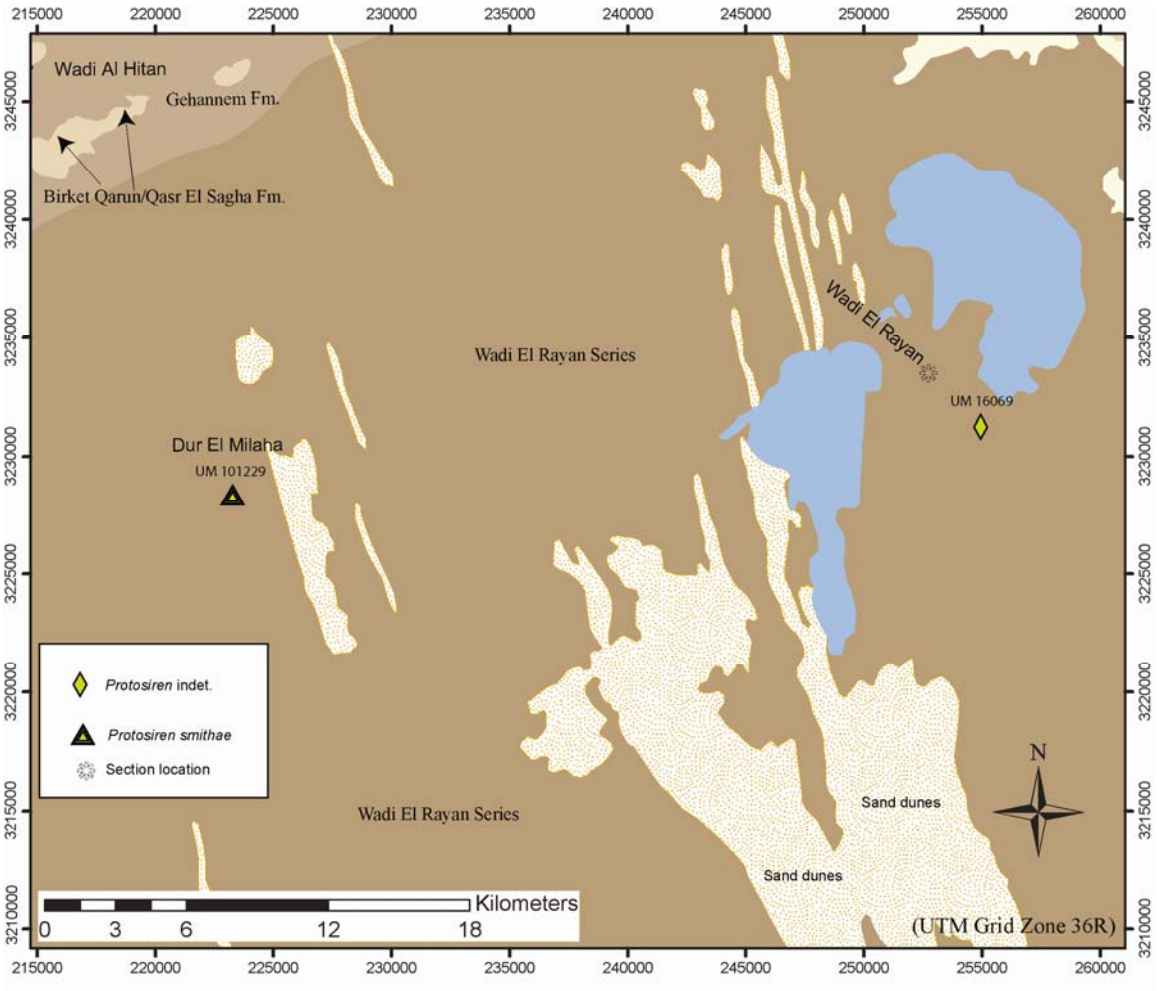

FIGURE 1.7. Sirenian fossil distribution north of Lake Moeris. The oldest rocks exposed here are located on the lower part of Qazeeret El Qurn and belong to the Gehannam Formation. Most o the sirenian in fossils in this area came from Qasr El Sagha Formation. *Eosiren imenti* came from the Rupelian beds of the Gebel Qatrani Formation.

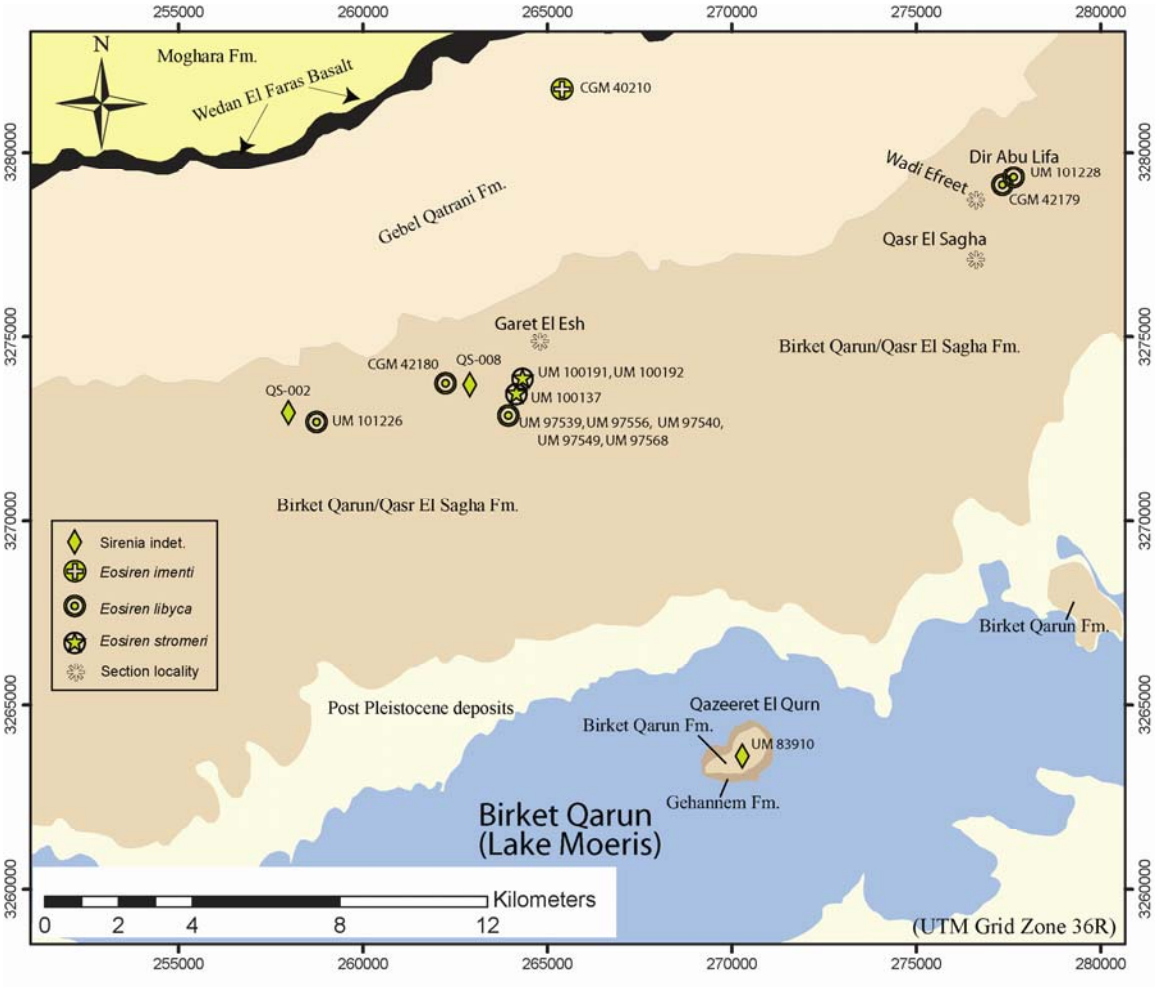

Literature Cited

ABEL, O. 1904. Die Sirenen der mediterranen Tertiarbildungen Osterreichs. Abhandlungen der Kaiserlich-Kiniglichen Geologischen Reichsanstalt (Wien), 19:1-223.

ABEL, O. 1907. Die Stammesgeschichte der Meeressäugetiere. Meereskunde 1:1-36.

ABEL, O. 1912. Die eocänen Sirenen der Mittelmeerregion. I. Teil: Der Schädel von Eotherium aegyptiacum. Palaeontographica, 59:289-360.

ANDREWS, C. W. 1902. Dr. C. W. Andrews on fossil vertebrates from Upper Egypt. . Proceedings of the Zoological Society of London, 1902:228-230.

ANDREWS, C. W. 1904. Further notes on the mammals of the Eocene of Egypt, Part III. Geological Magazine, 1:211-215.

ANDREWS, C. W. 1906. A descriptive catalogue of the Tertiary Vertebrata of the Fayãum, Egypt. Printed by order of the Trustees of the British museum [etc.], London, xxxvii, 324 p., 26 l. pp.

AS-SARURI, M. L., P. J. WHYBROW, and M. E. COLLINSON. 1999. Geology, fruits, seeds, and vertebrates (?Sirenia) from the Kaninah Formation (Middle Eocene), Republic of Yemen; pp. 443-453 in P. J. WHYBROW and A. HILL (eds.), Fossil vertebrates of Arabia: with emphasis on the Late Miocene faunas, geology, and palaeoenvironments of the Emirate of Abu Dhabi, United Arab Emirates. Yale University Press, New Haven & London.

ASTIBIA, H., A. PAYROS, X. P. SUBERBIOLA, J. ELORZA, A. BERRETEAGA, N. ETXEBARRIA, A. BADIOLA, and J. T. OSQUELLA. 2005. Sedimentology and taphonomy of sirenian remains from the Middle Eocene of the Pamplona Basin (Navarre, western Pyrenees). Facies, 50:463-475.

ARATA, A. A., and C. G. JACKSON JR. 1965. Cenozoic Vertebrates from the Gulf Coastal Plain. Tulane Studies in Geology, 3:175-177.

BAJPAI, S., J. G. M. THEWISSEN, V. V. KAPUR, B. N. TIWARI, and A. SAHNI. 2006. Eocene and Oligocene sirenians (Mammalia) from Kachchh, India. Journal of Vertebrate Paleontology, 26:400-410.

BATALLER, J. R. 1956. Contribución al conocimiento de los Vertebrados terciarios de España. Cursillos y Conferencias, Instituto Lucas Mallada, 3:11-28.

BATIK, P., and O. FEJFAR. 1990. Les vertébrés du Lutétien, du Miocène et du Pliocène de Tunisie centrale. Notes Service Géologique de Tunisie, 56:69-83.

BEADNELL, H. J. L. 1905. The Topography and Geology of the Fayum Province of Egypt. Survey Department Egypt, Cairo, 101 pp.

BIZZOTTO, B. 1983. *Prototherium intermedium* n. sp. (Sirenia) dell'Eocene Superiore di Possagna e proposta di revisione sistematica del taxon *Eotheroides* Palmer 1899. . Memorie de Scienze Geologiche (Memorie dell'Instituto Geologico della R. Università), Padua, 36:95-116.

BIZZOTTO, B. 2005. La struttura cranica di *Prototherium intermedium* (Mammalia: Sirenia) dell'Eocene superiore Veneto. Nuovi contributi alla sua anatomia e sistematica. Societa Veneziana di Scienze Naturali Lavori, 30:107-125.

BLAINVILLE, H. M. D. De. 1840. Ostéographie, Livr. 7, Des Phoques (*G. Phoca*, L.). Arthus Bertrand, Paris.

BLAINVILLE, H. M. D. De. 1844. Ostéographie, Livr. 15, Des Lamantins (Buffon), (Manatus, Scopoli), ou gravigrades aquatiques. Arthus Bertrand, Paris.

BOWN, T. M., and M. J. KRAUS. 1988. Geology and paleoenvironment of the Oligocene Jebel Qatrani Formation and adjacent rocks, Fayum Depression, Egypt, United States Geological Survey Professional Paper Volume 1452, Denver, CO, iv, 60, 4 pp.

DOMNING, D. P. 1978. Sirenian Evolution in the North Pacific Ocean. University of Californian Publications in Geological Sciences, 118:1-179.

DOMNING, D. P. 1994. A phylogenetic analysis of the Sirenia. Proceedings of San Diego Society of Natural History, 29:177-189.

DOMNING, D. P. 1996. Bibliography and Index of the Sirenia and Desmostylia. Smithsonian Contributions to Paleobiology, 80:1-611.

DOMNING, D. P. 2000. The readaptation of Eocene sirenians to life in water. Historical Biology 14(1-2):115-119.

DOMNING, D. P. 2001. The earliest known fully quadrupedal sirenian. Nature, 413(6856):625-627.

DOMNING, D. P., and P. D. GINGERICH. 1994. *Protosiren smithae*, new species (Mammalia, Sirenia), from the late Middle Eocene of Wadi Hitan, Egypt. Contributions from the Museum of Paleontology University of Michigan, 29(3):69-87.

DOMNING, D. P., G. S. MORGAN, and C. E. RAY. 1982. North American Eocene sea cows (Mammalia: Sirenia). Smithsonian Contribution to Paleobiology, 52:1-69.

DOMNING, P. D., P. D. GINGERICH, E. L. SIMONS, and A. F. ANKEL-SIMONS. 1994. A new early Oligocene Dugongid (Mammalia, Sirenia) from Fayum Province, Egypt Contributions from the Museum of Paleontology, University of Michigan, 29(4):89-108.

EMMONS, E. 1858. Agriculture of the Eastern Counties; together with descriptions of the Fossils of the Marl Beds. In *Report* of *the North-Carolina Geological Survey,* xvi + 314 pages, more than 256 figures. Raleigh: H. D. Turner. [Reprinted in part, 1969, *Bulletins of American Paleontology*, 56(249):57-230, with new index.].

FILHOL, H. 1878. Note sur la découverte d'un nouveau Mammifère marin (Manatus coulombi) en Afrique dans les carrières de Mokattam près du Caire. Bullétin de la Société Philomathique de Paris, Série 7, 2:124-125.

FLOWER, W. H., and J. G. GARSON. 1884. Class Mammalia, Other Than Man. *In* Catalogue of the Specimens Illustrating the Osteology and Dentition of Vertebrated Animals, Recent and Extinct, Contained in the Museum of the Royal College of Surgeons of England, part 2, xliii + 779 pages. London: J. & A. Churchill.

FRAAS, E. 1904. Neue Zeuglodonten aus dem unteren Mitteleocän vom Mokattam bei Cairo. Geologische und Paläontologische Abhandlungen, 6:197-220.

FREUDENTHAL, M. 1970. Fossiele zeekoeien in het Eoceen van Taulanne. Experimenteel Geologisch Onderwijs, 1969/70:64-65.

FURUSAWA, H. 1988. A new species of hydrodamaline Sirenia from Hokkaido, Japan. Takikawa Museum of Art and Natural History, Takikawa, 1-73 pp.

GHEERBRANT, E., D. P. DOMNING, and P. TASSY. 2005. Paenungulata (Sirenia, Proboscidea, Hyracoidea and relatives); pp. 84-105 in K. D. ROSE and J. D.

ARCHIBALD (eds.), The rise of placental mammals: origins and relationships of the major extant clades. Johns Hopkins University Press, Baltimore & London.

GILL, T. 1870. On the relations of the orders of mammals. Proceedings of American Association for the Advancement of Science 19:267-270.

GINGERICH, P. D. 1992. Marine mammals (Cetacea and Sirenia) from the Eocene of Gebel Mokattam and Fayum, Egypt: stratigraphy, age, and paleoenvironments. University of Michigan Papers on Paleontology, 30: 1-84.

GINGERICH, P. D., B. H. SMITH, and E. L. SIMONS. 1990. Hind Limbs of Eocene Basilosaurus - Evidence of Feet in Whales. Science, 249:154-157.

GINGERICH, P. D., M. ARIF, M. A. BHATTI, H. A. RAZA, and S. M. RAZA. 1995. *Protosiren* and *Babiacetus* (Mammalia, Sirenia and Cetacea) from the middle Eocene Drazinda Formation, Sulaiman Range, Punjab (Pakistan). . Contributions from the Museum of Paleontology, University of Michigan, 29:331-357.

GINGERICH, P. D., Y. ATTIA, F. EL-BEDAWI, and S. SAMEEH. 2007. Khasm El-Raqaba: a new locality yielding middle Eocene whales and sea cows from Wadi Tarfa in the Eastern Desert of Egypt. Journal of Vertebrate Paleontology, 27:81A.

HEAL, G. J. 1973. Contributions to the study of sirenian evolution. University of Bristol, London, 1-245 pp.

KOENIGSWALD, G. H. R. Von. 1952. Fossil sirenians from Java. Proceedings of the Section of Sciences, Series B, Koninklijke Nederlandse Akademie van Wetenschappen-Amesterdam, 55:610-612.

KORDOS, L. 1977. A new upper Eocene Sirenian (Paralitherium tarkanyense n.g.n.sp.) from Felsötrárkány, NE Hungary. Magyar Állami Földtani Intézet Évi Jelentése az 1975 Évröl, 1977:349-367.

KORDOS, L. 1978. Major Finds of Scattered Fossils in the Palaeovertebrate Collection of the Hungarian Geological nstitute (Communication No 3). Magyar Állami Földtani Intézet Évi jelentése az 1976 Evröl, 1978:281 -290, 1 plate. [Pages 281-284 in Hungarian.].

KORDOS, L. 1979. Major Finds of Scattered Fossils in the Palaeovertebrate Collection of the Hungarian Geological Institute(Communication No. 4). Magyar Állami

Földtani Intézet Évi jelentése az 1977 Evröl, 1979:313-326 [Pages 313-316 in Hungarian.].

KORDOS, L. 1980. Contribution to the knowledge of sirenians from the Hungarian Eocene. Magyar Allami Foldtani Intezet Evi Jelentese, 1978:385-397.

KORDOS, L. 2002. Eocene sea cows (Sirenia, Mammalia) from Hungary. Fragmenta Palaeontologica Hungarica, 20:43-48.

KRETZOI, M. 1941. Sirenavus hungaricus n.g. n. sp., ein neuer Prorastomide aus dem Mitteleozän (Lutetium) von Felsögalla in Ungarn. Annales Musei Nationalis Hungarici, Pars Mineralogica, Geologica et Palaeontologica, 34:146-156.

KRETZOI, M. 1953. A legidösebb magyar ösemlös-lelet. Földtani Közlöny, 83:273-277.

MCKENNA, M. C. 1975. Toward a phylogenetic classification of the Mammalia; pp. 21-46 in W. P. LUCKETT and F. S. SZALAY (eds.), Phylogeny of the Primates. Plenum Press, New York.

MÜLLERRIED, F. K. G. 1932. Primer hallazgo de un sirénido fósil en la República Mexicana. Anales del Institute de Biologia Universidad Nacional de México, 3:71-73.

MURPHY, W. J., E. EIZIRIK, S. J. O'BRIEN, O. MADSEN, M. SCALLY, C. J. DOUADY, E. TEELING, O. A. RYDER, M. J. STANHOPE, W. W. DE JONG, and M. S. SPRINGER. 2001. Resolution of the Early Placental Mammal Radiation Using Bayesian Phylogenetics. Science 294:2348-2351.

OWEN, R. M. 1855. On the fossil skull of a mammal (Prorastomus sirenoides Owen) from the island of Jamaica. Quarterly Journal of the Geological Society of London, 11:541-543.

OWEN, R.1875. On fossil evidences of a sirenian mammal (Eotherium aegyptiacum, Owen) from the Nummulitic Eocene of the Mokattam Cliffs, near Cairo . Quarterly Journal of the Geological Society of London, 31:100-105.

PILLERI, G., J. BIOSCA, and L. VIA. 1989. The Tertiary Sirenia of Catalonia. Brain Anatomy Institute, University of Berne, Ostermundingen, 1-98 pp.

REINHART, R. H. 1959. A Review of the Sirenia and Desmostylia. University of California Publications in Geological Sciences, 36:1-146.

REINHART, R. H. 1976. Fossil sirenians and desmostylids from Florida and elsewhere. Bulletin of the Florida State Museum of Biological Sciences, 20:187-300.

RICHARD, M. 1946. les gisements de mammifères tertiaires: Contribution à l'étude du Bassin d'Aquitaine. Mémoires de la société géologique de France (nouvelle série), 24(Mémoire n°52):1-380.

ROSE, K.D., T. SMITH, R.S. RANA, A. SAHNI, H. SINGH, P. MISSIAEN, and A. FOLIE. 2006. Early Eocene (Ypresian) continental vertebrate assemblage from India, with description of a new anthracobunid (Mammalia, Tethytheria). Journal of Vertebrate Paleontology, 26: 219-225.

SAGNE, C. 2001. *Halitherium taulannense*, nouveau sirenien (Sirenia, Mammalia) de l'Eocene superieur provenant du domaine Nord-Tethysien (Alpes-de-Haute-Provence, France) Comptes Rendus de l'Academie des Sciences Serie II A Sciences de la Terre et des Planetes, 333:471-476.

SAHNI, A., and V. P. MISHRA. 1975. Lower Tertiary vertebrates from western India. Monographs of the Palaeontological Society of India, 3:1-48.

SAID, R. 1990. Cenozoic; pp. 451-486 in R. SAID (ed.), The geology of Egypt. A.A. Balkema, Netherlands (NLD).

SAMONDS, K., I. ZALMOUT, and D. KRAUSE. 2005. New Sirenian fossils from the Late Eocene of Madagascar. Journal of Vertebrate Paleontology, 25:63A.

SAMONDS, K., I. S. ZALMOUT, M. T. IRWIN, and L. L. RAHARIVONY. 2007. Sirenian postcrania from Nosy Mahakamby, Northwestern Madagascar. Journal of Vertebrate Paleontology, 27:139A.

SANDERS, A. E. 1974. A Paleontological Survey of the Cooper Marl and Santee Limestone near Harleyville, South Carolina (Preliminary Report). South Carolina State Development Board, Division of Geology, Geologic notes, 18:4-12.

SAVAGE, R. J. G. 1969. Early Tertiary Mammal Locality in Southern Libya. Proceedings of the Geological Society of London, 1657:167-171.

SAVAGE, R. J. G. 1977. Review of early Sirenia. Systematic Zoology, 25:344-351.

SCHWEINFURTH, G. A. 1883. Ueber die geologische Schichtengliederung des Mokattam bei Cairo. Zeitschrift der Deutschen Geologischen Gesellschaft, 35:709-737.

SICKENBERG, O. 1934. Beträge zur Kenntnis tertiärer Sirenen. I. Die Eozänen Sirenen des Mittelmeergebietes. II. Die Sirenen des Belgischen Tertiärs. Mémoires de la Musée Royal d'Histoire Naturelle de Belgique, 63:1-352.

SIEGFRIED, P. 1967. Das Femur von *Eotheroides libyca* (Owen) (Sirenia). Paläontologische Zeitschrift, 41:165-172.

SILER, W. L. 1964. A Middle Eocene Sirenian in Alabama. Journal of Paleontology, 36:1108-1109.

SIMONS, E. L., and D. T. RASMUSSEN. 1990. Vertebrate paleontology of Fayum; history of research, faunal review and future prospects; pp. 627-638 in R. SAID (ed.), The geology of Egypt. A.A. Balkema, Rotterdam.

SCHLOSSER, M. 1923. Grundziige der Paliiontologie (Palaozoologie) von Karl A. von Zittel, II Abteilung- Vertebrata. Neuarbeitet von F. Broili und M. Schlosser. R. Oldenbourg, Munich and Berlin, 706 pp.

SHOSHANI, J. 1986a. Mammalian phylogeny: comparison of morphological and molecular results. Molecular Biology and Evolution, 3:222-242.

SIMPSON, G. G. 1945. The principles of classification and a classification of mammals. Bulletin of the American Museum of Natural History, 85:1-350.

STELLER, G. 1751. The beasts of the sea. (translated by W. Miller and J. E. Miller, orig. published in 1751).. Pp. 180-201 in D. Jordan, ed. The fur seals and fur seal islands of the North Pacific Ocean. Part 3. Washington, D.C.: U.S. Government Printing Office.

STROUGO, A. 1992. The Middle Eocene/Upper Eocene transition in Egypt reconsidered. Neues Jahrbuch für Geologie und Palaeontologie. Abhandlungen, 186:71-89.

STROUGO, A., and M. A. Y. HAGGAG. 1984. Contribution to the age determination of the Gehannam Formation in the Fayum Province, Egypt Neues Jahrbuch für Geologie und Palaeontologie. Monatshefte, 1984:46-52.

UHEN, M. D. 2003. Form, function and anatomy of *Dorudon atrox* (Mammalia, Cetacea) : an Archaeocete from the middle to late Eocene of Egypt. University of Michigan Papers on Paleontology, 34:1-222.

VERNON, R. O. 1951. Geology of Citrus and Levy Counties, Florida. Florida Geological

WELLS, N. A., and P. D. GINGERICH. 1983. Review of Eocene Anthracobunidae (Mammalia, Proboscidea) with a new genus and species, *Jozaria palustris*, from the Kuldana Formation of Kohat (Pakistan). Contributions from the Museum of Paleontology, University of Michigan, 26:117-139.

WING, S. L., and B. H. TIFFNEY. 1982. a paleotropical flora from the Oligocene Jebel Qatrani Formation of Northern Egypt: A preliminary report Miscellanous series of the Botanical Society of America, 162:67.

WING, S. L., S. T. HASIOTIS, and T. M. BOWN. 1995. First ichnofossils of flank-buttressed trees (late Eocene), Fayum Depression, Egypt. Ichnos, 3:281-286.

ZALMOUT, I. S., M. UL-HAQ, and P. D. GINGERICH. 2003a. New species of *Protosiren* (Mammalia, Sirenia) from the early middle Eocene of Balochistan (Pakistan). Contributions from the Museum of Paleontology. University of Michigan, 31:79-87.

ZALMOUT, I., P. GINGERICH, H. MUSTAFA, A. SMADI, and A. KHAMMASH. 2003b. Cetacea and Sirenia from the Eocene Wadi Esh-Shallala Formation of Jordan. Journal of Vertebrate Paleontology, 23(3, supplement):113.

ZDANSKY, O. 1938. *Eotherium majus* sp.n., eine neue Sirene aus dem Mitteleozän von Aegypten. Palaeobiologica, 6:429-434.

ZIGNO, A. DE. 1875. Sireni fossili trovati nel Veneto Memorie dell' Real Istituto Veneto di Scienze Lettere ed Arti, 18:427-456.

CHAPTER TWO

GEOLOGY AND STRATIGRAPHY

The origin and distribution of the Eocene deposits yielding sirenian fossils in Egypt were to a great extent controlled by the tectonic history of the African Continent. Major rifting events during the Late Jurassic and Early Cretaceous along the North African–Arabian margin of Tethys caused a series of pull-apart basins to form in northern Egypt and Sinai. This system, the Syrian Arc system of Krenkel (1924), extended as far north as western and central Jordan and most of Syria. Continuous movement of the Afro-Arabian plate to the northeast imposed severe compressional forces through the Late Cretaceous and middle and late Eocene, which gave the final shape to this system and its basins (Guiraud and Bosworth, 1999; Guiraud et al., 2001; Guiraud et al., 2005).

Two aspects are of interest here: first, the geology of the Fayum Basin and surrounding areas, and second: the stratigraphy of the sirenian-bearing formations in northern Egypt.

Geology of the Fayum Basin and Surrounding Areas

The Fayum Basin (also referred to as the Fayum-Gindi Basin) is a 120 km wide graben filled with 2 km of Eocene sediments (Salem, 1976). These lie unconformably on top of Upper Cretaceous strata. The basin is bounded by two major highlands: El Kattaniya-Abu Rosh in the north, and Nashfa to the south of Wadi El Rayyan. The latter forms the southern edge of the Syrian Arc System.

Within this grabben, the Fayum Basin represents a classic model of regression and/or progradation, with a carbonate shelf facies occupying the lower and lower middle parts of the Eocene and siliciclastic deltaic, lagoonal, and estuarine facies predominating in the upper middle and upper Eocene (Kostandi, 1959; Salem, 1976).

Northern Egypt, including the Fayum Basin, was a broad stable marine platform during the middle and late Eocene, following Syrian Arc rifting and compression, and preceding Red Sea rifting. The platform subsided passively, with little or no tectonic influence, and preserved a good record of shallow marine strata.

Stratigraphy of Sirenian-Bearing Formations in Cairo and Wadi Al Hitan

Gebel Mokattam (Mokattam Hills) near Cairo is considerably important because it is made up of Eocene sediments that produced informative marine mammal fossils and span middle and late Eocene (Figure 2.1). It produced the first sirenian, the type specimen of *Eotheroides aegyptiacum* (Owen, 1875), primitive whales such as *Protocetus atavus* and *Eocetus schweinfurthi* Frass (1904), and later another sirenian taxon known as *Protosiren fraasi* Abel (1907). These marine mammals are at least 8 million years older than the marine mammal assemblages of Wadi Al Hitan of the Fayum Basin.

Gebel Mokattam is famous for its nummulitic limestone that is also known as the Building Limestone in reference to the stones quarries that the Pyramids were built from.

Strougo (1986) and Said (1990: 459) divided the rocks in Gebel Mokattam into three Formations, the lowermost formation is the Mokattam Formation which is made of nummulitic limestone and produced all the Mokattamian marine mammals, followed by the Giushi Formation which is mostly coquina limestone of *Operculina* bivalves, and the Maadi Formation at the top which is mostly fine sandstones and silty marl. The Mokattam Formation and the Giushi Formation at Gebel Mokattam are Lutetian and Bartonian (middle Eocene) in age, and were deposed in offshore marine shelf and shallow shelf environments. The Maadi Formation at Gebel Mokattam is Priabonian and Bartonian (middle and late Eocene) in age, and was deposited in nearshore and lagoonal environments. According to Schweinfurth (1883) and later by Strougo (1985a, b), Gebel Mokattam has a thickness between 220 and 300 meters, depending on which side of the hill the section was measured.

Southwest of Cairo, in the Fayum Basin, the Eocene sedimentary exposure is almost twice as thick as in Cairo and more silisiclastic as well. The fossils are abundant and complete.

Our understanding of the Eocene stratigraphy in Fayum is mostly based on the Beadnell's (1901, 1905) and Blanckenhorn's (1903) diagnoses of stratigraphic levels and rock units at the Wadi El Rayan (the type locality for the Wadi El Rayan series) in the southwestern part of the Fayum Basin. Division and nomenclature of strata exposed in the Fayum Basin, starting from older formations of the Lutetian-Bartonian Wadi El Rayan series, heading north and northwest to the top of the Oligocene Gebel Qatrani terrestrial deposits, were reexamined after reading many paleontological and geological

descriptions and interpretations (Beadnell, 1901, 1905; Iskender, 1943; Said, 1990; Gingerich, 1992).

According to Beadnell (1901, 1905), the lower-most four formations of the Wadi El Rayan series (Figures 2.1 and 2.3) are Lutetian and Bartonian in age, and exposed in Wadi El Rayan valley and mesas. These were mapped by Beadnell (1905) and Iskender (1943, 1:100,000) as Wadi El Rayan Series which include:

A. Muweilih Formation (Figures 2.1 and 2.3): This is the lowest exposed formation in the area, and named Muweilih because it forms the floor of the Muweilih Oasis (the Salt Oasis). This formation represents bed number 6 in Minqar El Rayan section of Beadnell 1905. It is made of shallow marine, gray to dark colored, nummulitic, shaley, sandy, hard limestones. The exposed thickness of this formation is 36.5 m.

B. Midawara Formation (Figures 2.1 and 2.3): Iskender (1943) indicated that there is no physical interruption in the transition of between Muweilih and Midawara formations. The Midawara Formation is mostly thick brown and kaki shales, sandy shales, sandy limestones, and glauconitic sand. The maximum thickness of this formation may reach 127 meters at Gebel El Mishgega (Latitude 29º 12' N, Longitude 30º 21' E) (see: Iskander 1943:12). Sirenian and whale remains were recorded in the upper third of this formation in the bioturbated glauconitic sands near Dour El Milaha east of Qusor El Arab.

C. Sath El Hadid Formation (Figures 2.1 and 2.3): Iron surface in Arabic, it is a reef limestone bank with large and small sizes of *Nummulites*. It is 25 meters thick and caps the tops of Midawara Formation and covers most of the mesas in Wadi Al Rayan Area. The base of the Sath El Hadid is recognized as the contact between the snow-white

limestone and the brown sandy limestone of the Midawara Formation, while the upper contact with the El Gharag Formation is recognized by the appearance of brown and kaki shales above snow-white nummulitic limestone. The top of the Sath El Hadid Formation is recognized by the presence of secondary flint pockets and concretions.

D. El Gharaq Formation (Figures 1.2 and 2.3): According to the measured sections in Beadnell (1905) and Iskender (1943) this is the thickest formation of the Wadi El Rayan Series reaching 124 m at Ilw El Bireig in the SE of Wadi El Rayan. The El Gharaq Formation is made of nummulitic limestone and siltstone with glauconite, and shale at the top. This formation, conformably, overlies the Sath El Hadid Formation and the base is defined above the last appearance of the white-snow limestone of the Sath El Hadid Formation; while its top is defined as the abrupt absence of the large and small nummulites and increase in the glauconitic concentrations which marks the base of the Gehannam Formation. According to Boukhary et al. (2003), the age of this formation is Biarritzian (i.e., late middle Eocene, or Bartonian) based on the nummulitic scale of Schaub (1981). The top of this formation is exposed at the northern and eastern foot hills of Qaret Gehannam. Teeth of sharks and rays were collected from this formation; marine mammals here are fragmentary and rare.

E. Gehannam Formation (Figures 2.1, 2.4, and 2.5): Beadnell (1905) and Iskender (1943) called the Gehannam Formation the Ravine Beds because its sediments are exposed in ravines and small valleys. Said (1962, 1990) called the beds the Gehannam Formation as they best exposed at Garet Gehannam; Ismael and Abdel-Kereem (1971a, b) divided the Gehannam Formation into two members, a lower part which is equal to the Ravine Beds as the Gehannam Marl Member, and upper part which is the Birket Qarun

Formation, called the Gehannam Shale Member. However because the beds are exposed very well at Garet Gehannam with a defined base and top the name Gehannam Formation is used here rather than the Ravine Beds. It has a variable thickness and may reach 35 meters near Garet Gehannam plateau. The base of this formation is marked by thick deposits of glauconitic sandstone and marls lacking large forms of benthic forams, but is rich with fish scales, sharks and rays teeth, and marine mammal skeletons. The marl and glauconite deposits are replaced by gypseous fine sands and brown shale capped with pale sandstone at the top, marking the base of the Birket Qarun Formation. Eastward of the Qaret Gehannam and just to the west side of the Birket Qarun near the village of Guta, the Gehannam Formation appears in limestone and marly limestone facies (Strougo, 1992), this area also produced many skeletons of marine mammals.

In Wadi Al Hitan the middle and top part of the Gehannam Formation is exposed and mostly covers the base of the valley. Gingerich (1992) placed the boundary between the Birket Qarun and Gehannam formations at the bioturbated Camp White Layer with shrimp burrowing tubes and networks and other pneumatophore structures. The boundary probably should be extended down deeper in the valley to the top level of the calcareous sandstone that weathers into spherical masses where it is exposed 18 meters below the type locality of *Protosiren smithae* at locality ZV-54 (see Gingerich, 1992). Beadnell (1905: 38) placed the boundary between the Gehannam and Birket Qarun between two thick sandstones at meter 70 (see Gingerich, 1992, p.28), these two sandstone bodies are genealogically related and should be allocated in the same formation. So the boundary between the Gehannam and Birket Qarun formations assigned by Beadnell (1905: 38) along the exposed cliffs of Garet Gehannam Plateau

should be moved down to the top of the clayey limestone with fish scales at meter 37, as it is the end of a sedimentation cycle, and the base of the light brown gypseous clay, as it represents a beginning of a different cycle

Gingerich (1992) proposed a shallow open shelf environment for the Gehannam Formation. Abdou and Abdel-Kireem (1975), Strougo and Haggag (1984), Haggag (1995, 1990), assigned a Bartonian-Priabonian age to this formation based on its foraminiferal content.

F. Birket Qarun Formation (Figures 2.1, 2.4, 2.5, and 2.9): The Birket Qarun Formation is very well exposed along the northern cliffs of Lake Qarun and to the west in Wadi Al Hitan. Its thickness ranges between 20 and 85 meters. It is made of clays, shales, thick fine-grained sandstones, ferruginous bioclasts, and calcareous grits. Being thickest and well exposed in Wadi Al Hitan, the Birket Qarun Formation is made of alternations of two major lithologies; the first is greenish, gypseous shales with minor silts; the second is very fine, mature sandstones with severely bioturbated bases by *Ophiomorpha* and *Thalassinoides*. Gingerich (1992) stated that the Birket Qarun Formation represented a series of barrier bar deposits trapping clay and silts in small lagoons. However, information from recently studied sections covering a larger area of the Birket Qarun Formation exposure in Wadi Al Hitan revealed that this formation is thicker than was previously thought, and with very complex and different architecture in heterogeneous shallow shelf and shoreface settings with limited wave domination. The fossil marine mammals and other vertebrates of the Birket Qarun Formation were collected from many levels, from the lagoonal shale and from the sandstone barrier zone.

According to Strougo (Personal communication: April 2007), the marine mammal bearing beds from top of the Gehannam formation and the lower third of the Birket Qarun Formation at Wadi Al Hitan are early Priabonian in age based on the overlapping of NP18 calcareous nannoplankton zone and planktonic foraminifera zone P15 (*Globigerinatheka semiinvoluta*).

G. Qasr El Sagha Formation (Figures 2.1, 2.6, 2.7, and 2.8): The last and thickest Eocene series in Fayum is the Qasr El Sagah Formation, which may exceed 180 meters in total thickness. It tops the Birket Qarun Formation conformably most of the time (unless there are major channel cuts and redeposition from older and younger sediments). The base of this formation is defined by the first appearance of the papery *Carolia* bivalves, while the top is marked by a disconformity with the varicolored fluviomarine and terrestrial sandstones of the Gebel Qatrani Formation. According to Vondra (1974) and Bown and Kraus (1988), the Qasr El Sagha Formation was deposited in a retreating shallow sea which was receiving detritus from the exposed hinterland. The influx of terrigenous material became exceptionally high during the late Eocene when large rivers seem to have discharged in the sea forming submarine deltas. One of the best classic deltas that was deposited by these Eocene rivers is exposed to the north of the basin at the foot of the Qasr El Sagha Temple (the Temple Locality). The deltaic and interdeltaic sediments of the upper Eocene are exposed to the north of Birket Qarun, Fayum, where they form the Qasr El Sagha formation. Vondra (1974) listed four major facies dominated the Qasr El Sagha Formation, these are: 1-the *lowermost arenaceous bioclastic facies* is made up of bioturbated (mainly by the crustacean *Callianassa*) glauconitic and fossiliferous calcareous sandstone; 2- *gypsiferous and carbonaceous*

laminated claystone and siltstone facies which seem to have been deposited in back bar open and restricted lagoons; 3- *interbedded claystone, siltstone and quartz sandstone facies*, which is a fining upward cycle of very fine to fine-grained white quartz sandstone, pale yellowish brown and dark grey siltstone and claystone. Each unit constitutes a foreset of large-scale planar cross-stratification deposits, this facies was deposited in a rapidly prograding delta front environment in quiet shallow brackish marine waters; 4- *quartz sandstone facies* which seems to represent distributary channel deposits.

In Wadi Al Hitan the Qasr El Sagha Formation is divided into four members; from bottom to top they are: the Umm Rigl Member, Harab Member, Temple Member, and Dir Abu Lifa Member. The lowest two members were added to the Fayum stratigraphic system by Gingerich (1992) as they are recognized near Wadi Al Hitan and Garet Gehannam, while the top two were described in detail by Bown and Kraus (1988). According to Gingerich (1992) the Umm Rigl Member consists of an alternation of Vondra's arenaceous bioclastic carbonate facies (hard beds) and Vondra's gypsiferous and carbonaceous laminated claystone and siltstone facies, similar to that found in the Temple Member (but separated by the intervening Harab Member) of a shallow outer lagoonal setting; while the overlying Harab Member is deeper central lagoonal, and is made of a barren interval of brown shale and forms broad featureless plain; the Temple Member of Bown and Kraus (1988), is dominated by two of Vondra's (1974) Qasr El Sagha facies: the arenaceous bioclastic carbonate facies (facies 1), and the gypsiferous and carbonaceous laminated claystone and siltstone facies (facies 2). The Dir Abu Lifa Member is the fourth member of the Qasr El Sagha Formation, and it is made of cross-bedded sandstone, and appears to be composed of Vondra's facies 3, the inter-bedded

claystone, siltstone, and quartz sandstone facies (delta front), and Vondra's facies 4, the quartz sandstone facies (delta distributary facies).

H. Gebel Qatrani Formation (Figures 2.4): The Rupelian Gebel El Qatrani Formation disconformably tops the Priabonian Qasr El Sagha formation. Beadnell (1905), Vondra (1974), Bown et al. (1982), and Bown and Kraus (1988), studied this formation in depth and found that it is made of 110 to 340 m of fluvial sandstone, siltstones and claystones, and very minor carbonate lenses and carbonaceous shale. The lower third is characterized by a complex of large scale trough cross-stratified channel lag and point bar sands indicating deposition in a loosely sinuous, low gradient, medium velocity stream. The upper part of the formation is characterized by point bar, flood plain splay and channel fill deposits pointing to an overloaded and more tightly meandering stream. The point bar deposits are very fossiliferous in the lower as well as in the upper parts of the formation, containing abundant silicified tree logs and fossil vertebrates. Nearly all the sandstones show digenetic alteration reflecting ancient pedogenesis. Part of the lower part of this formation was deposited in a nearshore setting as indicated by the presence of shark teeth, ray mouth parts, brackish-water molluscs and abundant mangrove rhizoliths, and very recently a Sirenian skull (Domning et al., 1994). Among the diverse fossil vertebrates from Gebel Qatrani, the following are abundant: crocodilians, turtles, browsing artiodactyls and hyracoids, arboreal quadrupedal anthropoid primates, carnivorous mammals and phiomyid rodents (Andrews, 1906; Simons, 1968; Simons and Gingerich, 1974; El Khashab, 1974; Simons and Rasmussen, 1990; Gagnon, 1997). Ichnofossils and rhizoliths are abundant, well preserved and diverse in form (Bown, 1982); the ichnofauna contains traces of probable annelid, insect,

crustacean and vertebrate origin. These include fossil nest structures and gallery systems of subterranean termites. Rhizoliths associated with the ichnofauna document a variety of small wetland plants, coastal mangroves and large trees. Kortland (1980) believed that the Gebel Qatrani flora indicates a drier (Sahelian) climate. It differs from that of Qasr El Sagha in containing no identified leaves and in having only two fruit species (a waterlily and a relative of palms).

I. Widan El Faras Basalt (Figure 1.2 in Chapter 1): The Gebel Qatrani Formation is unconformably overlain by the Widan El Faras Basalt (Bowen and Vondra, 1974), the lower part of which is dated at 3 1±1 my (Fleagle et al., 1986a,b). The basalt occurs in three sheets. The lower and upper sheets are amygdaloidal, vesicular and intensely altered, whereas the middle sheet is massive, compact and fresh. Layering is noted in the upper sheet. The three sheets are similar petrologically and are of tholeiitic nature (Heikal et al., 1983).

Stratigraphic Levels Yielding Sirenia in Wadi Al Hitan

Two representative stratigraphic sections were measured at Wadi Al Hitan in order to append the collected fossils to their stratotypes. The first section (Figure 2.4) was measured to cover the areas of Minqar El-Hut, the University of Michigan Old Camp at Wadi Al Hitan and the Three Sisters Hill (see location of section in Figure 1.5); this section is referred to as Minqar El-Hut and Three Sisters section. The second section (see location of section in Figure 1.5) was measured at the eastern area of Wadi Al Hitan to cover the exposed lithologies around localities ZV-230 northeast of ZV-54 were sirenian

type specimens of Wadi AL-Hitan were found; this section is referred to as the Wadi Al Hitan ZV-230 section.

Other sections included in this study were re-illustrated and slightly modified from Beadnell (1905), Iskender (1943), Bown and Kraus (1988), and Gingerich (1992) in order to allocate fossils to their stratigraphic levels.

Minqar El-Hut and Three Sisters section: The stratigraphic section of Minqar El-Hut and Three Sisters (Figure 2.4) includes the top part of the Gehannam Formation which is marked by a thick layer of brown shale with gypsum. That is followed by a white marl bed with many skeletons of *Basilosaurus*; the marl bed can be easily seen at the bottom of the southern cliffs of Minqar El-Hut. This is followed by two white fine-sandstone beds that fine upward into another thick, light-brown shale; this brown shale is topped by another thin layer of marl that marks the top of the Gehannam Formation.

The top marl of the Gehannam Formation is topped by a white, very fine, highly bioturbated sandstones that extends for several kilometer in this area and marks the base of the Birket Qarun Formation. It is a prominent marker bed known as the Camp White Layer (CWL).that varies in thickness from 30 cm to 700 cm, and it may be synchronous and/or replaced by different facies in other areas of Wadi Al Hitan. CWL in most cases preserves infilled biological structures as *Callianassa* tubes. These tubes have a typical J shape, and are mostly filled with fine sand or nummulites. The base of the CWL contains fossil tree trunks that had been infested with *Teredo* worm tubes and later were replaced by celestite. The top of the CWL preserved many whale and sirenian fossils intact, but most of the time suffered severe sandblasting as they exposed on the surface.

The CWL is topped with 14 to 30 meters of thick, massive, cliff-forming, golden-colored, very fine, friable sandstone that produced many whale and sirenian skeletons. This bed starts at the base with white sandstone that is extremely rich with selachian teeth, turtles and crocodilian remains; the middle part is marked by a yellow and black gypsous clay.

The thick sandstone is followed by a 30-60 cm thick, hematite-stained, sheet-forming silty limestone, this is followed by 2.5 meters of golden and white colored friable sandstones with bioturbated hard base similar to the CWL lithology, this is then overlain by a 3 meters thick massive golden fine sandstone that gets very fine at the top. The top of this sandstone is capped by clayey sandstone preceding an episode of slow deposition in restricted environment; this episode is represented by a locally deposited gray to black clay bed ranging in thickness from 20 cm to 5 meters, with a maximum thickness in Qaret Gehannam (about 10 km NE of the Wadi Al Hitan), the clay is overlain by a thick bed of nummulitic, golden color sandstone.

The fine sandstones interrupted with minor clays and shales beds continue in appearance in the following 15 meters towards the top of the Birket Qarun Formation with minor change in the biological contents as the transition into the Qasr El Sagha Formation is marked by a 40 cm thick carbonaceous fine sandstone weathering out *Carolia* shells on flat benches. The rest of the section which is the entire 190 meters of Qasr El Sagha Formation capped by the Bare Limestone and the Gebel Al Qatrani Formation is already described in Gingerich 1992.

Wadi Al Hitan ZV-230 section: The second section is Wadi Al Hitan ZV-230 (Figure 2.5), located about 9 km northeast of Minqar El-Hut and Three Sisters section (Figure 1.5). The base of the section is located 150 meters east of locality ZV-230 (the type locality of *Eotheroides sandersi*, CGM 42181).

The top the Gehannam Formation furnishes the floor of the valley with gypsum and silty brown clays establishing the base of the stratigraphic section of Wadi Al Hitan ZV-230. These clays are followed by a 40 cm thick yellow calcareous sandstone topped by a 4 m thick friable white-pale sandstone; this sandstone is then followed by 1 m meter think white to gray bioturbated sandstone with its top weathering into sand concretions. This bed is the base of the section illustrated in Gingerich (1992: 43: fig. 35) and marks the top of the Gehannam Formation.

Just above this white calcareous sandstone a 2 meter thick unit of very friable silty shale marks the base of the Birket Qarun Formation. This bed has produced many marine mammals skeletons such as the type specimen of *Eotheroides sandersi*; a 50 cm thick yellow sandstone followed by a 4 m thick green shale; above this thick shale is a 3 m section of yellow and golden-colored sandstone that is equivalent to the CWL marker bed of the Birket Qarun Formation.

The top of the former sandstone bed is ferruginous and loaded with archaeocete skeletons and is the level that produced the famed skeleton of *Dorudon atrox* (UM 101215). A 2-meter thick shale bed tops the sandstone layer and is caped by a 30 cm thick terrace of sandstone. Above this is an 11-meter thick, massive bed of gypsiferous clay and shale marked by a thin yellow sulphurous layer in the middle. This thick mud bed is traceable and mapable for several kilometers in Wadi Al Hitan. This clayey shale

is overlain by a 5-meter thick fine, golden-colored sandstone; the base of this sandstone level produced the type specimen of *Protosiren smithae* (CGM 42292 at locality ZV-54). This sandstone is followed by a 2-meter thick, yellow colored, very fine-grained marly sandstone. This marly sandstone is slowly integrated into another calcareous, fine, white sandstone of 4 meters in thickness with pneumatic and J-shaped burrows that are similar to those in the marker bed CWL.

The pneumatic sandstone is followed by a thick alternation of thick , dark colored silty shale packages (3 of them at least) that are separated by thin layers of iron-stained, bioturbated, fossiliferous sandstone sheets; this is followed by a thick, dark green mudstone interrupted with fine sandstone at the top. Finally, a thick bedded, very fine, yellow colored sandstone is capping this shale.

All fossil sirenians from Wadi Al Hitan were collected from fine sandstone and silty facies; most of these fossils are either skeletons or partial skeletons found in articulation and/or association (Figure. 2.9). Preservation and articulation patterns in Wadi Al Hitan were mostly governed by physical factors rather than biological (bioturbation, scavenging or predatory behavior). The Birket Qarun and most of Qasr El Sagha formations were deposited in a quiet and restricted environment, close to the shoreface, and at the same time near a huge source of siliciclastic sediments. Repetition of thick fine sandstone, shale, and clays, and their lateral variations and shifting from one facies to another in a shallowing upward sequence, as in the Wadi Al Hitan, is diagnostic of a lagoonal or estuarine environment. These lagoons and estuaries were greatly controlled by the tectonically active NE Africa and eustacy. Lutetian and Bartonian carbonate rocks of the Wadi Al Rayan Series were mostly nummulitic with slightly siliciclastic and glauconitic

components, and were deposited in a deeper environment than those of the Birket Qarun and Qasr El Sagha formations.

FIGURE 2.1. Correlation of stratigraphic units of Cairo and Fayum areas (modified after: Schweinfurth, 1883; Said, 1990; Strougo and Haggag, 1984; Strougo 1985a,b; Strougo, 1992; Gingerich, 1992). The stratigraphic section of Gebel Mokattam near Cairo (on the left) may reach 220 meters, which is one third of the total stratigraphic thickness of the Eocene rocks in Fayum Basin (see Chapter 2). All known Eocene marine mammal from Jebel Mokattam (green diamonds) came from the Mokattam Formation Building Stone Member of the Mokattam Formation which is equivalent to Muweilih Formation. Most of the Fayum marine mammals were found and excavated from the Bartonian and Priabonian sediments of the Gehannam, Birket Qarun, and Qasr El Sagha formations. L. A. and F. A. refer to the last appearance and the first appearance of index fossil.

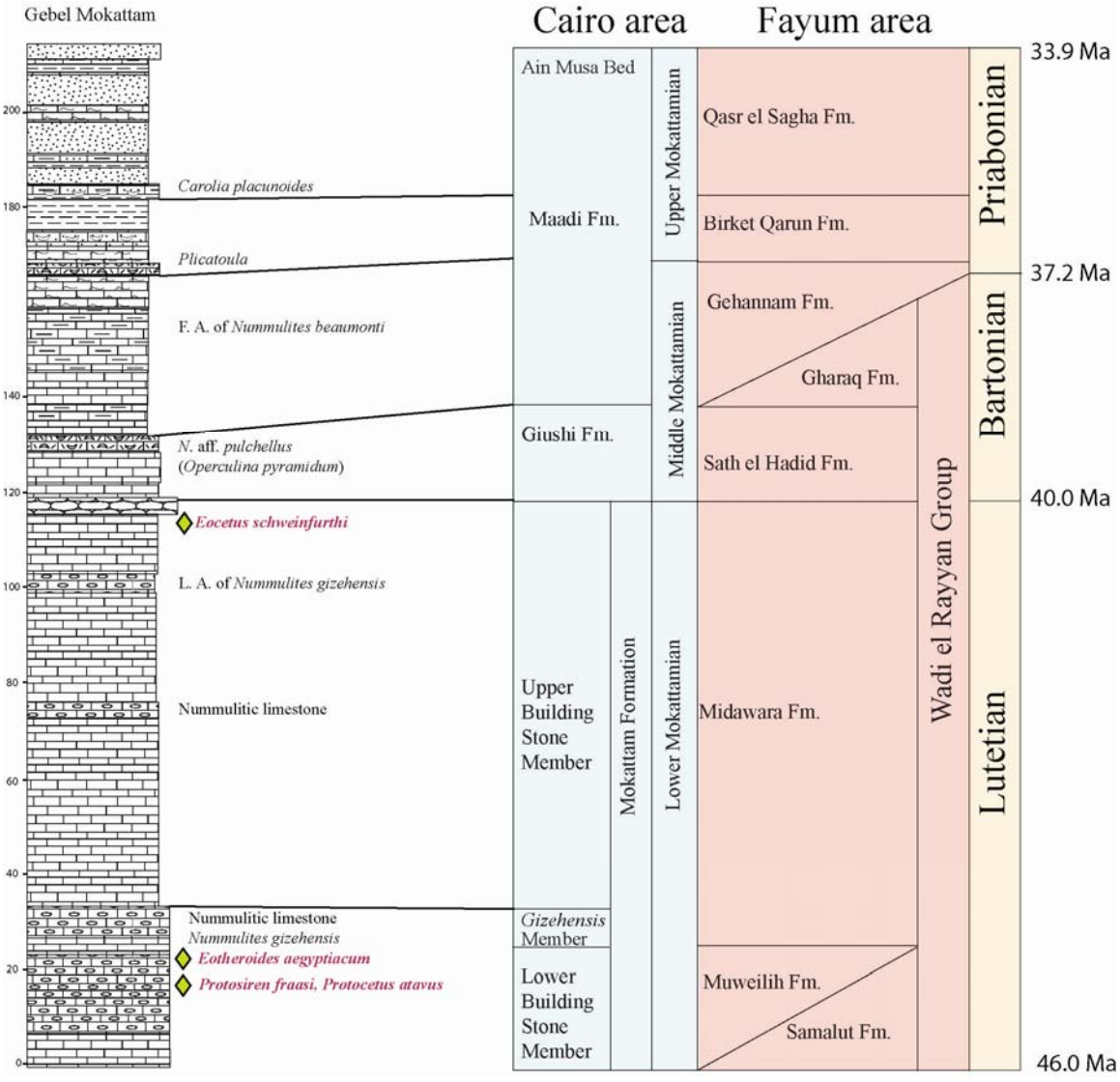

FIGURE 2.2. Legend for the stratigraphic sections illustrated in this study.

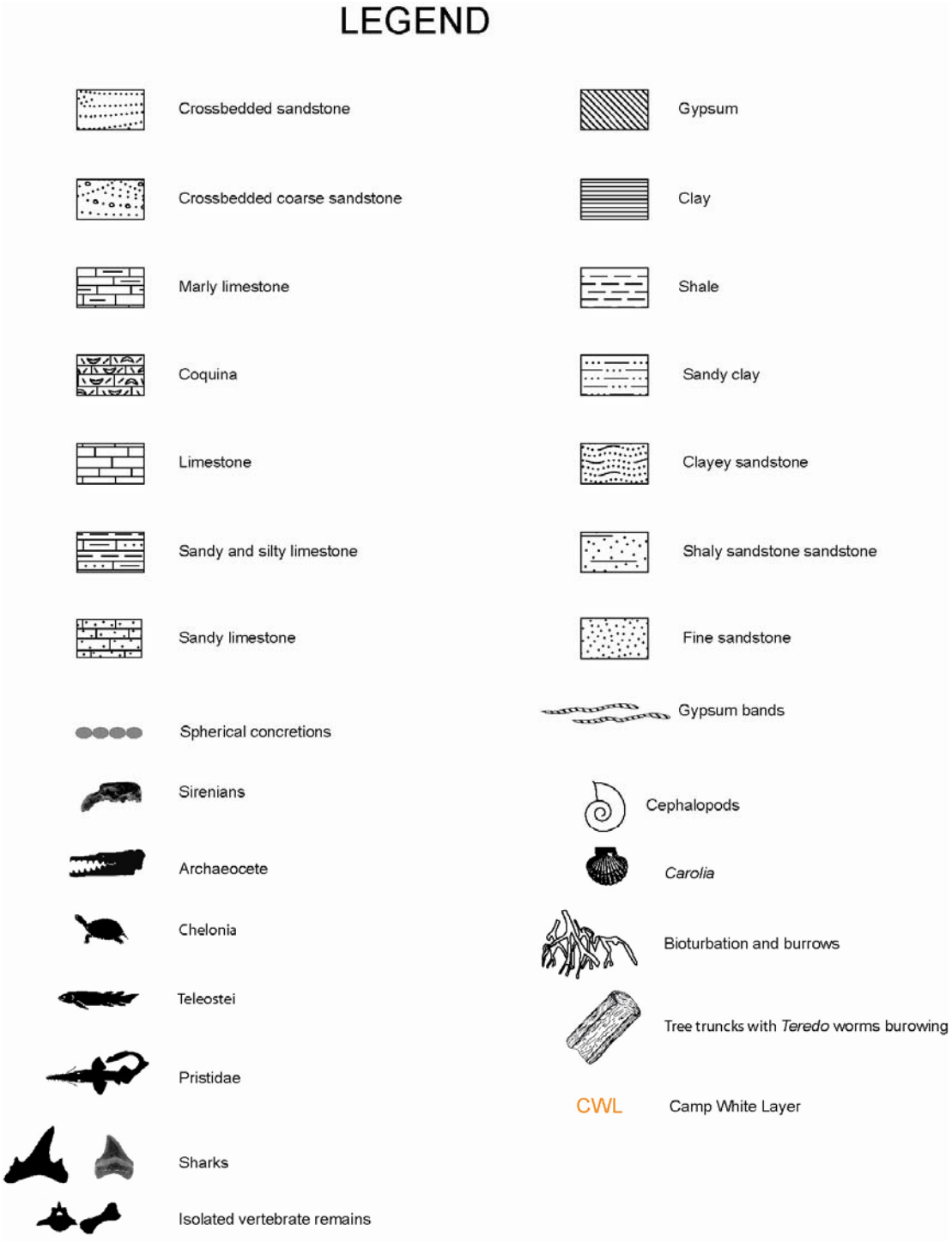

FIGURE 2.3. Stratigraphic section of Lutetian-Bartonian of the Wadi El Rayan Series in near Wadi El Ryan including: Muweilih, Midawara, Sath El Hadid, and El Gharaq formations, and fossil stratigraphic locations. Section was modified after Beadnell (1905) and Iskander (1943).

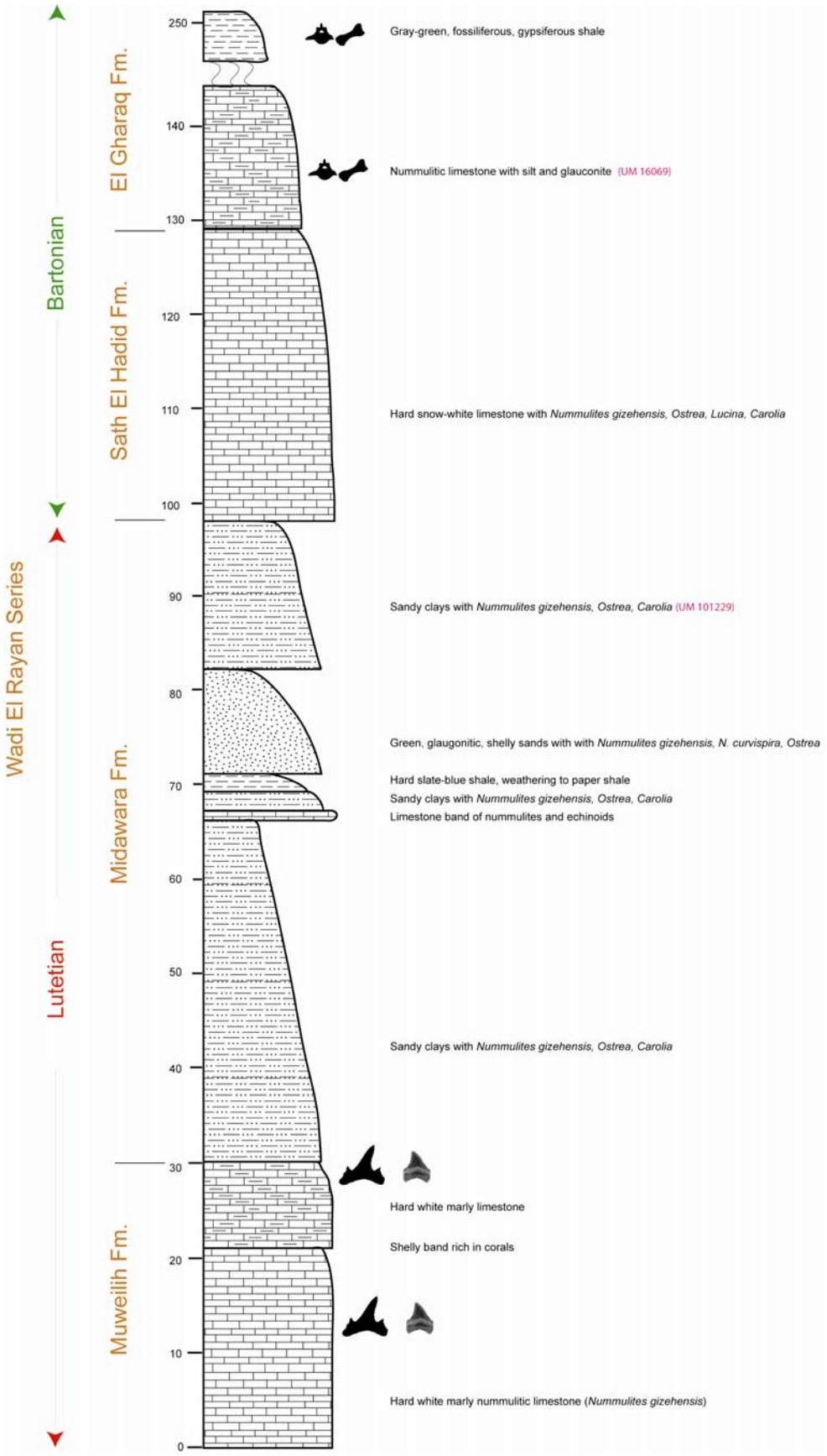
Wadi El Rayan Series
Bartonian
Lutetian
El Gharaq Fm.
Sath El Hadid Fm.
Midawara Fm.
Muweilih Fm.
250
140
130
120
110
100
90
80
70
60
50
40
30
20
10
0
Gray-green, fossiliferous, gypsiferous shale
Nummulitic limestone with silt and glauconite (UM 16069)
Hard snow-white limestone with Nummulites gizehensis, Ostrea, Lucina, Carolia
Sandy clays with Nummulites gizehensis, Ostrea, Carolia (UM 101229)
Green, glaugonitic, shelly sands with with Nummulites gizehensis, N. curvispira, Ostrea
Hard slate-blue shale, weathering to paper shale
Sandy clays with Nummulites gizehensis, Ostrea, Carolia
Limestone band of nummulites and echinoids
Sandy clays with Nummulites gizehensis, Ostrea, Carolia
Hard white marly limestone
Shelly band rich in corals
Hard white marly nummulitic limestone (Nummulites gizehensis)

FIGURE 2.4. Stratigraphic section of Minqar El-Hut and near Three Sisters in Wadi Al Hitan showing the Priabonian Gehannam, Birket Qarun, and Qasr El Sagha formations, followed by the terrestrial Oligocene beds of the Gebel Qatrani Formation. Fossil sirenians here were collected almost from every level of the formations. Location Of the section is marked in Figure (1-6). All fossil sirenians appearing on the section are listed in Table 1-2. Section was measured during this study.

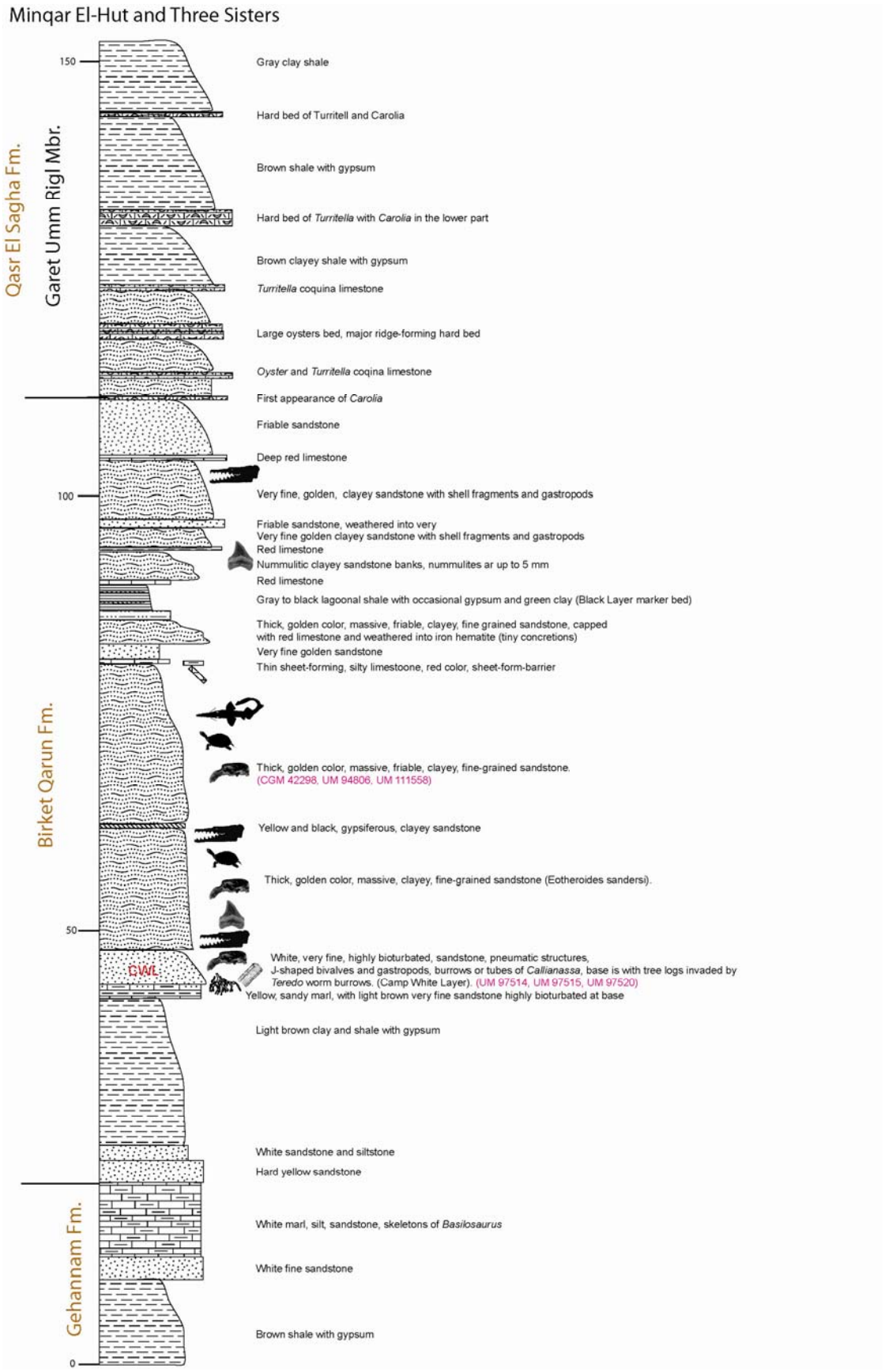
Minqar El-Hut and Three Sisters
Qasr El Sagha Fm.
Garet Umm Rigl Mbr.
Birket Qarun Fm.
Gehannam Fm.
150
100
50
0
CWL
Gray clay shale
Hard bed of Turritell and Carolia
Brown shale with gypsum
Hard bed of Turritella with Carolia in the lower part
Brown clayey shale with gypsum
Turritella coquina limestone
Large oysters bed, major ridge-forming hard bed
Oyster and Turritella coqina limestone
First appearance of Carolia
Friable sandstone
Deep red limestone
Very fine, golden, clayey sandstone with shell fragments and gastropods
Friable sandstone, weathered into very
Very fine golden clayey sandstone with shell fragments and gastropods
Red limestone
Nummulitic clayey sandstone banks, nummulites ar up to 5 mm
Red limestone
Gray to black lagoonal shale with occasional gypsum and green clay (Black Layer marker bed)
Thick, golden color, massive, friable, clayey, fine grained sandstone, capped
with red limestone and weathered into iron hematite (tiny concretions)
Very fine golden sandstone
Thin sheet-forming, silty limestoone, red color, sheet-form-barrier
Thick, golden color, massive, friable, clayey, fine-grained sandstone.
(CGM 42298, UM 94806, UM 111558)
Yellow and black, gypsiferous, clayey sandstone
Thick, golden color, massive, clayey, fine-grained sandstone (Eotheroides sandersi).
White, very fine, highly bioturbated, sandstone, pneumatic structures,
J-shaped bivalves and gastropods, burrows or tubes of Callianassa, base is with tree logs invaded by
Teredo worm burrows. (Camp White Layer). (UM 97514, UM 97515, UM 97520)
Yellow, sandy marl, with light brown very fine sandstone highly bioturbated at base
Light brown clay and shale with gypsum
White sandstone and siltstone
Hard yellow sandstone
White marl, silt, sandstone, skeletons of Basilosaurus
White fine sandstone
Brown shale with gypsum

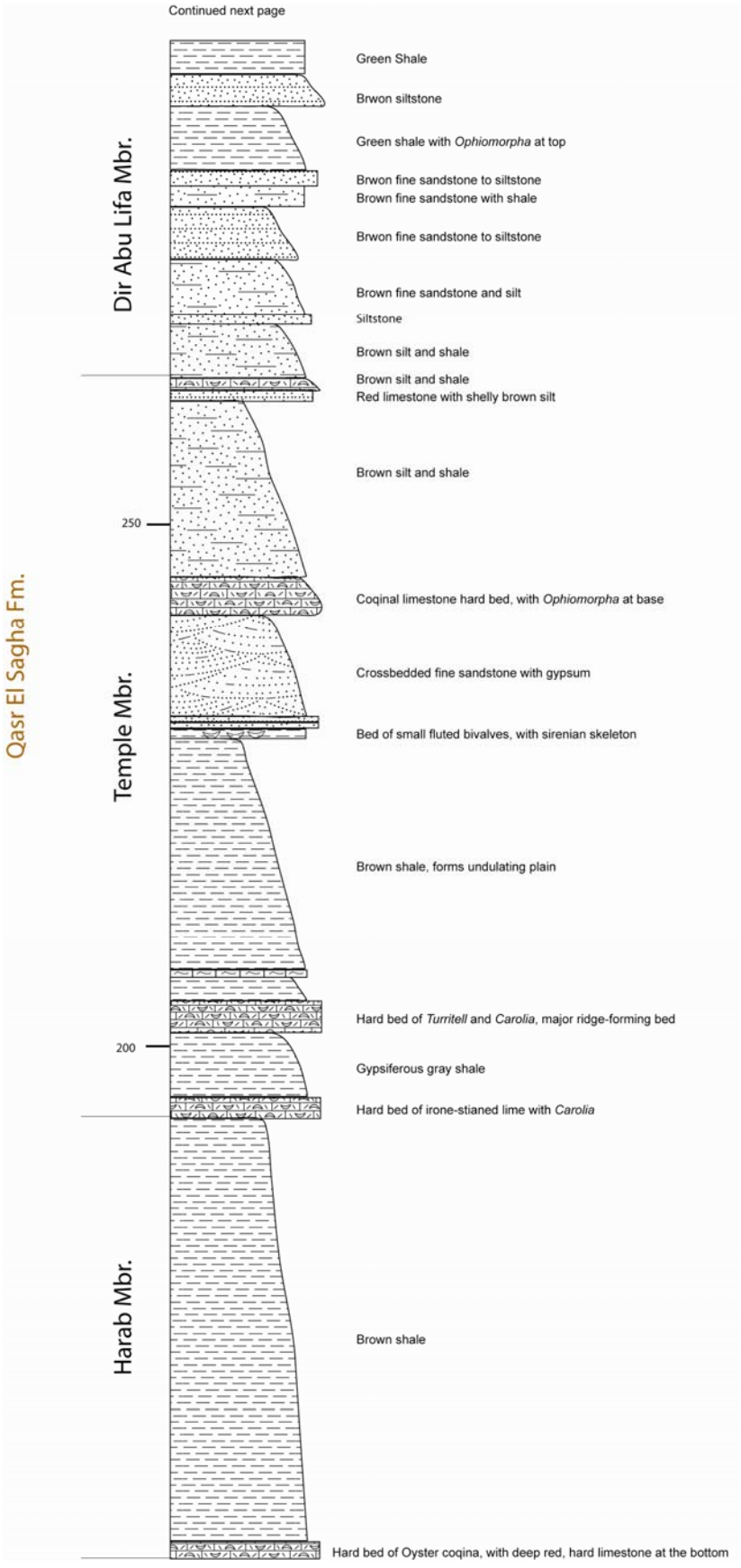
Continued next page
Qasr El Sagha Fm.
Dir Abu Lifa Mbr.
Temple Mbr.
Harab Mbr.
250
200
Green Shale
Brwon siltstone
Green shale with Ophiomorpha at top
Brwon fine sandstone to siltstone
Brown fine sandstone with shale
Brwon fine sandstone to siltstone
Brown fine sandstone and silt
Siltstone
Brown silt and shale
Brown silt and shale
Red limestone with shelly brown silt
Brown silt and shale
Coqinal limestone hard bed, with Ophiomorpha at base
Crossbedded fine sandstone with gypsum
Bed of small fluted bivalves, with sirenian skeleton
Brown shale, forms undulating plain
Hard bed of Turritell and Carolia, major ridge-forming bed
Gypsiferous gray shale
Hard bed of irone-stianed lime with Carolia
Brown shale
Hard bed of Oyster coqina, with deep red, hard limestone at the bottom

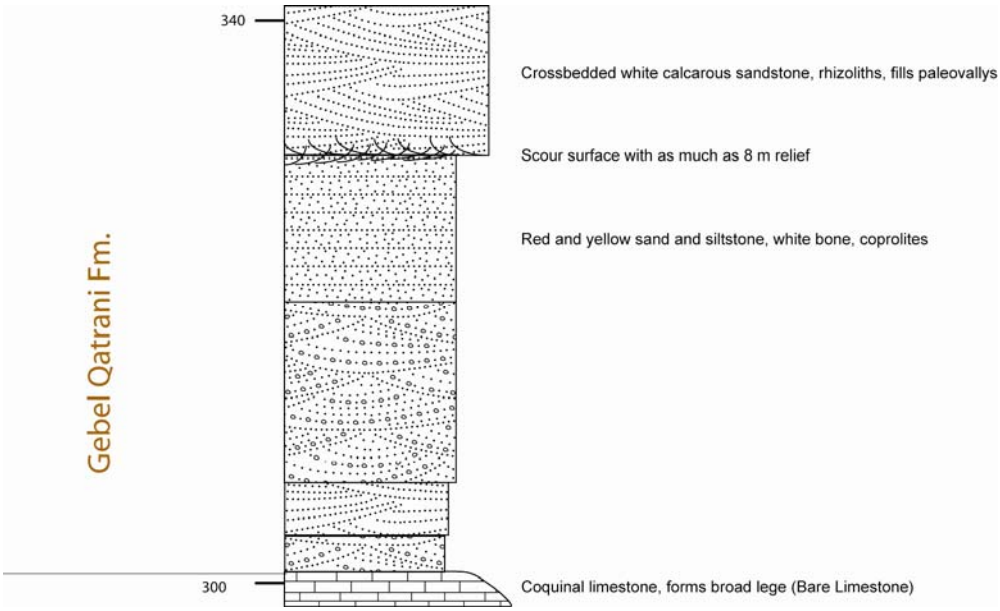
340
300
Gebel Qatrani Fm.
Crossbedded white calcarous sandstone, rhizoliths, fills paleovallys
Scour surface with as much as 8 m relief
Red and yellow sand and siltstone, white bone, coprolites
Coquinal limestone, forms broad lege (Bare Limestone)

FIGURE 2.5. Stratigraphic section of Wadi Al Hitan ZV-230 showing the Priabonian Gehannam and Birket Qarun formations. Location of the section is marked in Figure (1-6). All fossil sirenians appearing on the section are listed in Table 1-2. Section was measured during this study.

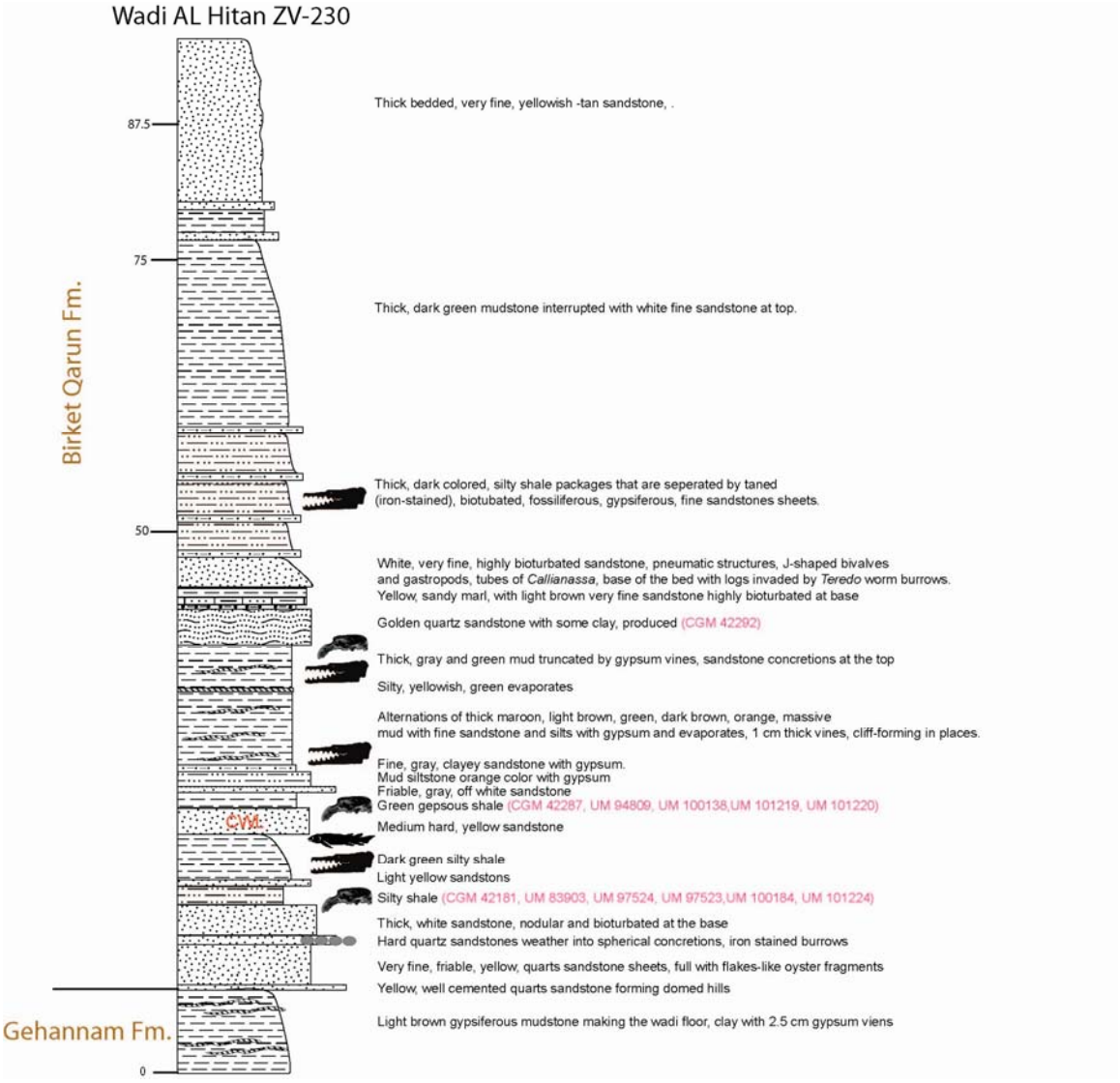

FIGURE 2.6. Stratigraphic section of the Qasr El Sagha Formation near Garet El Esh localities (modified after Gingerich 1992). Fossil sirenians were collected from the base of the Temple Member of the Qasr El Sagha Formation, a few meters above the Harab Member, that is equivalent to zone II-4 of Blanckenhorn (1903).

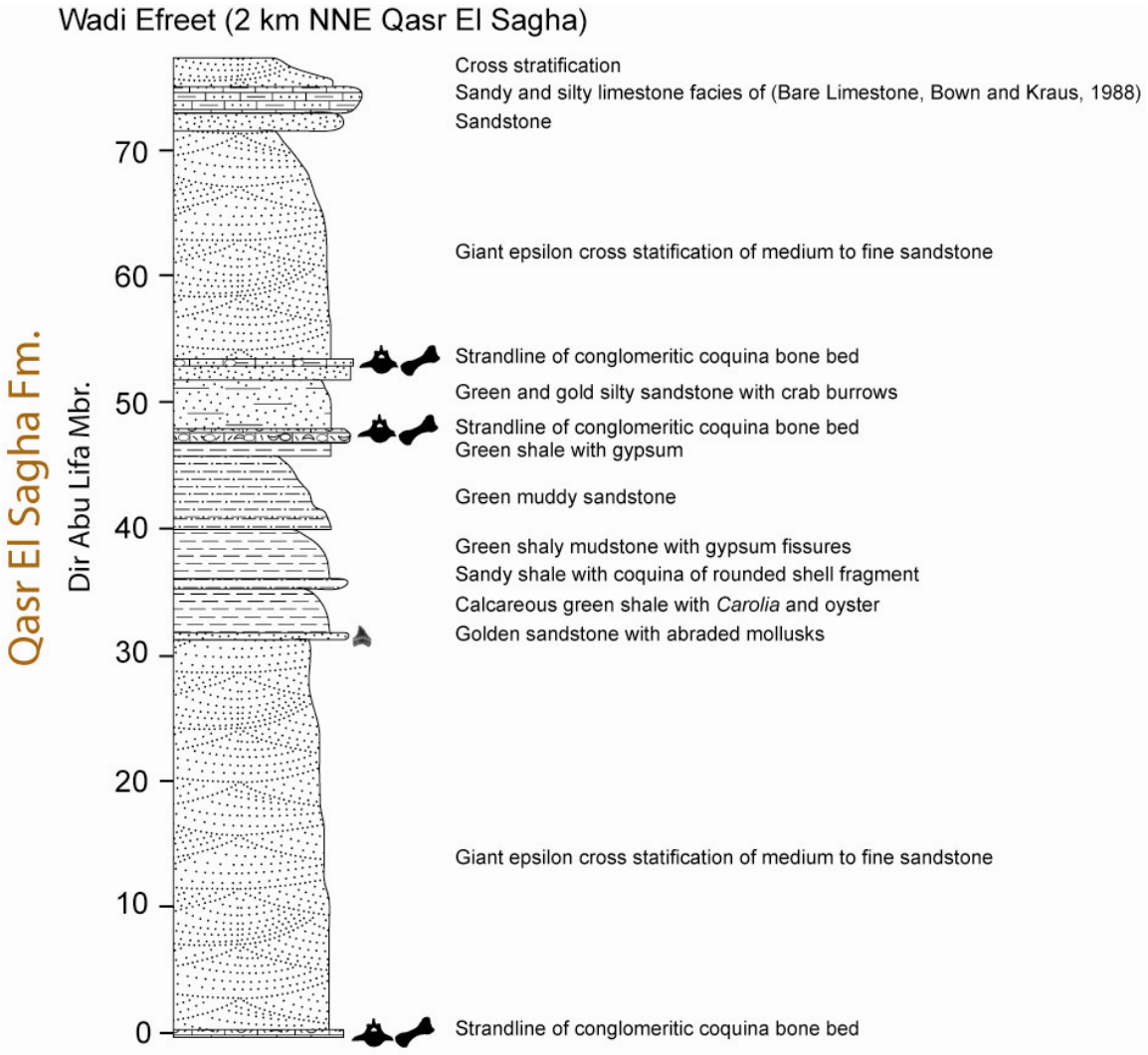

FIGURE 2.7. Bown and Kraus (1988) stratigraphic section of the uppermost Qasr El Sagha Formation along Wadi Efreet (Valley of the Ghost, 2 km NNE of Qasr El Sagha temple), showing deltaic giant cross stratifications of Dir Abu Lifa Member. Vertebrate fossils were collected from the base of the lag beds and are disarticulated.

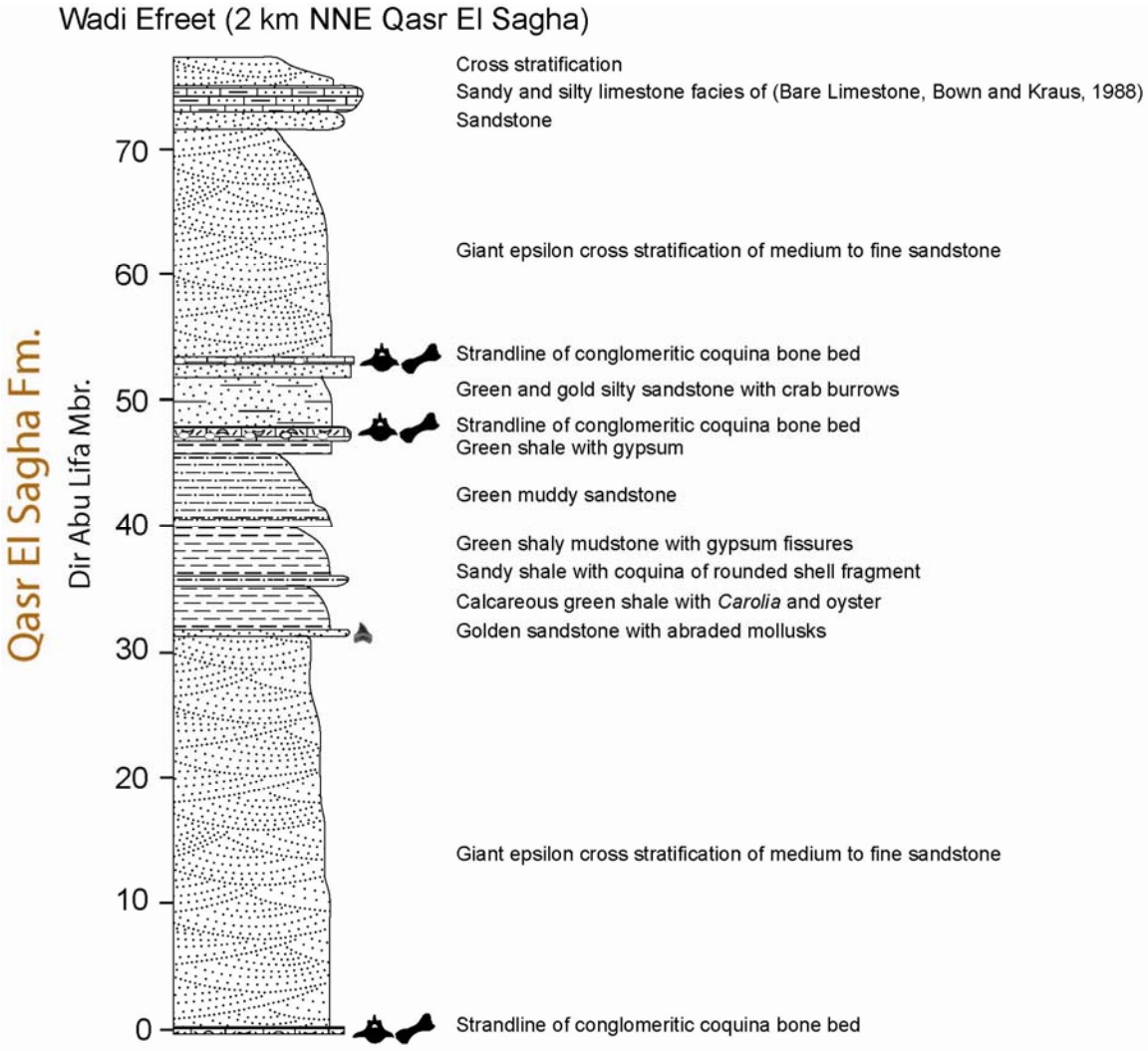

FIGURE 2.8. Stratigraphic section of the Qasr El Sagha Formation near Dir Abu Lifa fossil localities (Gingerich, 1992). Fossil sirenians were collected from the hematite-stained limestone 20 meters below the cross-bedded sandstone.

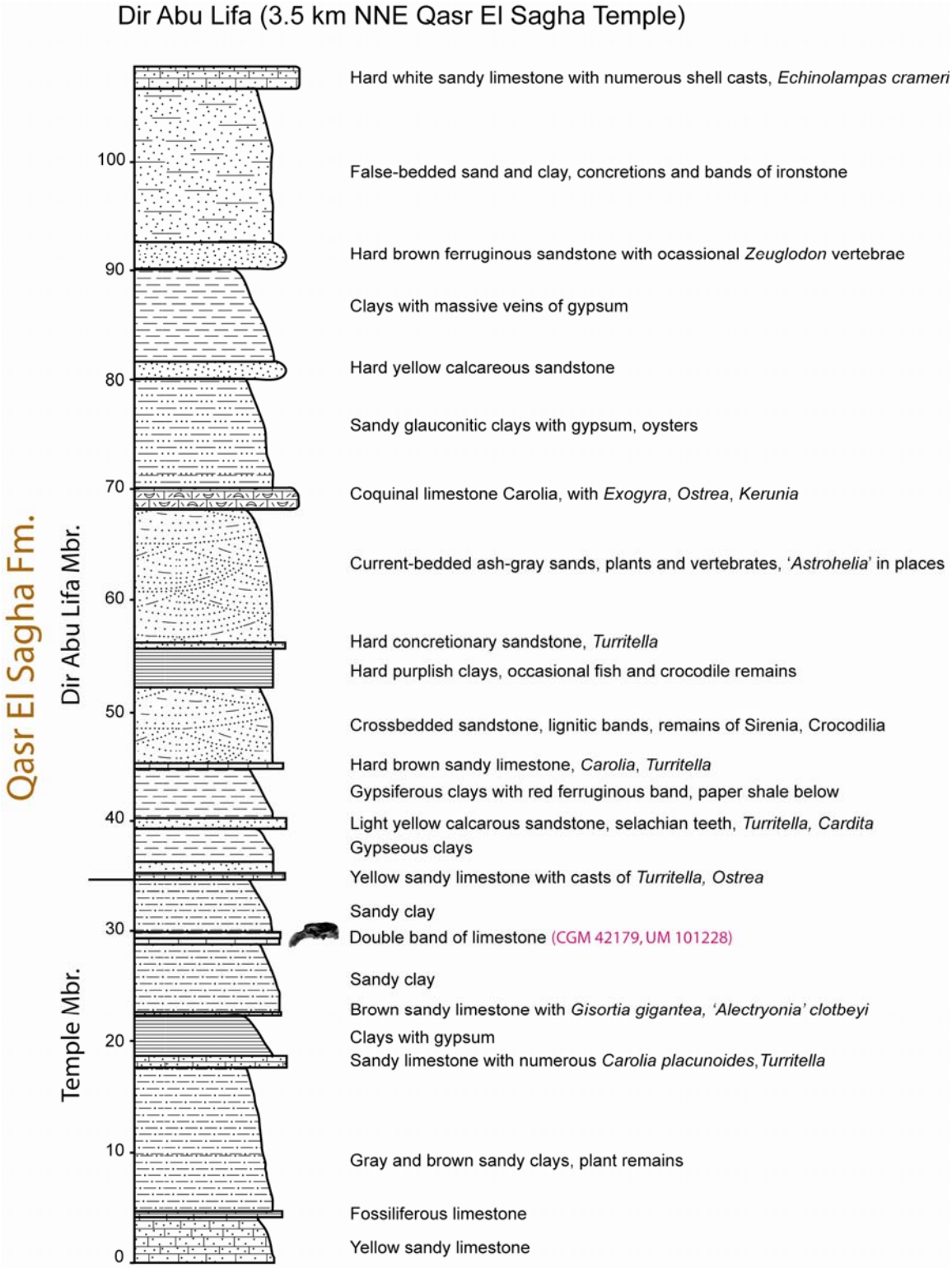

FIGURE 2.9. *Eotheroides sandersi* (UM 97514) during excavation processes at locality ZV-110, the matrix is friable sandstone at the top of the Camp White Layer (where William J. Sanders is wrapping a sirenian skeleton), these sandstones were deposited in a shoreface environment with limited wave action. Photo by Philip D. Gingerich.

Literature Cited

ABDOU, H. F., and M. R. ABDEL-KIREEM. 1975. Planktonic foraminiferal zonation of the middle and upper Eocene rocks of Fayoum Province, Egypt. Revista Espanola de Micropaleontologia, 7:15-64.

BEADNELL, H. J. L. 1901. The Fayum depression: a preliminary notice of the geology of a district in Egypt containing a new Palaeogene vertebrate fauna. Geological Magazine, Decade IV, 8:540-546.

BEADNELL, H. J. L. 1905. The Topography and Geology of the Fayum Province of Egypt. Survey Department Egypt, Cairo, 101 pp.

BLANCKENHORN, M. 1900. Neues zur Geologie und Paläontologie Aegyptens. II. Das Palaeogen. Zeitschrift der Deutschen Geologischen Gesellshaft, Stuttgart, 52: 403-479.

BLANCKENHORN, M. 1903. Neue geologisch-stratigraphische Beobachtungen in Aegypten. Sitzungsberichte der Mathematisch-physikalischen Classe der Königlichen bayerischen Akademie der Wissenschaften, München, 32: 353-433.

BOUKHARY, M., A. I. M. HUSSEIN, and D. KAMAL. 2003. *Nummulites issawii* n. sp., a new species of the N-laevigatus group from the Bartonian (Middle Eocene) of the southern Fayum area, Egypt. Neues Jahrbuch Fur Geologie Und Paläontologie-Monatshefte, 6:351-362.

BOWEN, B. W., and C. F. VONDRA. 1974. Paleoenvironmental interpretations of the Oligocene Gabal el Qatrani Formation, Fayum Depression, Egypt (Essays on African Paleontology). Annals of the Geological Survey of Egypt, 4:115-138.

BOWN, T. M., and M. J. KRAUS. 1988. Geology and paleoenvironment of the Oligocene Jebel Qatrani Formation and adjacent rocks, Fayum Depression, Egypt, United States Geological Survey Professional Paper, 1452:1-60.

BOWN, T. M., M. J. KRAUS, S. L. WING, B. H. TIFFNEY, J. G. FLEAGLE, E. L. SIMONS, and C. F. VONDRA. 1982. The Fayum primate forest revisited. Journal of Human Evolution, 11:603-632.

DOMNING, P. D., P. D. GINGERICH, E. L. SIMONS, and A. F. ANKEL-SIMONS. 1994. A new early Oligocene Dugongid (Mammalia, Sirenia) from Fayum

Province, Egypt Contributions from the Museum of Paleontology, University of Michigan, 29:89-108.

EL-KHASHAB, B. 1974. Review of the early Tertiary eutherian faunas of African mammals in Fayum Province, Egypt. Annals of the Geological Survey of Egypt, 4:95-114.

FLEAGLE, J. G., T. M. BOWN, J. D. OBRADOVICH, and E. L. SIMONS. 1986a. How old are the Fayum primates?; pp. 3-17 in J. G. ELSE and P. C. LEE (eds.), Primate Evolution. Cambridge University Press, Cambridge.

FLEAGLE, J. G., T. M. BOWN, J. D. OBRADOVICH, and E. L. SIMONS. 1986b. Age of the earliest African anthropoids. Science, 234:1247-1249.

GINGERICH, P. D. 1992. Marine mammals (Cetacea and Sirenia) from the Eocene of Gebel Mokattam and Fayum, Egypt: stratigraphy, age, and paleoenvironments. University of Michigan Papers on Paleontology, 30:1-84.

GUIRAUD, R., and W. BOSWORTH. 1999. Phanerozoic geodynamic evolution of northeastern Africa and the northwestern Arabian platform. Tectonophysics, 315:73-108.

GUIRAUD, R., B. ISSAWI, and W. BOSWORTH. 2001. Phanerozoic history of Egypt and surrounding areas; Peri-Tethys memoir 6; Peri-Tethyan rift/wrench basins and passive margins. Memoires du Museum National d'Histoire Naturelle, 186:469-509.

GUIRAUD, R., W. BOSWORTH, J. THIERRY, and A. DELPLANQUE. 2005. Phanerozoic geological evolution of Northern and Central Africa: An overview. Journal of African Earth Sciences, 43:83-143.

HAGGAG, M. A. Y. 1985. Middle Eocene planktonic foraminifera from Fayum area, Egypt. Revista Espanola de Micropaleontologia, 17:27-40.

HAGGAG, M. A. Y. 1990. *Globigerina pseudoamphiapertura* Zone, a new late Eocene planktonic foraminiferal zone (Fayoum area, Egypt). Neues Jahrbuch für Geologie und Palaeontologie. Monatshefte, 5:295-307.

HEIKAL, M. A., M. A. HASSAN, and Y. EL SHESHTAWI. 1983. The Cenozoic basalt of Gebel Qatrani, Western Desert, Egypt; as an example of continental tholeiitic basalt. Annals of the Geological Survey of Egypt, 13:193-209.

ISKANDER, F. 1943. Geological survey of the Gharag el Sultani sheet no. 68/54. Standard Oil Company, Egypt S. A., Reports, 51:1-29.

ISMAIL, M. M., and ABDEL-KIREEM. 1971. Microfacies of the Fayoum surface sections. part 1: middle Eocene. Bulletin of the faculty of Science (Alxidanderia University), 11:65-84.

ISMAIL, M. M., and ABDEL-KIREEM. 1971. Microfacies of the Fayoum surface sections. part 2: upper Eocene. Bulletin of the faculty of Science (Alxidanderia University), 11:85-105.

KORTLAND, A. 1980. The Fayum Forest: Did it exist? Journal of Human Evolution, 9:277-297.

KOSTANDI, B. 1963. Eocene facies maps and tectonic interpretation in the Western Desert, U.A.R. Revue de l'Institut français du pétrole, 18:1331-1343.

KRENKEL, E. 1924. Der Syrische Bogen. Zentralblatt fuer Mineralogie, Geologie und Palaeontologie, 9:274-281.

SAID, R. 1962. The geology of Egypt. Elsevier, 377 pp.

SAID, R. 1990. Cenozoic; pp. 451-486 in R. SAID (ed.), The Geology of Egypt. A. A. Balkema, Netherlands (NLD).

SALEM, R. M. 1976. Evolution of Eocene-Miocene sedimentation patterns in parts of northern Egypt. American Association of Petroleum Geologists Bulletin, 60:34-64.

SCHAUB, H. 1981. Nummulites et Assilines de la Tethys paléogene. Taxonomy, phylogenèse et biostratigraphie. Text and atlas. Schweizerische Paläontologisches Abhandlungen, 104-106:1-236.

SIMONS, E. L. 1968. Early Cenozoic mammalian faunas, Fayum Province, Egypt; Part I. African Oligocene Mammals: Introduction, history of study and faunal succession. Bulletin, Peabody Museum, 28:1-21.

SIMONS, E. L., and D. T. RASMUSSEN. 1990. Vertebrate paleontology of Fayum; history of research, faunal review and future prospects; pp. 627-638 in R. SAID (ed.), The Geology of Egypt. A. A. Balkema, Rotterdam.

SIMONS, E. L., and P. D. GINGERICH. 1974. New carnivorous mammals from the Oligocene of Egypt. Annals of the Geological Survey of Egypt, Essays on African Paleontology, 4:157-166.

STROUGO, A. 1985a. Eocene stratigraphy of the eastern greater Cairo (Gebel Mokattam - Helwan) area. Middle East Research Center, Ain Shams University, Scientific Research Series, 5:1-39.

STROUGO, A. 1985b. Eocene stratigraphy of the Giza Pyramids plateau. Middle East Research Center, Ain Shams University, Scientific Research Series, 5:79-99.

STROUGO, A. 1986. Mokattam stratigraphy of eastern Maghagha- El Fashn district. Middle East Research Center, Ain Shams University, Scientific Research Series, 6: 33-58.

STROUGO, A. 1988. Mokattamian Bivalvia of greater Cairo: an annotated list. Earth Science Series, Middle East Research Center, Ain Shams University, Cairo, 2:29-48.

STROUGO, A. 1992. The Middle Eocene/Upper Eocene transition in Egypt reconsidered. Neues Jahrbuch für Geologie und Palaeontologie. Abhandlungen, 186:71-89.

STROUGO, A., and M. A. Y. HAGGAG. 1984. Contribution to the age determination of the Gehannam Formation in the Fayum Province, Egypt Neues Jahrbuch für Geologie und Palaeontologie. Monatshefte, 1984:46-52.

VONDRA, C. F. 1974. Upper Eocene transitional and near-shore marine Qasr El Sagha Formation, Fayum Depression, Egypt (Essays on African Paleontology). Annals of the Geological Survey of Egypt, 4:79-94.

CHAPTER THREE

REVIEW OF THE CENOZOIC SIRENIA OF AFRICA

The first sirenian fossils reported from Africa, like most found subsequently, were from Egypt. These included indeterminate fragments from the Nile Valley (de Blainville, 1840, 1844) and from the Isthmus of Suez (O. Fraas, 1867, reported in Gervais, 1872). Discovery of *Eotheroides aegyptiacum* (Owen, 1875) in the middle Eocene nummulitic beds of the Mokattam Hills near Cairo was a precursor for subsequent finds at Gebel Mokattam (Abel, 1907; Sickenberg, 1934; Gingerich et al., 1994) and in late Eocene strata of Fayum (Andrews, 1906; Abel, 1907; Sickenberg, 1934; Domning and Gingerich, 1994; Domning et al., 1994; see Chapter 4).

Other African records of Sirenia, mostly indeterminate, have emerged, chronologically, from the Miocene of Madagascar (Collignon and Cottreau, 1927) and the Congo (Dartevelle, 1935); the Pliocene of Morocco (Ennouchi, 1954); the Eocene, Oligocene, and Miocene of Libya (Savage and White, 1965; Savage, 1967, 1969, 1971); the Eocene and Oligocene of Somalia (Savage, 1969); the Oligocene and Miocene of Tunisia (Robinson and Black, 1969; Savage, 1969?); the Eocene of Togo (Gingerich et al., 1992), and the Eocene of Madagascar (Samonds et al., 2005) (see Table 1, Figure. 2). Good specimens of *Metaxytherium serresii* from Sahabi, Libya, formerly considered early Pliocene, are now assigned to the late Miocene (Domning and Thomas, 1987; Boaz et al., 2004; Carone and Domning, 2007).

Egyptian sirenians, including new late Eocene and early Oligocene specimens, have been described in recent years, but important new Eocene and Miocene taxa from Libya (Heal, 1973) await formal publication. The sirenian history of the rest of the continent has barely begun to be investigated.

Domning (1978) summarized fossil and living sirenians of Africa, however, since then many new sirenian records have been added to the literature. Table 3.1 and Figure 3.1 represent a summary of all known Cenozoic fossil and living sirenians of Africa. This overview of African Sirenia provides a context for new specimens from Wadi Al Hitan being described here in Chapter 4.

*This chapter is a summary of a longer text by **D. P. Domning, I. S. Zalmout, and P. D. Gingerich** submitted to Cenozoic Mammals of Africa edited by Lars Werdelin and William J. Sanders.*

Institutional Abbreviations—**BMNH (=NHML)**, British Museum of Natural History (=Natural History Museum), London (England); **CGM**, Cairo Geological Museum, Cairo (Egypt); **SMNS**, Staatliches Museum für Naturkunde, Stuttgart (Germany); **UM**, Museum of Paleontology, University of Michigan, Ann Arbor (USA).

Systematic Paleontology

(For complete synonymies and bibliography, see Domning, 1994, 1996)

Order Sirenia Illiger, 1811

Family Protosirenidae Sickenberg, 1934 (Figs. 3.1, B; 3.4A, B)

Based on one genus and four species, this Tethyan Eocene group is known with assurance only from Africa and Asia (Abel, 1907; Domning and Gingerich, 1994; Gingerich et al., 1995; Zalmout et al., 2003; Bajpai et al., 2006). Reports of protosirenids from North America by Domning et al. (1982) require further study to determine the position of these taxa.

Members of this group are the largest of all known Eocene sirenians. The skull roof is robust and stout, and very broad across the supraorbital processes; the nasal bones are reduced and separated in some species; the alisphenoid canal is well defined; the rostrum is slightly deflected; the palatal region of the rostrum is wide; and the cheek teeth are large. Postcranial elements are pachyostotic, thoracic vertebrae have a keyhole-shaped vertebral canal, and the heads of the ribs display a cartilaginous rather than fully ossified articular surface. As shown by the well-preserved sacrum, pelvis, femur, patella, tibia, and fibula of *P. smithae*, *Protosiren* had well-developed hindlimbs and may have maintained mobility, but could not fully support its body weight on land.

Genus *PROTOSIREN* Abel, 1907

PROTOSIREN FRAASI Abel, 1907 (Figs. 3.2A, 3.4A)

Age and Occurrence—Lutetian of the Mokattam Hills near Cairo (Table 1, Figure 2).

Diagnosis—Tusk alveoli small. Nasals contact each other in midline. Orbital opening small and dorsoventrally compressed. Pelvis has a large obturator foramen and a deep acetabulum.

Description—Rostrum is slightly deflected, premaxillary-maxillary suture is shifted posteriorly, alisphenoid canal is present. Squamosal does not contribute to the back of the skull, squamosal and supraoccipital are completely separated by a parietal process, and posttympanic process of squamosal is absent. Dorsal surface of endocranium is smooth, with no bony falx cerebri, bony tentorium, or internal occipital protuberance. The pelvis has a rod-like ilium with a spindle-like end.

Remarks—*Protosiren fraasi* is known from skulls, a dentary, thoracic vertebrae, ribs, and innominates from the Lutetian of the Mokattam Hills near Cairo. The holotype skull and mandible (CGM 10171) were erroneously described as "*Eotherium aegyptiacum* (?)" by Andrews (1906: text-figs. 66-67). Innominates referred to "*Eotherium*" *aegyptiacum* (Abel, 1904: pl. 7, fig. 1) also pertain to *P. fraasi*.

PROTOSIREN SMITHAE Domning and Gingerich, 1994 (Figs. 3.2B, 3.4B)

Age and Occurrence—Early Priabonian of the Birket Qarun Formation, about 40 km west of Lake Qarun, 160 km SW of Cairo (Table 3.1, Figure 3.1).

Diagnosis—Upper incisor tusks enlarged. Rostral masticating surface trapezoidal. Rostral deflection increased. Pterygoid process long dorsoventrally. Nasals separated by frontals. Supraorbital processes massive. Exoccipitals widely separated in the dorsal midline. Sternebrae short and blocklike, resembling those of terrestrial mammals.

Description—The holotype (CGM 42292) is a mature adult represented by a skull and lower jaw with the upper and lower teeth, most of the vertebral column, some ribs, and front and hind limbs. The premaxillae are short, rostral deflection is about 60º, and the nasals are separated by the frontals in dorsal view (more clear in UM 101224,

Domning and Gingerich, 1994). The endocranial surface is smoothly concave with no bony falx cerebri; however, in UM 101224 the falx and tentorium are very faintly marked (Domning and Gingerich, 1994). An alisphenoid canal is present and well developed. Cervical vertebrae are short with flattened endplates, the neural spine is bifurcated on the posterior cervicals and the first thoracics, and the vertebral foramina are wide. Scapulae are sickle-shaped with a narrow supraspinous fossa. Innominates have a long ilium that is triangualar in cross-section and is flatten anterior third in some specimens, broad and flattened ischium, well-developed pubis and pubic symphysis, reduced obturator foramen, and shallow acetabulum. The femur is 140 mm long with distinct greater and lesser trochanters and no third trochanter; the femoral head is oval; and the shaft is flattened anteroposteriorly. The patellar surface and condyles are well developed.

Remarks—*Protosiren smithae* from the Priabonian of the Western Desert of Egypt is intermediate between amphibious and fully aquatic sirenians. Domning and Gingerich (1994) commented that the retention of functional hip and knee articulations and a well-developed tibia and fibula indicate that this taxon retained a mobile foot.

LIBYSIREN SICKENBERGI, n.gen. n.sp. Heal, 1973

Age and Occurrence—Middle Eocene (Lutetian) of Bu el Haderait, Libya (Table 3.1, Figure 3.1).

Diagnosis—The largest protosirenid to be described to date (total length of the skull is 45 cm, sagittal length of skull roof approximately 25 cm); nasals large; sagittal length of parietals much greater than that of frontals; length of m2 = 26 mm. Five lower premolars were likely present.

Description—The premaxillary symphysis forms one-third of the premaxillary length, the external nares are wide, the maxilla is almost straight, the lacrimal bone separates the premaxilla from the frontal, nasals and frontals are enlarged, frontals are heavy and thick and their supraorbital processes extend anterolaterally to reach the front of the nasals and lacrimals; parietal and frontal meet along a transversely wide and shallow suture, the zygomatic process of the squamosal is short and laterally compressed, the pterygoid process is short, an alisphenoid canal is present and its openings are narrow, and the tentative dental formula is 3.1.4.3/3.1.4(5?).3.

Postcranial elements are not well known; however, a recovered atlas and an anterior thoracic vertebra are larger than those of any other Eocene sirenians. The thoracic vertebra shows characteristics of typical protosirenid postcrania with its large vertebral canal and high neural spine.

Remarks—Described in an unpublished doctoral dissertation (Heal, 1973) and represented by good cranial material, this is the largest known Eocene sirenian. One specimen has an apparently supernumerary last lower molar (m4?) with a circular crown, reminiscent of the reduced M3 of *Miosiren kocki* (Sickenberg, 1934).

Family Dugongidae Gray, 1821

Subfamily Halitheriinae (Carus, 1868) Abel, 1913

The Dugongidae are the most diverse and successful group of sirenians. They made their first appearance in the middle and late Eocene of the Old World Tethys. Three major genera of Dugongidae dominate the Eocene record: *Eotheroides*, *Eosiren*, and *Prototherium*. These are fully aquatic with very reduced pelvic and femoral features,

including: reduced length of the ischium and ilium, a diminutive obturator foramen, and reduction or loss of the pubic symphysis, presaging the complete loss of function in hind limbs.

GENUS *EOTHEROIDES* Palmer, 1899

The first diagnosis of *Eotheroides* ("*Eotherium*"), by Richard Owen in 1875, was based on a cranial endocast from the Lutetian of the Mokattam Hills. The endocast (NHML 46722) contains enough information to visualize the braincase. Later more elements were recovered and assigned to this taxon. These include partial skulls and skeletons (Abel, 1913). So far the genus is known from the Lutetian of the Mokattam Hills near Cairo (Owen, 1875; Abel, 1913) and the Priabonian Birket Qarun Formation of the Fayum (Zalmout and Gingerich, 2005).

EOTHEROIDES AEGYPTIACUM (Owen, 1875) Trouessart, 1905

Age and Occurrence—Lutetian of the Mokattam Formation near Cairo (Table 3.1, Figure 3.1).

Diagnosis—Falx, bony tentorium, and internal occipital protuberance present. Nasals are long and in contact along the midline; however, their posterior extremities are separated slightly by the frontals (though not as much as in *Protosiren* or *Eosiren*). The lacrimal foramen opens laterally (Abel, 1913: plate 2). The palate is broad and its posterior border, which is formed by the palatines, lies abaft the rear of the toothrow. Anterior ribs are dense, thickened and swollen (pachyosteosclerotic, see: Domning and de Buffrénil, 1991), having a banana-like shape (see Abel, 1919: 836, fig. 663).

Description—The rostrum is deflected, the premaxillary-maxillary suture lies below the premaxillary symphysis, an alisphenoid canal is absent, the posttympanic process of the squamosal is present, the dental formula is 2-3.1.5.3/3.1.4-5.3, the fifth permanent premolar is lost, and the tri-rooted DP5 is retained and not replaced.

Remarks—*Eotheroides aegyptiacum* is distinctive among Eocene sirenians in having extensive pachyosteosclerotic banana-like ribs. New records from Priabonian beds in the Fayum, including articulated and more complete skeletons of new *Eotheroides* material, will reveal more information about the evolutionary history of this group.

EOTHEROIDES CLAVIGERUM sp. nov. (Figures. 3.2C and 3.4D)

Age and Occurrence—Early Priabonian of the Birket Qarun Formation (Table 3.1, Figure 3.1).

Diagnosis—Infraorbital foramen enlarged. Nasals highly arched upward, rising higher than parietals. Lacrimal faces posteriorly and is less exposed laterally, and lacrimal foramen absent. Pelvis has a short club-like ilium, flat ischium, tiny obturator foramen, and extremely long and narrow short pubic bone.

Description— I^2 is absent, DP^5 and dp_5 are not replaced , and the dental formula is 2.1.5.3/3.1.5.3. Mandibles are straight and parallel to each other. Anterior and middle ribs are swollen, posterior ribs are slender.

Remarks— This species is based on excellent material including fairly complete postcranial skeletons. The most characteristic element that distinguishes this species from the associated sirenian taxa is the, literally, club-like ilium. Reduction in the

number of upper incisors and the overall reduction in the pelvic girdle represent derived conditions for *Eotheroides*.

EOTHEROIDES SANDERSI sp. nov. (Figure 3.4C)

Age and Occurrence—Early Priabonian of the Birket Qarun Formation. (Table 3.1, Figure 3.1).

Diagnosis—Infraorbital foramen enlarged. Nasals are low, rising at the parietal level. Pelvis has a short club-like ilium, robust and massive ischium, 6-7 mm wide obturator foramen, and extremely long and cylindrical pubic bone.

Description— I^2 is absent, DP^5 and dp_5 are not replaced, and the dental formula is 2.1.5.3/3.1.5.3.

Remarks— this species is very close to *Eotheroides clavigerum*, however this is smaller species in possessing a different pelvic form, and is the most abundant dugong in Wadi Al Hitan.

GENUS *EOSIREN* Andrews, 1902

Age and Occurrence—Middle Eocene to early Oligocene (Table 3.1, Figure 3.1), known from the Mokattam Hills near Cairo (Lutetian), Qasr El Sagha in the Fayum (Priabonian), and Jabal Qatrani, north of Birket Qarun in the Fayum area (Rupelian).

Diagnosis— Rostrum strong and enlarged, premaxillary symphysis extends more than one-third of the skull length, supracondylar fossa of the occipital is deep and extends across entire width of the occipital condyle, anterior border of coronoid process extends

slightly anterior to base of the process, cheek teeth are enlarged. Ribs are osteosclerotic and gracile. Scapulae are flat and broad. Innominates are very reduced; ilium is short and gracile, obturator foramen is either closed or diminutive, and acetabulum (Figures 3.4E, F) is shallow and oval. Femora are reduced as well, with rounded cross section at the middle of the shaft. Dental formula is usually 1-3.1.5.3/3.1.5.3.

EOSIREN ABELI Sickenberg, 1934

Age and Occurrence—Lutetian of the Mokattam Hills near Cairo (Table 3.1, Figure 3.1).

Diagnosis—M2 differs in shape and size from *Eotheroides aegyptiacum* and *Protosiren fraasi*, and is slightly smaller than M2 of *Eosiren libyca*. The skull in general is short, and so is the braincase (the median length of the brain endocast is 52 mm, which is 10 mm shorter than *Eotheroides aegyptiacum*). The end of the olfactory bulb is notably steeper, and overall the brain morphology shows a great affinity with the braincase of *Eosiren libyca* described (reconstructed) by Andrews (1906: text-fig. 65, page 202).

Description—The most informative specimen (now destroyed) was Abel's (1913:309) individual VI of "*Eotherium" aegyptiacum,* which consisted of a skull (premaxilla, maxilla, skull roof, occipitals and basicranium, ear apparatus including tympanics, ossicles, and lower jaw), and an atlas and some other vertebrae. A squamosal and some vertebrae representing this species are illustrated in Sickenberg (1934: pl. 4, Figs. 3, 11). Only cranial elements seem to be characteristic in this species; vertebrae and ribs are similar to Qasr El Sagha *Eosiren*.

Remarks— The holotype was a right M2 destroyed during World War II along with a referred skull and other cranial and postcranial elements collected from the Mokattam Hills near Cairo. *E. abeli* is the third sirenian taxon in the Mokattam Hills. Sickenberg (1934) mentioned that finding *Eosiren* in the Mokattam Hills is not remarkable since the precursor of the Fayum *Eosiren* should have been present in older strata.

EOSIREN LIBYCA Andrews, 1902 (Figures. 3.3A; 3.4E, F)

Age and Occurrence—Late Priabonian of Qasr El Sagha Formation, north of Lake Qarun, Fayum area, Egypt (Table 3.1, Figure. 3.1).

Diagnosis—Differs from *Eosiren stromeri* in having a narrow palate, M2 smaller than M3, larger and more prominent tusk alveoli, and smaller temporal fossa. Frontals are shorter or slightly longer than parietals. Innominates are vestigial like those in *Halitherium* and have their obturator foramen almost closed.

Description—Nasals are shortened and are still joined in the midline with a slight posterior separation by the frontal. The nasal process of the premaxilla overlaps less than one-third of the anteroposterior length of the supraorbital process. A distinct crista intratemporalis is present, the parietal roof is usually bilaterally convex, and the ventral process of the jugal is positioned slightly abaft the dorsal process. Dental formula is 3.1.5.3/3.1.5.3.

Remarks—This species is the best known and documented dugongid from the late Priabonian Qasr El Sagha Formation of the Fayum area.

EOSIREN STROMERI (Sickenberg, 1934) Kordos, 1977

Age and Occurrence— Late Priabonian of Qasr El-Sagha Formation, north of Lake Qarun, Fayum area, Egypt(Table 3.1, Figure 3.1).

Diagnosis—Frontals are much longer than parietals along midline. M^2 is larger than M^3. I^1 is reduced although the premaxillary symphysis is heavy and enlarged. Anteroposterior length of the zygomatic process of the squamosal seems to be greater than in *E. libyca*.

Description—Very similar in size and overall morphology to *E. libyca* except for minor features.

Remarks— Illustrations and reconstructions in Sickenberg (1934) and Kretzoi (1941), showing the premaxillae separated from frontals in dorsal view, are erroneous. All examined specimens, including the holotypes of both *E. libyca* and *E. stromeri*, show that the premaxillae and frontals are always in contact. Minor differences between *E. libyca* and *E. stromeri* could reflect merely individual variation, but we provisionally consider the two species to be valid.

EOSIREN IMENTI Domning et al., 1994 (Figure 3.3B)

Age and Occurrence—Rupelian of the Jabal Qatrani Formation, north of Lake Qarun, Fayum area, Egypt (Table 3.1, Figure 3.1).

Diagnosis—Differs from *Eosiren libyca* in having more elongate skull and more overlap of premaxilla and frontal, narrower palate, separated nasals, no distinct crista intratemporalis, sharp and upraised temporal crests separated by broadly concave parietal roof, more anteriorly located ventral process of jugal, and loss of I^{2-3}. Differs from *Halitherium taulannense* in having more overlap of premaxilla and frontal, separated

nasals, no distinct crista intratemporalis, more anteriorly located ventral process of jugal, and loss of I^{2-3}. Differs from *H. schinzii* in retaining canines and DP or P^1.

Description—*Eosiren imenti* is the most derived form of *Eosiren*. It has an elongate skull (400 mm in total length; see Domning el al., 1994 for complete skull measurements). The premaxillary symphysis is enlarged relative to the cranium, the masticating surface of the rostrum is trapezoidal, the nasal opening is expanded anteroposteriorly, the supraorbital process is well developed, and the cranial vault is square in cross section with smoothly concave roof and sharp edges. The preorbital process of the jugal is flattened against the maxilla, and the jugal is separated from the premaxilla by a small portion of the maxilla. The upper dental formula (based on the only specimen, CGM 40210) is 1.1.5?.3. Tentorium osseum, transverse sulcus, internal occipital protuberance, and bony falx cerebri are prominent. *Eosiren* and early *Halitherium* are closely similar, generalized halitheriines with moderately deflected rostra and with tusks that were persistently small in *Eosiren* but became medium-sized in *Halitherium*.

HALITHERIUM Kaup, 1838

Age—All the supposed African records of *Halitherium* are said to be Miocene, but this genus is not validly recorded after the Oligocene (Table 3.1, Figure 3.1).

African Occurrence—All supposed African specimens are here considered to be indeterminate sirenians, with the exception of a dugongid from Madagascar that is potentially determinable (see below).

Description—A generalized halitheriine with moderate rostral deflection and a subconical tusk with an alveolus roughly one-half the length of the premaxillary symphysis. Single-rooted permanent premolars 2-4/2-4 are retained.

Remarks—*Halitherium* is the common Oligocene sirenian of Europe (Lepsius, 1882; Spillmann, 1959). As the senior available generic name proposed for a fossil sirenian, *Halitherium* has also served in its time as a wastebasket name for a variety of Eocene to Pliocene specimens, many fragmentary and indeterminable. Today it nominally comprises three valid Old World species, all European: *H. taulannense* Sagne, 2001a (late Eocene); the type species *H. schinzii* (Kaup, 1838) (early Oligocene); and *H. christolii* Fitzinger, 1842 (late Oligocene). Even the last of these is conceivably assignable to *Metaxytherium*. *Halitherium* may also occur in the New World.

METAXYTHERIUM de Christol, 1840 (= *Felsinotherium* Capellini, 1872)

METAXYTHERIUM sp.

Age—Early Miocene (Burdigalian).

African Occurrence—Jabal Zelten, Libya (Table 1, Figure 2), yielded fragments of two skulls described in an unpublished doctoral dissertation (Heal, 1973:141). Its age would make this animal a contemporary of the European *M. krahuletzi* Depéret, 1895, but the taxonomic assignment requires corroboration (Domning and Pervesler, 2001:41).

Description—This genus is characterized in part by absence of permanent premolars, a rather strongly deflected rostrum, long and thin nasal processes of the premaxillae, a flat or convex frontal roof, and (in species earlier than the latest Miocene) small subconical tusks.

Remarks—*Metaxytherium* is the most common fossil sirenian in the Neogene of Europe, where it is represented by four chronospecies (Domning and Thomas, 1987). It also occurs in the New World and is probably derived from *Halitherium*.

METAXYTHERIUM SERRESII (Gervais, 1847) Depéret, 1895

Partial Synonymy— *Halitherium serresii* Gervais, 1847; *Felsinotherium serresii* (Gervais) de Zigno, 1878.

Age—Late Miocene-early Pliocene.

African Range—North Africa (Sahabi, Libya; ?Dar bel Hamri, Morocco), (Table 3.1, Figure 3.1).

Diagnosis—Differs from both earlier and later European species of the genus in its smaller body size, and in having a tusk alveolus roughly one-half the length of the premaxillary symphysis (i.e., longer than in earlier species but smaller than in the later, middle Pliocene one). *M. serresii* is also intermediate in degree of reduction of the supracondylar fossa.

Description—Remains of *Metaxytherium serresii* from Sahabi include: partial skulls, cranial elements, cheek teeth, mandibles, and some postcranial elements (Domning and Thomas, 1987). The rostrum of this species is strongly deflected downward (50˚-75˚), and incisor alveoli extend about half the length of the premaxillary symphysis. Nasals are reduced compared to *Halitherium*. Frontals are relatively flat and supraorbital process has a distinct posterolateral corner. Palatine extends forward on the palate to about the level of the front of M1 and rear edge of the zygomatic-orbital bridge. The mandible has a deep and strongly arched horizontal ramus.

The manubrium has a broad anterior tongue that is expanded slightly at front; the xiphisternum is wide anteriorly with a small demifacet. Innominates show apparent sexual dimorphism (Domning and Thomas, 1987); supposed females have long and narrow innominates while supposed male innominates have broad ischiac and pubic regions.

Remarks—The reduced body size of this species, later reversed in the lineage, is interpreted as ecophenotypic dwarfing related to the late Tortonian-Messinian salinity crises in the Mediterranean Basin (Bianucci et al., 2008). The type locality of this species (Montpellier, France) is its latest known occurrence (early Pliocene); the earliest occurrence is in Calabria, Italy (latest Tortonian; Carone and Domning, 2007). The relatively abundant Sahabi material is now considered early Messinian rather than post-Messinian. The Moroccan record is based only on a lower molar and a skullcap (Ennouchi, 1954); their age and identity are uncertain.

Subfamily Dugonginae (Gray, 1821) Simpson, 1932

(including Rytiodontinae Abel, 1914)

RYTIODUS Lartet, 1866

Diagnosis—According to Abel (1928), *Rytiodus* has a strongly deflected rostrum, a large lacrimal lacking any duct, large flattened incisor tusks, and an unreduced and complex M3.

RYTIODUS sp. nov. Heal, 1973

Age—Early Miocene (Burdigalian).

African Occurrence—Jabal Zelten, Libya (Table 3.1, Figure 3.1).

Diagnosis—The premaxillary rami abut against the nasals; the lacrimal is triangular.

Description—Highly derived dugongine with short, strongly deflected rostrum and large, self-sharpening bladelike tusks with paper-thin enamel on the medial surface. Nasal processes of premaxillae short, thick, and abut against triangular nasal bones. Frontal roof concave. Temporal crests pronounced, concave laterad, meet in midline. Sagittal length of skull roof approximately 26 cm; length of m3 = 29.5 mm. Other character states listed by Bajpai and Domning (1997: table 3).

Remarks—Described in an unpublished doctoral dissertation (Heal, 1973) and represented by good cranial material. The referral to *Rytiodus*, a poorly-known dugongine from the Aquitanian of France, needs corroboration, but this is at least a closely allied and conceivably descendant form. Delfortrie's (1880: pl. 5) restoration of the type species *R. capgrandi* with a straight, undeflected rostrum is incorrect, as shown by the strongly downturned anterior end of its maxilla.

Indeterminate Sirenia of assorted ages

At this point may be listed several African occurrences of Tertiary sirenians that, unfortunately, do not yet include diagnostic material (Table 3.1, Figure 3.1).

Eocene: Isolated cheek teeth and other remains have been collected from the Carcar Series near Callis, Somalia (Savage, 1977; not near Mogadishu as stated; Dr. A. Azzaroli, *Personal communications to Daryl P. Domning in litt.*, 24 Sept. 1986), and further fragments from the middle Eocene *Nautilus* Beds southeast of Berbera, Somalia (MacFadyen, 1952). Middle Eocene of north central Tunisia, west of Gebel Torzza, south east of El Ala village; mostly vertebrae and ribs still in rocks (Batik and Fejfar,

1990). Upper Eocene beds at Dor el Talha, Libya, have also yielded rib fragments (Savage, 1971; Heal, 1973).

Oligocene: A tusk, possibly sirenian, has been reported from Bedeil, Somalia (Savage, 1969). A skeleton has been found at Djebel ech Cherichira, Tunisia (Savage, 1969).

Miocene: Dugongid teeth have been collected from the Serravallian Beglia Formation, Bled ed Douarah, Tunisia (Robinson and Black, 1969). Three other, supposedly Miocene records from the African region have been referred to *Halitherium*, but none is sufficiently diagnostic to justify assignment to this Eocene and Oligocene north-Tethyan genus:

1. Gervais (1872: 341) records ribs of "*Halithérium*" from "dépôts à *Carcharodon megalodon*" at Chalouf (= El Shallûfa), Isthmus of Suez, received by the Paris Museum. He also (p. 352) alludes to other ribs from Lower Egypt cited by de Blainville. In fact, de Blainville (1840: 43, 51) was originally inclined to refer the fragmentary vertebrae and ribs in question to a pinniped, but later (1844:119-120) concluded that they were sirenian. These remains, from the "left bank of the Nile Valley" and of uncertain age and unknown present location, appear to be the earliest-recorded sirenian remains from Africa.

2. A fragmentary skull and skeleton from Makamby Island on the northwest coast of Madagascar were recorded as *Halitherium* sp. by Collignon and Cottreau (1927), who considered the deposits Miocene (Burdigalian to Helvetian). They supposed that the latest European record of *Halitherium* was *"H." bellunense* from the basal Burdigalian of Italy; but the latter species is probably a dugongine. The Madagascar skullcap is elongated, with temporal crests meeting in the midline, somewhat resembling that of the

early Oligocene *H. schinzii*; but its apparently late date indicates a different generic referral. The published drawing appears to show a concave frontal roof, suggesting that this animal may in fact be a dugongine. It needs to be compared with the *Rytiodus* from Libya.

3. Ribs of probable Burdigalian age from Malembe, Congo, were referred to *Halitherium*(?) sp. (Dartevelle, 1935), but the only tenable identification is Sirenia indet.

4. Recent investigations in the Cenozoic deposits of Madagascar (Samonds et al., 2005, 2007) yielded a potentially Eocene sirenian, known from a fairly complete skull, that has yet to be examined and described. Moreover, Samonds et al. 2007 provided new material sirenian record form the Mahakamby Island of the shore of northwestern Madagascar.

Discussion

Sirenians first appear in the Eocene, and the abundance of their remains in the middle and upper Eocene of North Africa led to the labeling of that area (or even the Fayum in particular) as the center of origin of the group. This was corroborated by recognition of anatomical similarities between sirenians and other characteristically African groups, such as proboscideans and hyracoids. Now, however, it seems more prudent to be less geographically specific. The earliest and most primitive known sirenian fossils are from the late early or early middle Eocene of Jamaica (Savage et al., 1994; Domning, 2001b), with a possible middle Eocene record from Israel (Goodwin et al., 1998) and Jordan (Zalmout et. al. 2003); and the presently known distribution of Eocene sirenians from the Caribbean to the East Indies (Domning et al., 1982; Domning, 2001a) points to "the shores of the Tethyan Seaway, probably in the Old World", as the specification of choice for a "center" of origin. Significantly, the marine angiosperms (seagrasses) also show signs of an originally Tethyan distribution, although they entered the water during the Cretaceous, well before the appearance of sirenians (den Hartog, 1970).

Today, both morphological and molecular evidence support the concept of an Afro-Asian Tethytheria (Sirenia + Proboscidea, plus the extinct Embrithopoda, Desmostylia, and Anthracobunidae). Indeed, Tethytheria is one of the best-supported supraordinal monophyletic groupings among the ungulates. Molecular (though not morphological) support is even stronger for the concept of Paenungulata (Tethytheria + Hyracoidea). The interordinal relationships within these groupings, however, are not well resolved, nor are the (presumably Paleocene) origins of the groupings themselves, due to paucity of primitive fossils for some of the orders (Gheerbrant et al., 2005). Surprisingly, molecular

studies strongly support placement of the Paenungulata within the Afrotheria rather than the ungulates! If this proves true, we may have to return to thinking of an African origin for sirenians.

Sagne (2001b) has pointed out a persistent zoogeographic division between sirenian faunas on the north shore of the Paleogene Tethys (*Sirenavus, Prototherium, Halitherium*) and the south shore (*Protosiren, Eotheroides, Eosiren*). Although these and other Eocene sirenians still require extensive taxonomic revision, a picture seems to be emerging of largely separate evolutionary histories on either side of Tethys during this period, with the northern lineage leading to *Halitherium* being distinct from the African *Eosiren* at least as early as the late Eocene.

Fossil Sirenia from Africa have been collected from shallow marine, lagoonal, estuarine, deltaic, and riverine environments. The African landmass was changing during the early and middle Cenozoic, with the closure of the Tethyan Sea in the north, tectonic compression of the Syrian arc in the northeast, and opening of the Red Sea in the east, which were undoubtly responsible for the diversity of the ecological settings. The result was a notable diversification of the African (Tethyan) lineages. Climate and sea level changes undoubtly played a role as well. *Protosiren*, *Eotheroides,* and *Eosiren* are known from middle and late Eocene and in one case Oligocene beds. By the late Oligocene and early Miocene, the northern African continent had assumed much of its present form, with a notable drop in sea level and domination of deltaic and riverine environments (Jabal Qatrani and Moghara formations in Egypt and Sahabi Formation in Libya). Generally speaking, these are freshwater deposits with minor pulses of marine incursion. Isotopic analysis of dental enamel from contemporaneous Eocene sirenians in

Egypt (Clementz et al., 2006) has produced isotopic signatures of marine settings, suggesting that these marine herbivores were adapted to a predominantly marine seagrass-based diet. These authors concluded that the low variation in the $\delta^{13}C$ values between these Eocene sirenians suggesting that their dietary preferences were highly focused.

The ecology and geography of Recent Sirenia partly reflect the Recent distribution of seagrasses: *Dugong* and some *Trichechus* both depend largely on this food source, and the majority of extinct sirenians evidently did so as well. Seagrass fossils were found in association with sirenian remains from the Priabonian of the Fayum area and comprised two genera, *Thalassodendron* and *Cymodocea* (Zalmout and Gingerich, 2004). This is the only record of fossil seagrass from Africa, and it surely does not give us an adequate picture of the Eocene diversity of these important marine plants in the Tethyan realm, where they seem to have originated.

Summary

Protosirenidae, Dugongidae and Trichechidae (including: *Anomotherium* of Siegfried 1965 and *Miosiren* of Dollo 1889) are the only sirenian families that are known to have lived in the nearshore habitats of the African continent, although it is not unlikely that Prorastomidae were once represented there as well. Dugongidae account for more than 85% of Africa's sirenian fossil record. No trichechid fossils have been found in Africa at all, but the living West African manatee probably arrived there from the New World in the late Pliocene or Pleistocene.

The abundance of Eocene sirenians in northeastern Africa (now the Libyan Desert) gives us our best sample to date of the diversity of sirenians that once inhabited the

Tethyan Seaway (including Southeast Asia, South Europe, and North America). For the remainder of the Cenozoic the sirenian fossil record in Africa is much less complete, but Miocene records of *Rytiodus* and *Metaxytherium* indicate continuing faunal connections between Europe and North Africa. Further collecting in marine Tertiary strata of Africa will undoubtedly expand the diversity of African Sirenia.

African Sirenia provide some of the best documentation of reduction and loss of the hind limbs in formerly terrestrial vertebrates as a progressive adaptation for aquatic life in coastal and off-shore environments. Preserved pelvic girdles and limb bones of Protosirenidae and Dugongidae show that there was a gradual reduction in their size with loss of some features associated with hindlimb functions. The most primitive sirenian from the middle Eocene of Jamaica (*Pezosiren portelli*, Domning, 2001b) has quadrupedal body form, while middle-late Eocene *Protosiren* from Egypt show intermediate characteristics between incipiently aquatic and fully aquatic forms. Among Eocene sirenians, *Eotheroides* and *Eosiren* have the most reduced pelvis and femur, including: reduced length of the ischium and ilium, a diminutive obturator foramen, and unfused and distinctly separated left and right pubic bones that must have been connected to one another by ligaments and cartilage, presaging the complete loss of function in the hind limbs. Later sirenians (Oligocene to Recent) show further reduction of the pelvis, as seen for example in the innominates of the Sahabi *Metaxytherium* (Domning and Thomas, 1987).

TABLE 3.1. African fossil sirenian taxa, localities, ages, and distributions published to date.

Loc	Taxon	Locality	Age	Material	Author
	Protosirenidae		**Middle to Late Eocene**		
1	*Protosiren*?	Left side of the Lower Nile Valley, Egypt	Lutetian?, Mokattam Limestone?	Vertebra and rib fragments	Blainville, 1840, 1844
2	*Protosiren fraasi*	Jabal Mokattam, Egypt	Lutetian, Mokattam Limestone	Skulls and postcrania	Filhol, 1878; Abel, 1907
3	*Libysiren sickenbergi*	Bu el Haderait, Libya	Lutetian	Partial skeletons	Heal, 1973
4	*Protosiren* sp.	Wadi El Rayan, Fayum, Egypt	Lutetian, Wadi El Rayyan Series	Scapula	This study
5	*Protosiren smithae*	Wadi Al Hitan, Fayum, Egypt	Priabonian, Birket Qaroun Fm.	Skulls and skeleton	Domning et al., 1994
	Dugongidae		**Middle Eocene to Recent**		
6	*Eosiren abeli*	Jabal Mokattam, Cairo, Egypt	Lutetian, Mokattam Limestone	Skull, mandible, teeth, vertebrae (mostly destroyed)	Sickenberg, 1934
7	*Eotheroides aegyptiacum*	Jabal Mokattam, Egypt	Lutetian, Mokattam Limestone	Skulls and postcrania	Owen, 1875; Abel, 1913; Zdansky, 1938; Sickenberg, 1934
8	*Eotheroides sandersi* *Eotheroides clavigerum*	Wadi Al Hitan, Fayum, Egypt	Priabonian, Birket Qaroun Fm.	Skeletons	This study
9	Dugongidae	Callis, Somalia	Middle Eocene, Carcar Series	Teeth, rib	Savage, 1969, 1977; Savage and Tewari, 1977
10	Dugongidae	Ampazony, Majunga, Madagascar	Bartonian-Priabonian, Nummulitic Limestone	Skull	Samonds et al., 2005
11	Dugongidae	Dor el Talha, Libya	Priabonian, Idam Unit	Ribs	Savage, 1969, 1971, 1977; Heal, 1973; Wight, 1980
12	*Eosiren libyca*	Qasr El Sagha, Fayum, Egypt	Priabonian, Qasr El Sagha Fm.	Skulls and postcrania	Andrews, 1902; Sickenberg, 1934; Siegfried, 1967
13	*Eosiren stromeri*	Qasr El Sagha, Fayum, Egypt	Priabonian, Qasr El Sagha Fm.	Skull and postcrania	Sickenberg, 1934
14	*Eosiren imenti*	Jabal Qatrani, Fayum, Egypt	Rupelian, Jabal Qatrani Fm.	Skull and some ribs	Domning et al., 1994
15	*Rytiodus* n.sp.	Jabal Zelten, Libya	Burdigalian, Marada Fm.	Skulls, mandibles, etc.	Heal, 1973
16	*Metaxytherium* sp.	Jabal Zelten, Libya	Burdigalian, Marada Fm.	Fragments of 2 skulls	Heal, 1973
17	Dugongidae	Bled ed Douarah, Tunisia	Serravallian	Teeth	Robinson and Black, 1969
18	*Metaxytherium* sp.?	Qasr Sahabi, Libya	Late Miocene [Fm. M]	Articulated skeletons	Domning and Thomas, 1987
19	*Metaxytherium* sp.?	Qasr Sahabi, Libya	Late Tortonian or Early Messinian? [Fm. P]	Sirenian ribs	de Heinzelin and El Arnauti, 1987
20	*Metaxytherium serresii*	Qasr Sahabi, Libya	Early Messinian [Mbr. T]	Skull fragments, mandibles, postcrania	Domning and Thomas, 1987
21	*Metaxytherium serresii*	Qasr Sahabi, Libya	Early Messinian? [Mbr. U-2; also U-1]	Partial skeleton	Domning and Thomas, 1987
22	Dugongidae	Ile Makamby (E side of the island), Madagascar	Miocene, Nummulitic Marl Unit	Skullcap	Collignon and Cottreau, 1927

23	*Metaxytherium* cf. *serresii*	Dar bel Hamri, Morocco	Pliocene	Skullcap, tooth	Ennouchi, 1954
	Sirenia indet.				
24	Sirenia?	Gebel Torzza, Tunisia	Lutetian	Sirenian remains in block	Batik and Fejfar, 1990
25	Sirenian remains	Kpogamé-Hahotoé, Togo	Lutetian, Kpogamé-Hahotoé Phosphate level, Middle Eocene	Thoracic vertebrae, rib heads	Gingerich et al., 1992
26	Sirenia indet.	25 km SE of Berbera , Somalia	Middle Eocene, [Daban Series]	Ribs	Macfadyen 1952; Savage and Tewari, 1977; Savage, 1969
27	Sirenia indet.	Khashm El Raqaba, Eastern Desert of Egypt	Bartonian	Vertebrae	Gingerich et al., 2007
28	Sirenia indet.	Djebel ech Cherichira, Tunisia	Oligocene	Skeleton	Savage, 1969
29	Sirenia?	Bedeil, Somalia	Oligocene	Tusk	Savage, 1969
30	Sirenian	Nosy Mahakamby, Madagascar	Early Oligocene	Ribs and vertebrae	Samonds, 2007
31	Sirenia indet.	Jabal Zelten, Libya	Burdigalian, Marada Fm.	Sirenian remains	Heal, 1973
32	Sirenia indet.	Isthmus of Suez, Egypt	Miocene	Fragmentary ribs	Gervais, 1872
33	Sirenia indet.	Malembe, Congo	Miocene	Ribs	Dartevelle, 1935

FIGURE 3.1. African distribution of fossil and living sirenians (after Bertram and Bertram, 1973) known to date (fossil localities presented as open diamonds associated with numbers, Recent distribution of *Dugong dugon* Müller 1776 (light color) and *Trichechus senegalensis* Link 1797 (dark color) highlighted as narrow stripes along shores and rivers and in inland areas).

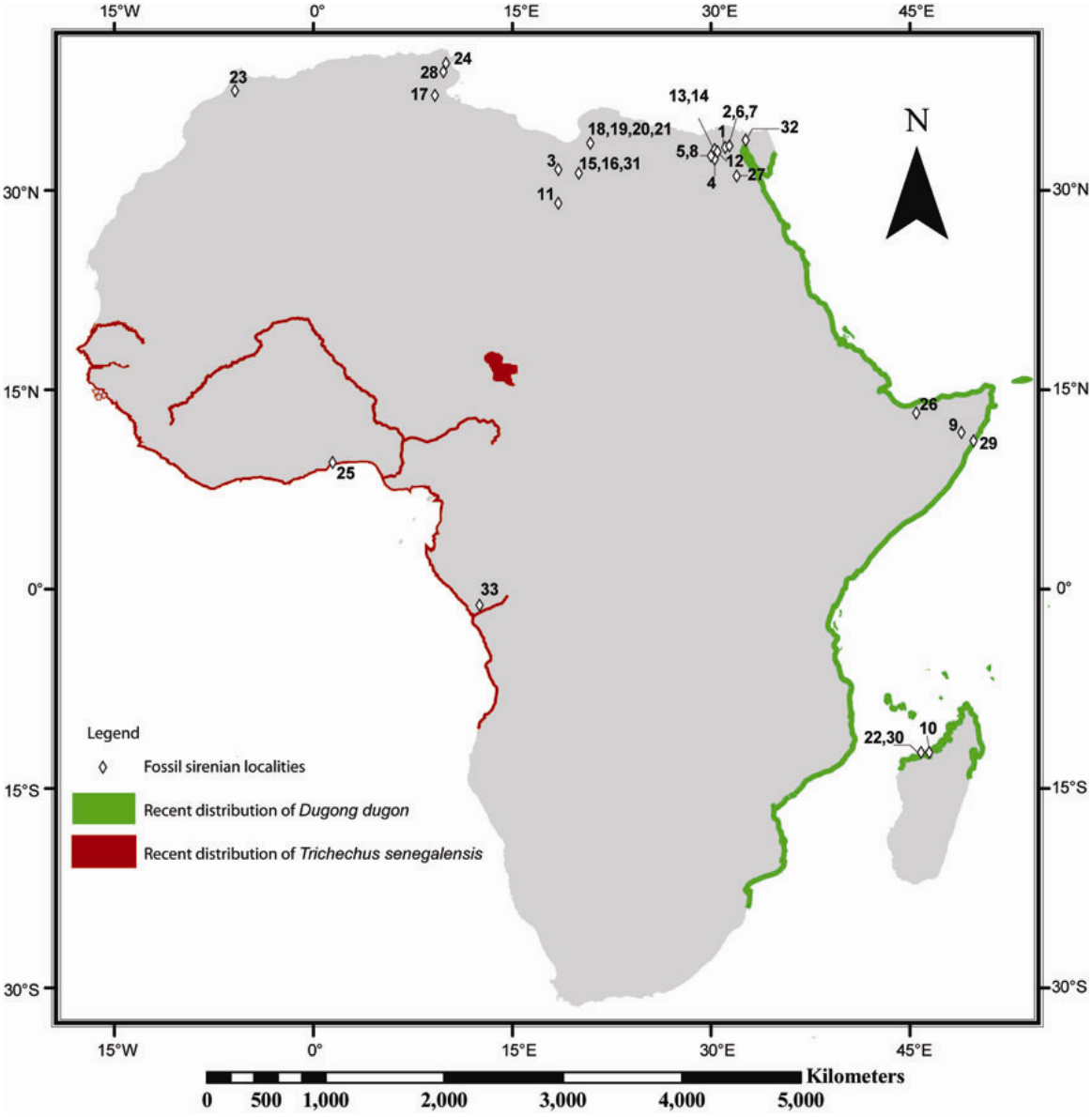

FIGURE 3.2. Cranial drawings of some African Paleogene sirenians (Protosirenidae and Dugongidae) in lateral views. A, Lutetian *Protosiren fraasi* (reconstructed from CGM 10171 and SMNS 10576; reconstruction of Gingerich et. al. 1994); B, Priabonian *Protosiren smithae* (CGM 43392; Domning and Gingerich, 1994); C, Priabonian *Eotheroides clavigerum* sp. nov. (UM 101219; see Chapter 4). Abbreviations: **AC**, alisphenoid canal; **AS**, alisphenoid; **BO**, basioccipital; **BS**, basisphenoid; **C^1**, upper canine; **DP**, deciduous premolar; **EO**, exoccipital; **FIO**, infraorbital foramen; **FR**, frontal; **FRT**, foramen rotundum; **I^1** etc., upper incisor; **J**, jugal; **LAC**, lacrimal; **M^1** etc., upper molar or alveoli; **MES,** mesethmoid; **MF**, mastoid foramen; **MX**, maxilla; **N**, Nasal; **OC**, occipital condyle, **P^1** etc., upper premolar alveoli; **PA**, parietal; **PM**, premaxilla; **SO**; supraoccipital; **SQ**, squamosal; **SR,** sigmoidal ridge; **T**, tympanic; **V**, vomer.

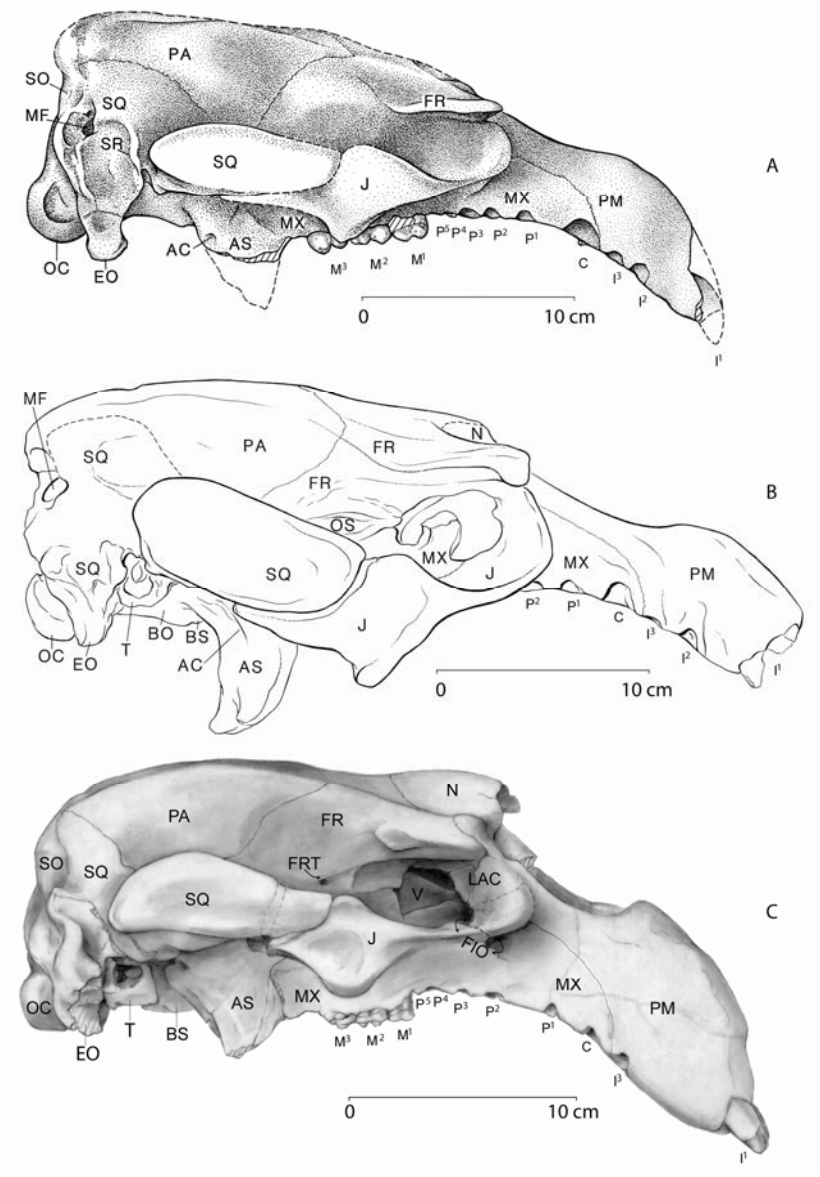

FIGURE 3.3. Eocene and Oligocene *Eosiren* from the Fayum area in Egypt. A, Dorsal view of Priabonian *Eosiren libyca* of Qasr El Sagha Formation (Andrews, 1902; illustration of Abel, 1929); B, Lateral view of Rupelian *Eosiren imenti* (CGM 40210, Domning et al., 1994). Abbreviations: see abbreviations in Figure 3.2.

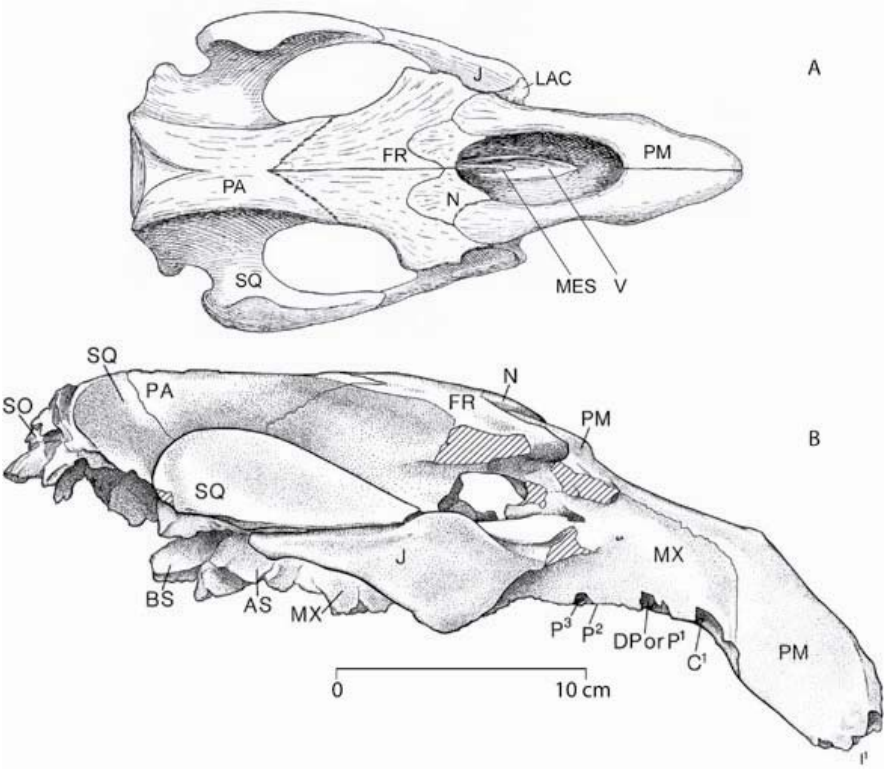

FIGURE 3.4. Right innominate bones of Paleogene African sirenians. A, *Protosiren fraasi* (SMNS 43976A, from Abel, 1904: pl. 7, fig. 1); B, *Protosiren smithae* (Domning and Gingerich, 1994, CGM 43392); C, *Eotheroides sandersi* sp. nov. (UM 97514); D, *Eotheroides clavigerum* sp. nov. (UM 101219); E, *Eosiren libyca* (UM 101226); F, *Eosiren libyca* (CGM 29774). Abbreviations: **act.,** acetabulum; **act. n.,** acetabular notch; **dor. il. sp.** dorso iliac spine; **il.,** ilium; **is.,** ischium; **obt. f.,** obturator foramen; **ps.,** pubis; **ps. sym.,** pubic symphysis.

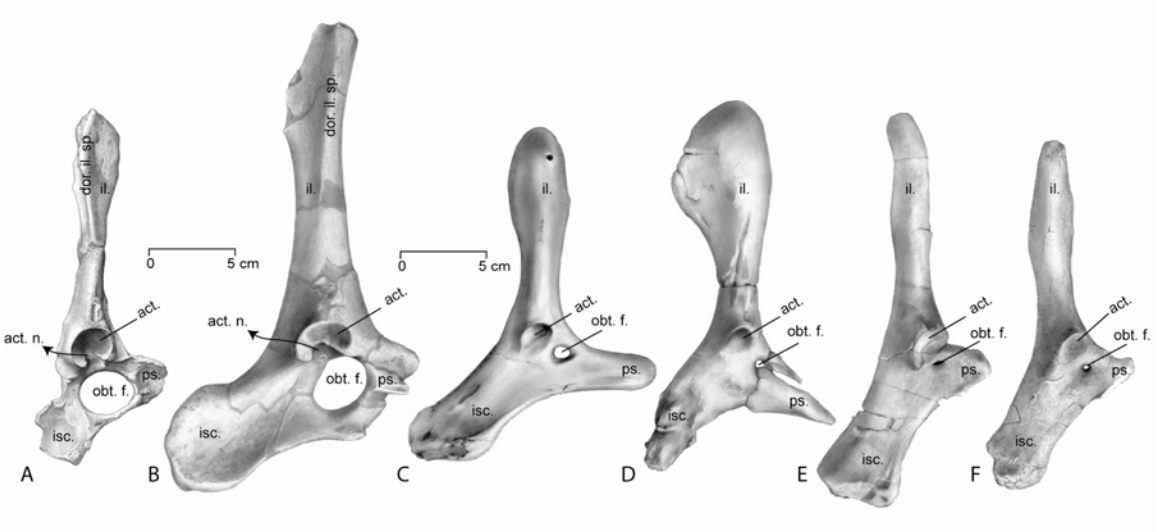

Literature Cited

ABEL, O. 1904. Die Sirenen der mediterranen Tertiärbildungen Österreichs. Abhandlungen der Kaiserlich-Königlichen Geologischen Reichsanstalt (Wien), 19:1-223.

ABEL, O. 1907. Die Stammesgeschichte der Meeressäugetiere. Meereskunde, 1:1-36.

ABEL, O. 1913. Die eozänen Sirenen der Mittelmeerregion. Erster Teil: Der Schädel von *Eotherium aegyptiacum*. Paläontographica 59:289-360 (title page bears date of 1912).

ABEL, O. 1919. Die Stämme der Wirbeltiere. Vereinigung Wissenschaftlicher Verleger, Walter de Gruyter & Co., Berlin and Leipzig, 914 pp.

ABEL, O. 1928. Vorgeschichte der Sirenia; pp. 475-504 in M. Weber (ed.), Die Säugetiere. Einführung in die Anatomie und Systematik der recenten und fossilen Mammalia. Gustav Fischer, Jena.

ANDREWS, C. W. 1902. Preliminary note on some recently discovered extinct vertebrates from Egypt. (Part III.) Geological Magazine, 9:291-295.

ANDREWS, C. W. 1906. A Descriptive Catalogue of the Tertiary Vertebrata of the Fayum, Egypt. British Museum of Natural History, London, 324 pp.

BAJPAI, S., and D.P. DOMNING. 1997. A new dugongine sirenian from the Early Miocene of India. Journal of Vertebrate Paleontology, 17:219-228.

BAJPAI, S., J. G. M. THEWISSEN, V. V. KAPUR, B. N. TIWARI, and A. SAHNI. 2006. Eocene and Oligocene sirenians (Mammalia) from Kachchh, India. Journal of Vertebrate Paleontology, 26:400-410.

BATIK, P., and O. FEJFAR. 1990. Les vertébrés du Lutétien, du Miocène et du Pliocène de Tunisie centrale. Notes Service Géologique de Tunisie, 56:69-83.

BERTRAM, G. C. L., and C. K. R. BERTRAM. 1973. The modern Sirenia: their distribution and status. Biological Journal of the Linnean Society of London, 5:297-338.

BIANUCCI, G., G. CARONE, D. P. DOMNING, W. LANDINI, L. ROOK and S. SORBI. 2008. Peri-Messinian dwarfing in Mediterranean Metaxytherium (Mammalia: Sirenia): evidence of habitat degradation related to the Messinian Salinity Crisis. Garyounis Scientific Bulletin, Special Issue 5: 145-157.

BLAINVILLE, H. M. D. DE. 1840. Ostéographie, Livr. 7, Des Phoques (G. *Phoca*, L.). Paris, Arthus Bertrand.

BLAINVILLE, H. M. D. DE. 1844. Ostéographie, Livr. 15, Des Lamantins (Buffon), (*Manatus*, Scopoli), ou gravigrades aquatiques. Paris, Arthus Bertrand.

BOAZ, N.T., A. EL-ARNAUTI, J. AGUSTI, R. L BERNOR., P. PAVLAKIS and L. ROOK. 2004. Temporal, lithostratigraphic, and biochronologic setting of As Sahabi Formation, north-central Libya. *Abstracts, Third Symposium on Geology of East Libya*, Binghazi, Libya, Nov. 21-23, 2004, p. 21.

CARONE, G., and D. P. DOMNING. 2007. *Metaxytherium serresii* (Mammalia: Sirenia): First pre-Pliocene record, and implications for Mediterranean paleoecology before and after the Messinian salinity crisis. Bollettino della Societ Paleontologica Italiana, 46:55-92.

CARUS, J. V. 1868. Handbuch der Zoologie. 1ster band. Wirbelthiere, Mollusken und Molluscoiden. Wilhelm Engelmann, Leipzig, 894 pp.

CAPELLINI, G. 1872. Sul Felsinoterio, sirenoide halicoreforme dei deposition littorali pliocenici dell'antico Bacino del Mediterraneo e del Mar Nero. Memorie dell'Accademia delle Scienze dell'Istituto di Bologna, 3:605-646.

CHRISTOL, J. D. 1840. Recherches sur divers ossements fossiles attributés par Cuvier à deux phoques, au lamantin, et à deux espèces d'hippoptames, et rapportés au *Metaxytherium*, nouveau genre de cétacé de la famille des dugongs. L'Institute Annales, 8:322-323.

CLEMENTZ, M. T., A. GOSWAMI, P. D. GINGERICH, and P. L. KOCH. 2006. Isotopic records from early whales and sea cows: contrasting patterns of ecological transition. Journal of Vertebrate Paleontology, 26:355-370.

COLLIGNON, M., AND J. COTTREAU. 1927. Paléontologie de Madagascar. XIV. Fossiles du Miocène marin. Annales de Paléontologie, 16:135-171.

DARTEVELLE, E. 1935. Les premiers restes de mammifères du tertiaire du Congo: la faune Miocène de Malembe. Comptes-Rendus du Congrès National des Sciences, (Brussels), 1:715-720.

DELFORTRIE, E. 1880. Découverte d'un squelette entier de *Rytiodus* dans le falun Aquitanien. Actes Societe Linneenne de Bordeaux, 34:131-144.

DEPÉRET, C. 1895. Ueber die Fauna von miocänen Wirbelthieren aus der ersten Mediterranustufe von Eggenburg. Sitzungsberichte. Akademie der Wissenschaften in Wien. Mathematisch-Naturwissenschaftliche Klasse, 104:395-416.

DOLLO, L. 1889. Prèmiere note sure les siréniens de Boom (résumé). Bulletin de la Société belge de Géologie, de Paléontologie et d'Hydrologie, 3:415-421.

DOMNING, D. P. 1977. An ecological model for Late Tertiary sirenian evolution in the North Pacific Ocean. Systematic Zoology, 25:352-362.

DOMNING, D. P. 1978. Sirenia. In: V.J. Maglio and H.B.S. Cooke, eds., Evolution of African Mammals, Harvard University Press, pp: 573-581.

DOMNING, D. P. 1994. A phylogenetic analysis of the Sirenia. Proceedings of the San Diego Society of Natural History, 29:177–189.

DOMNING, D. P. 1996. Bibliography and Index of the Sirenia and Desmostylia. Smithsonian Contributions to Paleobiology, 80:iii + 611.

DOMNING, D. P. 2001a. Sirenians, seagrasses, and Cenozoic ecological change in the Caribbean. In: W. Miller III & S.E. Walker (eds.), Cenozoic Paleobiology: The Last 65 Million Years of Biotic Stasis and Change. Palaeogeography, Palaeoclimatology, Palaeoecology, 166:27-50.

DOMNING, D. P. 2001b. The earliest known fully quadrupedal sirenian. Nature, 413:625-627.

DOMNING, D. P., G. S. MORGAN, and C. E. RAY. 1982. North American Eocene sea cows (Mammalia: Sirenia). Smithsonian Contribution to Paleobiology, 52:1-69.

DOMNING, D. P., and V. DE BUFFRÉNIL. 1991. Hydrostasis in the Sirenia: quantitative data and functional interpretations. Marine Mammal Science, 7:331-368.

DOMNING, D. P., and P.D. GINGERICH. 1994. *Protosiren smithae*, new species (Mammalia, Sirenia), from the late Middle Eocene of Wadi Hitan, Egypt. Contributions from the Museum of Paleontology. University of Michigan, 29:69-87.

DOMNING, D. P., P.D. GINGERICH, E.L. SIMONS, and F.A. ANKEL-SIMONS. 1994. A new early Oligocene dugongid (Mammalia, Sirenia) from Fayum Province, Egypt. Contributions from the Museum of Paleontology. University of Michigan, 29:89-108.

DOMNING, D. P., and P. PERVESLER. 2001. The osteology and relationships of *Metaxytherium krahuletzi* Depéret, 1895 (Mammalia: Sirenia). Abhandlungen der Senckenbergischen Naturforschenden Gesellschaft, 553:1-89.

DOMNING, D. P., and H. THOMAS. 1987. *Metaxytherium serresii* (Mammalia: Sirenia) from the Lower Pliocene of Libya and France: a reevaluation of its morphology, phyletic position, and biostratigraphic and paleoecological significance. In: N. Boaz, A. El-Arnauti, A. W. Gaziry, J. DE Heinzelin, and D. D. Boaz, eds., Neogene Paleontology and Geology of Sahabi. Alan R. Liss, New York, pp:205-232.

ENNOUCHI, E. 1954. Un sirénien, *Felsinotherium* cf. *serresi*, à Dar bel Hamri. Service Géologique du Marco, 121:77-82.

FILHOL, H. 1878. Note sur la découverte d'un nouveau Mammifère marin (Manatus coulombi) en Afrique dans les carrières de Mokattam près du Caire. Bullétin de la Société Philomathique de Paris, Série 7, 2:124-125.

FITZINGER, L. J. 1842. Bericht über die in dem Sandlagern von Linz aufgefundenen fossilen Reste eines urweltlichen Säugers, (*Halitherium cristolii*). Bericht ueber das Museum Francisco-Carolinum, 6:61-72.

FRAAS, O. 1867. Aus dem Orient. Geologische Beobachtungen am Nil, auf der Sinai-Halbinsel und in Syrien. Ebner and Seubert, Stuttgart, 222 pp.

GERVAIS, P. 1872. Travaux récents sur les sirénides vivants et fossiles (analyse des publications de MM. Van Beneden, E. Lartet, Delfortrie, Capellini, etc.). Journal de Zoologie, 1:332-353.

GHEERBRANT, E., D. P. DOMNING, and P. TASSY. 2005. Paenungulata (Sirenia, Proboscidea, Hyracoidea, and relatives). Chap. 7 in: K.D. Rose and J. D. Archibald (eds.), The Rise of Placental Mammals: Origin and Relationships of the Major Extant Clades. Baltimore, Johns Hopkins University Press, PP: 84-105.

GINGERICH, P. D. 1992. Marine mammals (Cetacea and Sirenia) form the Eocene of Gebel Mokattam and Fayum, Egypt: stratigraphy, age, and paleoenvironments. Contributions to the Museum of Paleontology, University of Michigan 30:1–85.

GINGERICH, P. D., H. CAPPETTA, and M. TRAVERSE. 1992. Marine mammals (Cetacea and Sirenia) from the middle Eocene of Kpogamé- Hahotoé in Togo (abstract). Journal of Vertebrate Paleontology 12 (3, supplement): 29A-30A.

GINGERICH, P.D., D.P. DOMNING, C.E. BLANE, and M. UHEN. 1994. Cranial morphology of *Protosiren fraasi* (Mammalia, Sirenia) from the Middle Eocene of Egypt: a new study using computed tomography. Contributions from the Museum of Paleontology. University of Michigan, 29:41- 67.

GINGERICH, P. D., M. ARIF, M. A. BHATTI, H. A. RAZA, and S. M. RAZA. 1995. *Protosiren* and *Babiacetus* (Mammalia, Sirenia and Cetacea) from the middle Eocene Drazinda Formation, Sulaiman Range, Punjab (Pakistan). Contributions to the Museum of Paleontology, University of Michigan, 29:331–357.

GOODWIN, M.B., D.P. DOMNING, J.H. LIPPS, and C. BENJAMINI. 1998. The first record of an Eocene (Lutetian) marine mammal from Israel. Journal of Vertebrate Paleontology, 18:813-815.

GRAY, J. E. 1821. On the natural arrangement of vertebrose animals. London Medical Repository, 15:296-310.

HARTOG, C. DEN. 1970. The Sea-Grasses of the World. Koninklijke Nederlandse Akademie van Wetenschappen Verhandelingen, Afdeling Natuurkunde, 59:1-275.

HEAL, G. J. 1973. Contributions to the study of sirenian evolution. Ph.D. thesis, University of Bristol, England (unpubl.).

HEINZELIN, J. DE and A. EL-ARNAUTI. 1987. The Sahabi Formation and related deposits; pp. 1-21 in N. T. Boaz, A. El-Arnauti, A. W. Gaziry, J. de Heinzelin, and D. D. Boaz (eds.), Neogene paleontology and geology of Sahabi. Alan R. Liss, Inc, New York.

ILLIGER, C. 1811. Prodromus systematis mammalium et avium additis terminis zoographicus utriusque classis, earumque versione Germanica. C. Salfeld, Berlin, 302 pp.

KAUP, J. J. 1838a. Über Zähnen von *Halytherium* und *Pugmeodon* aus Flonheim. Neues Jahrbuch für Geognosie, Geologie und Petrefactenkunde, 1838:318-320.

KAUP, J. J. 1838b. Über Zähnen von *Halitherium* und Dugong. Neues Jahrbuch für Geognosie, Geologie und Petrefactenkunde 1838:356.

KORDOS, L. 1977. A New Upper Eocene Sirenian *(Paralitherium tarkanyense* n.g.n.sp.) from Felsötrárkány, NE Hungary. Magyar Állami Földtani Intézet Évi Jelentése az 1975 Évröl, 1977:349-367.

KRETZOI, M.1941. *Sirenavus hungaricus* n.g. n. sp., ein neuer Prorastomide aus dem Mitteleozän (Lutetium) von Felsögalla in Ungarn. Annales Musei Nationalis Hungarici, Pars Mineralogica, Geologica et Palaeontologica, 34:146-156.

LARTET, É. 1866. Note sur deux nouveaux siréniens fossiles des terrains tertiaires du bassin de la Garonne. Bulletin de la Societe geologique de France, 2:673-686.

LEPSIUS, G. R.1882. *Halitherium Schinzi*, die fossile Sirene des Mainzer Beckens. Eine vergleichend-anatomische Studie. Abhandlungen des Mittelrheinischen Geologischen Vereins 1:vi + 200 + viii.

LINK, H. F. 1795. Beyträge zur Naturgeschichte. Vol. 1, part 2. K. C. Stiller, Rostock and Leipzig, 126 pp.

MACFADYEN, W. A. 1952. Note on the geology of the Daban area and the localities of the described nautiloids. In O. Haas and A. K. Miller, Eocene Nautiloids of British Somaliland. Bulletin of the American Museum of Natural History, 99:347-349.

MARSHALL, C. D., L. A. CLARK, and R. L. REEP. 1998. The muscular hydrostat of the Florida manatee (*Trichechus manatus latirostris*): a functional morphological model of perioral bristle use. Marine Mammal Science, 14:290-303.

MÜLLER, P. L. S. 1776. Des Ritters Carl von Linne' … vollständiges Natursystems Supplements- und Register-Band…. Nuremberg, Gabriel Nicolaus Raspe, 384 pp.

OWEN, R. 1855. On the fossil skull of a mammal (*Prorastomus sirenoides* Owen) from the island of Jamaica. Quarterly Journal of the Geological Society of London, 11:541-543.

OWEN, R. 1875. On fossil evidences of a sirenian mammal (*Eotherium aegyptiacum*, Owen) from the Nummulitic Eocene of the Mokattam Cliffs, near Cairo. Quarterly Journal of the Geological Society of London, 31:100-105.

PALMER, T. S. 1899. Catalogus Mammalium tam viventium quam fossilium [Review of Dr. E. L. Trouessart's Catalogus Mammalium]. Science 10:491-495.

PREEN, A. R. 1995. Diet of dugongs: are they omnivores? Journal of Mammalogy, 76:163-171.

ROBINSON, P., and C. C. BLACK. 1969. Note préliminaire sur les vertébrés fossils du Vindobonien (formation Béglia), du Bled Douarah, Gouvernorat de Gafsa, Tunisie. Notes du Service Géologique (Tunisie), 31:67-70.

SAGNE, C. 2001. *Halitherium taulannense*, nouveau sirenien (Sirenia, Mammalia) de l'Eocene superieur provenant du domaine Nord-Tethysien (Alpes-de-Haute-Provence, France) Comptes Rendus de l'Academie des Sciences Serie II A Sciences de la Terre et des Planetes, 333:471-476.

SAMONDS, K., ZALMOUT, I. S., and KRAUS, D. 2005. New sirenian fossils from the late Eocene of Madagascar. Journal of Vertebrate Paleontology, 25(3, supplement):108A.

SAMONDS, K., I. S. ZALMOUT, M. T. IRWIN, and L. L. RAHARIVONY. 2007. Sirenian postcrania from Nosy Mahakamby, Northwestern Madagascar. Journal of Vertebrate Paleontology, 27(3, supplement):139A.

SAVAGE, R. J. G. 1967. Early Miocene mammal faunas of the Tethyan region. Systematics Association Publication, 7:247-282.

SAVAGE, R. J. G. 1969. Early Tertiary mammal locality in southern Libya. Proceedings Geological Society of London, 1657:167-171.

SAVAGE, R. J. G. 1971. Review of the fossil mammals of Libya. In: Symposium on the Geology of Libya, University of Libya, pp: 215-225.

SAVAGE, R. J. G. 1977. Review of early Sirenia. Systematic Zoology 25:344–351.

SAVAGE, R. J. G., and M. E. WHITE. 1965. Exhibit: Two mammal faunas from the early Tertiary of central Libya. Proceedings Geological Society of London, 1623:89-91.

SAVAGE, R. J. G., and B. S. TEWARI. 1977. A new sirenian from Kutch India. Journal of the Palaeontological Society of India, 20:216-218.

SAVAGE, R. J. G., D.P. DOMNING, and J. G. M. THEWISSEN. 1994. Fossil Sirenia of the West Atlantic and Caribbean region. V. The most primitive known sirenian, *Prorastomus sirenoides* Owen, 1855. Journal of Vertebrate Paleontology, 14:427-449.

SICKENBERG, O. 1934. Beiträge zur Kenntnis Tertiärer Sirenen. I. Die Eozänen Sirenen des Mittelmeergebietes; II. Die Sirenen des Belgischen Tertiärs. Mémoires du Museé Royal d'Histoire Naturelle de Belgique, 63:1–352.

SIEGFRIED, P. 1965. *Anomotherium langewieschei* n.g. n. sp. (Sirenia) aus dem Ober-Oligozan des Dobergs bei Bunde/Westfalen. Sonder-Abdruck aus Palaeontolographica, 124:116-150.

SIEGFRIED, P. 1967. Das Femur von *Eotheroides libyca* (Owen) (Sirenia). Paläontologisches Zeitschrift, 41:165-172.

SIMPSON, G. G. 1932. A new classification of mammals. Bulletin of the American Museum of Natural History, 59:259-293.

SIMPSON, G. G. 1945. The principles of classification and a classification of mammals. Bulletin of the American Museum of Natural History, 85:1-350.

SPILLMANN, F. 1959. Die Sirenen aus dem Oligozän des Linzer Beckens (Oberösterreich), mit Ausführungen über "Osteoskelerose" und "Pachyostose". Österreichische Akademie der Wissenschaften, Mathematisch-Naturwissenschaftliche Klasse. Denkschriften, 110:1-68.

TROUESSART, E.-L. 1905. Catalogus mammalium tam viventium quam fossilium…. Quinquennale supplementum anno 1904, Volume 2. R. Friedländer and Sohn, Berlin, 547-929.

WIGHT, A. 1971. Paleogene vertebrates from Libya. 1: The Geology of the Eocene-Oligocene sediments at Dor el Talha, Southern Libya, with special reference to the vertebrate fauna. 2: the Proboscidea (excluding *Barytherium*) from Dor el Talha, southern Libya; and a study of the genus *Moeritherium*. University of Bristol, London.

ZALMOUT, I. S., M. UL-HAQ, and P. D. GINGERICH. 2003. New species of *Protosiren* (Mammalia, Sirenia) from the early middle Eocene of Balochistan (Pakistan). Contributions from the Museum of Paleontology. University of Michigan, 31:79-87.

ZALMOUT, I. S. and GINGERICH, P. D. 2004. Paleobiology of Tethyan seacows (Sirenia, Mammalia) from the marine Eocene Fayum Province, Egypt (abstract).

In K. Bice, M.-P. Aubry, and K. Ouda (eds.), Climate and Biota of the Early Paleogene - V: Abstract and Program Book, Luxor, p. B-31.

ZALMOUT, I.S., and P. D. GINGERICH. 2005. Eocene Sirenia of Egyptian Tethys: Aquatic Adaptations. Journal of Vertebrate Paleontology, 25(3, supplement):133A.

ZALMOUT, I. S., P. GINGERICH, H. MUSTAFA, A. SMADI, and A. KHAMMASH. 2003. Cetacea and Sirenia from the Eocene Wadi Esh-Shallala Formation of Jordan. Journal of Vertebrate Paleontology, 23(3, supplement):113A.

ZDANSKY, O. 1938. *Eotherium majus* sp.n., eine neue Sirene aus dem Mitteleozän von Aegypten. Palaeobiologica, 6:429-434.

ZIGNO, A. DE. 1875. Sireni fossili trovati nel Veneto. Memorie dell' Real Istituto Veneto di Scienze Lettere ed Arti, 18:427-456.

CHAPTER FOUR

NEW EOCENE SIRENIA FROM THE PRIABONIAN OF WADI AL HITAN

This chapter includes a description of two new species of Sirenia represented by skulls and exceptionally complete skeletons found in Wadi Al Hitan in the 1980s and 1990s: *Eotheroides clavigerum*, new species; and *Eotheroides sandersi*, new species. Sexual dimorphism in these skeletons is discussed in Chapter 5. Paleoenvironments, paleoecology, and paleobiology follow in Chapters 6 and 7.

Institutional and Field Abbreviations—**BMNH (=NHML)**, British Museum of Natural History (=Natural History Museum), London (England); **CGM**, Cairo Geological Museum (Egyptian Geological Museum), Cairo (Egypt); **MTM**, Magyar Természettudományi Múzeum (Hungarian Natural History Museum), Budapest (Hungary); **MÁFI**, Magyar Állami Földtani Intézet (Geological Institute of Hungary), Budapest (Hungary); **NSM-PV**, National Science Museum-Vertebrate Paleontology collection, Tokyo (Japan); **SMNS**, Staatliches Museum für Naturkunde, Stuttgart (Germany); **UM**, Museum of Paleontology, University of Michigan, Ann Arbor (USA); **UMMZ**, Museum of Zoology, University of Michigan, Ann Arbor (USA); **USNM**, former United States National Museum collections deposited in the National Museum of

Natural History, Smithsonian Institution, Washington D.C. (USA); **YPM**, Peabody Museum of Natural History, Yale University, Yale (USA); **ZV**, Wadi Al Hitan "Valley of Whales" field and map label for specimens in the Cairo Geological Museum (Egypt); Museum of Paleontology, University of Michigan, Ann Arbor (USA); and specimens remaining in the field.

SYSTEMATIC PALEONTOLOGY

Class MAMMALIA Linnaeus, 1758

Order SIRENIA Illiger, 1881

Family DUGONGIDAE Gray, 1821

Subfamily HALITHERIINAE (Carus, 1868) Abel, 1913

GENUS *EOTHEROIDES* Palmer, 1899

EOTHEROIDES CLAVIGERUM sp. nov.

(Figures 4.1, 4.2, 4.3, 4.4, 4.5, 4.6, 4.7, 4.8, 4.1, 4.11; Tables 4.1, 4.4, 4.5, 4.7, 4.8, 4.10, 4.11).

Holotype— UM 101219 (Figures 4.14.2-4.3, 4.54.74.84.1-4.11; Tables 4.1, 4.44.54.74.84.1-4.11) is a skeleton of a dentally-mature adult sirenian, includes a skull with left and right M^{1-3}, both dentaries with left and right M_{1-3}, in addition to right dp_5, most of the cervical and thoracic vertebrae, one sacral, and three caudals (C1-C3, C5, C7, Th1- Th13, Th17-Th18, S1, Ca2, Ca16, and Ca19), virtually complete ribcage, left scapula and humerus, left radius and ulna fused, several metacarpals and a phalanx, and both innominates.

Type Locality— University of Michigan field locality ZV-219 in Wadi Al Hitan (Zeuglodon Valley) (Figure 1.5), some 75 km west of the city of Fayum, and 140 SW of the city of Cairo. UTM grid coordinates for the holotype in zone 36R are 213606 m E and 3245831 m N.

Referred Specimens— UM 94806 (Figure 4.4), includes a left premaxilla, and right scapula and humerus from locality ZV-33 (UTM grid coordinates in zone 36R: 211669 m E and 3243892 m N); Priabonian, lower part of Birket Qarun Formation.

CGM 42298, right squamosal and right M^3 from locality ZV-101, (UTM grid coordinates in zone 36R: 212840 m E and 3241481 m N); Priabonian, lower part of Birket Qarun Formation.

UM 100184, partial skull roof includes the sutured area of the frontals and parietals from locality ZV-200 (UTM grid coordinates in zone 36R: 214537 m E and 3246438 m N); Priabonian, lower part of Birket Qarun Formation.

CGM 42287, lumbar vertebrae from locality ZV-190 (UTM grid coordinates in zone 36R: 213872 m E and 3240765 m N); Priabonian, lower part of Birket Qarun Formation.

UM 101220, fragments of rostrum and vertebrae (atlas and some thoracics) from locality ZV-220 (UTM grid coordinates in zone 36R: 213658 m E and 3245870 m N); Priabonian, lower part of Birket Qarun Formation.

UM 97520, fragments of isolated left scapula from locality ZV-128 (UTM grid coordinates in zone 36R: 212595 m E and 3242363 m N); Priabonian, lower part of Birket Qarun Formation.

UM 83903, five caudal vertebrae from locality ZV-207 (UTM grid coordinates in zone 36R: 214109 m E and 3245069 m N); Priabonian, lower part of Birket Qarun Formation.

Bed and Formation—The type specimen of *Eotheroides clavigerum* was excavated from the base of the Birket Qarun Formation of Beadnell 1905, a few meters above the top of the Gehannam Formation (Figure 2.3). This level was included in the Gehannam Formation (Gingerich, 1992), however recent stratigraphic revision of the Birket Qarun and Gehannam Formation by Gingerich et al. (2005) and Strougo (in preparation, personal communications 2007) assigned the thick brown shale with gypsum of Wadi Al Hitan to the base of the Birket Qarun Formation.

Age and distribution—The marine mammal-bearing beds from the lower third of the Birket Qarun Formation are early Priabonian in age based on overlap of calcareous nannoplankton zone NP18 and planktonic foraminifera zone P15 (*Globigerinatheka semiinvoluta*). *Eotheroides clavigerum* sp. nov. is only known from the lower and middle parts of the Birket Qarun Formation (Figure 2.3) in Wadi Al Hitan.

Associated Fauna—In addition to *Eotheroides clavigerum*, the same beds produced *Eotheroides sandersi* sp. nov., described later in this chapter. *Protosiren smithae* was described from nearby localities above the interval that produced *Eotheroides clavigerum*. Following Gingerich (1992), the Birket Qarun Formation also contains the archaeocete whales *Basilosaurus isis* and *Dorudon atrox*; with occasional *Moeritherium* (Proboscidea); *Crocodilus* and *Paratomistoma* (Crocodylia); Cf. *Podocnemis* sp., Cf. *Stereogenys* sp., and Cf. *Dermochelys* sp. (turtles); *Pterosphenus schweinfurthi*

(Squamata); *Fajumia* sp., Cf. *Arius* sp., *Cylindracanthus* sp., *Xiphorhynchus aegyptiacus* (bony fishes); and abundant teeth of selachian fishes (sharks and rays).

Diagnosis— *Eotheroides clavigerum* (Figures 4.1-4.11) differs from *Eotheroides aegyptiacum* (Owen, 1875; Abel, 1912) and *E. sandersi* (Figures 4.12 through 4.35) in having convex-upward and strongly arched nasals along midline that are higher than parietals; lacrimal is directed anteroposteriorly and barely exposed laterally; lacrimal foramen is closed. *E. clavigerum* also differs from *Eotheroides sandersi* in having a robust, rugose-edged atlas with knoblike transverse processes directed upward; first rib swollen with tapered end, and middle ribs are pachyosteosclerotic (i.e.: extensively swollen and thickened in bone according to Domning and de Buffrénil, 1991). Moreover, *E. clavigerum has a* short, club-like ilium; flat, broad, and thin ischium; small obturator foramen; short, gracile cleft on medially-pointed pubic bone on both sides, lacking any real symphysis. Dental formula is 2.1.5.3/3.1.5.3., I^1 is enlarged into a tusk; narrow and deep posterior palate, anterior palatal gutter across both upper second premolars (P^2) is narrow and deep. Mandibles run straight along the symphyseal axis.

Etymology— *clavigerum*, Latin. club-like, in reference to the swollen proximal end of the ilium (Figure 4.11).

Description

Premaxilla—Both premaxillae are well preserved in UM 101219 (Figure 4.1, 4.2, and 4.3). UM 94806 includes an isolated left premaxillary blade that is missing its anterior and posterior borders. The premaxillary length from the anterior tip of the symphysal process to the posterior end of the nasal process where it overlaps with the nasal and the frontal is 192 mm in UM 101219. At the tip of the rostrum is a pair of

enlarged alveoli for upper incisor tusks that measure 19 x 15 mm in diameter in UM 101219. Tusk alveoli do not rise higher than the lower third of the premaxillary symphysis. Deflection of the masticating surface of the rostrum is 43˚ from the occlusal plane (Table 4.1). The premaxillary symphysis in all specimens is enlarged relative to the cranium, with the ratio of symphysal length to total length of the skull being about 3:1 (Table 4.1). Left and right premaxillary symphyses meet along a gently convex dorsal border. The rostrum has a weak dorsal keel that is very pronounced at its anterior end and is broadened posteriorly into a strongly convex summit emerging in a flattened peak at the rear of the symphyseal suture.

The nasal processes of the premaxillae are curved in dorsal and lateral views. These have a length of 92 mm in UM 101219, while they are incomplete in UM 94806. The nasal processes of the premaxillae have a suboval cross-section that is 14 mm in diameter in UM 101219, with no sign of dorsoventral flattening (Figure 4.1, 4.2, and 4.3). The most posterior extensions of the premaxillary processes are angular and little-expanded mediolaterally. These are slightly flattened dorsoventrally, but not to the degree seen in *Protosiren*, where they overlap the nasal and frontal bones. As in more advanced dugongs, the mesorostral fossa opens dorsally, pertains an oval outline anteriorly, truncated by the nasals posteriorly as an indicator of an advance stage of adaptation into aquatic environments. The rostral end of the premaxillary canal in *E. clavigerum* enters the premaxilla and maxilla, and penetrates the medial wall of the infraorbital foramina, indicating that vines and nerves enters into the infraorbital canal.

The isolated partial left premaxilla of UM 94806 was somewhat more than 76 mm long, with a straight dorsal border. The rostrum apparently formed a thin dorsal keel

anteriorly, which broadened posteriorly into a strongly convex summit ending in a sharp peak at the rear of the symphysal suture (more or less similar to that in UM 101219). The thin anterior part of the bone is pierced by a large premaxillary canal, but no incisor alveoli are preserved, and there is no indication that the first incisor was enlarged. The nasal process is preserved for a distance of 40 mm behind the symphysis, at that point it has a suboval cross-section that is 7 mm in diameter, showing no sign of dorsoventral flattening. The mesorostral fossa appears to have been broadly semicircular in outline when viewed anteriorly.

Nasal—Nasal bones are elongated anteroposteriorly (Figures 4.1, 4.2, and 4.3). They are exposed dorsally, forming oval wings that reach a length of 65 mm; symmetrical and maintain a 30-mm long contact along their median borders; stout and highly arched upward, rising higher than both frontals and parietals. The lobes or wings are cleft by the frontals posteriorly. The nasals are set into a socket in the anteromedial margin of the frontals; they are exposed dorsally and measure 65 mm along their longest axis (anteroposteriorly). The maximum breadth of both nasals is equal to their anteroposterior axis. Anterolaterally the nasals bear a concavity for the nasal processes of the premaxillae. The lateral sides of the nasals covered by the frontals are 23 mm apart medially, and form the side walls of the upper part of the nasal cavity, which is roofed anteriorly by the arching dorsomedial flanges of the nasals. The ventrolateral side of each nasal is massive and fused to the ethmoid.

Ethmoid region—The nasal arch is long providing a large surface for attachment of the ethmoid. Ethmoid and mesethmoid are preserved in UM 101219, extending below the nasals and along the narial passages. Ethmoids (Figure 4.3) stand vertically and

almost parallel to the medial walls of the nasals; they are 11 mm apart. Turbinals and laminae papyraceae remains are not preserved.

Vomer—The vomer is partially preserved in UM 101219 (Figure 4.2 and 4.3). A 9 mm thick sheath runs along most the internal narial passage. It is exposed in the mesorostral fossa, opening as a U-shaped canal and becoming narrow and constricted laterally and posteriorly. It contacts the maxilla and the palatine before embracing the olfactory chamber.

Lacrimal—The lacrimal is large and irregular, and lacks a lacrimal foramen. It faces posteriorly and slightly laterally, with a distinct prominence laterally (Figure 4.1, 4.2, and 4.3). The lacrimal is surrounded by supraorbital process of the frontal, by the jugal, and by the maxilla.

Frontal—The frontals form the flat part of the skull roof, just behind the upwardly-arched nasals (Figure 4.1, 4.2, and 4.3). The lateral edges of the frontals are sharp and slightly overhanging. The lateral walls of the frontals are constrained and narrow, especially below the frontal-parietal suture. Anterior processes of the frontals on either side of the midline fill a wedge-shaped space between the posterior ends of the nasals, and these slope upward as do the nasals themselves, ending where the nasals meet in the midline. At this extremity the frontals are 7 mm thick where they cover the posterior end of the nasal cavity. The supraorbital process is stout and dense. It is extended anteriorly to embrace the nasal and the tip of the premaxillary processes. The posterolateral corner of the supraorbital process is prominent and distinct and lies forward of the posterior end of the nasal. No postorbital processes are present. The dorsolateral part of each frontal is marked by a distinct crista temporalis in UM 101219. The ratio of the maximum width

breadth across the supraorbital processes to the maximum length of the frontals, reaching the deepest point where the frontal meets the parietal posteriorly, is 0.82.

Parietal—The parietal is heavy and robust in the holotype and marked by a thick crista temporalis and a deep and wide interparietal groove (Figures 4.1 and 4.2). The lateral edges of the convex temporal crests are closest together just behind the frontoparietal suture, and are separated medially by about 29 mm. The parietal roof is more than 20 mm thick anteriorly along the midline. The squamosal overhangs and slightly indents the temporal crest.

Supraoccipital—The supraoccipital is very well preserved UM 101219 (Figures 4.1, 4.2, and 4.3). Very thick and massive, the supraoccipital measures 52 mm along the midline, and its maximum breadth is 70 mm. It has a relatively flat surface, and a pentagonal outline. The nuchal planum is bipartite; lateral to the nuchal planum is a pair of insertions for the rectus capitis dorsalis (Figure 4.3); insertions for capitis semispinalis muscle are not preserved. The anterolateral portion of the supraoccipital is fused with the dorsal process of the squamosal in UM 101219. The nuchal ridge shows weak rugosity. The parietal-supraoccipital angle is about 105º in UM 101219 and the posterior surface of the supraoccipital itself is broadly V-shaped.

Exoccipitals—The exoccipitals are well preserved in UM 101219 (Figure 4.3). They are hexagonal in shape, and connected along a median suture that measures 21 mm. The ratio of exoccipital maximum height to maximum breadth is 0.59. The supraoccipital-exoccipital suture is almost straight. The mastoid foramen is almost closed. The foramen magnum is dome-like, opening downward, with a width that exceeds its height. Occipital condyles are 15 mm apart. A pair of diminutive hypoglossal foramina (44 mm apart)

appear anteroventral to the occipital condyles. Paroccipital processes are very well developed. These separated by 11 mm from the occipital condyles, and extend ventrally deeper than the occipital condyles themselves. The paroccipital processes have tapered, slightly deflected, and curved ends to accommodate the tympanic along with the squamosal.

Basioccipital—The basioccipital is completely fused to the exoccipital and basisphenoid in UM 101219 (Figure 4.2); it is 52 mm long (from the base of the foramen magnum to the fusion line with the basisphenoid) and 22 mm wide. The union of the exoccipital and basioccipital produce an anchor-like bone in the posteroventral corner of the skull. The anterior edge is higher than its posterior. Ventrolaterally and more anteriorly are the insertions of the longus capitis muscles that are preserved as deep longitudinal grooves separated by a prominent median ridge.

Basisphenoid, **Presphenoid**—Both bones (Figure 4.2) are well preserved and are fused to the surrounding elements (orbitosphenoid, alisphenoid, pterygoid, and palatine); sutures are fused. The basisphenoid is flat ventrally and its posterior end higher than its front. The presphenoid is projected cranially out of the basisphenoid as it starts narrowing and its median crest becomes sheath-like and directed anterodorsally before joining the vomer.

Orbitosphenoid—The orbitosphenoid is partly destroyed by cementation, it is exposed laterally and is bounded by the frontal and alisphenoid dorsally, the alisphenoid posterolaterally, alisphenoid and palatine laterally, and the palatine ventrally. Foramen rotundum is exposed anterolaterally (Figure 4.1), the anteroposterior opening serves as a

canal between cranial and pterygoid-palatine fossae. Below the foramen rotundam is the optic foramen, which is partially open.

Alisphenoid—The alisphenoids have excellent preservation UM 101219 (Figure 4.1). They are 75 mm deep dorsoventrally, and are 82 mm apart. The squamosal, parietal, and frontal contact the alisphenoid dorsally; and the squamosal dorsolaterally. The alisphenoid is strongly fused with the palatine and the pterygoid, and covers the palatine posterior wing on both sides while the pterygoid covers its posteromedial wall. The alisphenoid canal is absent, instead the alisphenoid foramen (14 mm in diameter in UM 101219) opens posteriorly and directly to the base of the braincase. A pair of concavities occupy the most lateral posterior corners of the basisphenoid above the pterygoid fossa that might have been used the remains of the posterior openings for the alisphenoid canal.

Pterygoid—The pterygoid is preserved on both sides along with its processes and grooves (Figure 4.1, 4.2, and 4.3). Medial walls of the pterygoid are 45 mm apart as measured in UM 101219. It is fused to the basisphenoid dorsally, the palatine mediolaterally, and alisphenoid posterolaterally. Lateral and medial edges are strongly pronounced and converge posterodorsally at the posterior corner of the basisphenoid, they gently curves anteriorly and end projected backward ventrally; median edge stands vertical while lateral edge diverges 20º laterally.

Palatine—The palatine represents the anteromedial component of the pterygoid processes (Figures 4.1 and 4.2). Both palatines are curved anteromedially before re-joining posteroventrally along the midline; however the ventral reunion is not evident in UM 101219 since most of the palatine is damaged medial to M^3 and M^2, on the other hand the anterior edge along the ventral midline lies between P^4 and dP^5. The palatines

contact the pterygoid posteromedially and alisphenoid posterolaterally, and overlap the posterior edge of the maxillae anteriorly and anteroventrally. They also form the posterior wall between the internal nares and the temporal fossa by contributing most their plates by merging with the presphenoid medially and the orbitosphenoid anterolaterally.

Maxilla—Maxillae are very well preserved in UM 101219 (Figures 4.1, 4.2, and 4.3). They have a lyre-shaped palate. Molar teeth (M^{1-3}), alveoli for a triple rooted dP^5, and single-rooted alveoli for P^4 through C^1 are clear. The maxillary dental battery extends posteriorly with a 16 mm atrophied behind M^3 in UM 101219. The orbital bridge (zygomatic bridge), which provides the ventral and mediolateral cover for the infraorbital foramen, is 65 mm long UM 101219. The infraorbital foramen is almost suboval and opens anteriorly with width and height of about 21 X 26 mm in UM 101219, and are placed about 61 mm from each other across the rostrum. The depth of the zygomatic bridge above the alveolar shelf of M^1 in UM 101219 is 26 mm. Ventrally, the maxilla is slightly curved and narrow. In a lateral profile, it is deflected 30º downward from the horizontal palate at the narrowest point in the rostrum where the lyriform edges of the palatal ventral gutter are 12 mm wide and 11 mm deep. Furthermore this deflection is anterior to the zygomatic-orbital bridge and exactly at the alveoli of P^1 on both sides. After the anterior constriction and narrowing the maxillae forms a slightly broad shelf before splitting laterally and ending with a large incisive foramen (the anterior palatine foramen). The latter foramen has a heart-like cross-section, lies in a deep concavity where it is formed together by the maxilla and the premaxilla, and opens downward.

UM 97524 includes a virtually complete right maxilla (Figure 4.4) with all alveoli of (P^{1-4}) and four three-rooted molariform teeth (dP^5-M^3). The palatal gutter that would have been about 1.5 cm wide and 0.5 cm deep lay between the toothrows anteriorly. The zygomatic-orbital bridge is about 50 mm long anteroposteriorly, and reaches a thickness of 16 mm near its posterior edge which lies at the level of the anterior alveoli of M^2. The ventral side of the bridge is elevated about 1 cm above the alveolar margin.

Squamosal—The squamosal makes a large portion of the posterolateral sides of the skull, and it extends dorsally high enough to indent the temporal crest (Figures 4.1, 4.2, and 4.3). The mastoid foramen in UM 101219 is almost closed. The sigmoidal ridge is laterally projected in the posterolateral edge the squamosal, it appears below the mastoid foramen and extends down to the ventral tip of the post-tympanic process. The sigmoidal ridge is eroded in UM 101219. The zygomatic process is roughly lozenge-shaped in lateral view, with a nearly straight posterodorsal edge that is very slightly convex laterally. The processus retroversus of the squamosal is slightly developed. The anterior end tapers somewhat without reaching the level of the supraorbital process; the anterodorsal edge is distinctly concave in outline. The zygomatic process in UM 101219 is 96 mm long and 39 mm wide dorsoventrally; its root is 43 mm long anteroposteriorly. Ventrally, the mandibular fossa, entoglenoid bar, and temporozygomatic suture are all shallow and weakly defined. The sphenosquamosal suture is flat and indented; and the suture with the parietals is interdigitated with rugose posteromedially. The cranial portion of the squamosal, along with the basioccipital, capsulates the periotic in semicircular socket which is deep and cylindrical in shape in the cranial portion of the squamosal root.

Jugal—The jugal is very well preserved on both sides in UM 101219 (Figures 4.1, 4.2, and 4.3). The total length of the jugals is about 177 mm with a maximum dorsoventral height of 44 mm below the postorbital process. The preorbital process is thin and lies against the maxillae. The deepest point, the ventral process of the jugal, is smooth and curved surfaced with a rounded tip, mediolaterally compressed, and it lies directly beneath postorbital process, and above the maxillary shelf. The postorbital process is a blunt summit and lies against the anterior tip of the zygomatic process of the squamosal. The zygomatic process is gracile, rounded behind the postorbital process, flattened and thin posteriorly, and curved medially at its posterior tip just to the front of the mandibular fossa. The zygomatic process of the jugal is very well preserved; it is directed more laterally than medially; posterior end of the jugal is rounded and slightly curved-back medially just to the front of the glenoid process.

Periotic—The petrotympanic bone is damaged on both sides by gypsum, however only the tympanic ring (Figures 4.1 and 4.2) is preserved and directed and inclined medially forming an angle less than 45 degree with the pars mastoidea.

Mandible—UM 101219 has the best and the only preserved lower jaw in the collected material of this species (Figures 4.1, Table 4.5).

The lower jaw of UM 101219 preserves almost all of its morphological features on both dentaries (mandibular rami with coronoid and condylar processes, mandibular corpora, mental and mandibular foramina, symphysis and masticating surfaces, and number of check teeth). The total length of the mandible is approximately 210 mm plus the length of the broken anterior tip of the symphysis. The depth of the mandibular corpus below M_1 is about 48 mm. Dental rows (magazines) run parallel to each others

from M_3 to P_1 where both sides start converging to seal the posterior side of the symphysis. Anterolateral sides of the mandibular corpora are characterized by the presence of a large mental foramen (12 mm in diameter) located just below the canine; 3 or 4 secondary mental foramina decreasing in size posterodorsally are located behind the main mental foramen; in addition to these there are at least two more foramina positioned above the mental foramen and its downwardly open groove and below the alveoli of the masticating surface.

The symphysis is strongly fused, deeply cleft ventrally, deflected about 38 degrees from the mandibular corpus, and bulbous posteroventrally; it has a length of 62 mm, plus the length of the broken tip of the mandible (protuberantia mentalis=mental protuberance), and is 71 mm high as measured below the posterior edge of I_3 and the base ventrally. The outline of the ascending ramous is perpendicular to the mandibular corpus posteriorly, curved at its posteroventrad, and ascends upward smoothly. The masticating surface of the symphysis consist of a pair of rows with rounded alveoli (sockets) for three incisors, the widest are the most anterior pair. The masticating surface is narrow anteriorly (18 mm wide across I_1) and widen posteriorly (36 mm across the I_3) and has a length of 50 mm plus the length of the mental protuberance. The posteromedial portion of the masticating surfaces is connected to a narrow gutter that is 3 mm wide and 3 mm deep. This short gutter intially emerges as forward continuation of the labial rims in the symphysal area as both mandibular corpora start converging medially near the canine alveolus; after this the gutter disappears while a weak ridge runs along the rest of the rostrum medially to the broken end of the mental protuberance (Figure 4.1).

The length of the mandibular ramus and corpus are perfectly perpendicular to each other; the mandibular ramus is 64 mm; it is very thin at the temporalis and zygomatico-mandibular muscle scar attachment. The condyle process is oval in shape, about 23 mm wide and 14 mm long anterodorsally, and extends 117 mm from the base of the angular process. Coronoid process is thin and raised 130 mm from the most ventral point of the angular process to its back-ward curved dorsal peak. The mandibular notch is quite well preserved on the right side of UM 101219; it is deep and subcircular to crescent-shape. The internal oblique line connecting the mandibular ramus with mandibular corpus is robust and stronger than the external line. A prominent shallow trough (coronoid canal) is located just behind M_3 is partly filled with cancellous bone; in fact the coronoid foramen appears to be exposed in the dental capsule in the median side of the mandibular ramus behind M_3 and the mandibular foramen. The mandibular foramen opens below the anterior edge of M_3; it is 14 mm in diameter at this point and extends posterodorsally in an acute angle to form a flute-like groove. The posteroventral corner of the angular process is rounded with a thick edge, the internal side of the angular process (surface attachment for pterygoidus internus) is flanged and curved medially on both sides.

Upper Dentitions—The quality of the preserved material and number of specimens allowed for determination of the formula for the upper dentition of *Eotheroides clavigerum* (Figures 4.1, 4.2, and 4.38; Table 4.2). The dental formula for the upper dentations is 2.1.5.3 and 3.1.5.3 for the lower counterparts.

The upper first incisor is a medium-sized tusk positioned at the anterior tip of the premaxilla of UM 101219 (Figures 4.1, 4.2, and 4.3). The total length of tusk with its root is 36 mm; the crown is 13 mm long and the base is between 8 and 10 mm wide. The tusk

has an oval crosssection; the crown is cone-shaped and its tip is worn out exposing its dentine. There is no sign of I^2 or its alveolus; the alveolus at the posterior end of the premaxilla thus was assigned to I^3. However, I^3 is not preserved, its alveolus is the only alveolus lies between the canine and tusk, it follows the tusk after a 46 mm diastema in UM 101219.

The upper canines are not preserved, but their alveolae that are separated from I^3 by a 13 mm diastema in UM 101219. Following the canine alveoli, there are 4 pairs of single rooted alveoli marking the locus for P^{1-4}, followed by a three-rooted pair of empty alveoli for dP^5. The distemata between the alveoli of C and P^1, P^1 and P^2, P^2 and P^3, P^3 and P^4, and P^4 and dP^5, are 13, 25, 7, 3, 2 mm, respectively, in UM 101219.

Associated with the skull of UM 101219 is what seems to be a right P^2 (Figure 4.1); the tooth has been assigned to the P^2 because the roots fits in the alveolus. The root and the crown are preserved and they are measured together about 21.4 mm in total height. The crown is 8.00 mm high, 7.62 mm long and 6.45 mm wide; it consists of a large centrolabial cusp directed lingually showing slight wear that increases labially; a smaller cusp is lingually associated with the main centrolabial cusp; together, both cusps separate the cingulum into two heels or valleys. To the front of the two cusps a pair of cusplets marks the lingual cingulum; posterior to the main cusp, and still lingually, another pair of cusplets takes a lower position on the postcingulum.

dP^5 is missing on all maxillae; the three alveoli (one of them is damaged) that follow M^1 in UM 101219 are the only marks left from its root. M^{1-3} are preserved on both maxillae of UM 101219. The cheek teeth are bilophodont, trigon higher than talon, proloph is larger than metaloph, and there is a gradual increase in the teeth size distally.

M^1 exposes the most wear facets of all molars, width slightly exceeds length, and labial cusps are deeper and with less wear than lingual ones, with paracone being the highest. Para- and lingual cingulae are more developed than meta- and labial cingulae. The occlusal surface of M^1 in UM 101219 has suffered excessive honing and grinding. M^2 is more or less square, cusps are higher than those in M^1 and lower than M^3, paracone is the highest cusp as in M^2. Interlophs (intervalleys) are deeper than these in M^1 (Figures 4.2 and 4.38). Dentine is less exposed in the lophs than in M^1. Cingulum is weakly developed or almost absent labially, and cingulum obliqum is very well developed.

M^3 has the best preservation, showing the least wear and is the largest of all molars in UM 101219, being 32% larger than M^1 and 15% larger than M^2. The protoloph is wider and slightly lower than metaloph, and both are separated lingually and labially by deep valleys; a lingual cingulum blocked these valleys, and no labially cingulum appears on M^3 in UM 101219. The metacone is the highest cusp and the smallest major cusp, and protocone is the largest. Protoconule is relatively large and positioned equidistant between the protocone and paracone; the three cusps were aligned to form a transverse ridge in early stages before the appearance of wear surfaces. The precingulum is a simple transverse ridge; initially it arises from the most anterolabial corner just at the base of the paracone, extends lingually and reaches its peak just in front of the protocone, its anterolingual corner bears a single cusp that is mostly obscured by wear in older individuals. The lingual cingulum is marked by up to four small cuspules; it extends from the anterolingual base of hypocone then gently curves and ascends to join the posterolingual base of the protocone. The postcingulum is a low transverse ridge that is confined posteriorly behind the metaloph, higher at the posterior base of the hypocone,

and it is cleft with a wide angle. The valley between the metaloph and the postcingulum in UM 101219 has an open v-shape and the valley between the metaloph and the postcingulum is open mesiodistally.

The maxilla of UM 97524 (Figure 4.4) contains alveoli for four large single-rooted premolars (P^{1-4}) and four three-rooted molariform teeth (dP^5-M^3). These alveoli contain roots for dP^5-M^2; M^3 was fully erupted as its roots were distinct and separate. The four anterior alveoli are each about 7 mm in diameter; the anteroposterior lengths of each set of alveoli for the molariform teeth are 11, 12, 15, and >15 mm, and their transverse widths are about 14, 15, 17, and >16 mm, respectively. The bone extends for 28 mm anterior to the P^1 alveolus, and only a small part of it is missing where a canine might have been located. The alveoli of P^1 and P^2 are separated by a 12 mm diastema. The surface of a break passing just behind dP^5 was excavated in search of an unerupted P^5, but none was found. The toothrow is distinctly convex laterad from P^2 to M^3. The posterior end of the intermaxillary suture (i.e., the location of the anterior end of the palatine) lies at the level of the posterior dP^5 alveoli.

Lower Dentitions—The lower dental formula of *Eotheroides clavigerum* (UM 101219 in Figure 4.1; Table 4.2) is 3.1.5.3. UM 101219 has dp_5 - m_3 preserved on the right side; m_{1-3} are partially preserved on the left side. In front of dp_5 there are 9 or 10 single alveoli for the roots of p_4-i_1; extra alveoli are remnant of incomplete resorbtion of the alveoli in deciduous postcanine teeth that often appeared as small rounded alveoli in front of the permanent alveoli.

i_1 through p_4 are missing from the lower jaw on both sides; all alveoli are empty and shallow indicating that lower premolars and incisors were replaced and lost long before

actual death of UM 101219. Alveoli of i_1 through C are 16, 11, 10, and 10 mm, in anteroposterior length, respectively; and 7, 8, 9, 12 mm, in mediolateral width, respectively. There is a 3-4 mm of medial separation between the left and right canines and incisors. i_1 and i_2 alveoli are separated from each other by an 8 mm diastema; i_3 and c alveoli follow after 6 mm diastemata each. Diastemata between the successive teeth of c, p_1, p_2, and p_3 are all equal to 2 mm, respectively. There is a notable diastema between p_3 and p_4 and is measured 7 mm on the right side and 4 mm on the left side. p_4 and dp_5 are separated by a 3 mm diastema.

dp_5-m_3 are bilophodont (Figure 4.1; Table 4.2), double-rooted teeth increasing in size distally, and m_1-m_3 possessing well-developed talonids; occlusal surfaces are strongly worn with m_1 and dp_5 exhibiting extreme wear. The transverse crest shows a steep lateral wear gradient where the lingual cusps are higher and sharper than the buccal cusps.

dp_5 is the smallest and the highest of all molariform teeth; it is heavily worn; metalophid (entoconid and hypoconid) is wider and longer than protolophid (entoconid and hypoconid); crista obliqua is absent and there are no signs of hypoconulids; a posterior facet on the crown fits with the front wall of m_1.

m_2 is smaller than m_3 and larger than m_1 and dp_5; metaconid and entoconids are very well preserved, crista obliqua extends for 3 mm between the metalophid and protolophid into two lakes of dentine; hypolophid is obscured by wear. m_1 and m_2 have no hypoconulids, instead a posterior cingulid or distocristid is very prominent. In m_1 the metalophid is longer and narrower than the protolophid and both are slightly separated from each other by a crista obliqua that is only 1 mm in length.

m_3 is partially preserved on both sides and is the largest in the series; the hypoconulid is small, low and prominent, consisting of a sharp cusp; metalophid is larger than protolophid; crista obiqua is broken on both sides; interlophids (intervalleys) are narrow and shallow.

Vertebrae— UM 101219 (Figures 4.5, 4.6, and 4.7; Table 4.6) preserves the atlas, axis, centrum of the third cervical, the fifth cervical, and the centrum of the last cervical; thoracic series include 16 vertebrae arranged serially based on their size and morphology of their capitular-tubercular facets, and missing the fourteenth through sixteenth thoracic vertebrae and the lower most thoracic ones; the lumbar region is completely missing in the type specimen; what seems to be a sacral vertebra preserves a centrum, and has a broken transverse process bearing a rounded and robust medial crosssection. The tail is represented by a proximal vertebra with articulation facet for the chevron bones on the ventral side of the centrum, the transverse processes are broad and erected horizontally. The end of the tail preserves two medially elongated centra, and the most posterior caudal preserved here has distinctive flatten anterior and posterior epiphyses. All vertebrae have their end plates perfectly fused to the centra. UM 101220 preserves an atlas that is identical to that, of UM 101219, and a posterior caudal vertebra. In addition to that UM 83903 contains five caudal vertebrae. The vertebral series in this taxon may include 7 cervicals, 19 thoracics, 4-6 lumbars, 1 sacral, and 22-24 caudal vertebrae.

The atlas (Figures 4.5, 4.6, and 4.7; Table 4.6) has a robust, rugose edge, and knoblike transverse processes directed dorsolaterally. The dorsal arch bears a pyramid-like summit protuberance. Articular facet for the odontoid process is smooth and tilted posteriorly as in *Eotheroides sandersi*, the cranial edge is slightly notched cranially, and

its distal edge protrudes for a distance caudally longer than that in *Eotheroides sandersi*. Cranial cotyles are larger and deeply concave than the caudal sides.

The axis (Figures 4.5, 4.6, and 4.7; Table 4.6) has a neural spine that is robust and swollen, and is directed cranially downward. Neural canal is oval. Centrum has a semicircular outline caudally bearing a keel on its ventral surface. The transverse processes are short, thin and directed posterolaterad; transverse foramina are unusually large, occupying most of the area of the transverse processes. The cotyles are relatively convex; the projecting odontoid process is shorter than the centrum, and its ventral surface bears only the keel but not any other structures.

C3 (Figures 4.5, 4.6, and 4.7; Table 4.6) lacks its neural arch; centrum is short, craniocaudally flattened "compressed", and bears a keel ventrally; transverse processes are flanged and directed anteroventrally with its base flattened horizontally. The transverse foramina are 6-8 mm in diameter.

C5 (Figures 4.5, 4.6, and 4.7; Table 4.6) bears a neural spine that has a pointed summit. The zygapophyseal articular surfaces face ventrally and dorsally. The centrum is marked by a short keel dorsally and is smooth ventrally. The transverse foramina measures 14 x 12 mm. the transverse processes stand in the same plane as the centrum, however, their ventral sides (below the foramina) form a ventral lamina horizontal and prolonged caudally and bear a keel or a ridge on their ventrally face. This distinguishes C5 from C6 in *Eotheroides*. C6 is not known from this species, however in *Eotheroides aegyptiacum* (Sickenberg, 1934: pl. 4, fig. 1) the ventral lamina bears on its ventromedial surface a distinct low ridge inclined posteroventrally.

C7 (Figures 4.5, 4.6, and 4.7; Table 4.6) has a centrum bearing the right transverse processes. The centrum is compressed craniocaudally but is relatively longer than the anterior cervicals (excluding the axis), cranial and caudal outlines are rectangular in shape, cranial articulation surface is more flattened than its caudal. Dorsal keel is weak and no sign of a ventral keel exists. The transverse process is projected anterolaterally; it is robust with a ventrolateral knob-like process. Transverse foramen is open in a form of a deep notch. Demifacets for first rib are present at the lateroventral end of the caudal articulation surface.

Th1 (Figures 4.5, 4.6, and 4.7; Table 4.6) is the tallest and widest of all thoracics. Neural spine widest anteroposteriorly just above the neural canal, anterior edge is slightly sharp at its lower third and blunt dorsally and flat at top. Posterior surface is concave anteriorly with lateral edge forming thin wall to engulf the anterior edge of the spinous process of the succedent vertebra. Neural canal is semicircular, enlarged and widen, it is the largest neural canal posterior to C7, and caudally it is subcircular with width exceeds height. Transverse processes are stout and short, and bear articulate facets for rib tuberculum on their ventrolateral corner. Prezygapophyses are 45 mm distant from each others, slightly straight, and shallow; postzygapophyses are partially preserved, flat, and meet along median line forming an angle of 150˚. The base of the neural arch (pedicle) is massive and robust on both sides. The centrum is almost twice as long as the last cervical, width is twice the height and length, caudal and cranial articulation surfaces are flatten and fused to the body. Dorsal surface of centrum is flat cranially and slightly elevated, 2-3 mm, caudally; ventral surface lacks any pillar or keel; rib capitular articulations form small cups that are deep.

Th2 (Figures 4.5, 4.6, and 4.7; Table 4.6) has the spinous process convex cranially, and has the widest anteroposterior length of any spine in the vertebral series; anterior edge blunt with an extended dorsal surface longer than that of Th1. Anterior edge is blunt, slightly bent backward in profile view; posterior surface engulfing the anterior edge of the spinous process of Th3 is fusiform, convex and expanded laterally at its base. Prezygapophyses are 35 mm distant from each others, asymmetrical, left side is deeper and more flatten that the right; postzygapophyses are more or less flatt and separated from each other by a median groove. Neural canal is narrower than the antecedent counterpart and larger than the succedent (Th3), it has a more or less triangular crosssection cranially and more rounded caudally. Transverse processes are more rounded and shorter than those of Th1, and demifacets of tuberculum articulation are more laterally positioned and larger and more circular than those in Th1. Centrum is slightly eroded and a bit longer than the first thoracic, end plates are firmly fused to the centrum body, posterior articulation surface is wider laterally and shorter dorsoventrally than the cranial face; ventral surface is gently concave downward but not forming an arch. Rib capitular articulations are larger and deeper on the caudal surface.

Th3 and Th4 (Figures 4.5, 4.6, and 4.7; Table 4.6) have massive spinous processes that are directed backward, and are more robust and anteroposteriorly shorter than the spine of Th2. Transverse processes are elevated above the dorsal surface of centrum, shorter, rounded and more massive than the anterior ones. Prezygapophyses are close to each others, symmetrical, deep laterally and elevated medially. Postzygapophyses are slightly tilted from midline sliding more ventrolaterally, and notably separated by a groove that is slightly wider than that which appears on Th2. Neural canal is smaller and

more rounded than those in Th1 and Th2. Epiphyses are firmly fused to the centrum; anterior surface is convex while the posterior side is concave.

Th5 and Th6 (Figures 4.5, 4.6, and 4.7; Table 4.6) bear heavy and massive spinous processes. Transverse processes are more elevated, and more massive and more bent dorsally. Neural canal as small as in Th4. Centra are more enlarged and widen caudally; their dorsal surface lack any ridges; epiphyses are fused to the centrum; ventrally they show slight convexity; vascular foramen is small and preserved on the right side only.

Th7 through Th9 (Figures 4.5, 4.6, and 4.7; Table 4.6) have their spinous processes shorter, less bent backward, and less robust with a sharp anterior edge than in the antecedent thoracics. Cranial epiphyses are flattened and enlarged and slightly concave; caudal epiphyses are heart shape due the presence of a depression on the dorsal surface of the centrum and the extension of the rib facet more laterally. Ventral surface of centra is slightly concave, however at Th8 a ventral pillar is developed that is more pronounced.

Th10 through Th12 (Figures 4.5, 4.6, and 4.7; Table 4.6) possess spinous processes that are thinner and shorter posteriorly; neural canals are smaller and wider than high; anterior and posterior epiphyses are heart shape. Pre- and postzygapophysis are longer and are elongate rather than flat; postzygapophyses are divergent laterally from midline. Rib demifacets are smaller and shallower signaling the shift of the rib articulation facets towards the center of the centrum.

Th13 (Figures 4.5, 4.6, and 4.7; Table 4.6) is partially preserved, but it has both rib capitular and tubercular articulation surfaces convoluted in the transverse process.

Th17 and Th18 (Figures 4.5, 4.6, and 4.7; Table 4.6) are almost identical. However the spinous process of Th18 is more flattened, larger, and compressed mediolaterally than

Th17, and continues with sharper anterior and posterior edges. Prezygapophyses protrude more cranially and closer to each others than those in the antecedent vertebrae; also the prezygapophyses have their articular facets or plane inclined dorsomedially about 45˚. Capitular and tubercular articulation surfaces show convolution into one open shallow socket divided equally between the top of the centrum and below the base of the neural arch. Centum has heart-shaped outline, strongly biconcave toward its center; ventral surface bears a narrow pillar directed anteroposteriorly, and lateral to the pillar two vascular foramina open laterally. Epiphyses are strongly fused to centrum and both are concave caudally.

There probably were one or two more thoracic vertebrae following Th18, since the capitular and tubercular articulation surfaces are not completely closed and developed into a short transverse process.

The sacrum (Figures 4.5, 4.6, and 4.7; Table 4.6) is a single, partially preserved vertebra that is missing its neural arch and transverse processes; the base of the transverse processes have rounded cross section on both sides of the centrum. The sacral vertebra is short in craniocaudal length, has a wide epiphyses, and is reduced in height; its ventral surface is concave, lacking any keels or ridges.

The caudal region (Figures 4.5, 4.6, and 4.7; Table 4.6) is preserved in three vertebrae; the size and morphology of the largest of these three make it a strong candidate for the second (Ca2) or third (Ca3) caudal vertebra. Both transverse processes are straight, horizontal, and flatten; the neural arch and postzygapophyses are very reduced compared to the anterior vertebrae in the trunk, prezygapophysis are missing; neural canal is narrow and dorsoventrally compressed caudally. The centrum has hexagonal

outlines; its epiphyses are fused to centrum and partly eroded, and are flat cranially and concave caudally; demifacets for both anterior and posterior chevrons on ventral surface are preserved.

The remaining two caudals are from the distal end and were assigned to ?Ca16 and ?Ca19, and both of them are almost certainly positioned in the fluke and beyond the peduncle since they have greatly diminished transverse processes and also because they have dorsoventrally compressed centra, and lack neural arches, and articulation on their ventral surface.

The more anterior caudal vertebra (?Ca16) has very short transverse processes close to the centrum, directed and tapered posteriorly; the centrum has a larger epiphysis anteriorly than posteriorly; cranial and caudal ends of the dorsal surface along the midline are slightly elevated. The ventral side sides of the transverse processes are truncated by a pair of shallow grooves one on each side. These grooves probably served as an attachment for the sacrococcygeus ventralis tendons. The extreme distal vertebra (?Ca19) is asymmetrical and very small, biconvex anteroposteriorly and dorsoventrally; the dorsal surface bears a fine keel, while there are laterally remains of the diminutive transverse processes. Anterior and posterior articulation areas are oval in shape. This is not the last vertebra in the tail since it has a concave caudal epiphysis.

UM 83903 consists of five associated caudal vertebrae, comparable in size to those above. The centra have distinct, sharp midventral and middorsal keels. The thin epiphyses, tightly connected to the centra, are clearly visible. In the two most anterior vertebrae, the ventral sides are nearly flat and the transverse processes are scarcely elevated above this level.

CGM 42287 is a series of six more or less eroded vertebrae from the anterior caudal region. The largest and presumably most anterior of these (probably Ca2) bears on its underside what may be traces of chevron demifacets on the rear edge only. The ventral side of the centrum is almost flat, with only a very faint median keel, and gives the centrum a distinctly trapezoidal shape in end view. The undersides of the transverse processes lay in almost the same plane as that of the centrum, as in the sacral and caudals described for UM 97514. The centrum is 61 mm wide, 40 mm high, and 43 mm thick; the neural canal was about 23 mm wide. The other caudals all exhibit small demifacets for chevrons on both ends. The transverse processes are gently inclined downward and backward. The fifth and best-preserved vertebra in the series had an estimated width across the transverse processes of 132 mm; the centrum measures about 56 mm wide, 42 mm high, and 38 mm thick; and the neural canal is 16 mm wide.

Chevrons—A few chevron bones were preserved with caudal vertebrae of UM 101219. The anterior pairs are long dorsoventrally, short anteroposteriorly, and unfused at their distal end. The angle between both bones in all chevron is less than 30º and consistent craniocaudally.

Ribs—UM 101219 has 19 rib pairs (Figure 4.8; Table 4.7), of which 4 or 5 pairs were connected to sternum, and the last rib is extremely reduced and probably was fused to the last thoracic vertebra. All ribs, excluding the 19th, have real capitular facets that connect directly to the articular surface on the centrum.

First rib (R1) is perfectly preserved from the left side of the ribcage with considerable pachyosteosclerosis and missing from the right series (Figure 4.8; Table 4.7). It connects C7 with Th1, it has a tapered distal end, not a truncated end as in other contemporaneous

taxa including *Eotheroides sandersi.* The anterior capitular facet is rounded and is twice the size of the posterior facet. The neck is 20 mm long, cylindrical and almost straight. The tubercular facet is level with the capitulum, forming a knoblike summit. The angle of external deflection between the proximal end and the shaft, is about 150˚, and the angle region is characterized by a flat, circular (10 mm in diameter) ligament attachment. There is considerable variation in thickness and crosssectional area along the shaft; proximal end of the shaft is oval in crosssection, midshaft is more or less triangular in crosssection and swollen laterally and posses a prominent ridge posteromedially. Just below midshaft, the anterior edge bears a prominent anterior protuberance; just below this protuberance the distal end begins to flatten and tapers toward the broken rogues end.

Second through fourth rib (R2-R4) are perfectly preserved on both sides, are banana-like in over all morphology (Figure 4.8; Table 4.7), and show extreme pachyosteosclerosis.

Second rib (R2) is larger than R1, bears prominent anterior and posterior capitula; neck is almost straight and more robust than the neck of R1; tuberculum is very weak and small, followed by a small mediolateral elongate depression or fossa. The angle is almost the same as of R1, however the proximal mediolateral surface is broader and inclined dorsally lowering the tangent of the surface almost to 45˚ with the mediolateral horizontal surface. Proximal crosssection of the shaft is rounded and becomes more or less square just above midshaft; midshaft is almost quadratic to trapezoid crosssection. The distal third of the rib shows the greatest degree of swelling with the widest crosssection in the rib; the tip of the lower third ribs tapers abruptly to the apical point forming a cone whose summit is the attachment area for the coastal cartilage.

Third and fourth ribs (R3 and R4) are biconvex anteroposteriorly; they have more rounded and more robust heads and shaft than R2; the widest crosssection is at midshaft. Capitular facets are rounded and are lower than the tubercular facet; ventral surface of the head is broader and more straight mediolaterally than those in R1 and R2. Distal end tapers abruptly towards the apical area for the attachment of the coastal cartilage.

Fifth and sixth ribs (R5 and R6) have more or less cylindrical shafts, that are rounded and uniform in cross-sectional area along most of the shaft before the distal end tapers gently towards the apical attachment area. The ventral faces of the neck and head are flatten and broad. Iliocostalis thoracic muscle attachment areas are large in both ribs. The end of the distal third of the shaft is compressed mediolaterally.

Rib seven through fourteen (R7-R14) are compressed mediolaterally (Figure 4.8; Table 4.7); heads project horizontally and are reduced in length; proximal end of the shaft has an oval crosssection before becoming rounded distally; the lower third of the shaft is swollen. The distal end, which tapers toward the coastal attachment region, is flatten and more compressed mediolaterally than those of the antecedent ribs.

The posterior third of the ribcage (R15-R17) is partially preserved, represented by heads and/or proximal shafts (Figure 4.8; Table 4.7). Heads are small with broad ventral faces; capitular and tubercular regions are almost convolute and more closer to each other in posterior ribs. Shaft crosssection is more or less rounded.

R18 is partly preserved on both sides; it is the shortest “functional rib” at an estimated length of 220 mm; the head is straight and very reduced anteroposteriorly; shaft is gracile and cylindrical in shape; the distal end tapers very gently towards the apical attachment

area and has a small oval crosssection. It is not clear whether the last thoracic vertebrae (Th19), the prelumbar, had a fused rib (Figure 4.8; Table 4.7).

Scapula—The right scapula of UM 101219 (Figure 4.9; Table 4.8) is perfectly preserved but missing its acromion process; UM 94806 partially preserved, sandblasted and broken cranial and dorsal margin, and missing acromion process; UM 97520 preserved the proximal side however the acromion process and coronoid process were not fused to the glenoid cavity and are missing.

The scapula of UM 101219 is sicklelike, stout, and is marked by a robust spinous process missing the acromion process. The total length of the blade is 228 mm, and the maximum breadth of the dorsal portion across the spine is 76 mm. The spine is thick dorsoventrally bearing dull edges; at midsection the spine is thinner but still blunt. The glenoid fossa is deeply concave anteroposteriorly and shallowly concave transversely; it is measured 51, 38, 29 mm for its anteroposterior length, mediolateral breadth, and depth, respectively. The coracoid process is broken, but bears a well-defined oval muscle scar on its medial side; when scapula and humerus are articulated, this muscle scar lines up precisely with the bicipital groove. The supraspinous fossa is broad with well defined cranial and superior angle, and marked by striations towards the vertebral border; it is twice as large as the infraspinous fossa which is very narrow but gets larger towards the vertebral border; striations also mark the vertebral border of the infraspinous fossa. The subscapular fossa on the medial side of the blade is slightly concave bearing an enormous striation.

In UM 94806 the maximum length of the blade is 218 mm, width of the dorsal part of the blade (which is probably a little short of the actual width) is 65 mm; the width of the

dorsal-most part, at the level of the sharp teres major protuberance, is 58 mm. Dorsally, the spine rises to a height (measured from the medial side of the scapula) of 26 mm; more ventrally it is reduced to a height of about 21 mm before rising again to more than 30 mm at the acromion, whose tip is missing. The spine is thickest dorsally (the remnant of a tuber spine) and elsewhere very thin, due in part to erosion. Except for a very faint ridge extending for about 2 cm parallel to the midsection of the spine, the infraspinous fossa bears no trace of the "crista postscapularis" described by Sickenberg (1934: 28) in *E. aegyptiacum*. The glenoid fossa is similar to the one in UM 101219 from the same side, but slightly wider transversely. The coracoid process is very small and bears the well-defined oval muscle scar on its medial side. Subscapular fossa is broader than UM 101219 and lacks any striations due to sandblasting.

Humerus—The humerus of the holotype UM 101219 (Figure 4.9; Table 4.8) and the right humerus of UM 94806 are almost identical, although the latter is few mm longer. UM 94806 shows better preservation and more anatomical details since the humerus in UM 101219 has been partially damaged by mineralization. In UM 94806 the proximal epiphysis is partly fused to the shaft, but the suture is still conspicuous. The head is irregularly heart-shaped, being notched anteriorly at the top of the bicipital groove. The greater tubercle forms a thin but prominent flange, with a narrow surface for muscle attachment on its summit. The lesser tubercle has an irregular surface and forms the medial edge of a shallow bicipital groove. This groove continues proximally over a low threshold and ends in a shallow cul-de-sac on the bone's proximal surface, bounded posteriorly by the notched border of the head (cf. Sickenberg, 1934: fig. 4b). The deltoid crest, located some 70 mm from the summit of the greater tubercle, is distinct but small

and thin in comparison to that of Neogene dugongids; an almost flat, rectangular surface separates it from the bicipital groove. A slightly accentuated ridge marks the insertion of the pectoralis major, another 4.5 cm distally. A continuation of this ridge joins the medial edge of the trochlea. On the posterior side, a convex, somewhat spiral ridge (ectocondyloid crest) extends from midshaft to the ectepicondyle. The sagittal diameter of the shaft (about 28 mm) greatly exceeds the transverse diameter (18 mm). The entepicondyle is very strong, protruding far posterior as well as distal to the trochlea. The coronoid fossa is distinct; the olecranon fossa is very deep. The axis of the trochlea is inclined about 85˚ to that of the shaft.

The only humerus of *Eotheroides aegyptiacum* hitherto described was an incomplete juvenile specimen (Sickenberg, 1934: p. 29-30); apart from its smaller size, it closely resembles the humerus of UM 94806, but it is not clear how reliably these can be distinguished from *Protosiren fraasi*, whose humerus is also inadequately known (Sickenberg, 1934: 93-94). However, UM 94806 is clearly different from the humerus of *Protosiren smithae* described above. Although these bones are almost exactly the same size and have the same general appearance and proportions, UM 94806 is distinguished by possession of the cul-de-sac on the proximal end, a more mediolaterally compressed shaft, a prominent ectepicondylar crest, a smaller trochlea, and a much more posteromedially salient and mediolaterally compressed entepicondyle.

Radius and Ulna—The right radius and ulna of UM 101219 are very well preserved and fused together at their proximal and distal ends leaving a 7-8 mm space between both shafts in lateral view (Figure 4.9; Tables 4.10 and 4.11). The ulna is missing the top of the olecranon making its end roughened and rugose; both radius and ulna are missing

their distal epiphyses. The preserved length of the ulna is 145 mm, and 120 mm for radial length. The ulna and radius of this species are the longest among contemporaneous Fayum sirenians.

The ulna is slightly convex posteriorly; olecranon is tilted 20˚ backward and is coaxially aligned with the main axis of the shaft; the olecranon rises 26 mm above the ulnar articular surface and is 35 mm long anteroposteriorly across its tuberosity.

Both ulnar (proximal) and radioulnar (distal) articular surfaces for humerus articulation are asymmetrical and separated by a non articular surface; ulnar surface is strongly concave anteriorly; ulnar notch is narrow at its proximal end (16 mm wide), while the radioulnar measurers 38 mm mediolaterally at marking the widest region of the shaft. The proximal radioulnar tuberosity where both bones are fused is triangular in shape, runs for 26 mm distally (as measured medially) and 30 mm mediolaterally. Below the notch articulation, the shaft is stout and robust; its medial surface measures 16 x 20 mm for its mediolateral and posterior diameters at the diaphysis, respectively, and 65 mm for circumference; the shaft is wide distally, and is slightly projecting at its lowest posteromedial corner. The distal end is rectangular in shape with a rugose surface and indented outline where the missing epiphysis used to fit.

The radius is slender and gracile; the dorsal surface of the head (the articulation surface) is semicircular and is divided into two regions, medial (small and shallow), and lateral (enlarged and deep). The neck is as wide as the head and bears the radial tuberosity. The shaft has a uniform ovoid crosssection between the head and just 15 mm above the distal end; it is slightly convex posteriorly, and is slightly compressed anteroposteriorly; mediolateral and anteroposterior width at midshaft measure 19 and 12

mm, respectively, and 55 mm for the circumference. The groove of extensor tendons facing anteriorly and slightly laterally, is shallow and walls of the groove are thin and weak, they are thinner and less prominent than those found in *Protosiren smithae*. The distal epiphysis is missing leaving a rugose surface for attachment with curved square outline that is more rounded posteromedially.

Metacarpals and Phalanges—Identifiable hand bones of UM 101219 (Figure 4.10; Table 4.12) are all from the right side and these include: metacarpals I, II, and III, and a proximal phalange. All metacarpals have their proximal epiphysis fused, however only metacarpal III retained a solidly ossified distal epiphysis. The only phalange from the right hand is fairly well preserved although is missing its proximal epiphysis.

Metacarpal I is the shortest of all metacarpals of UM 101219; its proximal articulation surface with the trapezium is triangular in shape; shaft has an oval crosssection; slightly flattened in dorsal plane while ventral plane curves inward; distal articulation end with the first phalanx is larger and wider than proximal end; articulation with metacarpal II is notched along a proximal posterior rugose surface.

Metacarpal II is distinguished in having the largest proximal and distal articulation surfaces and crosssectional area at midshaft. It may have an equal length to metacarpal III considering that the distal epiphysis of metacarpal II has the same length of the associated distal epiphysis. Carpal articulation surface has trapezoidal outlines. Intermetacarpal facets between both anterior and posterior metacarpals are shallow and curved inward.

Metacarpal III has a slightly complicated proximal end that is compressed anteroposteriorly, and the proximal articular surface with the carpal facet is extended

dorsoventrally, and intermetacarpal facets are grooved on both sides. The dorsal surface of the shaft is flattened while the ventral surface is slightly keeled, midshaft is oval in crosssection, and the distal epiphysis is wider than the proximal one.

The only preserved phalanx is most probably proximal phalanx I or II. It has an oval proximal end that has a dorsoventral height that exceeds its anteroposterior width. The dorsal plane of the shaft is slightly concave, while its ventral side is almost convex inward. The distal half of the shaft, including distal epiphysis, is flattened, and retained an elongated tuberosity along its distal edge. The distal articulation surface is tightly fused to the end of the shaft, articulation facet is smooth and rectangular in shape.

Innominates—Both innominates of UM 101219 (Figure 4.11; Table 4.13) are well preserved; the left side has better preservation since it was found covered in the original matrix, while the right side is partly sandblasted with an eroded ischium and minor damage in the ilium. The total length for the left side is 215 mm while the right side is 10 mm shorter (Figure 4.11; Table 4.13).

The ilium is short (145 mm in the left side and 128 for the right side), massive and bears extreme swelling (clubbing) on its proximal side especially in the lateral (external) view, the medial side where it contacts the pleurapophyses of the sacral vertebra (sacroiliac joint) is oval in shape (52 x 44 mm as measured on the left side for its anteroposterior length and dorsoventral height, respectively), and concave laterally, and is extremely rugose indicating strong attachment with the sacrum via cartilage. Distal to the sacroiliac joint, the ilium narrows and becomes rounded as it reaches midshaft, 23 mm in diameter, then gets broader by towards the acetabulum.

The acetabulum is rounded and is 19 mm in diameter and 9 mm deep, it is deep and closed anterodorsally and posterodorsally, and is shallow and open downwardly. The acetabular notch is very weak, but still marked by a fine ridge in the lower third of the socket. The ischium is long, broad, and curved medially and makes an angle of 160˚ with the long axis of the ilium and 110˚ with the pubic bone; it is 88 mm long as measured from the center of the acetabulum, dorsoventral breadth is 33 mm midway between the acetabulum and the posteriormost edge of its tuberosity; internal and external sides are smooth, except on its distalmost edge where its slightly thickened and roughened as it is striated. The pubis is short, gracile, and triangular in shape with a pointed distal end lacking any pubic symphysis; both pubic bones are cleft on both sides; the clefts intrude the ventral wall of the 5-mm diameter obturator foramen.

EOTHEROIDES SANDERSI sp. nov.

Figures 4.12 through 4.36; Tables 4.14 through 4.25

Holotype—CGM 42181, Cairo Geological Museum. This specimen is an association of cranial and postcranial elements (Figures 4.12, 4.18, 4.26, 4.30, and 4.34; Tables 4.14, 4.18, 4.21, 4.22, and 4.25), including the skull roof (composed of nasals, frontals, parietals and supraoccipitalis), exoccipitals, sphenoid, parts of the right squamosal, mandibular symphysis, three thoracic vertebrae, five caudals, 16 ribs from the right side (missing the first and second ribs), left second rib, right scapula, left and right humeri, left innominate and right ilium, and both femora (missing epiphyses).

Geological Occurrence—*Eotheroides sandersi* skeletons and partial skeletons were collected from the lower and middle part of the Birket Qarun Formation of Beadnell 1905 (Figure 2.3).

Age—The lower part of the Birket Qarun Formation is equivalent to the upper Mokattam series, which is Priabonian in age (Gingerich, 1992).

Type locality—The University of Michigan field locality in Wadi Al Hitan ZV-230 (Figures 1.4 and 1.5; Table 1.2), some 75 km west of the city of Fayum, and 140 km southwest of Cairo. UTM grid coordinates for the holotype are within zone 36R and read as 215294 m E and 3247161 m N.

Referred Specimens—UM 111558 (Figures 4.13, 4.14, 4.16, 4.19, 4.20, 4.21, 4.23, 4.29, 4.31, 4.33, 4.36, 4.38 and 4.50; Tables 4.14, 4.15, 4.15, 4.16, 4.20, 4.21, 4.22, 4.23, 4.24, 4.25 and 4.26) includes a cranium of an adult individual, missing its lower jaw. Preserved teeth with crowns include left and right M^{1-3}, P^{2-3} and C. X-RAY images show that all teeth are erupted. Postcranial elements include a partial vertebral series (C1, C5,

Th2-Th16, Th18, L1, ?Ca5-Ca7, ?Ca12-Ca13, ?Ca16, and ?Ca19), 13 ribs from the right side (R1-R11 and R13, ?R17) and eight from left side, xiphisternum, left scapula and humerus, right ulna, metacarpal, and left femur missing its epiphyses. Locality ZV-174 (Figures 1.4 and 1.5; Table 1.2) (UTM grid coordinates within zone 36R: 212541 m E and 3243789 m N); Priabonian, middle part of Birket Qarun Formation, collected from the fine gold thick sand some seven meters above the White Camp Layer (Gingerich 1992).

UM 97514 (Figures 4.22, 4.23, 4.25, 4.28, 4.35; Tables 4.17, 4.19, and 4.25) includes a partial vertebral series (Th4-Th15, Th17, L2-L4, S, Ca1-Ca6, Ca8-Ca10, and ?Ca16), the posterior two-thirds of the ribcage, and both innominates. Locality ZV-110 (Figures 1.4 and 1.5; Table 1.2) (UTM grid coordinates within zone 36R: 211562 m E and 3242250 m N); Priabonian, lower part of Birket Qarun Formation, friable sandstone layer just above “the White Camp Layer” (Gingerich 1992).

UM 94809, a skull roof including nasals, frontals and the parts of the parietals (Figure 4.15). Locality ZV-079 (Figures 1.4 and 1.5; Table 1.2), (UTM grid coordinates within zone 36R: 210909 m E and 3241668 m N), Priabonian, lower part of the Birket Qarun Formation.

UM 100138, partial right and left dentaries (Figure 4.15), vertebrae and ribs. Locality ZV-180 (Figures 1.4 and 1.5; Table 1.2), (UTM grid coordinates within zone 36R: 212541 m E and 3243088 m N), Priabonian, lower part of the Birket Qarun Formation.

UM 97515, isolated ulna of a juvenile individual (Figure 4.32, Table 4.23). Locality ZV-117 (UTM grid coordinates within zone 36R: 214945 m E and 3242312 m N); Priabonian, lower part of Birket Qarun Formation.

Diagnosis—Small; enlarged infraorbital foramen (Figure 4.14); slightly concave nasals (Figure 4.13); slender, straight processes running at an acute angle to the midline, with posterior edge slightly curved with no major scour or corner; dental formula 2.1.5.3/3.1.5.3.; alveolus for I^1 for a small tusk; I^3 precedes upper canine immediately without a diastemata, short [what?] atrophied behind M^3; mid palate wide, broad and shallow; shallow and slightly constricted ventral rostral gutter across P^1. The atlas has squared transverse processes (Figure 4.19), extended laterally and directed downward. The first rib is compressed anteroposteriorly at its mid shaft and has a broad distal end (Figure 4.27). The innominate has a short, swollen, and club-like ilium (Figure 4.34). Innominates bear extremely long and narrow pubic bones (Figure 4.35); robust, and considerably laterally projected ischia; the obturator foramen is larger than any other in Dugongidae.

Etymology—Named after Dr. William J. Sanders of The University of Michigan for his contributions to the Cenozoic mammals of Africa, especially Tethytheres, and who has also collected and prepared many of the sirenian fossils from the Eocene of Egypt.

Description

Premaxillae—Both premaxillae are perfectly preserved in UM 111558 (Figure 4.13). The premaxillary length from the anterior tip of the symphyseal process to the posterior end of the premaxillary arm (nasal process), where it overlaps with the nasal and the frontal, is 170 mm. The premaxilla-maxilla lateral contact is steep. At the tip of the rostrum is a pair of small and shallow alveoli that are filled with sand; tusks are absent and appear to have been diminutive based on alveolar diameter. Deflection of the masticating surface of rostrum from the occlusal plane is about 50˚. Rostral length to the

total length of the skull is about 1:3 (Table 4.14). The rostrum forms a dorsal keel which is very pronounced anteriorly and broadened posteriorly at the rear of the rostral suture. The nasal processes (the premaxillary arms behind the rostrum) are relatively concave in lateral profile, with a length 85 mm. These processes have sub-oval cross-sections of seven mm in diameter. The posterior ends of the premaxillary processes are angular and pointed, and overlap the nasal and the frontal bones. The mesorostral fossae each have an oval outline anteriorly, truncated by the nasals posteriorly.

Nasals—Nasals (Figures 4.12, 4.13, 4.14, and 4.15) are slightly concave upward, rising at the level of frontals and parietals; are long and in contact along the midline, with the lobes separated by the frontals posteriorly.

Dorsally, the nasal is exposed on the skull roof for a distance ranging from 50 mm (in UM 94809) to 59 mm (in UM 111558) (Table 4.14); the ratio of the maximum breadth of both nasals to their anteroposterior axis is 0.83 (Table 4.14). The nasals form a forward-pointed median projection, on either side of which a V-shaped indentation of the anterior nasal margin intervenes between the midline and the premaxilla. The dorsomedial margin of the nasal is prolonged into a flange to meet its opposite side in a suture that is 29 mm long ventrally (measured in UM 94809), 40 mm long where exposed dorsally. The sutural surface bears posteroventrally-inclined interdigitations.

In the holotype (CGM 42181) (Figure 4.12) the nasals are broken anteriorly but are large, separated posteriorly by frontal internasal processes about 25 mm long, and form a high arch over the nasal cavity. Between the bodies of the nasals, the nasal cavity is 16 mm wide

Lacrimals—The lacrimal is relatively large (Figure 4.13 and 4.14), slightly exposed laterally with a distinguished prominent knob, and lacks a foramen; it is bounded by the supraorbital process, premaxilla, maxilla, and jugal.

Frontal— In CGM 42181 (Figure 4.12), the frontal roof is convex, with a median trough on its posterior half that is bordered by a pair of low ridges. The lateral edges of the broadly convex temporal crests are closest together just behind the frontoparietal suture, and are separated medially by about 10 mm. The frontals form the flat part of the skull roof just behind the concave nasals. The lateral walls of the frontals are narrow especially below the frontal-parietal suture. Medial and most anterior processes of the frontals incise between the posterodorsal corner of the nasal lobes. At this extremity, the frontals are at least seven mm thick (CGM 42181), and roof the posterior part of the nasal cavity.

The ratio of the maximum breadth across the supraorbital processes to the maximum length of the frontals reaching their deepest points (exposed dorsally along the midline) where the frontal meets the parietals posteriorly is measured as 0.86 and 0.70 in CGM 42181 and UM 111558, respectively (Table 4.14). The supraorbital processes are thin dorsoventrally, and intersect the mid-line at a 30° angle. Crista temporalis is weak on both sides of the frontal (Figures 4.12, 4.13, and 4.14). The posterior dorsolateral contact between the frontals and parietals is marked by a pair of prominences appearing only in UM 111558 (Figure 4.13).

UM 100184 (not illustrated) is comprised of the thick and dense posterior part of the frontals and anterior part of the parietal of a small sirenian. The frontal portion has a flat roof and is square in cross-section; the parietal is slightly more trapezoidal in section due

to the rounding of the temporal crests. These begin at the anterolateral corners of the parietal roof, converge backward, and are separated by a furrow only five mm wide where the bone is broken. The medial edges of the crests are steep and distinct, the lateral surfaces gently rounded and continuous with the temporal wall. The parietal roof is 16 mm thick in the midline where broken; the width of the roof at the frontoparietal suture is 34 mm. The suture is V-shaped dorsally and broadly V-shaped on the endocranial surface. The interfrontal suture is 22 mm long endocranially. The bony falx is either broken or eroded along the 10 mm of the preserved frontoparietal suture.

Parietals—These bones are narrow and elongate dorsally in all specimens (Figures 4.12, 4.13, 4.14, and 4.15); they each have a thick crista temporalis that curves to produce a deep and narrow interparietal groove. The minimum separation between both cristae is 14 mm in UM 111558. The squamosal overhangs and slightly indents the temporal crest in all cases, but they are not exposed dorsally.

The skull roofs of UM 94809 and UM 100184 have only fragments of their parietal portions; these form the usual V-shaped suture with the frontals. The skull roof where this suture intersects is very narrow, especially in UM 100184, and the thickness of the parietal roof in the anterior midline is less than 15 mm. In CGM 42181 the bony falx, internal occipital protuberance, and tentorium are all prominent.

Supraoccipital— The supraoccipital of the holotype CGM 42181 (Figure 4.12) is 12 mm thick at the posterior end of midline, 43 thick mm along the midline slope posteriorly, and 57 mm wide. In UM 111558 (Figures 4.13 and 4.14) the supraoccipital is very well preserved, and is detached from exoccipital, as in the holotype. It has a relatively flat surface, and a hexagonal outline. The nuchal planum is bipartite with a

weak median ridge, most prominent along the medial line from the top, and fades out downwardly; this ridge separates concavities for the rectus capitis dorsalis muscle insertions. Lateral to the rectus capitis dorsalis muscle insertions are the sites for another pair of insertions for capitis semispinalis, which are smaller and closer to the lateral, stout borders of the supraoccipital. The anterolateral portion of the supraoccipital is partly fused with the squamosal upper processes. The nuchal ridge (a crest in *Protosiren*) is semicircular in shape, curved laterally, and lacks rugosities. The parietal-supraoccipital angle is 120º, and the posterior surface of the supraoccipital itself is broadly V-shaped. The anterior top of the exoccipital and the posterior end of the parietals bare an emissary foramen, in some cases closed due to fusion, which pierces the external occipital protuberance close to the midline, and leads into the transverse sulcus.

Exoccipitals— The exoccipitals (Figures 4.13, and 4.14) are well preserved, connected along a 15 mm median suture, so that the foramen magnum is separated from supraoccipital. The ratio of maximum exoccipital height to maximum breadth is 0.49. The supraoccipital-exoccipital sutures form a V-shaped angle of 130º in UM 111558. Dorsolateral edges are thickened and flanged laterally, providing room for the mastoid foramen. The foramen magnum is 24 mm high mm and 32 mm wide. Occipital condyles are large and kidney-like, and are greatly separated at their bases in the holotype. Hypoglossal foramina are located anteroventrally to the occipital condyles and are 45 mm distant from each other. The paroccipital processes extend down deeper than occipital condyles; they are eight mm below the base of the occipital condyles, and are 12 mm distant from them ventrally; these processes are very well developed and prominent.

The exoccipitals are badly eroded in CGM 42181(Figure 4.12), but share a common median suture about 10 mm long; the ratio of their maximum height to maximum breadth is 0.49. The supraoccipital-exoccipital suture forms an angle of 132º in CGM 42181.

Basioccipital— The basioccipital is well preserved and completely detached from the basisphenoid in UM 111558 (Figures 4.13 and 4.14). It measures 43 mm along its ventral length (from the base of the foramen magnum to the fusion line with the basisphenoid) and 18 mm across its waist. The anterior edge is higher than its posterior. Longus capitis muscles are weak and asymmetric. The epiphysis is concave with trapezoidal outlines.

Basisphenoid, **Presphenoid**— Are fused together to form a gentle arch similar to that in UM 101219. The basisphenoid is wide open at the pterygoid process (Figures 4.12, and 4.13). Cranial and posterior contacts of the presphenoid are not defined since the internal nares are closed with cemented sediment.

Orbitosphenoid—This element is perfectly preserved with all foramina open from bottom to top: the alisphenoid opening, optic canal in the middle, and foramen rotundum at top (Figure 4.13). The alisphenoid opening (a canal in primitive sirenians including protosirenids, but not in *Eotheroides* or *Eosiren*) extends anteroposteriorly for about 30 mm inside the cerebral chamber as a shallow groove and ends open in the pterygoid glenoid fossa; the anterior opening is connected with a downwardly groove for the external pterygoid muscles. The optic foramen is seven mm in diameter; it enters the through the orbitosphenoid toward the antero-lateral portion of the cerebrum chamber as it opens medially to the alisphenoid groove cerebrally. Foramen rotundum is open at the

top, lateral corner of the orbitosphenoid and enters the cerebral chamber medial to the ethmoidal region.

Alisphenoid—Both sides in UM 111558 are perfectly preserved (Figure 4.13). The alisphenoids are 68 mm high, and 67 mm distant from each other at the base of their walls. However, they are shorter than the alisphenoids in *Eotheroides clavigerum*. The squamosal, parietal, and frontal contact the alisphenoid dorsally, and the squamosal dorsolaterally. On each side, the alisphenoid is strongly fused with the palatine and the pterygoid, and covers the palatine posterior wing while the pterygoid covers its posteromedial wall. An alisphenoid canal is absent; instead, the alisphenoid foramen, about 11 mm in diameter in UM 111558, opens posteriorly and directly to the base of the braincase.

Pterygoid—In the holotype, the pterygoid is very damaged (Figure 4.12); however, UM 111558 preserves both sides with distinct processes and deeply grooved posterior trochlear surfaces (Figure 4.13 and 4.14). It is completely fused to the surrounding elements as in other dugongs.

Palatines—These elements are flat in UM 111558 (Figure 4.13), narrowest posterior to M^3, and slightly wider when they contacts the maxilla anteriorly, just 10 mm behind the anterior opening of the infraorbital foramen. The posteroventral edge of each palatine is strongly concave inward where the posteroventral edge of the internal nares is located. The posterolateral walls of the palatines extend behind M^3 to contact the pterygoid.

Maxilla—Maxillae are very well preserved in UM 111558 (Figures 4.13 and 4.14). Molar teeth (M^{1-3}), alveoli for a triple rooted dP^5, and single-rooted alveoli for P^4 through C^1 are clear. The atrophied portion of the bone behind M^3 is short. The orbital

bridge (zygomatic bridge), which provides the ventral and mediolateral cover for the infraorbital foramen, is about 53 mm long in UM 111558 and extends ventrally from the end as far as M^2 to the posterior edge of the P^2 alveoli. The infraorbital foramen is sub-oval and opens anteriorly with width and height of about 20 mm x 21 mm in UM 111558. The depth of the zygomatic bridge above the alveolar shelf of M^1 is about 20 mm in UM 111558. Ventrally, the maxillae and the palatines form a spear-like palate with its widest breadth across the anterior edge of M^2 in UM 111558. The maxilla is smoothly deflected about 30º downward from the horizontal palate at the narrowest point in the rostrum at the beginning of the ventral gutter across P^1, where the palatal surfaces are 14 mm closest to each other in UM 111558.

Squamosals—The dorsal ends of the squamosals (Figures 4.12, 4.13, and 4.14) overhang the posterolateral corner of the parietal roof on each side. Its indentations are just 5 mm from the temporal crest. Mastoid foramina open on both posterior sides (Figures 4.13, and 4.14). The zygomatic process in UM 111558 is 86 mm long and 32 mm wide dorsoventrally; its root is 36 mm long anteroposteriorly. It is roughly lozenge-shaped in lateral view, with a nearly straight posterodorsal edge that is very slightly convex laterad as in UM 101219. The rear edge of the zygomatic root is notched with a distinct processus retroversus. This process is well-developed and slightly inflected (Figure 4.13). The anterior end tapers somewhat without reaching the level of the posterior end of the supraorbital processes (Figures 4.13); the anterodorsal edge is distinctly concave in outline. Ventrally, the mandibular fossa, entoglenoid bar, and temporozygomatic sutura are shallow and slightly pronounced (Figure 4.13). The mandibular fossa, entoglenoid bar, and temporozygomatic sutures are shallow and less

pronounced than those in UM 101219. The postglenoid process is knoblike and raised 11 mm above the mandibular fossa; between the post-tympanic process and the postglenoid process is the arcuate-shaped external auditory meatus, which is nine mm in antero-lateral length and about eight mm in mediolateral diameter (Figure 4.13). The posterior wall formed by the post-tympanic process extends deeper downwardly than the anterior wall that is formed by the posterior edge of the postglenoid process. The post-tympanic process is enlarged and ends with a projecting facet for insertion of the sternomastoid muscle, which is a primitive feature according to Domning (1994). A sigmoidal ridge is present but weak in UM 111558.

Jugals—The jugals are complete and 133 mm long in UM 111558 (Figures 4.13 and 4.14). The preorbital process of the jugal is thin and laid against the maxillae, and is isolated from the premaxilla. The deepest point in the jugal, the ventral process of the jugal, has a smooth, curved surface with a rounded, knoblike, mediolaterally compressed projection and it lies directly beneath the lower postorbital process and above the maxillary shelf. The postorbital process is a blunt projection and lies against the anterior tip of the zygomatic process of the squamosal. The posterior (zygomatic) process of the jugal is slender and oval in cross-section, complete at its tip in UM 111558, and reaches a little behind the edge of the temporal fossa (Figures 4.13 and 4.14).

Periotics—The petrotympanic bone (Figure 4.16) has an excellent preservation in UM 111558 and is not fused to any of the skull bones (Figure 4.16); however, it fits in a socket formed by the posteromedial wall of the squamosal and partially by the exoccipital. The squamosal covers the lateral and dorsolateral portions of pars mastoid leaving the posterolateral corner (processes fonticulus) of it exposed; the exoccipital

covers the periotic posteroventrally and partially posteromedially. The tympanic ring is directed anteroposteriorly (Figure 4.16); it is dense, flat and thin ventromedially; it has a length of 22 mm, a maximum height 30 mm, and the internal diameter of the ring is 10 mm. The malleus is very well preserved; it is small, cone-like, stout and rounded at it base narrow, and pointed at the top; the manubrium mallei appears as a distinct ridge along malleus and reaches the sulcus tympanicus. The processus folianus (processus folii of the malleus, according to Robineau, 1969) and incus are pushed medially by the tegmen tympani; the tympanohyale is narrow and short.

The pars temporalis (=tegmen tympani) is lenticular in shape extending 14 mm below tegmen tympani and slightly squished dorsoventrally (Figure 4.16); and is perpendicular to the tympanicum ring. The stapes are not preserved in any specimen. The pars mastoidea forms the posterolateral third of the pterotympanic bone. The pars mastoidea and pars temporalis are solid and dense; they are separated by the perlymphatic conchoidal groove posteromedially where the perilymphatic duct used to be attached and penetrate both parts laterally through the perilymphatic foramen; the promontorium connects both pars. In cerebral view both parts are smooth and separated by the sulcus facialis and foramen endolymphaticum.

Dentaries—The dentaries of CGM 42181 are incomplete (Figure 4.12); only the front portion of the lower jaw and symphysis is preserved. The symphysis is synostotic. The height at the deflection point of mandibular corpus is a little more than 54 mm. Minimum dorsoventral breadth of mandibular corpus is more than 37 mm; the maximum breadth of the masticating surface is 21 mm. At least one accessory mental foramen is

present on left side, above the principal foramen. Alveoli are obscure. The masticating surface is narrow and incomplete.

UM 100138 (Figure 4.17) is a sandblasted and toothless mandible of *E. sandersi*. Both corpora are complete on the right side but considerably damaged on the left, and the rami are missing. The symphysis is fused but marked ventrally throughout its length by a deep, narrow cleft. The symphyseal deflection is between 40^{o} and 50^{o}. The symphyseal masticating surface is badly weathered but relatively narrow, and bore two rows of alveoli that were not separated by any appreciable space. At least three small accessory mental foramina lie posterior to the principal foramen on the right side. The mandibular corpus is slender; its ventral margin is asymmetrical and moderately arched and sharply downturned at the symphysis. The mandibular foramen is not bridged or divided.

Upper dentitions— The dental formula for the upper dentations is 2.1.5.3 (Figures 4.13 and 4.38; Table 4.15). The anterior tip of the premaxilla of UM 111558 has a pair of broken alveoli for the first incisor (Figures 4.13 and 4.14), which was smaller than the tusk in *Eotheroides clavigerum*. The alveolus of I^3 is preserved at the posterior end of the premaxilla; and there is no indication of I^2. However, I^3 is separated from I^1 by a 38 mm diastema in UM 111558; in the same specimen, the upper canine alveolar is reduced and follows I^3 by a diastema of three mm. The only canine known for the species is partially preserved from the left side of UM 111558, and is missing its root. Its crown is very well preserved:it is 4.2 mm long, 3.7 mm wide, and 4.7 mm high, stumpy and barrel-like showing elliptical wear with its labial edge higher than its lingual edge.

Following the canine alveoli, there are four pairs of single-rooted alveoli marking the loci for P^{1-4}, followed by a triple-rooted pair for dP^5. The distemata between the alveoli

of C and P^1, P^1 and P^2, P^2 and P^3, P^3 and P^4, and P^4 and dP^5 are 14, 18, 10, 3, and 2 mm, respectively, in UM 111558.

P^1 is missing, leaving an empty alveolus. P^2 and P^3 are complete teeth preserved from the right side of the maxilla of UM 111558, while P^4 is missing from the maxillae, and dP^5 is missing in all maxillae. P^2 has a height of 18.8 mm, including the root and the crown together. It consists of a large single labial cusp. Height, length, and width of the crown are 7.0, 6.8, and 6.4 mm, respectively. The central cusp is directed inward; the lingual cingulum is deep and crenulated while the labial cingulum is weak and faded in the labial heel of the central cusp. The root is 11.6 mm high, with roughly a triangular cross-section 4.5 mm in diameter. P^3 has a height, length and width of 7.0, 6.7, and 6.1 mm, respectively. The central labial cusp is directed inward as well, associated with a smaller lingual cusp, and another posterior cusp that is not part of the cingulum. The cingulum is very well developed lingually and less pronounced labially. The root has an oval cross-section, and measures between 4.2 and 4.5 mm for its diameter.

M^{1-3} are exceptionally preserved on both sides of the maxillae of UM 111558, converse of the condition of the teeth in *Eotheroides clavigerum*. Almost all cusps are preserved, with very minor tooth wearing.

M^1 has a perfectly preserved crown with slight wear on its proloph; its width slightly exceeds its length, and anterior width exceeds posterior width. Labial cusps are higher than lingual ones, with the paracone being the highest cusp. Para- and lingual cingulae are more developed than meta- and labial cingulae.

M^2 is 28% larger than M^1, and the paracone is the highest cusp. Interlophs are deeper on the labial side, while they are wide and shallow lingually. Dentine is exposed as small

transverse lakes in the lophs on the lingual side. Cingulae border the M^2 lingually and labially, and the cingulum obliqum is long and very well developed.

M^3 is the largest of all molars. It is 18.5% larger than M^2 and about 41.5% larger than M^1. It shows no wear. Like the teeth of UM 101219, the protoloph is wider and slightly lower than the metaloph, and both are separated lingually and labially by deep valleys; however, a lingual cingulum blocks these valleys, while labially a shallow cingulum appears on both M^3 in UM 111558, though it is absent in UM 101219. The precingulum extends labiolingually, covering the anterior front of the protoloph. The lingual cingulum is distinct. The labial cingulum is short, and bears a cleft extending from anterior base of the metacone to the posterior base of the paracone. The postcingulum is higher lingually than labially; it is shallower than the one in UM 101219. The valley between the metaloph and the postcingulum is narrow.

Lower dentitions— No tooth crowns are preserved in the mandible of UM 100138 (Figure 4.17). The trough behind M_3 area is sealed with bone, with only a circular outline preserved. A fully erupted M_3 was present and had an anteroposteriorly-elongate posterior root. Forward of this tooth are preserved the two roots of M_2 and the two much smaller roots of M_1, immediately in front of which is a piece of matrix 3 mm in diameter which appears to occupy the anterolabial corner of the M_1 alveolus. Anterior to this is another alveolus 5 mm in diameter, for P_5 or the posterior root of a dP_5. The alveolar row is damaged for the next 25 mm, then a section with four alveoli is preserved near where the mandible's dorsal edge is turned down. Forward of this are only uncertain traces of incisor alveoli. All that can be said is that there was more than ample room for a 3.1.5.3 dentition.

Vertebrae— The holotype CGM 42181 (Figure 4.18) preserves two cervicals, three thoracic and five caudal vertebrae. The more complete individual UM 111558 (Figures 4.19, 4.20, and 4.21; Table 4.17) contains a perfectly preserved atlas, third cervical, second through sixteenth thoracic serially in order, the last thoracic, three middle tail vertebrae, and four posterior tail vertebrae.

UM 97514 includes the fourth through sixteenth thoracic (Figures 4.22, 4.23, 4.24, and 4.25; Tables 4.17), three lumbars (L2-4), a single sacral, caudals Ca1-6, Ca8-10, and one of the most posterior caudals; all these vertebrae have thin but well-developed epiphyses, firmly fused to the vertebral bodies. The vertebral bodies are mainly composed of cancellous bone and are connected to dense neural arches and spines. UM 100138 has four mid-thoracic vertebrae; The vertebral formula for *Eotheroides sandersi* is reconstructed as C7, T18-19, L4-5, S1, and Ca 20-22.

The atlas (Figures 4.19, 4.20, and 4.21) is smaller in size than that of *Eotheroides clavigerum*, and its transverse processes are square-like. They extend laterally and tilt posteriorly downward, keeping the vertebral artery passage visible craniocaudally; the first cervical nerve ran transversely behind the top of the anterior condyles and its passage is visible dorsolaterally. Lateral to that and still behind the condyles is a deep sulcus for the vertebral artery runs down to the transverse foramen. The dorsal arch bears a weak pointed summit and preserves the scars of rectus capitis dorsalis minor cranially, while caudally the summit is gentle and smooth. The ventral surface of the atlas is concave and smooth, the articular facet for the odontoid process is smooth and tilted posteriorly, the cranial edge is slightly concave cranially, and its distal edge slightly

protrudes caudally. The condyles are larger and more deeply concave on the cranial than caudal side. The vertebral canal is wide and keyhole-shaped, higher than wider.

C3 (Figures 4.19, 4.20, and 4.21) of UM 111558 has a damaged vertebral body; however the body seems to be flattened craniocaudally and lacks a ventral keel. The neural arch has knob-like summit. The neural canal is subtriangular. The prezygapophyses are flattened and face ventromedially, and postzygapophyses face ventrolaterally. Transverse processes are wide, flattened, and tilted from the main vertical plane of the vertebral body. The transverse foramen is damaged. The holotype (Figure 4.18) seems to have the centrum of C3; however, meaningful landmarks are broken away..

T2 (Figures 4.19, 4.20, and 4.21) is preserved in UM 111558; it has a thick, long neural spine that is straight, with a concave anterior edge and bluntly straight apex, transverse processes perpendicular to the arch and the neural spine and extended laterally more than the following thoracics; the vertebral foramen is oval in shape; prezygapophyses are inclined medially and facing anteroventrally, while postzygapophyses are directed posterodorsally; zygapophyses do not project beyond the most anterior tip of the transverse process or the most posterior edge of the neural spine.

T3 (Figures 4.19, 4.20, and 4.21) is partially preserved in UM 111558. Its vertebral body length is the same as in T2, and its ventral surface is concave anteriorly without a keel. The transverse processes are knoblike; the remaining preserved prezygapophysis is flat, horizontal, and directed forward. The shape of the vertebral canal is ovoid, but smaller than that of T2.

T4 (Figure 4.19, 4.20, and 4.21) is preserved in UM 111558. Its neural spine is shorter than that of T2 and is directed backward; the transverse processes make an angle relative to the neural arch and spinous process; the zygapophyses are in the same planes as of T2; and the vertebral canal is smaller, subrounded and notched at the top. The vertebral body is heartlike, with its prezygapopyses positioned at its top lateral sides, while the postzygapophyses are more elongated than the cranial ones.

T5- T11 (Figures 4.19, 4.20, 4.21, 4.22, 4.23, and 4.25) bear thick, heavy neural spines that are strongly inclined backward, with bluntly rounded apices and concave posterior surfaces. More posteriorly, the latter surfaces develop a median ridge, faint at first but eventually becoming so prominent that the spines have no posterior surface but only a sharp posterior edge. The spines progessively become thinner and more vertical. Transverse processes are angled upward from the neural arches. In dorsal view, they are irregularly rectangular in outline and are perpendicular to the body axis. More posteriorly, they are shorter and appear more horizontal, and their forward edges are swept back, making them more triangular in dorsal view.

The pedicles of the neural arches are very thick and massive, visually dominating the relatively small and constricted neural canal, which on all the thoracics has a sharply peaked apex. A thick, rounded ridge extends from the front edge of the tubercular costal facet down and medially to the forward edge of the prezygapophysis. This ridge separates the ventrolateral surface of the transverse process and pedicle from the more or less broad and flat anterior surface, which is especially distinct on the more anterior thoracics. This feature also is common in all Eocene Tethyan genera, including *Protosiren* and *Eotheroides*, and was designated the "Vorderfeld: the border of the field"

of Sickenberg (1934). Posterior and more or less parallel to this ridge is another, irregular and ill-defined one (crista subcostalis) that descends beneath the posterior edge of the tubercular facet. Between the zygapophyses and the base of the neural spine, on both front and back sides, the surfaces of the neural arch are sculpted by ridges into pairs of crescentic concavities to which Sickenberg (1934) applied the term "Area". According to his description, these features are characteristic of all Priabonian *Eotheroides* in contrast to *Eotheroides aegyptiacum* from the middle Eocene of Gebel Mokattam. The vertebral bodies have dorsal indentations and concave ends, and lack any distinct midventral keel; although the undersides of the vertebral bodies are convex, the epiphyseal surfaces of some appear irregularly and asymmetrically flat-bottomed in end view.

T12- T16 (Figures 4.19, 4.20, 4.21, 4.22, 4.23, and 4.25; Tables 4.16 and 4.17) have long zygapophyses projecting beyond the length of the vertebral bodies; neural spines are shorter, longer anteroposteriorly and compressed mediolaterally; and the top of the spinous process is blunt and convex. Neural canals are more or less diamond-shaped due to the degree of narrowing in the apex and the presence of a shallow groove on the dorsal side of the vertebral body. The epiphyses are strongly fused with the vertebral bodies; lateral sides of the vertebral bodies are notably concave inward; ventrally vertebral bodies lack any keel. Zygapophyses progressively move towards the transverse processes, joining the tubercular facet. In the most caudal thoracic vertebrae, but not the last one, only a single rib facet is present on the end of a stubby process jutting out from the side of the centrum. T17 and T18 were not preserved.

T19 (Figure 4.19) is the last thoracic, and is only known from the thoracic series in UM 111558; it is very distinct in having a short (about 25 mm long), and rounded transverse processes on the left side, this transverse process was formed from the fusion of the last rib, which is the shortest rib in the ribcage, with the stubby root of the transverse process of the centrum. The right transverse process is broken and missing, leaving the stubby process empty. The neural spine is shorter than in vertebrae more anterior in the series, wide anteroposteriorly, and thin. Zygapophyses are long, and the neural canal is more a spade-like ,lacking a slitted apex (Figure 4.19). The vertebral body is heart-shaped, has a gently convex dorsal surface (the base of the vertebral foramen), is laterally biconcave in the middle, and is characterized by a flat midventral pillar, too flat to be called a keel. The midlateral sides to the pillar are marked by a pair of vascular foramina. Epiphyses are fused strongly fused to the vertebral body.

L1 (Figures 4.19, 4.20, and 4.21) is preserved in UM 111558. The transverse process of the first lumbar is flat, short, and directed posteriorly; the vertebral body is markedly heart-shaped, with a distinct dorsal indentation and a thick midventral pillar, and has concave epiphyses. The neural spine is similar to that of the last thoracic; the neural canal is almost round in shape, and the zygapophyses are slightly shorter than those in the last thoracic, as well.

L2, L3, and L4 (Figures 4.22, 4.24, 4.25; Table 4.17) are preserved in UM 97514. L2 is missing it neural spine and the right transverse process is incomplete; the left transverse process is short, flattened, and posteromedially indented; the midventral pillar on the vertebral body is more pronounced than the that in L1 of UM 111558.

L3 and L4 have transverse processes longer and more flattened than those in L1 and L2 (Figures 4.22 and 4.24; Table 4.17); these extend nearly horizontally from the middle of the centrum, and are curved forward; their tips are flattened dorsoventrally, with their most anterolateral corners pointed forward. The apex of the neural canal is not slit-like. The neural spine is thin and sharp on both edges, and slightly inclined backward. The neural spines progressively become thinner and lower caudally. The zygapophyseal articular surfaces are inclined about 45º to the horizontal. The midventral pillar in L4 is more flattened than the one in Lr3.

The sacrum (S1) (Figures 4.22, 4.24, and 4.25; Table 4.17) is only known from UM 97514, and is characterized by stout, downward-sloping transverse processes with thickened extremities with rugosities on their ends for attachment to the ilia. The rugose ends measure up to 29 mm thick dorsoventrally, and extend well below the bottom of the centrum. Near their ends the transverse processes are also somewhat expanded anteriorly in an asymmetrical manner. The neural canal widens posteriorly and does not have a slit-like apex. The neural spine is thin and sharp on both edges, and is nearly vertical. The zygapophyseal articular surfaces are inclined about 45° to the horizontal. The ends of the vertebral body are concave; the ventral side is flat. The dorsal side of the vertebral body is indented anteriorly but not posteriorly.

Caudal vertebrae are best preserved in UM 97514; UM 111558 also has vertebrae from the posterior portion of the tail. The first six caudal vertebrae Ca1-Ca6 (Figures 4.22, 4.24, and 4.25; Table 4.17) of UM 97514 are perfectly preserved, along with three of the more posterior ones.

Ca1 (Figures 4.22, 4.24, and 4.25; Table 4.17) is unusual in that its transverse processes are inclined forward slightly, nearly horizontal, and even appear turned up slightly at the tips (due to thickening of the tips), in contrast to both the sacral and the succeeding caudal, whose transverse processes are perpendicular to the body axis and markedly inclined downward. However, in the shape of its vertebral body, degree of separation of its zygapophyses, and overall dimensions, this vertebra fits better in the first caudal position than elsewhere in the column. The vertebral body is flat-bottomed like that of the sacrum, and not indented dorsally. Like the other caudals, the ends of the centrum are concave and the neural spine is thin, with sharp front and back edges. The neural spine is vertical. Small postzygapophyseal articular facets are present. Ca2 (Figures 4.22, 4.24, and 4.25; Table 4.17) has very faint chevron attachments on the caudal edge of its ventral side. It also has downward-directed transverse processes that are still more recurved at their tips, which are slightly expanded and rugose. Ca3 (Figures 4.22, 4.24, and 4.25; Table 4.17) lacks these recurved tips, and bears rather indistinct demifacets for a chevron bone at each end. Ca4 (Figures 4.22, 4.24, and 4.25; Table 4.17) and subsequent vertebrae have distinct anterior and posterior chevron demifacets and lack postzygapophyses; the prezygapophyseal processes thereafter remain large, but lack articular facets and serve only as mammillary processes for transversospinal muscle insertion. The spinous process of Ca4 shows a hint of posterior inclination, which becomes distinct on Ca5 and quite marked on Ca6 (Figures 4.22, 4.24, and 4.25; Table 4.17). Backward inclination of the transverse processes also begins with Ca5 and gradually increases toward the peduncle (Figures 4.21 and 4.25).

In UM 97514 (Figures 4.22 and 4.25), at least one vertebra is missing immediately subsequent to Ca6. Ca8 through Ca10 continue the trends described above; the latter exhibits the lowest and most inclined neural spine and the most sharply swept-back transverse processes. One isolated vertebra from the posterior part of the fluke region probably represents the third or fourth vertebra from the end. It has only a very short transverse process and no trace of a neural arch. In its lack of long transverse processes it has a general resemblance to a posterior caudal of modern dugong.

The caudal series in UM 111558 (Figures 4.20 and 4.21) is missing all the anterior caudals, estimated to be Ca1 through Ca4; but preserves Ca5 through Ca7, Ca12 and Ca13, ?Ca16, and a very posterior caudal that is close to the measured centrum height of the last vertebra available from UM 97514. The trend in tapering, decreasing in size more caudally, and dorsoventral flattening of the caudal vertebral bodies are the same in both vertebral columns.

Ribs—The holotype, CGM 42181 (Figure 4.26; Table 4.18), includes nearly the entire right rib series, missing only the first and second ribs, and also preserves the second left rib. The second through sixth ribs are swollen (pachyostotic)and massive in construction. The seventh through eleventh ribs are the longest and have the greatest arc widths; all are rounded in cross-section and equally massive and thick. The twelfth rib to the last rib are cylindrical and more gracile.

The second rib is pachyosteosclerotic. Its neck is straight and diminutive; the head is as small as the capitular facets; the tuberculum is slightly higher than the head with a small pointed facet; the ligament fossa lateral to the tuberculum is very shallow and poorly developed. The shaft is thick, oval-shaped and has a smoothed outline. The shaft

maintains a consistent thickness and shape proximally; just before midshaft becomes more swollen and increases its thickness with a rectangular to quadratic cross-section; heading distally, the shaft reaches its greatest thickness and swollenness, measuring 37 mm mediolaterally and 26 mm anteroposteriorly. The distal end of rib is banana-shaped, tapering into a pointed end. The lower posteromedial area is characterized by irregular surface for muscle attachment.

Ribs 3-5 are missing their heads, all are pachyosteosclerotic and taper distally into a banana-shaped; the third rib has the greatest pachyosteosclerosis and swollenness of all ribs, and has the greatest width around its midshaft perimeter; the fifth rib has the greatest crescent in the series.

The sixth rib is complete, slightly compressed anteroposteriorly, and the tip of its head is missing. The tuberculum is less pronounced than those of the posterior ribs. Cross-sectional area at midshaft is greater than those of more posterior ribs.

Ribs 7-10 have oval anterior and posterior capitular head facets slightly connected at their summit. In each, the neck is slightly straight, long, flat ventrally, semicircular crosssection, and plunges cranially. The tuberculum is elevated, with a rounded ligament fossa medial to it. Cross-section is of the shaft is constant along the upper two thirds; the distal end is slightly tilted medially.

Rib 11 exhibits shortening in its neck, and the cross-section after the tuberculum is rounded. The twelfth and the succeeding ribs are slender, gracile, and semicircular in cross-section, and taper distally very gently. The most posterior ribs have their head and tuberculum joined together to form a flat, straight articular facet.

UM 111558 preserves the anterior and middle part of the ribcage (Figure 4.27; Table 4.19) comprising 13 ribs from the right side (R1-R11, ?R15 and R17 or R18) and 8 ribs from left side (R2-R6, R12 and 13, an possibly R14). Ribs arrangement is based on the overall shape and morphology the ribs of the single individual, and on recent and fossil analogy of ribcages of dugongs and from the Eocene Mokattam beds Eocene of Egypt.

The first rib (R1) in UM 111558 (Figure 4.27; Table 4.19) has a well developedhead, neck, and tuberculum . The anterior capitular facet is larger than the posterior one; the neck possesses a sulcus cranially and a shallow transverse concavity caudally; the tuberculum is lower than the capitulum; the tubercular fossa is facing laterally as a vertical notch, not a depression as in the succeeding ribs. The proximal end of the shaft is triangular in shape and compressed mediolaterally into a slight concavity posteriorly for muscle attachment. Midshaft, the rib is convex anteriorly with a distinct ridge formed posteriorly. The distal end of the shaft is flattened antero-posteriorly and the end is straight and truncated.

The second rib in UM 111558 (Figure 4.27; Table 4.19) ismorphologically like that of CGM 42181. It is a banana-like rib with strong pachyosteosclerosis.

The third rib (Figure 4.27; Table 4.19) is the heaviest and widest in diameter of all ribs in the ribcage of this individual; it is convex anteroposteriorly. The capitulum is rounded; the anterior capitular facet is smaller than its posterior counterpart; the neck is straight, cylindrical and thickened; the tuberculum is rounded, flat, and lower than the head; and the tubercular fossa is shallow and small. The proximal end of the shaft is oval; and the lower two-thirds of the shaft maintain a constant thickness and structure. Just 20 mm before the distal end, the shaft tapers rapidly.

The fourth rib (Figure 4.27; Table 4.19) is similar to that in CGM 42181, with a rounded capitulum that is lower the tuberculum,; the anterior tubercular surface is oval in shape, and is twice as large as the posterior one; the neck is straight; the tuberculum is slightly higher than the capitulum; and the tubercular fossa is larger than that in rib 3, shallow and connected to a superficial sulcus running ventrolaterally. At the posterior side and just above the midshaft, the second and third ribs retained a 30 mm long scar on each, running mediolaterally; the succeeding rib 4 possesses a depression anteriorly just below the angle. The scars and the depression are all aligned at the same level, and it is not clear whether this was a pathology or healed injury from an accident suffered by this animal.

The fifth rib (Figure 4.27; Table 4.19) is longer, less pachyosteosclerotic and slightly thinner than the forth rib; its neck is widened anteroposteriorly and more conformable to the body of the rib; its capitular facets are roughly subequal. The midshaft of the bone is rectangular to semicircular in shape. Internal muscle attachments are preserved on the medial surface as downwardly trending striations. The distal end tapers into a straight attachment area for the costal cartilage.

Ribs 6 and 7 are longer than rib 5 (Figure 4.27; Table 4.19). In these ribs, the ventral surface of the neck is flat; and the posterior surface of the neck is triangular in shape, flat and pitted. Their tubercular fossae are small and shallow. The distal third of the shaft in both ribs is twisted posteriorly from the mediolateral position of neck and head.

Rib 8 preserves its proximal half but is missing its capitular facets; its tuberculum is slightly elevated and the tubercular fossa is narrow, shallow, and triangular in shape. Rib 9 preserves the upper two thirds of its extent. It is distinct in having the largest flat

attachment area posterior to the head and neck. The shaft is uniformly oval in cross-section. The tuberculum is roughly pyramidal in shape.

Rib 10 is the longest rib in the series (Figure 4.27; Table 4.19), and is compressed mediolaterally along its shaft. The posterior capitular facet is circular in shape and larger than the anterior facet; the dorsal surface of the neck shows a mediolateral scar that disappears at the base of the pyramidal tuberculum; and the tubercular facet is a shallow, transversal groove. The posterior of the neck and proximal side of shaft are flat, with two rows of pits. The cross-section of the shaft is uniformly oval; the anterior distal end tapers with an angle towards the costal cartilage attachment end, while the posterior distal end is straight right to its end.

Rib 11 (Figure 4.27; Table 4.19), along with the rest of the more posterior ribs, is shorterand more gracile. The neck is short, the shaft is thinner and less convex than the neck of the more anterior ribs, and the shaft cross-section is oval and smaller than in the shafts of the more anterior ribs.

Ribs 12 and 13 are partially preserved on the left side. Both show reduced shaft diameters and are more elliptical in cross-section.

Rib 14 preserves a partial shaft from the left side. The length between the capitulum medial end and the tubercular fossa is about 42 mm, which is shorter than the length of any of its antecedents.

The only free rib preserved posterior to rib 15 in UM 111558 (Figure 4.27) fits with either thoracic vertebra rib facet 17 or 18, but not the last thoracic. It is distinct in having a straight proximal end, as the tuberculum and capitulum are joined on the same surface. The proximal end is compressed anteroposteriorly, forming an anterodorsal ridge; the

posterior proximal surface exhibits a shallow median grove; the cross-section of the shaft is oval. The last rib is distinct in being fused to the last the last thoracic vertebra (Figure 4.27; Table 4.19).

In UM 97514 (Figure 4.28; Table 4.20), all preserved ribs are from the posterior half of the ribcage, and are arranged in pairs in serial order from rib 6 through 16. . The recovered ribs were serially arranged based on size and morphology of the tuberculum and capitulum, size and shape of the midshaft, and also the fit of the capitulum-tuberculum to the rib facets on the vertebral bodies, and also by comparison with specimens having more complete ribcages, such as UM 111558. The ribs of UM 97514 are equally dense (osteosclerotic), completely lacking any cancellous bone, but the anterior ones (the second third of the ribcage) are much more swollen (pachyostotic) than those of the posterior section of the ribcage, and therefore much heavier. The more anterior ribs in this specimens (R6 through R10) are slightly sigmoid in lateral view, with swept-back distal ends. The articular surfaces are well defined. A pit is present between the capitulum and tuberculum, with another just lateral to the tuberculum. The tuberculum protrudes in pyramidal fashion well above the rib's dorsal surface as in the ribs of UM 97514. The distal end tapers abruptly in its last 40 mm. Ribs from the last third of the thorax (R11 through R16) are likewise oval in cross-section and have subcylindrical shafts, but are much more slender. The capitular and tubercular facets are still distinct, but there is no space separating them. The anterior surface of the tuberculum slopes more gradually than the vertical posterior surface. The tuberculum continues to rise prominently above each rib’s dorsal surface to the end of the ribcage, in contrast with some later dugongids, in which the tuberculum of the posterior ribs is

reduced and circumscribed feature on a broad and dorsoventrally compressed shaft. The last pair of ribs from this series (R16) has unequal lengths. The broken right rib was more than 118 mm long, while the left is only 64 mm long which is its natural length since its distal end shows the remnant of the costal attachment of the cartilage ligament. Both are only slightly curved and have dorsoventrally expanded proximal ends, the summits of which are formed by the tubercula. The capitulum is stubby, and neither it nor the tuberculum has a well-defined articular surface. Whether it is the last rib in the series in UM 97514 is not clear, since the last thoracic vertebra is not preserved.

Xiphisternum —(Figure 4.29) UM 111558 preserves a sternal element that best fits in the xiphisternum position in the sternal series. The bone is asymmetrical due to deformation. It is elongate craniocaudally, flattened dorsally, and slightly convex ventrally. It is greater than 102 mm in total length, 18 mm wide, 8 mm in dorsoventrally diameter, and it is wider and thicker cranially, while its distal portion is flattened. The proximal end has a central articulation for the last mesosternum, and two lateral articulations for rib ends. The distal portion of the xiphisternum is perforated by a large elliptical foramen that measures 15 mm long and 4 mm wide; usually, this foramen is formed as a congenital oval defect in the lower third of the sternal series, either by incomplete fusion of sternal elements or disturbed ossification of cartilage.

The morphology of this sternal bone implies that the cranial sternal elements of this taxon and narrow and thickened; *Eosiren* sternal elements are flattened dorsoventrally, while in *Protosiren* they are blocklike series (Figure 4.50).

Scapula—Two scapulae are known for this species. The first is the right scapula of the holotype (CGM 42181) (Figure 4.30; Table 4.21), and the second is a perfectly preserved left scapula from UM 111558 (Figure 4.31; Table 4.21).

The right scapula in the holotype (Figure 4.30; Table 4.21) has total length of 198 mm and has a maximum breadth of 61 mm across the spine. The scapular spine is 103 mm long, but missing its acromion process; it is slightly thickened and bears dull edges. The sickle-like scapula has its subscapular fossa literally flattened with a slightly thickened anterior edge (cranial border) that has a semicircular outline and projects laterally, making the supraspinous fossa more or less convex. Its glenoid fossa is ovoid and deep, wider and broader posteriorly, and is smaller than those in *Eotheroides clavigerum*. Both the coracoid and the oval muscle scar on the medial side, which is shallow, are present.

The scapula of UM 111558 (Figure 4.31; Table 4.21) is so far the most complete scapula to be recovered from an Eocene of dugongid. It is 4 mm shorter than the scapula of the holotype. The spine is 106 mm thick, bearing a 23 mm long acromion process that projects downward and medially; and the acromion process rises 21 mm above the surface blade. The spine is thickened and widened at its dorsal end, and the middle part of the spine is thin and narrow. The glenoid fossa is similar to that of the holotype. Cranial and dorsal borders of the blade have semicircular and smooth outlines; the caudal and posterodorsal borders have anteriorly concave outlines; and more posterodorsally the blade is marked by a straight, 35 mm long ridge (bordering the teres fossa). The infraspinous fossa and the anterior face of the spine are marked by rough striations. The subscapular fossa is concave and marked by a fan-shaped group of striations.

Humerus—In the holotype (Figure 4.30; Table 4.22), the right humerus is somewhat damaged and missing its greater tubercle; and its proximal epiphyses are slightly fused. The left humerus is fragmentary. UM 111558 has a perfectly preserved humerus (Figure 4.31; Table 4.22), with its proximal epiphyses fused. Both humeri are at least 10% shorter than the humerus of *Eotheroides clavigerum*.

In general, the humerus of this species is long and slender compared to most sirenians; its internal structure is dense and compact. The head has a rounded outline, and is notched anteriorly at the top of the narrow and deep bicipital groove. The greater tubercle forms a thick and prominent flange, with a narrow surface for muscle attachment on its summit. The lesser tubercle is robust and rounded at the top, forming the medial wall of the bicipital groove. This groove ends in a shallow cul-de-sac, bounded posteriorly by the notched border of the head (cf. Sickenberg, 1934: fig. 4b). The deltoid crest is distinct and prominent, located about 58 mm from the top of greater tubercle. The sagittal diameter of the shaft (about 23 mm) exceeds the transverse diameter (18 mm).

Ulna — Only the right ulna is preserved is known for this species, from UM 111558 (Figure 4.31; Table 4.23), and it is missing its olecranon and distal epiphyses. There is no sign that it was ever ankylosed to its radius (Figure 4.31). It is slender and gracile, with a preserved length of 135 mm. The olecranon is short (rises 20 mm above the crescent notch), and has and an oval occlusal surface measuring 23 mm anteroposteriorly and 14 mm mediolaterally. The olecranon is tilted backward slightly (18˚) from the axis of the shaft.

The lateral surface bears no grooves similar to those found in *Protosiren smithae* below the level of the semilunar notch. The proximal part of the articular surface is distinct and mediolaterally convex, while the distal end of this articular surface is clearly notched and indented. A slightly depressed, nonarticular surface (perhaps for a humero-ulnar ligament) extends medially beyond the midline of the joint surface. Still more distally, the ulna widens suddenly and bears two articular surfaces: a lateral surface facing anteroproximally, and a medial surface more proximally. These are nearly separated anteriorly by a median notch, but no laterally-positioned radial notch is present. There are no signs of a rough surface for radius attachment below the front edge of the semilunar articular. The shaft is triangular in cross-section and becomes oval at its distal end (and convex medially). Medial and lateral margins of the distal end of the ulna bear slight rugosities, but not enough to ankylose with the radius.

UM 97515 is a very short ulna (Figure 4.32; Table 4.23), only 95 mm in total length; it lacks its distal epiphysis and was not ankylosed with the radius, and clearly represents an immature animal. Nonetheless it is slightly larger than the specimen referred to *Eotheroides aegyptiacum* by Sickenberg (1934: 30-31, pl. 4, fig. 6; note that this illustration is about two-thirds natural size, not natural size as stated). It also differs from the latter in having a shorter olecranon (possibly due to loss of an epiphysis), whose anterior edge is less vertical and not as sharp; an articular surface not divided into lateral and medial portions by a ridge; and a shaft that is semicircular rather than triangular in cross-section. The flat, rugose area where the bone was sutured to the radius has an oblique orientation, suggesting a degree of torsion of the radius and ulna similar to that seen in Sickenberg's specimen. Medial to this area is a large and distinct oval pit. The

shaft has a perfect oval cross-section; its distal end remains oval, but with slight enlargement of the cross-sectional area.

Manus—The known hand elements for *Eotheroides sandersi* include a left metacarpal III (Figure 4.33; Table 4.24), and probably left metacarpal V; both elements belong to UM 111558.

Metacarpal III is 53 mm long, minus its distal epiphysis. The proximal third of the metacarpal is compressed anteroposteriorly; its midshaft has a rounded cross-section; and distally it is hemispherical. The proximal articular surface possesses three small facets connected with sharp edges and grooves; the most anterior of these facets is a 5-mm rounded circular surface separated from the posterior facets by a shallow groove; and the posterior facets are connected along a sharp edge that runs dorsoventrally. Metacarpal ?V, preserved in UM 111558, is missing its distal shaft; its proximal end and shaft are flattened dorsoventrally. The proximal carpal articulation facet is partly preserved;it originally had a trapezoidal outline with a wide ventral extent that is marked by a groove.

Innominates— The holotype CGM 42181 (Figure 4.34; Table 4.25) has its left innominate ., It is missing its pubic portion, portions of the ventral side of the ischium, and the acetabulum is sandblasted. The right right innominate has a poorly preserved ilium. The pelvis of this individual is small; the proximal end of the ilium is a clublike but is not as swollen as in the case of UM 97514 (Figure 4.35; Table 4.25); the medial side of ilium is flat, bears irregular bumps and pits where it attached to the sacrum, but no large cavity had yet developed. The acetabulum is shallow, the posterior end of the ischium flat, and the obturator foramen is damaged. The flattened ischium and its lack of rugosity or tuberosity indicate that each of these are female innominates.

The pelvic bones of UM 97514 (Figure 4.35; Table 4.25) are well preserved. The ilium is club-shaped, with a convex lateral surface; the proximal half of its medial surface is flat and rugose, and was in direct contact, via cartilage and ligaments, with the rugose lateral surface of the sacral alae. After narrowing slightly distal to the sacroiliac joint, the shaft of the ilium broadens again at the acetabulum, which has a diminutive, deep, smooth-surfaced, ellipsoid cavity 18 mm in greatest diameter. Its dorsal lip overhangs the socket, and lies in approximately the same horizontal plane as the ventromedial limit of the articular surface when the bone is held in its correct anatomical position. There is no distinctly demarcated acetabular notch; the entire ventral third of the acetabulum is roughened, in contrast to the smooth, obviously articular upper portion. Distal to the acetabulum is the broad, flat ischium, whose dorsal edge continues the gentle concave curve of the ilium. Its long axis forms an angle of about 135º with that of the ilium. The posterior end of the ischium is thickened, and abruptly flares outward below a line extending from the middle of its ventral edge to its posterodorsal corner. The entire margin of this flared portion is 10-15 mm thick and rugose; also roughened somewhat are its posteromedial surface and the vertical medial surface of the its posterodorsal end. The latter two surfaces, both slightly concave, are separated by a broadly convex horizontal ridge. The degree of lateral flaring of the distal end of the ischium is comparable to or greater than that which today characterizes male *Dugong*, in contrast to females (Domning, 1991). The most notable features of this specimen are its extremely long and narrow pubic ramus, and the small obturator foramen which it partly surrounds. The foramen is oval, with maximum diameters of 14 x 8 mm, and lies about 10 mm below the acetabulum (Figure 4.35; Table 4.25). The pubic ramus is about 18 mm wide and 10 mm

thick, and extends 53 mm downward, medially and slightly forward from the obturator foramen. Here it ends in a rugose symphyseal surface 20 mm long and 12 mm wide, flat ventrally and convex dorsally (preserved only on the left side).

Femur— Three femora of *Eotheroides sandersi* are known from two individuals, and all are missing their proximal and distal epiphyses; the holotype CGM 42181 (Figure 4.36; Table 4.26) preserves both of its femora, while UM 111558 preserves only the left femur.

The proximal end of these bones is broad and flat, lacking trochanteric fossa; the lesser trochanter is faintly marked; the shaft has a rounded cross-section, and is nearly straight and slightly concave forward. The distal end is ovoid to diamond in shape. The length of the femur in CGM 42181 is 91 mm, which is
10 % shorter than that of UM 111558 (Figure 4.36; Table 4.26).

When compared to *Protosiren* femoral and tibial elements (Figure 4.37; Table 4.26), and based on morphology and their size, the femora of *Eosiren* and *Eotheroides* are grouped together because they represent an advanced stage of hindlimb reduction and adaptation to a fully aquatic mode. *Eosiren* has a femur with a rounded shaft; the head is reduced and oval-shaped; the proximal end is broad and flat; it has no trochanteric fossa; and the lesser trochanter is not preserved. *Eotheroides* has nearly straight, broad shaft, that is slightly concave forward. Unfortunately, proximal and distal condyles have not been recovered for this taxon.

Comparison and Relationships

The phylogeny and systematics of fossil and living Sirenia have been reviewed by Domning (1994, 1996), where he identified many synapomorphies of Dugongidae and its subgroups useful for placing the Eocene Fayumian fossil sirenians in their proper evolutionary framework. Based on Domning's analysis, *Eotheroides clavigerum* and *Eotheroides sandersi* belong to the family Dugongidae because they have the following derived characters: enlarged premaxillary rostrum; enlarged infraorbital foramen; incised palate; extension of the squamosal to the temporal crest; well developed processus retroversus of the squamosal; dp5 is not replaced by a permanent premolar in the upper and lower jaws; the innominate has a short, rounded ilium (Figure 4.43), and femora are very reduced (Figure 4.36) compared with femora of the Protosirenidae (Figures 4.37).

Eotheroides clavigerum and *Eotheroides sandersi* from the Priabonian of the Birket Qarun Formation are phylogenetically closest to *Eotheroides aegyptiacum* (Owen, 1875) from the Lutetian Nummulitic Limestone beds near Cairo, as they share the following derived characters: prominent falx and bony tentorium at the roof of the braincase; nasals are long and in contact along the midline; the palate is broad and its posterior border lies posterior to the toothrow; and pachyosteosclerotic anterior ribs.

E. sandersi differs from *E. aegyptiacum* in being slightly larger; bearing arched nasals; having frontals contact parietals along a deep V-shaped suture which is laterally marked by a pair of prominences (in *E. aegyptiacum* the contact is W-shaped); and in having a longer, wider, and less arched cerebrum compared to the holotype of Owen (1875) and the braincase published in Abel (1913: plate 4, figs. 3-5). The supraoccipitals of *Eotheroides sandersi* (CGM 42181) are hexagonal in shape, projecting posteriorly

from the parietals at an angle of 133º, its muscle insertions form rounded depressions, and the distal lateral sides intersect one another posteriorly to form a V-shaped corner. Conversely, the supraoccipitals of *E. aegyptiacum*, as illustrated in Abel (1913: plate 2, Fig.1 and plate 4, figs. 3-5;1928: p. 496), have a straight contact with the exoccipitals, their muscle insertions are not in depressions, and they are shifted towards the upper and lateral corners of the supraoccipitalis. Also, the supraoccipital and parietals of *E. aegypticum* are perpendicular. The ribcage structure of the *Eotheroides aegyptiacum* specimen illustrated in Abel (1912: fig. 13, 1919: 836, fig. 663) and discussed in Senckenberg (1937: p. 24.25) differs slightly from those of the Priabonian *Eotheroides* of Wadi Al Hitan in that the fifth rib in *E. aegyptiacum* is the most pachyosteosclerotic, while the third rib is the most pachyosteosclerotic in *E. sandersi* and *E. clavigerum*.

E. clavigerum is at least 30% larger than *E. aegyptiacum* of Owen (1875) in overall skeletal dimension and is at least 70% larger in dental dimensions. The larger species has its unusual nasals concave upward while the nasals of *E. aegyptiacum* are more or less flattened dorsally and level with the frontals and parietals. Postcranial elements of both species show pachyosteosclerosis in the thoracic vertebrae and ribs; however, *Eotheroides clavigerum* exhibits extreme pachyosteosclerosis in its anterior ribs.

Eotheroides clavigerum is at least 7% larger than *Eotheroides sandersi* in cranial dimensions, and is 25% to 44% larger in dental dimensions. It is also 7- 31% larger in skeletal dimensions; moreover, its nasals are more concave upward and more arched than in *E. sandersi*. In addition, the innominate of *Eotheroides clavigerum* bears a short, club-like ilium, a flat, broad, and thin ischium, a small obturator foramen;, and a short, gracile, unfused, and medially pointed pubic ramus on each side, lacking a true symphysis. The

pelves of *Eotheroides sandersi* differ from those of the larger, contemporaneous *Eotheroides clavigerum* by their unusually long pubic rami, unlike those in any other sirenian, and by their variability in robustness and thickening of the ischiac tuberosity, interpreted as sexual dimorphism in the pelvic region.

Domning et al. (1982: 56, fig. 34) described a partial lower jaw of a dentally immature dugong thought to be from the Qasr El Sagha Formation near Wadi Al Hitan. However, the preservation almost certainly indicates derivation from the Birket Formation (although without a specific locality); the preservation and mineralization of this jaw is common in the fine sandstone facies above what is called the University of Michigan Camp White Layer (Gingerich 1992). The specimen (YPM 24851) is interpreted as *Eotheroides* from Wadi Al Hitan because it has a laterally compressed mandibular symphysis; unfortunately the partial mandible of the holotype of *E. sandersi* (CGM 42181) lacks features which would aid comparison with YPM 24851.

In Dugongidae, the nearest relatives to *Eotheroides* (Own, 1975) are: *Eosiren* (Andrews, 1902), *Prototherium* (de Zigno, 1875), *Sirenavus* (Kertzoi, 1941), and *Halitherium* (Kaup, 1838a,b). *Eosiren* has partial temporal and spatial overlapping with *Eotheroides*, as it is known from the Lutetian (middle Eocene) through the Priabonian (late Eocene) of Egypt. *Prototherium*, *Sirenavus*, and *Halitherium* are spatially separated from *Eotheroides*, as they were restricted to the middle and late Eocene of Europe. Nevertheless, *Eosiren*, including all the known species from the Eocene and Oligocene of Egypt, is distinguished from *Eotheroides* in having the following characters: larger body size; robust skull and lower jaws; broad and flattened skull roof with laterally flared supraorbital processes (as seen in *Eosiren imenti* from the Oligocene

of the Jabal Qatrani [Domning et al., 1994]); nasals are either separated from each others (e.g. *Eosiren imenti*) or in slight contact (e.g. *Eosiren libyca*); the maxillary-palatal gutter is very narrow; the jugals extensively contribute to the anteromedial margins of the orbit; at least *Eosiren abeli* (Abel, 1913: 55, fig. 4 "skull IV") and *Eosiren stromeri* (UM 100137) have a true foramen ovalis (i.e.; the fissura ovalis is closed posteriorly by a bony bridge); enlarged cheek teeth bearing the dental formula 1-3.1.5.3 /3.1.5.3 (Figures 4.38); and lower jaws lack a compressed anterior lip (see UM 100137, Figure 4.40). In addition, their vertebrae retained large, heart-shaped centra, marked by a ventral keel in the thoracic region (Figures 4.44, 4.45), and long neural spines in the anterior and mid-thoracic region (but shorter than those in P*rotosiren*); their ribs are osteosclerotic but gracile, lacking pachyostosis (Figure 4.49); their innominates are very reduced (Figure 4.43), with ilia that are short and gracile with no signs of swellings, and the obturator foramen is either closed or extremely diminutive.

Prototherium is known from two species based on cranial and postcranial elements from the late Eocene of Italy: *P. veronense* (de Zigno, 1875) and *P. intermedium* Bizzotto (1983 and 2005). Pilleri et al. (1989) have erected two new Bartonian species from Spain, *P. solei* and *P. montserratense*, but these seem similar if not identical to the Priabonian *P. intermedium* (Domning, 1994). At any rate, the major feature in *Prototherium* is the unusual anteroposterior elongation of the skull that makes it look relatively laterally compressed; *Prototherium* anterior ribs are pachyosteosclerotic, and the ilium is swollen, as shown in Bizzotto (1983, plate II) and Pilleri et al. (1989: 42, fig. 12).

Sirenavus hungaricus of Kretzoi (1941), which is based on a partial skull (MTM V.60.1712) and dentaries (MTM V.83.42) from the middle Eocene of Hungary, shows some affinities with *Eotheroides clavigerum* and *Eotheroides sandersi* in retaining strongly arched upward-concave nasals, large infraorbital foramina, and enlarged ribs associated with its partial skull. Further examination of S*irenavus hungaricus* by Kordos (1981) and Domning (1994,1996) shows that it is more closely related to Dugongidae rather than Protosirenidae and Prorastomidae. The innominate (MÁFI V.15366) and femur (MÁFI V.15367) of *Sirenavus hungaricus* mentioned in Kordos (2002) represent a dugongid evolutionary stage: the ilium is rod-like, the acetabulum is reduced, the pubic ramus is retracted medially, and the obturator foramen is diminutive. In addition, the femur is morphologically typical of an *Eosiren* femur, and is particularly similar to specimen UM 101226 (Figure 4.36 F) from the Qasr El Sagha Formation of the Fayum province.

Halitherium (Kaup, 1838a,b) includes three European Paleogene species: *Halitherium taulannense* from the Priabonian of Haute Province of France (Sagne, 2001a); *H. schinzii* (Kaup, 1838) from the early Oligocene (Rupelian) of Germany, Hungary, Switzerland, Belgium, and France (Lepsius, 1882; Spillmann, 1959); and *H. christolii* (Fitzinger, 1842) from late Oligocene Austria. *Halitherium taulannense* shares several cranial synapomorphies with *Eotheroides*; however, *Halitherium taulannense* is more derived because it possesses the following characters: contact between the lacrimal and premaxilla, and an enlarged first incisor as its alveoli reache about half the length of the rostrum (Sagne, 2001a). The right innominate of *H. taulannense* (NSM PV 20523) is 248 mm in total length, bears a rod-like ilium (130 mm in total length), and lacks any

swelling; the ischium is long, the obturator foramen (18x12 mm) is wider than those in *Eotheroides*, and the pubic ramus and symphysis are very reduced; its femur is incomplete, as it is missing its distal end, but is reduced as well. The head of its femur still articulated with the acetabulum, and was rounded in cross-section.

Smithsonian specimens (USNM 214596) from the Eocene of North Carolina , described as *Protosiren* sp. by Domning et al. (1982), is indeed the first potential *Eotheroides* sp. from North America. This assessment is based on cranial and postcranial elements that include a very well preserved lower jaw with permanent teeth (Figure 4.42), cervical and thoracic vertebrae, anterior ribs with strong pachyosteosclerosis and quadric cross-sections, partial humerus and ulna, and a partial pelvic bone. The ribs and vertebrae are similar to those of *Eotheroides* from Mokattam and Fayum. However, the North Carolina taxon differs from *Eotheroides sandersi* and *Eotheroides clavigerum* in having a gently arched ventral outline of the mandible and very small degree of deflection of the mastication surface (symphysis) (which is greater in the Egyptian *Eotheroides*), and in retaining a very narrowed mandibular lip (see Figure 4.42). The dental formula of the lower jaw in USNM 214596 (Figure 4.42) is 3.1.5.3, the same as in *Eotheroides clavigerum* (UM 101219, Figure 4.1) and *E. sandersi* (UM 100138, Figure 4.17). The rudimentary innominate associated with the postcranial and cranial elements is described in Domning et al. (1982: fig. 33), who described it as belonging to an animal in an advanced stage of aquatic adaptation similar to that of *Eosiren libyca*.

Beyond Dugongidae, Protosirenidae *Protosiren fraasi* of Abel (1907) from the Lutetian of the Mokattam Hills and the contemporaneous *Protosiren smithae* from the

Priabonian of the Fayum have major morphological differences with *Eotheroides* species. Cranial and postcranial differences between of *Protosiren* and *Eotheroides* were listed in Sickenberg (1934, p. 192-193) and then recounted in Gingerich et al. (1994:44, table 1). However, since *Protosiren smithae* was recently added to the Protosirenidae and is slightly different from the type "*P. fraasi*," a slight modification to the list is necessary. *Protosiren* differs from *Eotheroides* in the following characters: larger body size; slight rostral deflection in the maxilla and premaxilla; premaxillary-maxillary suture is pushed much farther back than the premaxillary symphysis; presence of an alisphenoid canal; the squamosal does not contribute to back of skull; the squamosal and supraoccipital are completely separated by a process of the parietal; the posttympanic process of the squamosal is absent; the supra-auditory region is thickened and outer ear passage somewhat elongated; the lamina orbitalis of the frontal contributes substantially to separation of the orbits and the nasal cavity; large brain; bony falx, bony tentorium, and internal occipital protuberance absent; the infraorbital foramen is relatively small compared to cranium size; lack of a pterygoid fossa; elongate cheek teeth (Figure 4.38); large incisors; dp5 is replaced in the upper jaw and lost in the dentaries (Figure 4.41); postcranial elements are osteosclerotic but lack swellings; thoracic and lumbar vertebrae have their neural spines higher than any other sirenian described (Figure 4.47); thoracic vertebrae have a keyhole-shaped vertebral canal (Figure 4.46); rib heads display a cartilaginous rather than fully ossified articular surface (Figure 4.48); and well-developed hindlimbs. However, one major character in the postcrania that unifies *Protosiren* with *Eotheroides* and other dugongs, is the reduction of the sacrum to a single sacral vertebra with transverse processes that serves as a sacral rib connected to the ilia by a cartilage.

Prorastomidae, the oldest and most primitive of known Sirenia, are endemic Caribbean sirenians that lived in the early middle Eocene, and are known from two species: *Prorastomus sirenoides* of Owen (1855) and Savage et al., (1994), and *Pezosiren portelli* of Domning (2001b). Both species are known from sufficient cranial and postcranial elements to supportinterpretation of an amphibious and quadrupedal lifeway. *Prorastomus sirenoides* is clearly different from *Eotheroides* and other known Eocene dugongs in having a horizontal rostrum and mandibular ramus, double-rooted canine, enlarged first premolar, periotic still connected to the alisphenoid, and presence of an alisphenoid canal. However, it shares some features in common with *Eotheroides* and Eocene dugongs, as it has a mediolaterally compressed mandibular symphysis, and the dental capsule is wholly enclosed by the bone of the mandible. *Pezosiren portelli* is unique, as it retained a sagittal crest, has an enlarged first premolar, the fifth premolar is single-rooted (i.e.: dp^5 was lost and replaced), multiple sacral vertebrae are fused together, and possesses a large and presumably functional pelvic girdle articulated with hindlimbs capable of supporting body weight. It does share some synapomorphies with Eocene dugongs, such as: anteroposterior width of the auditory meatus is equal to its height, the periotic and alisphenoid are not fused together, the ventral border of the horizontal mandibular is turned down anteriorly, and anterior thoracic ribs are pachyosteosclerotic.

Discussion

The new *Eotheroides* species increases the number of species that lived during the Paleogene in Egypt to at least nine valid taxa. These include: *Protosiren fraasi* Abel (1907), *Eotheroides aegyptiacum* Owen (1875), and *Eosiren abeli* (Sickenberg, 1934),

which dominate the Lutetian-aged Mokattam Nummulitic Limestone; *Protosiren smithae,* which derives from the base of the Birket Qarun Formation (Domning and Gingerich, 1994); *Eotheroides clavigerum* sp. nov. and *Eotheroides sandersi* sp. nov. from the Birket Qarun Formation; *Eosiren libyca* Andrews (1902), and *Eosiren stromeri* (Sickenberg, 1934) from the Qasr El Sagha Formation, and *Eosiren imenti* Domning et al. (1994) from the Oligocene Jabal Qatrani Formation. So far, no record of Prorastomidae is known for Africa, though the assumption of an early radiation of Sirenia beginning in Africa cannot be ruled out. Extant African Sirenia include two species: *Dugong dugon* (Müller, 1776) which inhabits the eastern and southeastern coast of the African continent, and *Trichechus senegalensis* (Link, 1795), the West African Manatee from the western side of the content (Bertram and Bertram, 1973). The sirenian fauna represents less than 5% of all the marine mammals found in the Birket Qarun Formation, far less than the dominant Archaeoceti, which represents 94% of all marine mammals collected or marked. *Moeritherium* is the least common aquatic or semi-aquatic mammal from Birket Qarun (however, this could change as a wealth of unpublished specimens have recently been collected [W. J. Sanders, pers. comm..]; these percentages are based on a count of 470 skeletons of marine mammals mapped in Wadi Al Hitan (Gingerich, 1992).

The skeletal and cranial material of new *Eotheroides* species from the Priabonian Birket Qarun Formation of Wadi Al Hitan are very important because they present novel information that help refine identification and phylogeny of the three Eocene genera that are known from the Tethyan Sea. *Eotheroides aegyptiacum* is known from partial skulls and lower jaws but lack cranial rostra, caudal vertebrae, pectoral and pelvic elements, which complicated attempts to better understand the paleobiology and systematics of this

taxon. Fayum *Eotheroides* were medium-to-large sized dugongs: *Eotheroides clavigerum* may have reached 2.2 m in total length, while *Eotheroides sandersi* was approximately 1.5 m long. Both have stout, heavy skulls, and rostra deflected downward between 43° and 50° from the horizontal plane and bearing a pair of medium sized tusks in *E. clavigerum*, and diminutive ones in *E. sandersi*; dental formula is $2.1.3.4.dp^{5}.3/3.1.3.4.dp_{5}.3$; vertebral count in *Eotheroides clavigerum* is reconstructed as 7C, 19Th, 4Lr, 1S, and 19-22Ca, associated with 19 pairs of ribs; for *Eotheroides sandersi* the vertebral count is 7C, 17-19Th, 4Lr, 1S, and 19-22Ca associated with 17-19 pairs of ribs; the trunk in each is widest between the ninth and eleventh thoracics, with the posteriormost of the tail presumably having supported a fluke in both species; hindlimbs are reduced to a short and slender femur attached to reduced innominates that had shallow, crescent-like acetabulae.

The pelves of Fayum *Eotheroides* make a substantial contribution to the generic diagnosis of the Eocene Sirenia. The ilia and femora of *Eotheroides clavigerum* and *E. sandersi* are the first definitive posterior girdle elements to be assigned to *Eotheroides,* as they were found in association with cranial and other postcranial elements. The pelves are unlike any sirenian pelvic bones heretofore described (see Abel 1906, 1907, Domning 2000, 2001b); they are intermediate between those referred to *Protosiren fraasi* (SMNS 43976A, from Abel, 1904: pl. 7, fig. 1; illustrated in Figure 4.43 in the present work) and *Protosiren smithae* (CGM 42292 in Domning and Gingerich, 1994; illustrated in the present work in Figure 4.43), and those of *Eosiren libyca* (UM 101226) (illustrated in the present work in Figure 4.43). Both species of *Eotheroides* from Fayum retained a long pubic rami with very limited symphyses, and obturator foramina are greatly reduced

compared with the former taxa, but have not been totally lost. The extensively swollen proximal ilium in *Eotheroides* is distinctive among Eocene sirenians; the ilium of *Eosiren* is reasonably constant in its diameter and cross-section, as illustrated in Andrews (1906), Stromer (1921), and Siegfried (1967), and those illustrated in Figure 4.43 of this work. This swelling in the ilium is similar to that which appears on the innominates of the European late Eocene *Prototherium intermedium* (See Bizzotto 1983, 2005). The iliosacral articular surface that appears on the dorsolateral surface of the ilium in *Eotheroides* is very shallow but larger than what is found in *Eosiren*, implying that there was still a connection between the ilium and the sacrum via a cartilagenous ligament. The femora of *Eotheroides* are also very reduced and small, similar in size and morphology to those *Eosiren* discussed in Siegfried (1967).

The record of *Eotheroides* is not known from other portions of Africa where sirenians have been extensively documented (see Savage 1969, 1971, 1977; and Domning 1978); however, the newly recovered Eocene dugongid from the western coast of Madagascar (Samonds et al., 2005), not yet fully described, may represent a dwarf species of *Eotheroides*. Marine mammal remains from the Eocene of Togo (Gingerich et. al., 1992) contain some isolated sirenian elements showing dugongid affinities. Out of Africa, the record requires more investigation; *Eotheroides* is known from the Eocene of the East Tethyan deposits of India, along with *Eosiren* and *Protosiren* (Bajpai et al., 2006); although it was based on a single mandible (IITR-SB 2775), *Eotheroides babiae* is similar "in part" to *Eotheroides* jaws from the Birket Qarun Formation (e.g., YPM 24851 and CGM 42181) in having a slightly arched ventral outline in lateral view, and mediolaterally compressed mandibular lip.

Conclusions

Eotheroides clavigerum sp. nov. and *Eotheroides sandersi* sp. nov. from the Priabonian Birket Qarun Formation of the Fayum Province are, phenetically and phylogenetically, closest to and possibly direct descendants of *Eotheroides aegyptiacum*. They all have a prominent falx and bony tentorium on the roof of the braincase; long nasals in contact along the midline; a broad palate with its posterior border posterior to the toothrow; and pachyosteosclerotic anterior ribs. The new species represent a derived form of dugongid, as they possess large infraorbital foramina, long premaxillary canals, and reduced pelvic girdles.

The most important skeletal elements for the diagnosis of the genus and its species are the anteriorly extensively pachyosteosclerotic ribs, and the innominates with their club-like ilia. The morphology of the skeletal elements of Lutetian and Priabonian *Eotheroides* are characteristic of fully aquatic marine mammals.

These large marine herbivores were fully aquatic and spent all their life in water either grazing on seagrass meadows in the tidal zone or consuming planktonic algae and floats from the surface. Based on paleontological and geological evidence, these animals lived in shoreface settings during a highstand in restricted and stable habitats (lagoons and estuaries), although some may have ventured into deltaic, keys, and bays. The presence of associated seagrass fossils in both the Birket Qarun and Qasr El Sagha Formations implies that they were deposited in settings that are less than 10 meters deep.

TABLE 4.1. Measurements of cranial elements of the holotype skull of *Eotheroides clavigerum* sp. nov. (UM 101219) from the Priabonian of the Birket Qarun Formation, and compared to the cranial measurements of *Eotheroides sandersi* sp. nov. (UM 111558) from the Priabonian of the Birket Qarun Formation, and *Eotheroides aegyptiacum* of Sickenberg (1934) SMNS St. III from the Eocene Mokattam Hills. All measurements are in mm. Measurements are after Domning 1978. See appendix for key to the measurements.

Abbr.	Measurement	*Eotheroides clavigerum* UM 101219	*Eotheroides sandersi* UM 111558	*Eotheroides aegyptiacum* SMNS St. III
AB	Condylobasal length	335	309	----
ab	Height of jugal below orbit	37	37	----
AH	Length of premaxillary symphysis	112	97	----
BI	Rear of occipital condyles to the anterior end of interfrontal suture	182	194	180
CC'	Zygomatic breadth	187	142	----
cc'	Breadth across exoccipitals	104	95	72
de	Top of supraoccipital to ventral sides of occipital condyles	103	92	79
F	Length of frontals, level of tips of supraorbital processes of frontoparietal suture	126	120	85
FF'	Breadth across supraorbital processes	107	82	89
ff'	Breadth across occipital condyles	73	65	54
GG'	Breadth of cranium at frontoparietal suture	44	50	49
gg'	Width of foramen magnum	32	32	26
HI	Length of mesorostral fossa	78	69	----
hi	Height of foramen magnum	25	25	26
JJ'	Width of mesorostral fossa	39	37	----
KL	Maximum height of rostrum	65	56	----
MM'	Posterior breadth of rostral masticating surface	43	42	----
no	Anteroposterior length of zygomatic-orbital bridge of maxilla	65	53	52
OP	Length of zygomatic process of squamosal	98	88	----
OT	Anterior tip of zygomatic process to rear edge of squamosal below mastoid foramen (length of the squamosal)	120	117	----
P	Length of parietals, frontoparietal suture to rear of external occipital protuberance	62	56	78
Pq	Length of the alveoli tooth row (dP^5-M^3)	54	44	42
QR	Anteroposterior length of zygomatic process of squamosal	47	35	34
rr'	Maximum width between labial edges of left and right alveoli across M^1	70	59	57
ST	Length of cranial portion of squamosal	78	57	----
ss'	Breadth across sigmoid ridges of squamosals	147	126	106
T	Dorsoventral thickness of zygomatic-orbital bridge	18	12	15
tt'	Anterior breadth of rostral masticating surface	28	25	----
UV	Height of posterior part of cranial portion of squamosal	92	77	72
WX	Dorsoventral breadth of zygomatic process	38	34	
yy'	Maximum width between pterygoid processes	38	41	29
YZ	Length of jugal	177	133	----
LFr	Length of frontals in midline	123	88	57
Hso	Height of supraoccipital	53	50	41
Wso	Width of supraoccipital	69	68	55
HIF	Height of infraorbital foramen	27	30	20
WIF	Width of infraorbital foramen	19	20	11
RD	Deflection of masticating surface of rostrum from occlusal plane (degrees)	43	49	----

TABLE 4.2. Measurements of right upper and lower teeth preserved in *Eotheroides clavigerum* sp. nov. in UM 101219, collected from the Priabonian of the Birket Qarun Formation. Abbreviations: **AW**, anterior width; **CH**, crown height labially; **L**, length; **PW**, posterior width. All measurements are in mm; see appendix for key to the measurements.

Tooth	L	AW	PW	CH
I^1	13.09	8.40	----	----
I^2	----	----	----	----
I^3	----	----	----	----
C^1	----	----	----	----
P^1	----	----	----	----
P^2	7.62	6.45	6.45	8.00
P^3	----	----	----	----
P^4	----	----	----	----
dP^5	----	----	----	----
M^1	12.61	15.57	14.16	6.00
M^2	13.98	17.59	14.60	8.83
M^3	16.53	17.55	12.35	7.89
dP_5	11.78	9.47	9.47	6.31
M_1	12.13	10.73	10.73	6.55
M_2	14.88	12.12	12.12	7.03
M_3	17.76	12.82	12.82	9.15

TABLE 4.3. Dental measurements of upper right cheek teeth *Eotheroides aegyptiacum* (SMNS St.XI (XIV)) from the Lutetian of the Mokattam Hills near Cairo. Abbreviations: **AW**, anterior width; **CH**, crown height labially; **L**, length; **PW**, posterior width. All measurements are in mm; see appendix for key to the measurements.

Tooth	L	AW	PW
M^1	9.80	11.20	9.60
M^2	12.00	12.30	10.70
M^3	12.70	11.90	8.70

TABLE 4.4. Measurements of the mandibles of *Eotheroides clavigerum* sp. nov (UM 101219) collected from the Priabonian of the Birket Qarun Formation compared to *Protosiren smithae* (CGM 42292) from Birket Qarun Formation, and *Eosiren stromeri* (UM 100137) from the Qasr El Sagha Formation, and "*Eotheroides* sp." from the Eocene of North America published in Domning., et al. (1982). All measurements are in mm; see appendix for key to the measurements.

Abb.	Measurement	*Eotheroides clavigerum* UM 101219 (holotype)	*Protosiren smithae* CGM 42292 (Domning & Gingerich, 1994)	*Eosiren stromeri* UM 100137	*Eotheroides* sp. USNM 214596 (Domning et al., 1982)
AA	Total Length	216	222	213	181+
AG	Anterior tip to front ascending ramus	150+	154	170	147
AP	Anterior tip to rear of mental foramen	43	70	54	52
AQ	Anterior tip to front of mandibular foramen	132	160	155	---
AS	Length of symphysis	62	65	68	69
BG	Posterior extremity to front of ascending ramus	64	74	----	----
BQ	Posterior extremity to front of mandibular foramen	36	65	50	----
CD	Height of coronoid process	130	154	----	----
DF	Distance between anterior and posterior ventral extremities	120	113	56	----
DK	Height of mandibular notch	106	114	----	----
DL	Height of condyle	119	131	----	----
EF	Height at deflection point of horizontal ramus	69	66	83	55
EU	Deflection point to rear of alveolar row	77	86	105	87
GH	Minimum anteroposterior breadth of ascending ramus	63	63	----	----
GP	Front of ascending ramus to rear of mental foramen	100	76	112	----
IJ	Maximum anteroposterior breadth of dorsal part of ascending ramus	65	76	----	----
MN	Top of ventral curvature of horizontal ramus to line connecting ventral extremities	32	26	37	18
MO	Minimum dorsoventral breadth of horizontal ramus	38	37	46	37
RR'	Maximum breadth of masticating surface	37	51	26	25
SQ	Rear of symphysis to front of mandibular foramen	72	99	88	----
TU	Length of the alveolar row (M_{1-3})	44	64	46	46
VV'	Maximum width between labial edges of left and right alveoli across M_1	56	59	65	40
WW'	Minimum width between angles	89	70	65	----
XX'	Minimum width between condyles	99	100	----	----
MD	Deflection of symphysal surface from occlusal plane (degrees)	50	58	43	37

TABLE 4.5. Dental measurements of the lower teeth preserved in USNM 214596 dugongid from the Eocene of North Carolina published in Domning et al. (1982). Abbreviations: **AW**, anterior width; **CH**, crown height labially; **L**, length; **PW**, posterior width. All measurements are in mm; see appendix for key to the measurements.

Tooth	L	AW	PW	CH
i_1	----	----	----	----
i_2	----	----	----	----
i_3	----	----	----	----
c	----	----	----	----
p_1	----	----	----	----
p_2	----	----	----	----
p_3	9.69	7.40	7.40	10.0
p_4	9.89	8.35	8.35	9.60
dp_5	12.17	9.05	9.80	5.50
m_1	12.94	10.10	10.60	7.80
m_2	14.50	11.27	----	9.80
m_3	18.21	12.10	12.00	9.10

TABLE 4.6. Measurements of vertebral elements of *Eotheroides clavigerum* (UM 101219) sp. nov. from the Priabonian of Birket Qarun Formation. Abbreviations: **C**, cervical vertebra; **Ca**, caudal vertebra; **CH,** centrum height; **CL**, centrum length; **CW**, centrum width; **DTF**, distance across transverse foramina in cervical vertebrae; **Lr**, lumbar vertebra, **NCW**, neural canal width; **NCH**, neural canal height ; **THT**, total height; **TW**, total width; **V**, vertebra. All measurements are in mm; see appendix for key to the measurements.

V	THT	TW	CL	CW	CH	NCW	NCH
C1	68	116	22	---	---	38	41
C2	73	70	44	37	26	26	26
C3	---	---	14	39	31	---	---
C5	84	107	15	29	39	37	32
C7	---	---	18	41	27	33	---
Th1	123	108	28	35	27	42	27
Th2	120	100	31	36	25	31	23
Th3	116	100	35	42	27	21	20
Th4	122	94	38	42	30	21	19
Th5	121	90	40	46	33	23	15
Th6	---	93	42	41	34	---	---
Th7	---	86	47	49	39	20	16
Th8	123	87	45	36	40	21	16
Th9	120	87	45	51	36	20	15
Th10	---	86	47	53	40	20	16
Th11	---	85	47	56	35	---	14
Th12	118	91	41	48	39	17	16
Th13	---	79	49	59	36	19	10
Th14	---	---	---	---	---	---	---
Th15	---	---	---	---	---	---	---
Th16	---	---	---	---	---	---	---
Th17	126	82	50	59	43	21	13
Th18	---	---	48	56	41	---	---
Th19	---	---	---	---	---	---	---
S	---	---	36	67	42	---	---
Ca2	78	182	41	63	38	18	12
Ca16	27	67	24	37	27	---	---
Ca19	12	23	17	18	12	---	---

TABLE 4.7. Measurements of left and right ribs of *Eotheroides clavigerum* (UM 101219) sp. nov. from the Priabonian of Birket Qarun Formation. Abbreviations: **CM**, circumference around midshaft; **CT**, capitulum to tubercle length; **EAL**, external arc length; **IAL**, internal arc length; **L**, left rib; **MAWM**, maximum anteroposteriorly width of midshaft; **MLWM**, maximum medolateral width at midshaft; **ND**, neck diameter; **R**, right rib; **TL**, total length. All measurements are in mm; see appendix for key to the measurements.

Rib	TL	EAL	IAL	CT	ND	CM	MLWM	MAWM
L1	158	240	160	45	26	112	37	34
L2	240	---	---	44	32	140	41	38
L3	243	370	275	53	33	154	55	40
L4	270	413	315	54	34	155	54	43
L5	---	---	---	54	35	140	42	46
L6	---	---	---	49	27	133	36	43
L7	315	457	205	52	27	130	35	45
L8				53	26	130	31	46
L9	330	451	385	55	24	118	30	45
L10	---	---	---	55	22	117	30	45
L11	---	---	---	---	19	---	---	---
L15	---	---	---	45		---	---	---
L16	---	---	---	37	28	---	---	---
L17	---	---	---	36		---	---	---
L18	220	230	225	32	28	65	---	---
R2	206	310	212	45	38	140	47	39
R3	241	365	273	49	38	159	53	43
R4	246	413	311	54	39	153	53	43
R5	284	---	345	58	36	143	45	42
R6	---	---	---	---	31	142	48	46
R7	328	452	381	58	32	133	35	44
R8	328	456	387	54	25	126	33	46
R9	330	452	399	52	23	121	32	46
R10	---	---	---	---	22	120	31	43
R11	335	430	393	52	22	117	30	41
R12	331	435	380	48	21	110	29	38
R13	325	430	370	45	24	108	26	40
R14	315	419	303	49	21	110	27	39
R15	---	---	---	42	21	108	23	36
R16	---	---	---	39	21	105	23	34
R17	---	---	---	36	19	93	21	33
R18	---	---	---	33	23	70	25	25

TABLE 4.8. Scapular dimensions of *Eotheroides clavigerum* sp. nov. (UM 101219) and (UM 94806) from the Birket Qarun Formation, compared to those scapulae of *Eotheroides sandersi* sp. nov. (UM 111558), and *Protosiren smithae* (UM 101224) as they were found in the same formation. All measurements are in mm; see appendix for key to the measurements.

Key.	Measurement	*Eotheroides clavigerum* UM 101219 (left scapula)	*Eotheroides clavigerum* UM 94806 (left scapula)	*Eotheroides sandersi* UM 111558 (left scapula)	*Protosiren smithae* UM 101224 (left scapula)
1	Scapular length along the spine	226	218	192	230
2	Spine length	137	118	106	144
3	Scapular breadth	76	---	65	78
4	Infraspinous fossa breadth	51	57	46	60
5	Neck breadth	46	40	34	44
6	Neck height	19	19	15	27
7	Distance from median glenoid cavity to acromion	30	36	29	31
8	Glenoid process breadth	51	52	43	56
9	Glenoid cavity breadth	38	43	34	43
10	Glenoid cavity height	29	30	26	34
11	Breadth of the acromion	---	---	6	11
12	Spine height from dorsal surface	---	---	21	34
13	Spine height from ventral surface	54	48	39	64
14	Distance between anterior tip of glenoid process and anterodorsal edge of blade	142	---	123	153
15	Distance between posterior tip of the glenoid process and first posterior edge of blade	99	---	85	89
16	Circumference of the blade	565	---	475	583

TABLE 4.9. Measurements of humeri of *Eotheroides clavigerum* (UM 101219) and UM (94806) sp. nov. compared to those of *Protosiren smithae* (42292) collected from a nearby localities from the same formation in Wadi Al Hitan. All measurements are in mm; see appendix for key to the measurements.

Key	Measurement	*Eotheroides clavigerum* UM 101219 (right humerus)	*Eotheroides clavigerum* UM 94806 (right humerus)	*Eotheroides sandersi* UM 111558 (left humerus)	*Protosiren smithae* CGM 42292 (left humerus)
1	Length (greater tubercle to distal end)	169	179	155	158
2	Length from the head to the distal end	159	164	142	155
3	Proximal end maximum breadth	59	56	51	57
4	Head height	16	18	17	26
5	Head length	42	43	36	45
6	Head width	36	39	31	37
7	Bicipital groove width	13	12	9	18
8	Maximum width of the shaft in the middle	37	29	23	23
9	Minimum width of the shaft in the middle	25	18	19	21
10	Minimum circumference of the shaft	97	76	70	70
11	Distal end maximum breadth	50	39	42	54
12	Trochlea breadth	34	27	31	31
13	Trochlea height	29	19	24	25
14	Trochlea height n the middle	18	11	18	16
15	Olecranial fossa width	18	23	20	21
16	Olecranial fossa height	20	21	28	23
17	Olecranial fossa depth	13	15	8	10

TABLE 4.10. Ulnar measurements of the Priabonian *Eotheroides clavigerum* (UM 101219) compared to ulnae of *Eotheroides sandersi* (UM 111558) and *Eotheroides aegyptiacum* (SMNS St. XXX) illustrated in Sickenberg (1934, page 30; plate 4, Figs. 6 a-b) from the Lutetian of the Mokattam hills, and also *Protosiren smithae* (CGM 42292) from the Birket Qarun Formation. All measurements are in mm; see appendix for key to the measurements.

key	Measurement	*Eotheroides clavigerum* UM 101219 (right ulna)	*Eotheroides sandersi* UM 111558 (right Ulna)	*Protosiren smithae* CGM 42292 (right ulna)	*Eotheroides aegyptiacum* SMNS St.XXX (right ulna)
1	Greatest length	146	136	138	----
2	Length of the olecranon	30	21	34	22
3	Smallest depth of olecranon	32	24	24	15
4	Greatest depth at the anconeal process	35	26	29	13
5	Height of the trochlear notch	26	22	24	21
6	Breadth across the coronoid process	35	30	23	25
7	Height from the coronoid process to the distal epiphysis	110	98	94	----
8	Circumference of midshaft	61	50	56	----
9	Width of the distal epiphysis	21	16	16	----
10	Length of the distal epiphysis	29	24	28	----

TABLE 4.11. Radial measurements of *Eotheroides clavigerum* (UM 101219) compared to those of an incomplete radius of *Eotheroides aegyptiacum* (SMNS St. XXX) illustrated in Sickenberg (1934, page 30; plate 4, Figs. 6 a-b) from the Lutetian of the Mokattam hills and *Protosiren smithae* (CGM 42292) from the Birket Qarun Formation. All measurements are in mm; see appendix for key to the measurements.

key	Measurement	*Eotheroides clavigerum* UM 101219 (right radius)	*Eotheroides aegyptiacum* SMNS St.XXX (right radius)	*P*rotosiren *smithae* CGM 42292 (right radius)
1	Greatest length	120	----	95
2	Minimum length	112	----	92
3	Breadth of the proximal surface	28	9	26
4	Breadth across the humeral articular surface	24	8	22
5	Maximum width at mid shaft	19	8	21
6	Minimum width at mid shaft	12	6	20
7	Circumference of the mid shaft	55	----	49
8	Greatest breadth of the distal radial end	24	----	24
9	Breadth of the distal articular surface	22	----	23
10	Epiphysis height	----	----	----

TABLE 4.12. Metacarpal and phalange bones dimensions of *Eotheroides clavigerum* sp. nov. (UM 101219). Abbreviation: **Met**, metacarpal; **Phl,** phalange. All measurements are in mm.

Measurement	Right Met I	Right Met II	Right Met III	Right Phl I
Total length	>43	>53	57	33
Proximal width	10	14	12	9
Distal width	13	19	17	11
Proximal height	16	15	15	11
Distal height	8	13	11	6
Midshaft width	9	11	10	7
Midshaft height	6	9	8	5

TABLE 4.13. Measurements of left and right innominates of the holotype *Eotheroides clavigerum* (UM 101219) sp. nov compared to innominate measurements of *Eotheroides sandersi* (UM 111558) from the Birket Qarun Formation, and *Eosiren libyca* (UM 101226) from the Qasr El Sagha Formation, and *Protosiren smithae* (CGM 42292, holotype). All measurements are in mm; see appendix for key to the measurements.

Key	Measurement	*Eotheroides clavigerum* (holotype) UM 101219 (right pelvis)	*Eotheroides clavigerum* (holotype) UM 101219 (left pelvis)	*Eotheroides sandersi* UM 97514 (left pelvis)	*Eosiren libyca* UM 101226 (right pelvis)	*Protosiren smithae* CGM 42292 (right pelvis)
1	Total length	205	215	186	197	250
2	Ilium length (acetabulum to proximal end)	128	145	107	119	165
3	Ilium dorsoventral diameter at midshaft	22	23	21	17	27
4	Ilium mediolateral diameter of at midshaft	20	24	20	18	18
5	Ilium circumference	75	76	65	49	81
6	Symphysis length	0	2	18	12	35
7	Pubic line length	74	70	75	29	56
8	Pubic ramus thickness in front of the obturator foramen	13	13	12	13	19
9	Pubic ramus thickness behind the obturator foramen	16	16	21	22	16
10	Acetabulum diameter	18	19	17	20	24
11	Acetabulum external diameter	21	24	23	24	30
12	Acetabulum depth	9	11	10	10	11
13	Obturator foramen length	4	5	8	5	28
14	Obturator foramen height	5	5	13	4	22
15	Ischium length from center of the acetabulum to distal end	84	89	91	105	105
16	Ischial ramus thickness dorsoventral	30	34	34	32	48
17	Ischiac ramus thickness mediolaterally	9	10	11	12	10
18	Dorsoventral length of the distal end of the ischium	---	28	52	47	54
19	Mediolateral thickness of the distal end of the ischium	---	9	16	28	22
20	Distance between the inner posterior edge of the obturator foramen and the ischiac tuberosity	82	86	94	86	73
21	Length of the sacral articulation surface with the sacrum (anteroposterior length of the oval articulation)	58	53	45	12	26
22	Height of the sacral articulation surface with the sacrum (dorsoventral height of the oval articulation)	46	41	33	16	14
23	Maximum height of the proximal end of the ilium dorsoventrally	52	47	33	17	40
24	Maximum width of the proximal end of the ilium mediolaterally	47	43	28	15	21

TABLE 4.14. Measurements of cranial elements of *Eotheroides sandersi* sp. nov. (CGM 42181, holotype) and UM 111558 collected from the Priabonian of the Birket Qarun Formation compared to the crania measurements *Eotheroides aegyptiacum* of Sickenberg (1934) SMNS St. III, from the Lutetian of Mokattam the Mokattam Hills. All measurements are in mm; see appendix for key to the measurements.

Abbr.	Measurement	*Eotheroides sandersi* CGM 42181	*Eotheroides sandersi* UM 111558	*Eotheroides aegyptiacum* SMNS St. III
AB	Condylobasal length	---	309	----
ab	Height of jugal below orbit	---	37	----
AH	length of premaxillary symphysis	---	97	----
BI	Rear of occipital condyles to the anterior end of interfrontal suture	---	194	180
CC'	Zygomatic breadth	---	142	----
cc'	Breadth across exoccipitals	90	95	72
de	Top of supraoccipital to ventral sides of occipital condyles	---	92	79
F	Length of frontals, level of tips of supraorbital processes of frontoparietal suture	89	120	85
FF'	Breadth across supraorbital processes	92	82	89
ff'	Breadth across occipital condyles	68	65	54
GG'	Breadth of cranium at frontoparietal suture	48	50	49
gg'	Width of foramen magnum	35	32	26
HI	Length of mesorostral fossa	22	69	----
hi	Height of foramen magnum	---	25	26
JJ'	Width of mesorostral fossa	---	37	----
KL	Maximum height of rostrum	---	56	----
MM'	Posterior breadth of rostral masticating surface	---	42	----
no	Anteroposterior length of zygomatic-orbital bridge of maxilla	---	53	52
OP	Length of zygomatic process of squamosal	---	88	----
OT	Anterior tip of zygomatic process to rear edge of squamosal below mastoid foramen	---	117	----
P	Length of parietals, frontoparietal suture to rear of external occipital protuberance	79	56	78
Pq	Length of the alveoli tooth row (Dp5-M3)	---	44	42
QR	Anteroposterior length of zygomatic process of squamosal	---	35	34
rr'	Maximum width between labial edges of left and right alveoli across M^1	---	59	57
ST	Length of cranial portion of squamosal	---	57	----
ss'	Breadth across sigmoid ridges of squamosals	---	126	106
tt'	Anterior breadth of rostral masticating surface	---	25	----
UV	Height of posterior part of cranial portion of squamosal	---	77	72
WX	Dorsoventral breadth of zygomatic process	33	34	----
yy'	Maximum width between pterygoid processes	---	41	29
YZ	Length of jugal	87+	133	----
LFr	Length of frontals in midline	---	88	57
Hso	Height of supraoccipital	45	50	41
Wso	Width of supraoccipital	48	68	55
HIF	Height of infraorbital foramen	---	30	20
WIF	Width of infraorbital foramen	---	20	11
RD	Deflection of masticating surface of rostrum from occlusal plane (Degrees)	---	49	----

TABLE 4.15. Dental measurements of the maxillary teeth preserved in *Eotheroides sandersi* sp. nov. in UM 111558, collected from the Priabonian of the Birket Qarun Formation. Abbreviations: **AW**, anterior width; **CH**, crown height labially; **L**, length; **PW**, posterior width. All measurements are in mm; see appendix for key to the measurements.

Tooth	L	PW	AW	CH
I^1	----	----	----	----
I^2	----	----	----	----
I^3	----	----	----	----
C^1	4.20	----	3.70	4.70
P^1	----	----	----	----
P^2	6.80	----	6.40	7.10
P^3	6.70	----	6.10	7.57
P^4	----	----	----	----
dP^5	----	----	----	----
M^1	9.65	10.74	11.28	6.29
M^2	11.06	11.75	13.75	7.17
M^3	14.29	10.51	14.51	8.27

TABLE 4.16. Vertebrae dimensions of *Eotheroides sandersi* of UM 111558. Abbreviations: **C**, cervical vertebra; **Ca**, caudal vertebra; **CH**, centrum height; **CL**, centrum length; **CW**, Centrum width; **Lr**, lumbar vertebra; **NCW**, neural canal width; **NCH**, neural canal height; **Th**, thoracic vertebra; **THT**, total height; **TW**, total width; **V**, vertebra. All measurements are in mm; see appendix for key to the measurements.

V	THT	TW	CL	CW	CH	NCW	NCH
C1	57	106	----	----	----	27	41
C3	65	84	15	36	28	26	24
Th2	113	101	26	33	23	18	23
Th3	----	----	25	----	20	----	20
Th4	103	93	30	34	26	17	21
Th5	----	----	33	33	27	17	21
Th6	103	86	33	36	27	17	23
Th7	103	82	36	40	30	17	21
Th8	99	81	36	38	27	19	23
Th9	----	81	37	42	30	18	21
Th10	101	98	39	43	28	19	12
Th11	109	79	39	45	32	22	22
Th12	108	80	39	47	33	21	20
Th13	110	78	40	50	37	22	20
Th14	105	79	41	54	33	21	19
Th15	----	77	40	56	33	18	19
Th16	108	78	41	53	35	21	22
Th17?	----	----	----	----	----	----	----
Th18	----	----	----	----	----	----	----
Th19	105	118	45	53	33	20	21
Lr1	104	168	44	53	34	22	21
Ca5?	66	144	39	50	35	19	----
Ca6?	----	120	36	51	35	16	12
Ca7?	----	----	35	49	36	17	16
Ca12?	----	----	27	34	32	----	----
Ca13?	----	95	27	29	26	----	----
Ca16	20	40	23	40	20	----	----
Ca19	----	----	18	22	15	----	----

TABLE 4.17. Measurements (in mm) of vertebrae of *Eotheroides sandersi* UM 97514. Abbreviations: **C**, cervical vertebra; **Ca**, caudal vertebra; **CH**, centrum height; **CL**, centrum length; **CW**, Centrum width; **Lr**, lumbar vertebra, **NCW**, neural canal width; **NCH**, neural canal height; **Th**, thoracic vertebra; **THT**, total height; **TW**, total width; **V**, vertebra. All measurements are in mm; see appendix for key to the measurements.

V	THT	TW	CL	CW	CH	NCW	NCH
Th4	120	----	----	----	----	----	----
Th5	116	99	31	40	29	19	23
Th6	109	91	35	44	31	18	23
Th7	111	93	36	47	34	17	20
Th8	----	----	35	46	----	14	----
Th9	----	89	37	53	34	15	18
Th10	----	87	38	54	39	15	21
Th11	111	88	38	50	36	18	18
Th12	116	83	38	52	38	16	15
Th13	119	81	40	57	41	19	17
Th14	----	86	40	57	44	18	16
Th15	----	79	41	57	39	19	----
Th16	----	----	----	----	----	----	----
Th17?	----	70	40	57	39	18	----
Th18	----	----	----	----	----	----	----
Lr1	----	----	----	----	----	----	----
Lr2	----	----	41	60	42	22	----
Lr3	112	190	42	63	39	19	16
Lr4	106	188	43	62	41	31	18
Lr5	----	----	----	----	----	----	----
Lr6	----	----	----	----	----	----	----
S	98	191	42	61	39	30	14
Ca1	94	192	42	60	37	26	12
Ca2	89	175	40	61	39	23	14
Ca3	83	177	40	62	41	19	13
Ca4	81	168	38	63	42	24	10
Ca5?	76	156	38	56	41	14	90
Ca6?	74		39	61	47	16	11
Ca7?	----	----	----	----	----	----	----
Ca8	65	143	37	53	41	15	8
Ca9	58	136	35	53	38	10	7
Ca10	43	114	28	48	36	8	----
Ca16?	14	33	17	26	14	----	----

TABLE 4.18. Measurements of the preserved ribs of the holotype of *Eotheroides sandersi* CGM 42181; most of the left side of the ribcage is weathered away and never been recovered. Abbreviations: **L**, left rib; **MAWM**, maximum anteroposteriorly width of midshaft; **MLWM**, maximum mediolateral width at midshaft; **R**, right rib; **TL**, total length. All measurements are in mm; see appendix for key to the measurements.

Rib	TL	MLWM	MAWM
L2	145	38	27
R3	----	41	32
R4	----	----	----
R5	----	36	30
R6	230	32	28
R7	260	34	25
R8	265	35	24
R9	260	32	23
R10	----	----	----
R11	----	32	22
R12	----	31	21
R13	----	28	21
R14	----	27	18
R15	----	24	14
R16	242	23	15
R17		22	13
R18	225	22	15

TABLE 4.19. Measurements of preserved ribs of *Eotheroides sandersi* UM 111558. Abbreviations: **CM**, circumference around midshaft; **CT**, capitulum to tubercle length; **EAL**, external arc length; **IAL**, internal arc length; **L**, left rib; **MAWM**, maximum anteroposterior width of midshaft; **MLWM**, maximum mediolateral width at midshaft; **ND**, neck diameter; **R**, right rib; **TL**, total length. All measurements are in mm; see appendix for key to the measurements.

Rib	TL	EAL	IAL	CT	ND	CM	MLWM	MAWM
L12	----	----	----	49	21	----	18	29
L13	----	----	----	48	20	----	18	29
R1	109	141	91	32	12	78	27	23
R2	151	212	145	36	13	107	33	29
R3	193	283	173	40	15	119	38	37
R4	212	322	200	43	16	112	38	31
R5	246	340	228	48	18	96	33	26
R6	264	352	245	49	19	92	24	34
R7	----	352	----	50	19	89	22	33
R8	----	----	----	----	----	88	31	23
R9	----	----	----	48	18	80	18	30
R10	312	374	295	47	20	78	20	29
R11	309	372	290	46	20	77	18	30
R15	----	----	----	42	18	70	18	25
R16	----	----	----	----	----	----	----	----
R17	----	----	----	28	12	48	16	12

TABLE 4.20. Measurements of left and right preserved ribs of *Eotheroides sandersi* UM 97514. Abbreviations: **CM**, circumference around midshaft; **CT**, capitulum to tubercle length; **EAL**, external arc length; **IAL**, internal arc length; **L**, left rib; **MAWM**, maximum anteroposteriorly width of midshaft; **MLWM**, maximum mediolateral width at midshaft; **ND**, neck diameter; **R**, right rib; **TL**, total length. All measurements are in mm; see appendix for key to the measurements.

Rib	TL	EAL	IAL	CT	ND	CM	MLWM	MAWM
L8	329	416	374	45	24	90	31	23
L9	326	414	367	43	23	87	31	22
L10	310+	396	356	42	22	83	29	20
L11	----	----	----	40	22	84	31	20
L12	294	365	325	35	22	78	28	21
L13	272	330	342	31	22	74	26	19
L14	265	280	315	30	21	63	23	16
L15	215	225	251	27	18	59	21	15
L16	64	58	62	22	13	35	15	9
R6	324	428	368	47	27	102	35	28
R7	320	428	370	49	26	99	33	27
R8	315	421	360	47	24	94	36	30
R9	310	412	300	43	24	89	30	22
R10	----	----	----	42	----	87	29	23
R11	295	375	334	40	23	81	29	21
R12	270	358	318	32	20	76	25	19
R13	268	350	310	31	21	73	25	19
R14	228	288	262	32	18	65	22	15
R15	215	252	235	26	18	53	18	11
R16	118	120	115	22	12	37	13	12

TABLE 4.21. Scapular measurements of *Eotheroides sandersi* sp. nov. CGM 42181, (holotype) and UM 111558 from the Birket Qarun Formation. All measurements are in mm; see appendix for key to the measurements.

Key	Measurement	*Eotheroides sandersi* CGM 42181 (right scapula)	*Eotheroides sandersi* UM 111558 (left scapula)
1	Scapular length along the spine	196	192
2	Spine length	103	106
3	Scapular breadth	61	65
4	Infraspinous fossa breadth	43	46
5	Neck breadth	36	34
6	Neck height	17	15
7	Distance from median glenoid cavity to acromion	38	29
8	Glenoid process breadth	47	43
9	Glenoid cavity breadth	36	34
10	Glenoid cavity height	25	26
11	Breadth of the acromion	---	6
12	Spine height from dorsal surface	---	21
13	Spine height from ventral surface	---	39
14	Distance between anterior tip of glenoid process and anterodorsal edge of blade	123	123
15	Distance between posterior tip of the glenoid process and first posterior edge of blade	93	85
16	Circumference of the blade	490	475

TABLE 4.22. Measurements of humeri of *Eotheroides sandersi* sp. nov. CGM 42181 (holotype) and UM 111558. All measurements are in mm; see appendix for key to the measurements.

Key	Measurement	*Eotheroides sandersi* CGM 42181	*Eotheroides sandersi* UM 111558
1	Maximum Length (greater tubercle to distal end)	137	155
2	Length from the head to the distal end	137	142
3	Maximum breadth of the proximal end	43	51
4	Head height	17	17
5	Head length	35	36
6	Head width	33	31
7	Width of the bicipital groove	13	9
8	Maximum width of the shaft in the middle	26	23
9	Minimum width of the shaft in the diaphyses	18	19
10	Minimum circumference of the shaft	71	70
11	Maximum breadth of the distal end	46	42
12	Breadth of the trochlea	32	31
13	Height of the trochlea	21	24
14	Height of the trochlea in the middle	15	18
15	Width of the olecranial fossa	20	20
16	Height of the olecranial fossa	16	28
17	Depth of the olecranial fossa	12	8

TABLE 4.23. Ulnar measurements of a fully mature *Eotheroides sandersi* (holotype) and juvenile individual (UM 97515) compared to an incomplete ulna of *Eotheroides aegyptiacum* (SMNS St. XXX) illustrated in Sickenberg (1934, page 30; plate 4, Figs. 6 a-b) from the Lutetian of the Mokattam hills. All measurements are in mm; see appendix for key to the measurements.

Key	Measurement	*Eotheroides sandersi* UM 111558 (right Ulna)	*Eotheroides sandersi* UM 97515 (left ulna)	*Eotheroides aegyptiacum* SMNS St.XXX (right ulna)
1	Greatest length	136	98	----
2	Length of olecranon	21	21	22
3	Smallest depth of olecranon	24	24	15
4	Greatest depth at the anconeal process	26	26	13
5	Height of the trochlear notch	22	23	21
6	Mediolateral breadth of proximal articular surface (coronoid process)	30	26	25
7	Height from the coronoid process to the distal epiphysis	98	66	----
8	Mid shaft circumference	50	44	----
9	Width of the distal epiphysis	16	13	----
10	Length of the distal epiphysis	24	20	----

TABLE 4.24. Dimensions of metacarpal bones dimensions of *Eotheroides sandersi* sp. nov. (UM 111558). Abbreviation: **Met.**, metacarpal. All measurements are in mm; see appendix for key to the measurements.

Measurement	Met. III	Met. V
Total length	>53	---
Proximal width	14	18
Distal width	14	---
Proximal height	15	10
Distal height	10	---
Midshaft width	9	11
Midshaft height	8	6

TABLE 4.25. Measurements of innominate pelvic bones of the *Eotheroides sandersi* sp. nov. (CGM 42181, holotype) and UM 111558 from the Birket Qarun Formation, and *Eosiren libyca* (UM 101226) from the Qasr El Sagha Formation. All measurements are in mm; see appendix for key to the measurements.

Key	Measurement	*Eotheroides sandersi* CGM 42181 (left pelvis)	*Eotheroides sandersi* UM 97514 (right pelvis)	*Eotheroides sandersi* UM 97514 (left pelvis)
1	Total length of the pelvis	153	190	186
2	Length of the ilium from the center of the acetabulum to proximal end	107	113	107
3	Dorsoventral diameter of ilium at midshaft	17	21	21
4	Mediolateral diameter of ilium at midshaft	19	21	20
5	Circumference ilium at midshaft	60	67	65
6	Symphysis length	---	18	18
7	Length of the pubic line from the center of the acetabulum	---	66	75
8	Pubic ramus in front of the obturator foramen	7	12	12
9	Pubic ramus behind the obturator foramen	7	22	21
10	Acetabulum diameter	16	18	17
11	External diameter of the acetabulum	18	21	23
12	Acetabulum depth	5	10	10
13	Obturator foramen length	5	9	8
14	Obturator foramen height	5	13	13
15	Length of the ischium from the center of the acetabulum	48	89	91
16	Dorsoventral depth of the ischiac ramus	30	34	34
17	Ramus of Ischium thickness (mediolaterally)	6	13	11
18	Maximum dorsoventral length of the distal end of the ischium	27	53	52
19	Maximum mediolateral thickness of the distal end of the ischium	6	16	16
20	Distance between the inner posterior edge of the obturator foramen and the ischiac tuberosity	47	99	94
21	Length of the sacral articulation surface with the sacrum (anteroposterior length of the oval articulation)	31	52	45
22	Height of the sacral articulation surface with the sacrum (dorsoventral height of the oval articulation)	16	31	33
23	Maximum height of the proximal end of the ilium dorsoventrally	27	31	33
24	Maximum width of the proximal end of the ilium mediolaterally	23	29	28

TABLE 4.26. Femoral dimensions Eocene Egyptian sirenians, including those of *Eotheroides sandersi*, *Eosiren libyca*, and *Protosiren smithae* from the Priabonian of Birket Qarun and Qasr El Sagha formations. *Protosiren smithae* has larger dimension. Both specimens of *Eotheroides sandersi* are missing their proximal and distal epiphysis. All measurements are in mm; see appendix for key to the measurements.

Key	Measurement	*Eotheroides sandersi* CGM 42181 (right femur)	*Eotheroides sandersi* UM 111558 (left femur)	*Eosiren libyca* UM 101226 (right femur)	*Protosiren smithae* CGM 42292 (right femur)
1	Greatest length	----	----	108	144
2	Total length from the femoral head	----	----	108	138
3	Head height	----	----	9	13
4	Head length anteroposteriorly	----	----	13	20
5	Head width mediolaterally	----	----	20	27
6	Greatest proximal width	19	20	26	48
7	Length of the femoral body	91	102	98	122
8	Width across the second trochanter	14	15	18	30
9	Minimum width of the diaphysis	9	7	11	19
10	Minimum circumference of diaphysis	28	25	14	52
11	Minimum width of the distal end	12	11	16	21
12	Greatest width of the distal end	12	12	13	35
13	Width between the external ends of the distal lateral condyles	----	----	6	26
14	Internal distance between the lateral condyle	----	----	----	5

FIGURE 4.1. Holotype skull and mandibles of *Eotheroides clavigerum* (UM 101219) from the Priabonian Birket Qarun Formation of Wadi Al Hitan. A, Lateral view of the cranium; illustration is based on the complete skull deposited at the Museum of Paleontology at the University of Michigan. The zygomatic process of the jugal was removed temporarily to expose the alisphenoid opening. B and C, Lateral and occlusal views of the lower dentaries, tightly fused together. Abbreviations: **AC**, alisphenoid canal (foramen in *Eotheroides*); **ANG. P.**, angular process; **AS**, alisphenoid; **BO**, basioccipital; **BS**, basisphenoid; **COND. P.**, processus condylus; **COR. CAN.**, coronoid canal; **COR. P.**, coronoid process**;** **CT**, temporal crest; **C**, upper canine; **c**, upper canine; **dP**, deciduous premolar; **dp alv.**, alveolar of deciduous premolar; **ENR**, external nares (mesorostral fossa); **EO**, exoccipital; **FIO**, foramen infraorbital; **FOV**, foramen ovalis; **FPT**, fossa pterygoidea; **FR**, frontal; **FRT**, foramen rotundum; **G**, glenoid articulation; **HOR. RAM.**, horizontal ramus**;** $\mathbf{I^1}$ etc., upper incisor; $\mathbf{i_1}$ etc., lower incisor; **J**, jugal; **LAC**, lacrimal, $\mathbf{M^1}$ etc., upper molar or alveoli; $\mathbf{m_1}$ etc., lower molar or alveoli; **MAL**, Malleus; **MAND. RAM.**, mandibular ramus; **MENT. FOR.**, mental foramen**;** **MENT. PROT.**, mental protuberance**;** **MF**, mastoid foramen; **MX**, maxilla; **N**, Nasal; **OCC**, occipital condyle, **OF**, optic foramen; **OVF**, oval foramen; $\mathbf{P^1}$ etc., upper premolar alveoli; $\mathbf{p_1}$ etc., lower premolar alveoli; **PA**, parietal; **PAL**, palatine; **PM**, premaxilla; **PT**, pterygoid; **PTP**, pterygoid process; **POP**, post occipital process; **SO**, supraoccipital; **SOP**, supraorbital process; **SQ**, squamosal; **T**, tympanic; **V**, vomer; **ZP**, zygomatic process of the jugal.

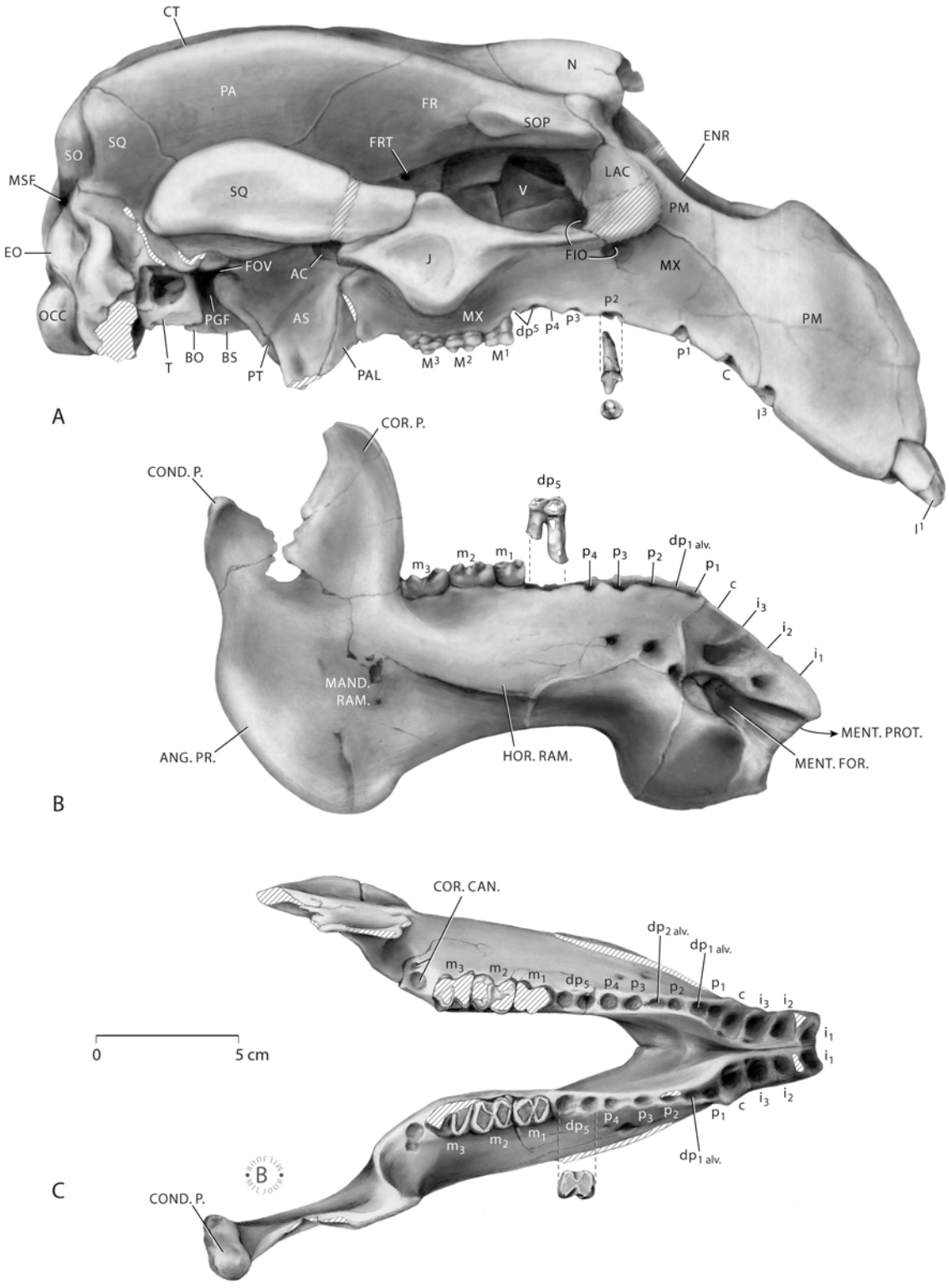
CT
PA
N
FR
SOP
SQ
SO
FRT
ENR
MSF
SQ
V
LAC
PM
EO
FOV
AC
J
FIO
MX
OCC
PGF
AS
MX
P2
PM
dp5
P4
P3
P1
T
BO
BS
PT
PAL
M3
M2
M1
C
I3
I1
A
COR. P.
COND. P.
dp5
m3
m2
m1
p4
p3
p2
dp1 alv.
p1
c
i3
i2
i1
MAND.
RAM.
MENT. PROT.
ANG. PR.
HOR. RAM.
MENT. FOR.
B
COR. CAN.
dp2 alv.
dp1 alv.
m3
m2
m1
dp5
p4
p3
p2
p1
c
i3
i2
i1
i1
0
5 cm
m3
m2
m1
dp5
p4
p3
p2
p1
c
i3
i2
dp1 alv.
C
COND. P.

FIGURE 4.2. Holotype cranium of *Eotheroides clavigerum* (UM 101219). A, Dorsal view. B, Ventral view. The skull is tilted more caudally in B to expose greater detail in the ventral view of the rostrum. Abbreviations: **APF**, anterior palatine foramen; **AS**, alisphenoid; **BO**, basioccipital; **BS**, basisphenoid; **C^1**, upper canine; **CF**, condyloid foramen; **CT**, temporal crest; condyloid foramen; **dP**, deciduous premolar of maxilla; **dp alv.**, alveolar of deciduous premolar; **E**, ethmoid; **ENR**, external nares (mesorostral fossa); **EO**, exoccipital; **FR**, foramen rotundum; **FIO**, foramen infraorbital; **FM**, foramen magnum; **FPT**, fossa pterygoidea; **F**, frontal; **G**, glenoid articulation; **I^1** etc., first upper incisor; **i_1** etc., first lower incisor; **INR**, internal nares; **INP**; interparietal groove; **J**, jugal; **LAC**, lacrimal, **M^1** etc., first upper molar or alveoli; **m_1** etc., first lower molar or alveoli; **MAL**, Malleus; **MAND. FOS.**, mandibular fossa**; ME**, Mesethmoid; **MF**, mastoid foramen; **MX**, maxilla; **N**, Nasal; **OCC**, occipital condyle; **P^1** etc., first upper premolar alveoli; **p_1** etc., first lower premolar alveoli; **PA**, parietal; **PAL**, palatine; **PAR. O. P.**, paroccipital processes**; PGF.,** postglenoid fossa; **PM**, premaxilla; **POST. T. P**, posttympanic process**; PR**, periotic; **PT**, pterygoid; **PS**, presphenoid, **SO**; supraoccipital; **SOP**, supraorbital process; **SQ**, squamosal; **T**, tympanic; **TF**, temporal fossa; **V**, vomer.

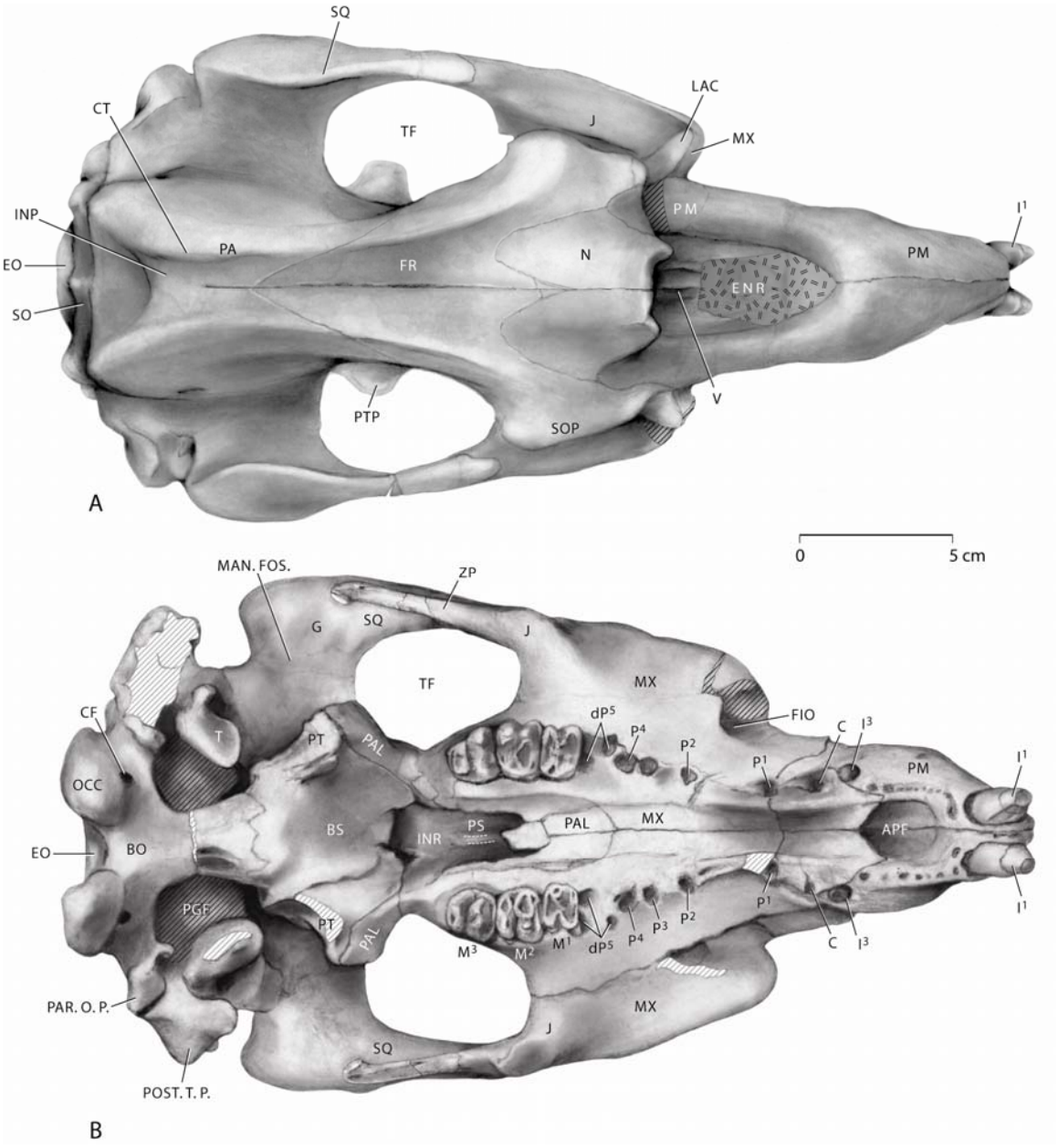
SQ
CT
TF
J
LAC
MX
INP
PA
FR
N
PM
I1
EO
SO
ENR
V
PTP
SOP
A
0
5 cm
MAN. FOS.
ZP
G
SQ
J
TF
MX
CF
T
PT
PAL
dP5
P4
P2
FIO
C
I3
P1
PM
I1
OCC
BS
INR
PS
PAL
MX
APF
EO
BO
PGF
PT
PAL
M3
M2
M1
dP5
P4
P3
P2
P1
C
I3
I1
PAR. O. P.
MX
J
SQ
POST. T. P.
B

FIGURE 4.3. Holotype cranium of *Eotheroides clavigerum* (UM 101219). A, Anterior view. B, Posterior view. Abbreviations: **BO**, basioccipital; **CT**, temporal crest; **E**, ethmoid; **ENR**, external nares (mesorostral fossa); **EO**, exoccipital; **FR**, foramen rotundum; **FIO**, foramen infraorbital; **FM**, foramen magnum; **FR**, frontal; **I^1** etc., first upper incisor; **INP**; interparietal groove; **J**, jugal; **LAC**, lacrimal, **M^1** etc., first upper molar or alveoli; **ME**, mesethmoid; **MSF**, mastoid foramen; **MX**, maxilla; **N**, nasal; **OCC**, occipital condyle; **P^1** etc., first upper premolar alveoli; **PA**, parietal; **PAL**, palatine; **PAR. O. P.**, paroccipital processes**; PGF.,** postglenoid fossa; **PM**, premaxilla; **PR**, periotic; **SO**; supraoccipital; **SOP**, supraorbital process; **SQ**, squamosal; **V**, vomer.

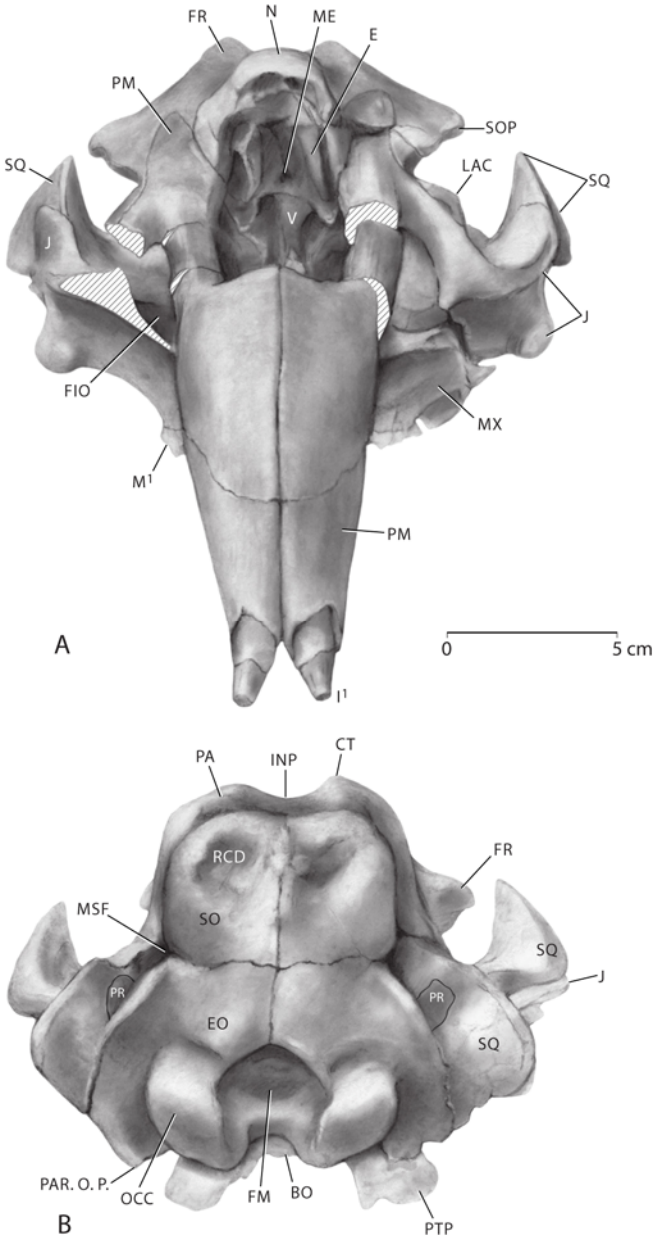

FIGURE 4.4. Toothless right maxillary bone of *Eotheroides clavigerum* (UM 97524) bearing alveoli of P^1 through M^3. dP^5 through M^3 are triple-rooted, while P^1 through P^4 are single-rooted.

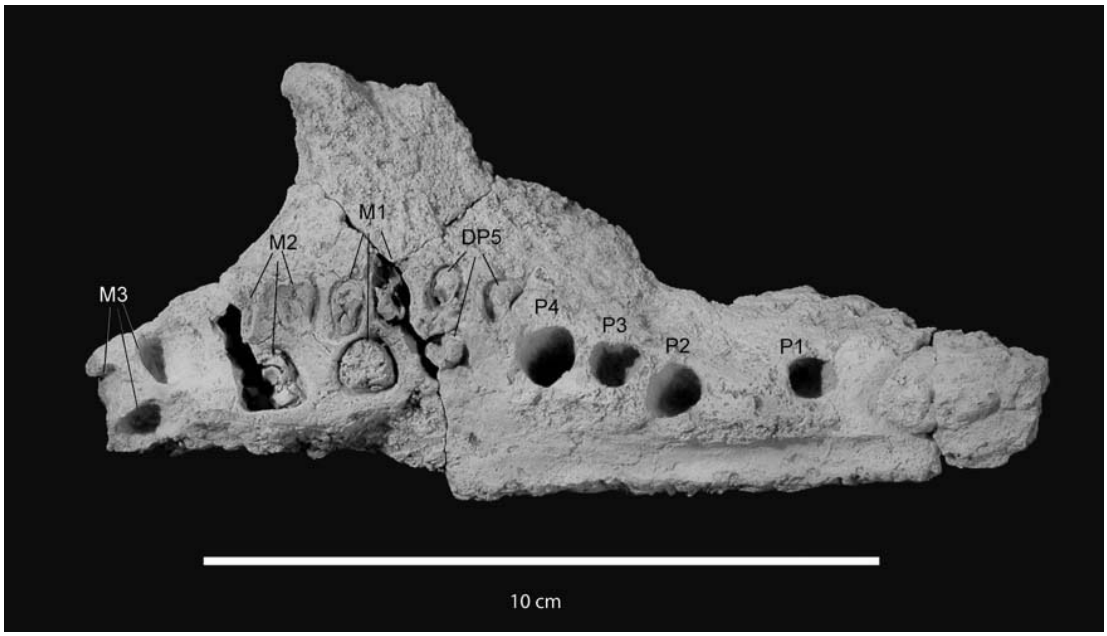

FIGURE 4.5. Cranial (anterior) view of cervical, thoracic, sacral, and caudal vertebrae of the holotype of *Eotheroides clavigerum* (UM 101219). Vertebrae recovered include **C1**, **C2**, **C3**, **C5** and **C7**, **Th1** through **Th13**, **Th17** and **Th18, S**, **Ca1**, ?**Ca16**, and ?**Ca19**. Abbreviations: **C**, cervical; **Ca**, caudal; **Th**, thoracic; **S**, sacral.

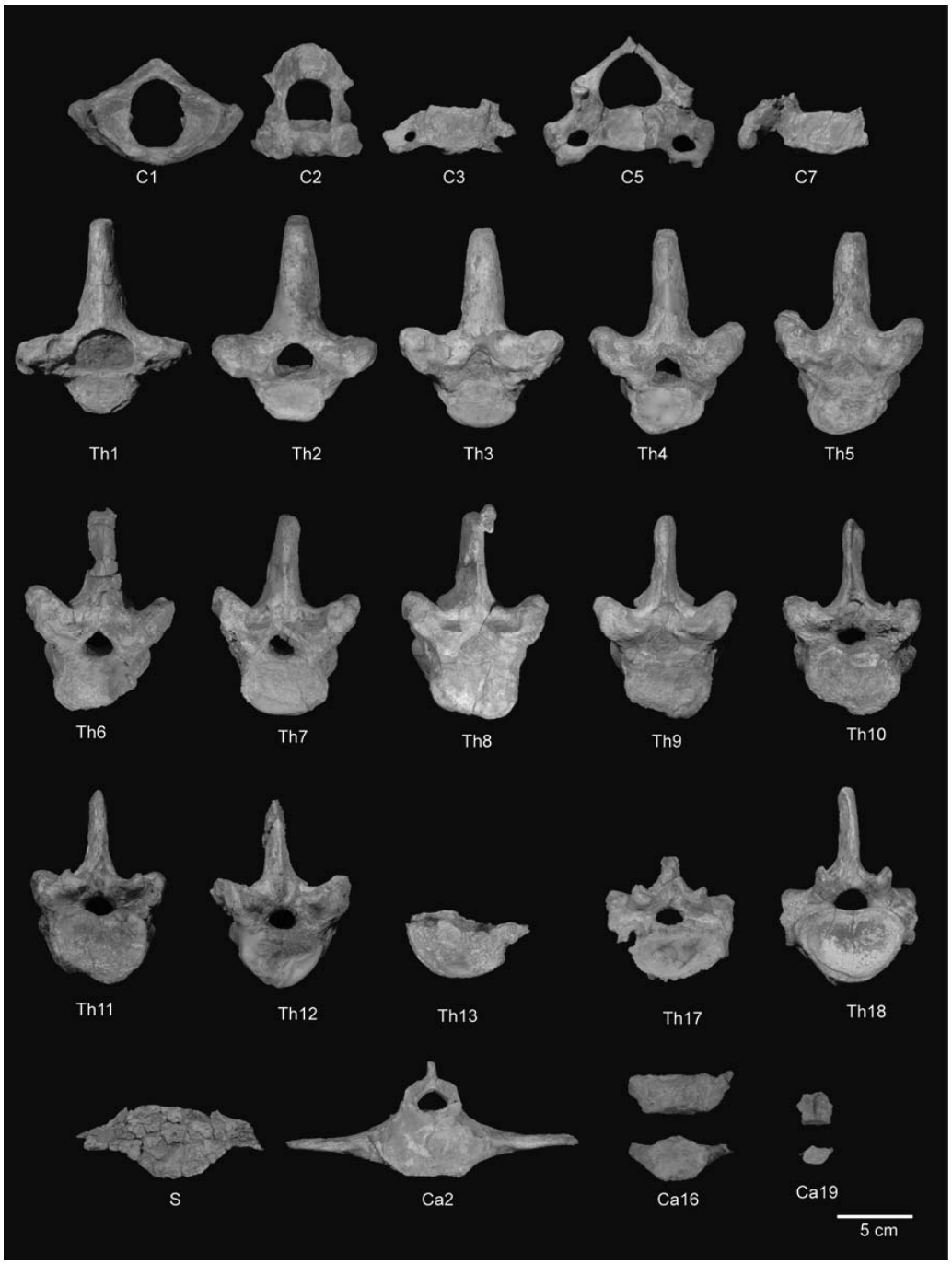

FIGURE 4.6. Dorsal view of cervical, thoracic, sacral, and caudal vertebrae of *Eotheroides clavigerum* (UM 101219) in articulation and serial arrangement of the holotype. Abbreviations: **C**, cervical; **Ca**, caudal; **Th**, thoracic; **S**, sacral.

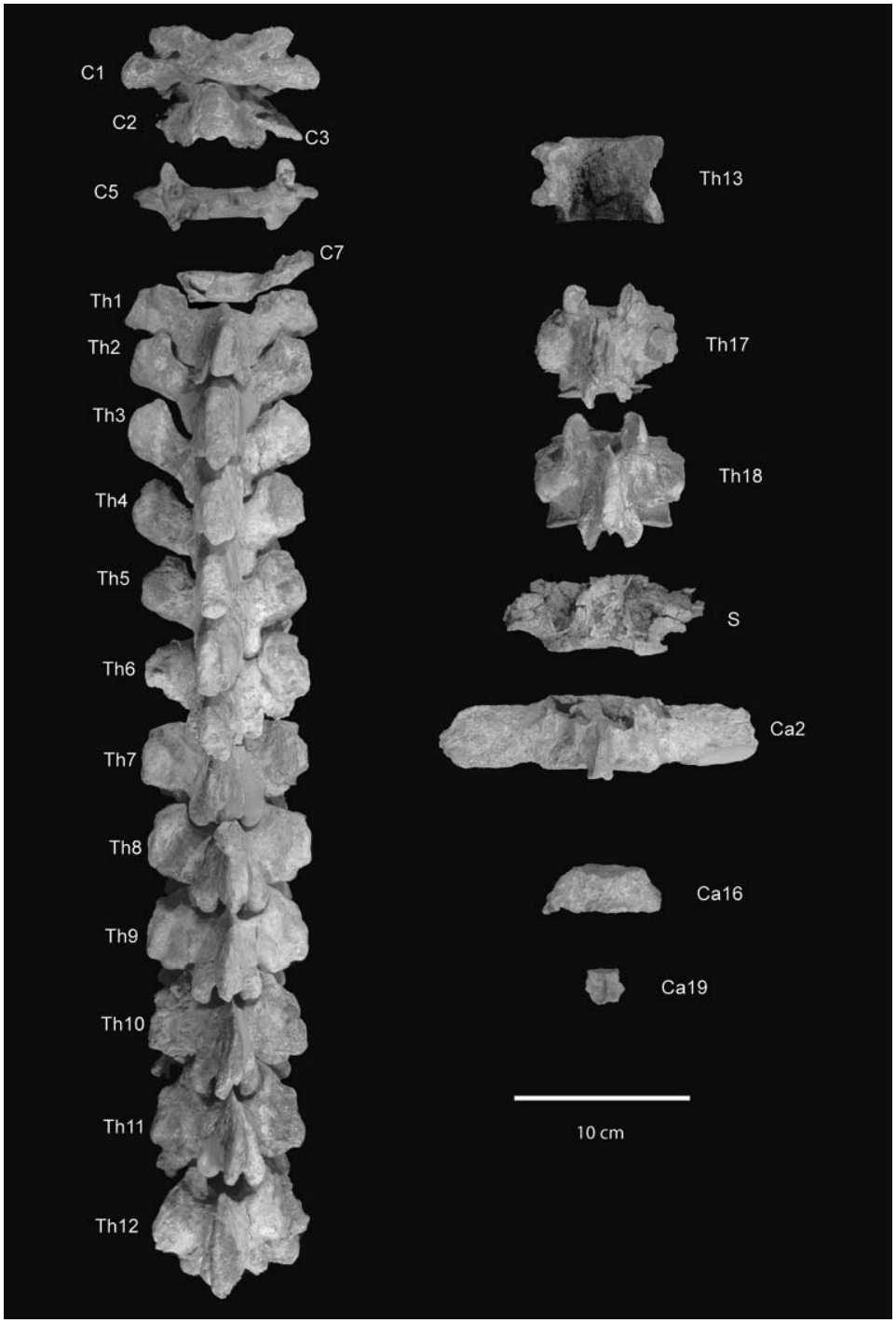

FIGURE 4.7. Lateral view of cervical, thoracic, sacral, and caudal vertebrae of the holotype of *Eotheroides clavigerum* (UM 101219) in articulations. Abbreviations: **C**, cervical; **Ca**, caudal; **Th**, thoracic; **S**, sacral.

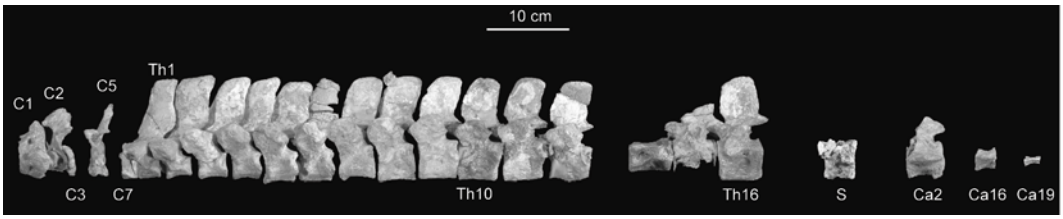

FIGURE 4.8. Cranial (anterior) view of the left and right ribs of the holotype of *Eotheroides clavigerum* (UM 101219). Ribs are arranged from 1 through 18 based on morphology and size of both rib body and proximal articulation of the tuberculae and facets of the head, fit with thoracic vertebrae, degree of pachyosteosclerosis, and length and straightness of the rib shaft. Left rib side preserved the upper half of rib series and the last rib. Right rib series is almost complete missing the first rib, and the distal portions of the posterior ribs. Abbreviations: **L**, left rib; **R**, right rib.

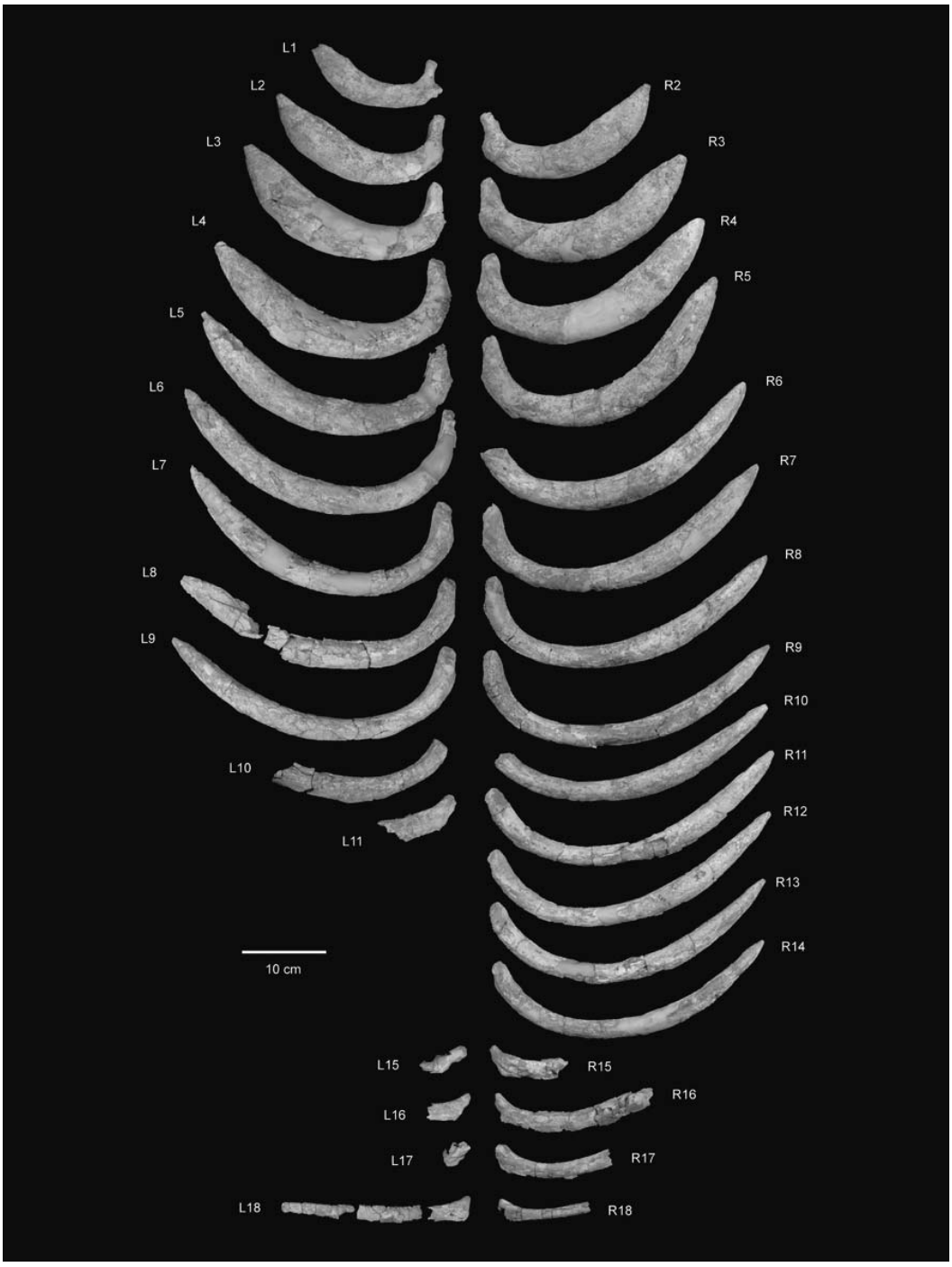

FIGURE 4.9. Forelimb elements of the holotype of *Eotheroides clavigerum* UM 101219. **A**, Right radius and ulna, medial view. **B**, Right humerus, posterior view. **C**, Right scapula, lateral view.

FIGURE 4.10. Right metapodials of *Eotheroides clavigerum* (UM 101219). First and second metacarpals (Met. I and II) have a best fit as shown here; the third metacarpal (Met. III) has a slightly weathered proximal end. Phalanx II has a flattened distal end.

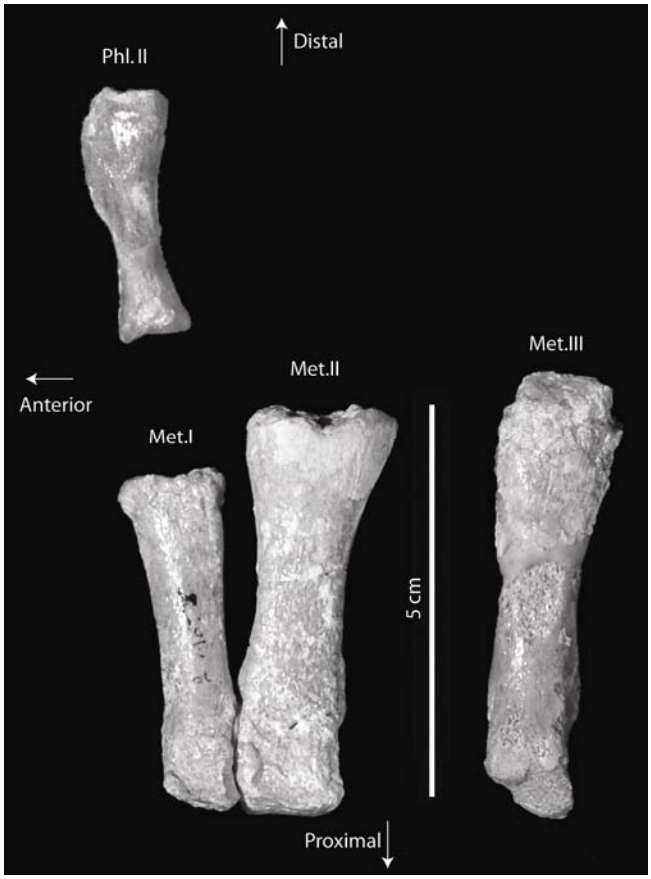

FIGURE 4.11. Left and right innominate pelvic bones of *Eotheroides clavigerum* (UM 101219, holotype) from the Birket Qarun Formation. **A**, Left innominate lateral view. **B**, Right innominate lateral view. **C**, Right innominates medial view. **D**, Left innominate in medial view. Notice the club-like anterior portion of the ilium; the long and cleft pubis, and the reduced acetabulum. Abbreviations: **act.,** acetabulum; **act. n.,** acetabular notch; **dor. il. sp.** dorso iliac spine; **il.,** ilium; **isc.,** ischium; **isc. tub.,** ischiac tuberosity; **isc. shft.,** ischiac shaft; **obt. f.,** obturator foramen;; **ps.,** pubis; **pub. symph.,** pubic symphysis; **pub. clft,** pubic cleft; **pub. ram. ant.,** anterior pubic ramus; **pub. ram. post.,** posterior pubic ramus; **sac. il. artic.**, sacroiliac articulation surface.

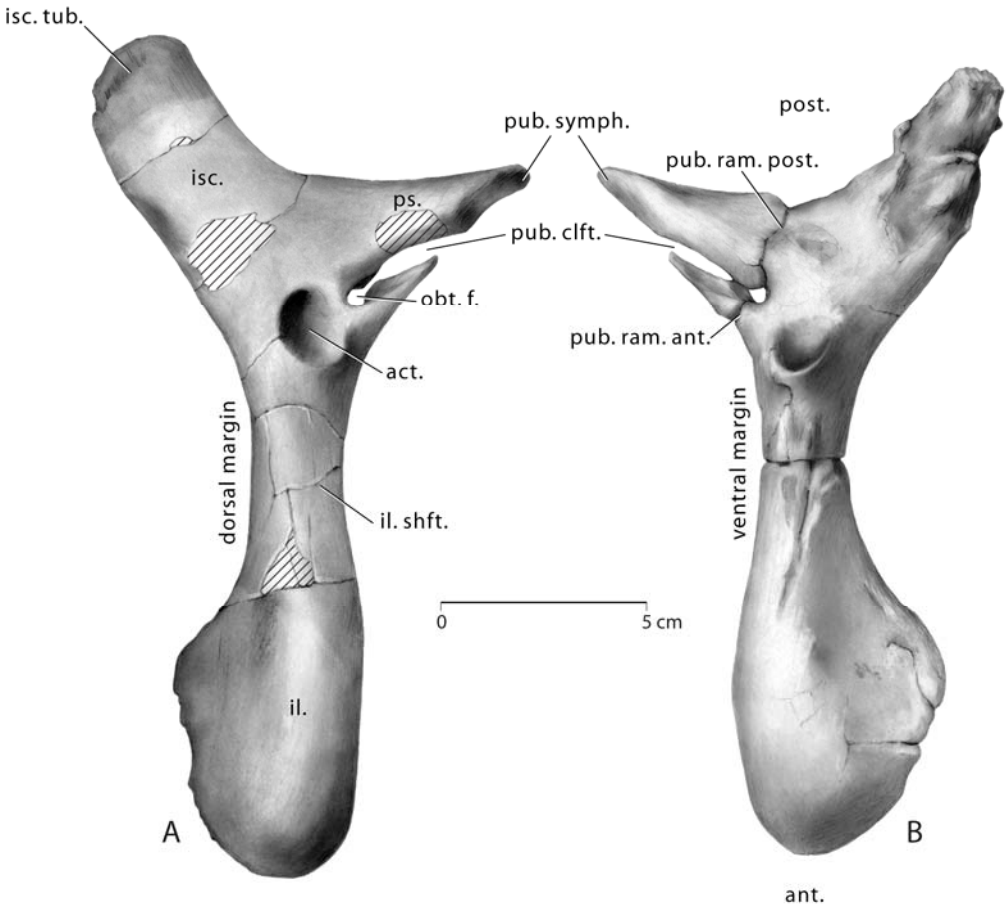

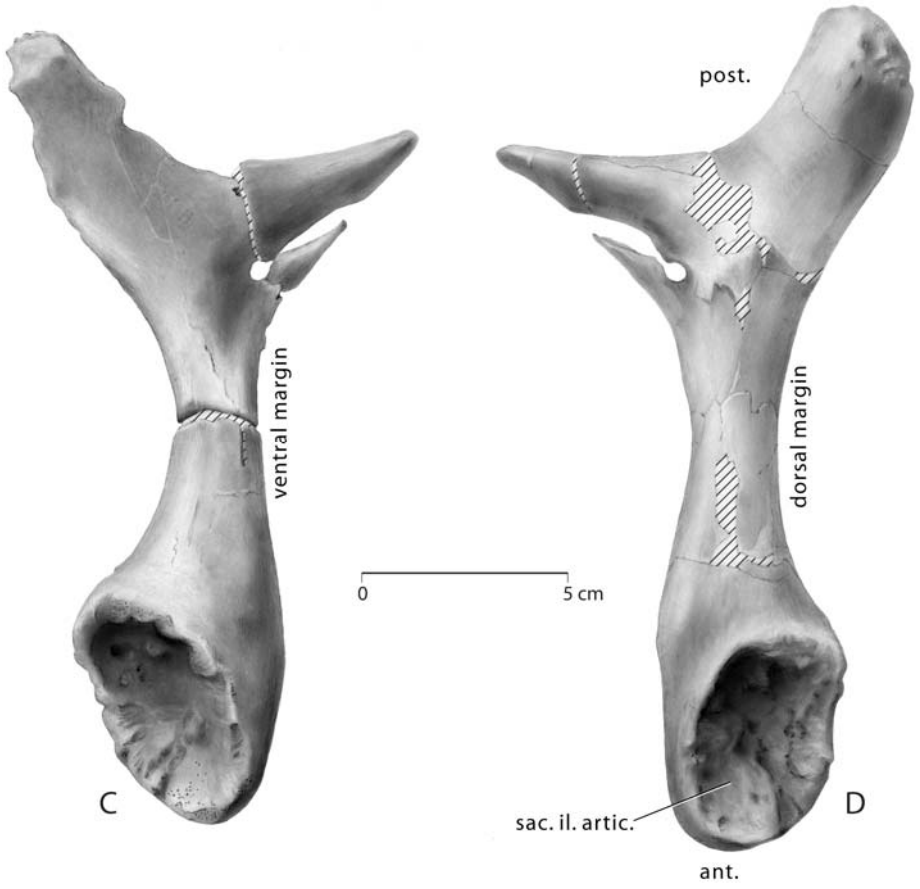
ventral margin
C
0
5 cm
post.
dorsal margin
D
sac. il. artic.
ant.

FIGURE 4.12. Cranial elements of *Eotheroides sandersi* CGM 42181 (holotype). A and D, Dorsal views of the skull roof including nasal, frontal, parietals, supraoccipital, and portions of the right squamosal; note that the parietals and frontals were connected with each others along a deep V-shaped suture. **B** and **F**, Ventral view of skull roof. **E**, Dorsal view of the right squamosal process. **C** and **G**, Dorsal and ventral views of the basisphenoid and presphenoid. **H**, Exoccipitals in posterior view showing the occipital condyles and foramen magnum. **I**, Symphysal processes of the lower jaw.
Abbreviations: **AC**, alisphenoid canal (foramen); **AS**, alisphenoid; **BS**, basisphenoid; **CT**, temporal crest; **E**, ethmoid; **EO**, exoccipital; **FM**, foramen magnum; **FPT**, fossa pterygoidea; **FR**, frontal; **INP**; interparietal groove; **ME**, Mesethmoid; **N**, Nasal; **OCC**, occipital condyle; **PA**, parietal; **PR**, periotic; **PT**, pterygoid; **PTP**, pterygoid process; **PS**, presphenoid, **SO**; supraoccipital; **SOP**, supraorbital process; **SQ**, squamosal.

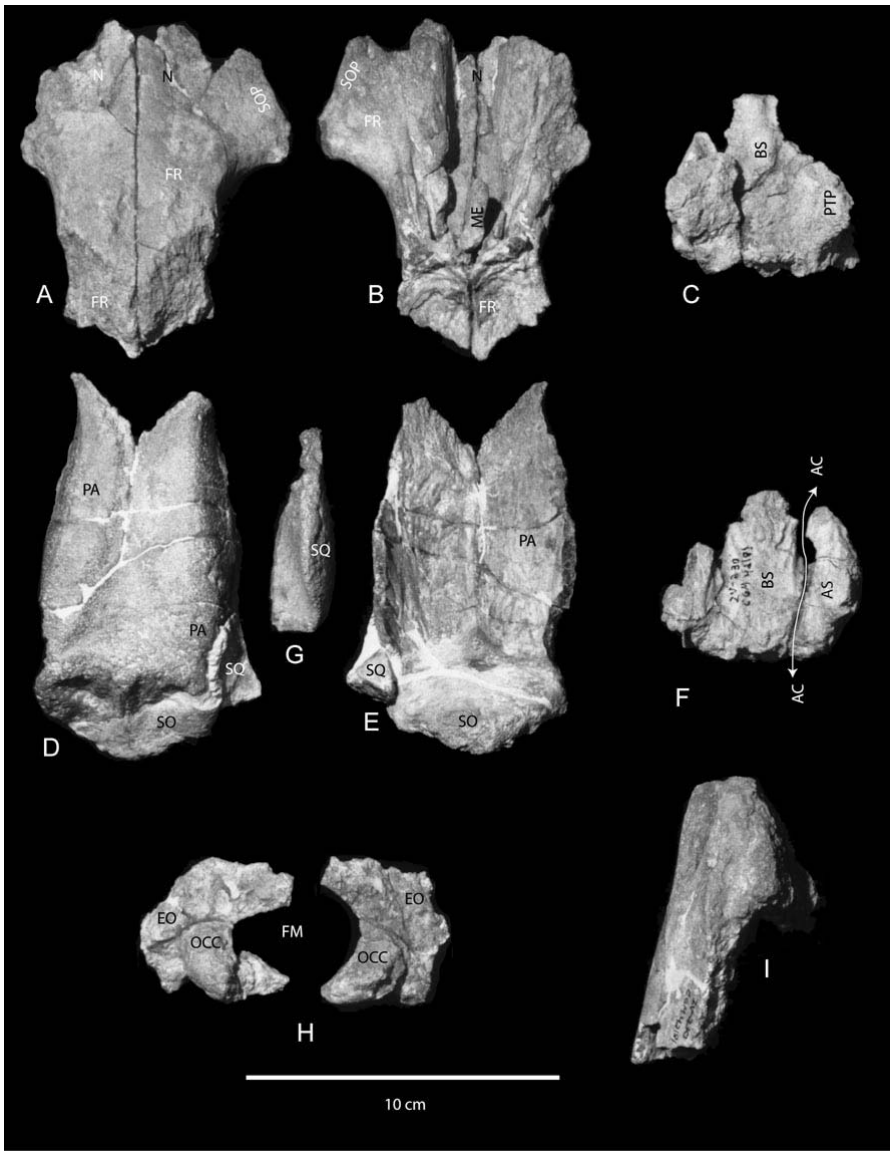

FIGURE 4.13. Cranium of *Eotheroides sandersi* (UM 111558). **A**, Dorsal view. **B**, Lateral view. **C**, Ventral view. Abbreviations: **AC**, alisphenoid canal (foramen); **APF**, anterior palatine foramen; **AS**, alisphenoid; **BO**, basioccipital; **BS**, basisphenoid; **C^1**, upper canine; **CF**, condyloid foramen; **CT**, temporal crest; **dP**, deciduous premolar of maxilla; **dp alv.**, alveolar of deciduous premolar; **E**, ethmoid; **ENR**, external nares (mesorostral fossa); **EO**, exoccipital; **FRT**, foramen rotundum; **FIO**, foramen infraorbital; **FM**, foramen magnum; **FOV**, foramen ovalis; **FPT**, fossa pterygoidea; **FR**, frontal; **G**, glenoid articulation; **I^1** etc., first upper incisor; **INR**, internal nares; **INP**; interparietal groove; **J**, jugal; **LAC**, lacrimal, **M^1** etc., first upper molar or alveoli; **MAL**, Malleus; **MAND. FOS.**, mandibular fossa**;** **ME**, Mesethmoid; **MSF**, mastoid foramen; **MX**, maxilla; **N**, Nasal; **OCC**, occipital condyle; **P^1** etc., first upper premolar alveoli; **PA**, parietal; **PAL**, palatine; **PAR. O. P.**, paroccipital processes**;** **PGF.,** postglenoid fossa; **PM**, premaxilla; **POST. T. P**, posttympanic process**;** **PR**, periotic; **PT**, pterygoid; **PTP**, pterygoid process; **PS**, presphenoid, **SO**; supraoccipital; **SOP**, supraorbital process; **SQ**, squamosal; **T**, tympanic; **TF**, temporal fossa; **V**, vomer; **ZP**, zygomatic process of the jugal.

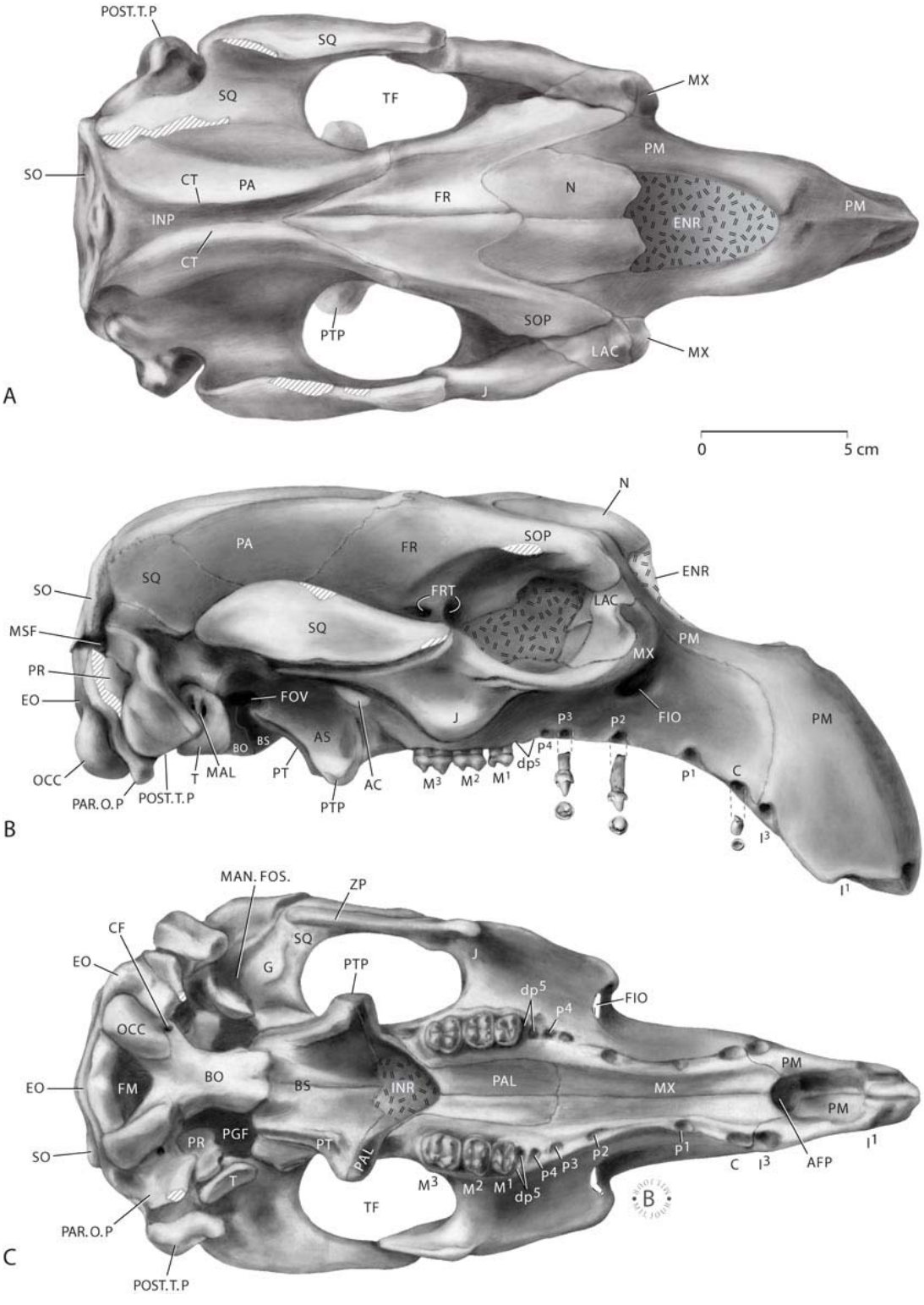
A
POST.T.P
SQ
SQ
TF
MX
PM
SO
CT
PA
FR
N
PM
INP
ENR
CT
SOP
PTP
LAC
MX
J
0
5 cm
B
N
PA
FR
SOP
SQ
ENR
SO
FRT
LAC
SQ
MSF
PM
MX
PR
EO
FOV
J
P3
P2
FIO
PM
BO
BS
AS
P4
OCC
T
MAL
PT
AC
M3
M2
M1
dp5
P1
C
PAR.O.P
POST.T.P
PTP
I3
I1
C
MAN. FOS.
ZP
CF
SQ
EO
G
PTP
J
dp5
FIO
P4
OCC
PM
EO
FM
BO
BS
INR
PAL
MX
PM
PR
PGF
PT
I1
SO
PAL
P3
P2
P1
T
M3
M2
M1
P4
C
I3
AFP
dp5
TF
PAR.O.P
POST.T.P

FIGURE 4.14. Cranium of *Eotheroides sandersi* (UM 111558). **A**, Anterior view. **B**, Posterior view. Abbreviations: **BO**, basioccipital; **CT**, temporal crest; **ENR**, external nares (mesorostral fossa); **EO**, exoccipital; **FR**, foramen rotundum; **FIO**, foramen infraorbital; **FM**, foramen magnum; **FR**, frontal; **I^1** etc., first upper incisor; **INP**; interparietal groove; **J**, jugal; **LAC**, lacrimal, **M^1** etc., first upper molar or alveoli; **MSF**, mastoid foramen; **MX**, maxilla; **N**, nasal; **OCC**, occipital condyle; **P^1** etc., first upper premolar alveoli; **PA**, parietal; **PAL**, palatine; **PAR. O. P.**, paroccipital processes; **PGF,** postglenoid fossa; **PM**, premaxilla; **PR**, periotic; **RCD**, rectus semispinalis dorsalis **SO**; supraoccipital; **SOP**, supraorbital process; **SQ**, squamosal; **SSC**, semispinalis capitate.

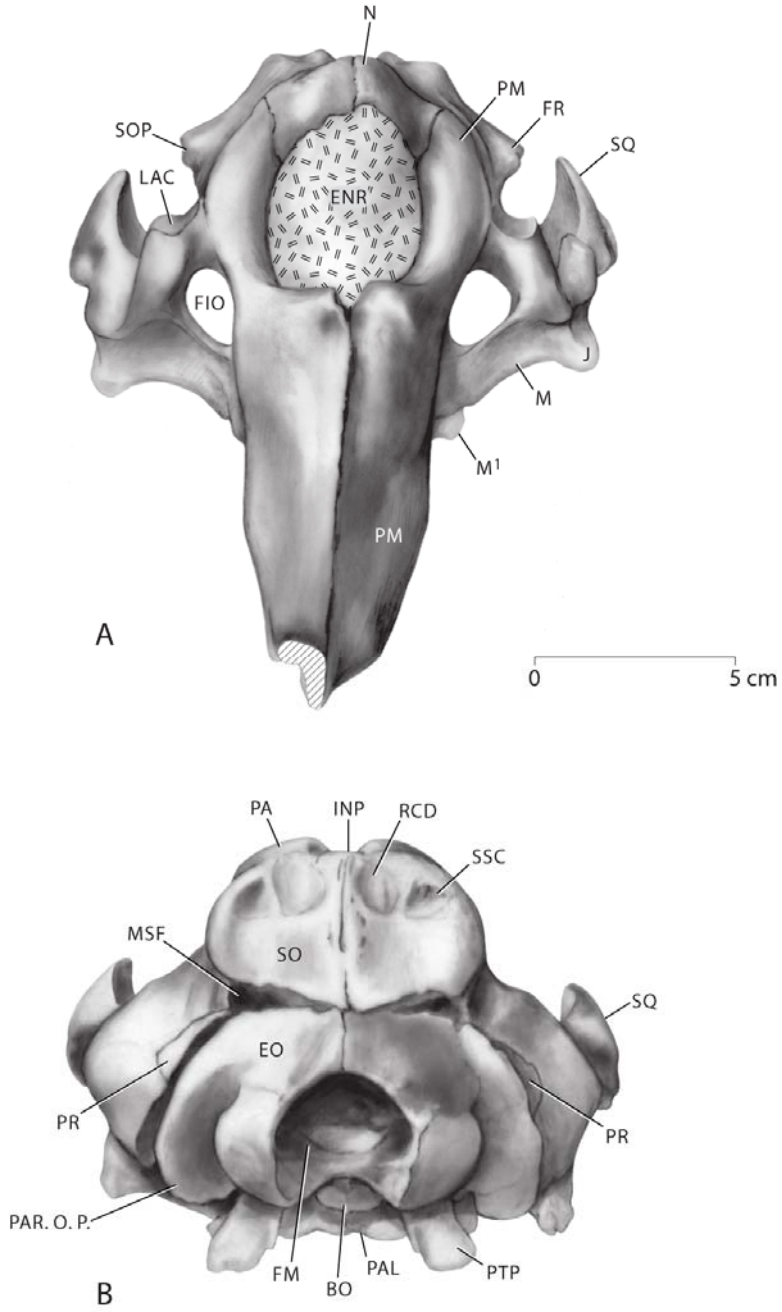

FIGURE 4.15. *Eotheroides sandersi* skull roof of (UM 94809) in dorsal view (**A**), and ventral view (**B**). Abbreviations: **FR**, frontal; **N**, Nasal; **PA**, parietal.

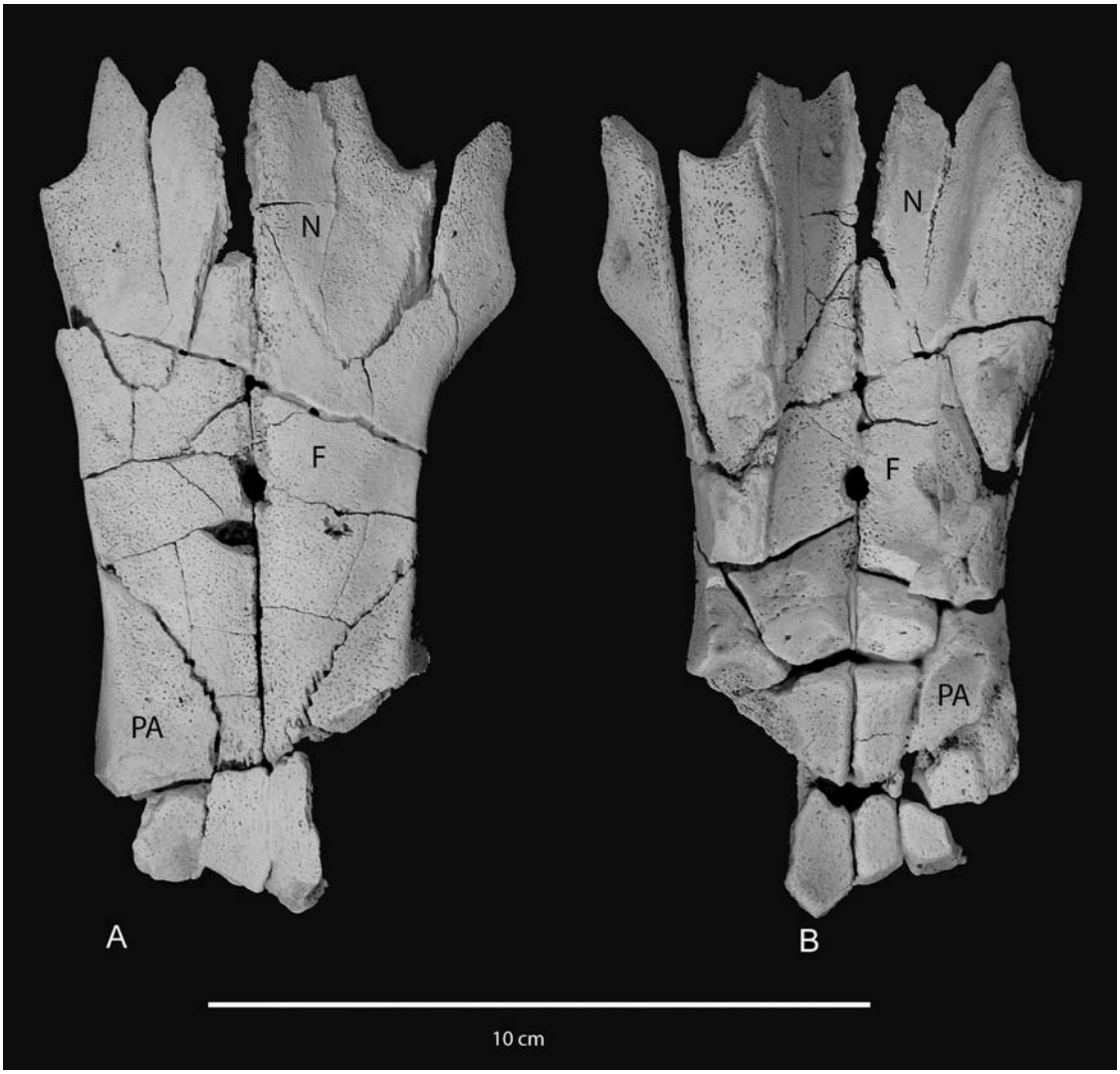

FIGURE 4.16. Anatomy of the ear region of *Eotheroides sandersi* (UM 111558). **A**, **B**, and **C**, Ventral, posterior, and cerebral views, respectively, of the left squamosal and pterotympanic elements. **D**, Lateral view of the right tympanic region of UM 111558. The ear region of is divided into three major components "bones": pars mastoidea, pars temporalis, and the tympanic ring; the largest is pars mastoidea, which is exposed posteriorly (pars fonticulus). Abbreviations: **FOV**, foramen ovalis; **IC**, incus; **MAL**, malleus; **MAL. M.**, manubrium mallei, **PF**, processus folianus; **PFT**, pars fonticulus; **PLG**, perlymphatic glenoid; **PM**, pars mastoidea (=pars petrosa, pars labyrinthica, also pars fonticulus "PFT"); **POST.T.P**, post tympanic process; **PRTM**, promontorium, **PT**, pars temporalis (=tegmen tympani); **SF**, sulcus facialis; **SQ**: squamosal; **ST**, sulcus tympanicus; **T**, tympanic ring; **TH**, tympanohyale.

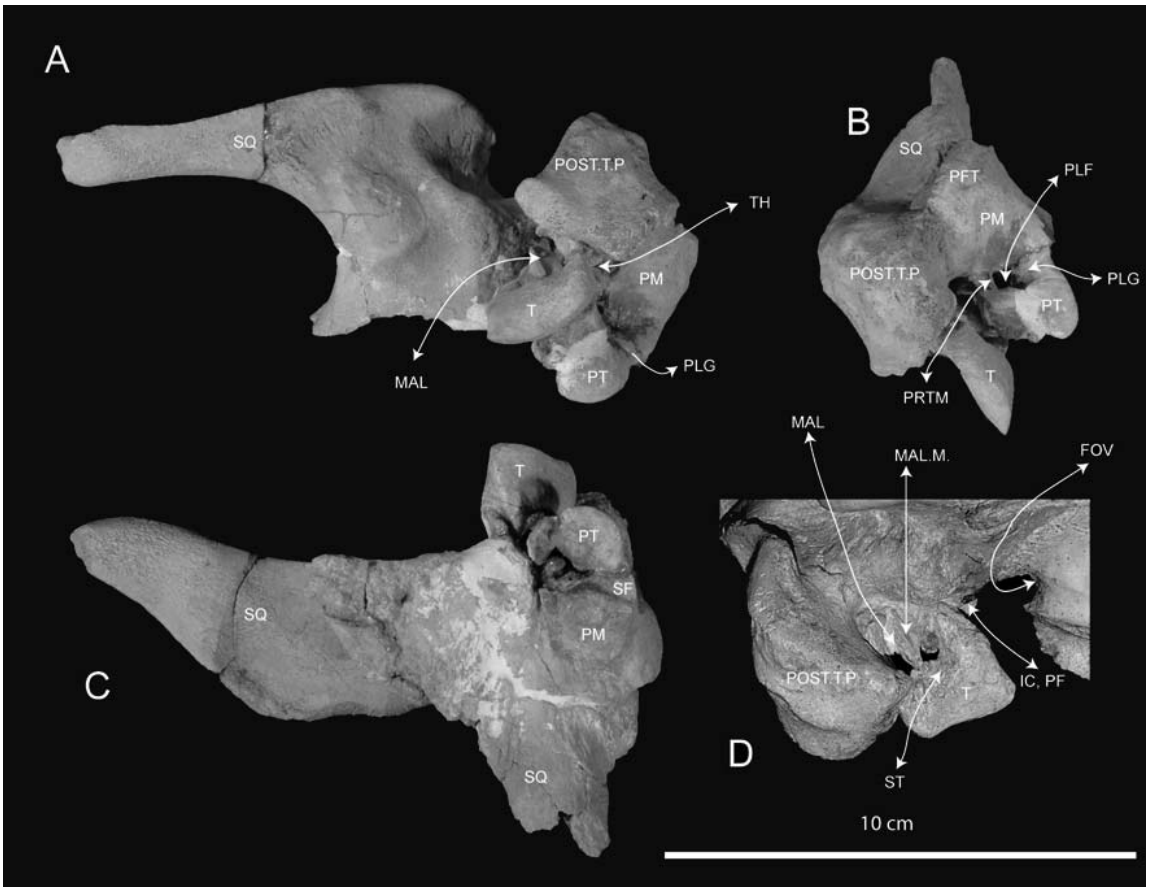

FIGURE 4.17. Mandibles of *Eotheroides sandersi* UM 100138 in dorsal view (**A**) and lateral view (**B**).

FIGURE 4.18. Anterior view of mid cervical, thoracic, and caudal vertebrae of *Eotheroides sandersi* CGM 42181 (holotype). **A** and **B**, vertebral bodies (centra) of the third and fourth cervical vertebrae. **C**, Second thoracic vertebra bearing a long spine and horizontal transverse processes. **D**, Third or fourth thoracic vertebra. **E,** Fourth or fifth thoracic vertebra. **F**, **G**, and **H** Ninth through the eleventh caudal vertebrae. **I** and **J**, Anterior view of ore posterior tail vertebrae.

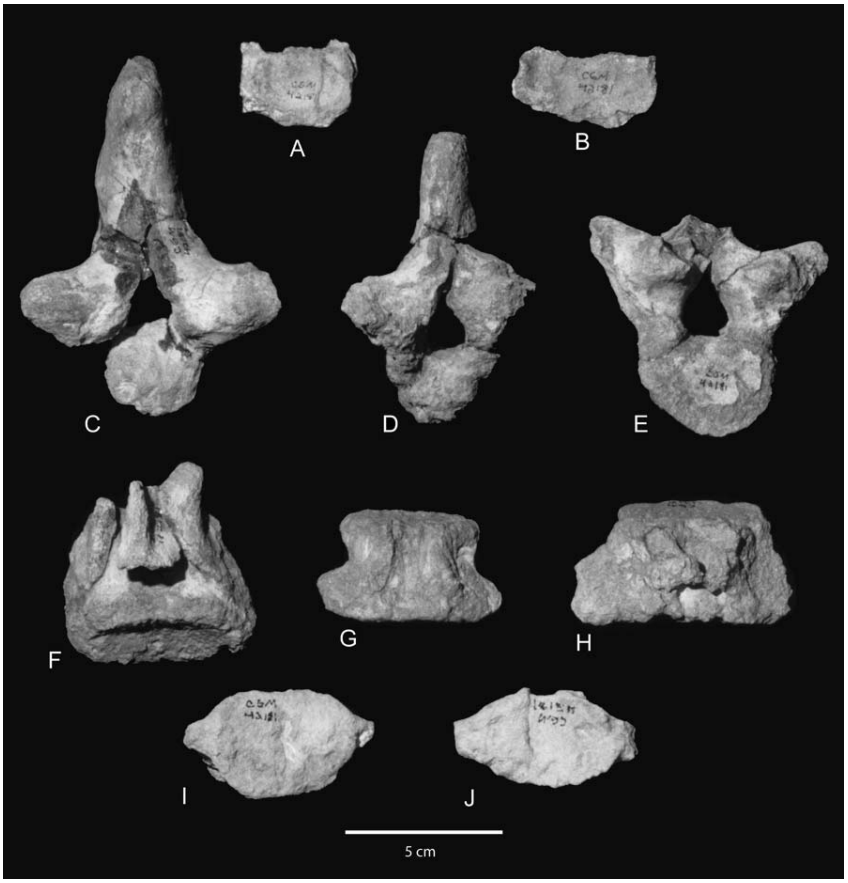

FIGURE 4.19. Cranial (anterior) view of cervical, thoracic, lumbar, caudal vertebrae of *Eotheroides sandersi* (UM 111558). Vertebrae shown are **C1** and **C3**, **Th2** through **Th16, Th 19** (pre lumbar), **Lr1**, **Ca5** through **Ca7**, **Ca12** and **Ca13**, **Ca16** and **Ca19**. The atlas has squared transverse processes in outline. The thoracic vertebrae were arranged according to their central length, spinous process height, and transverse process curvature; the anteriormost thoracic vertebrae have high spines, almost horizontal transverse processes, and large neural canals; the last thoracic vertebra possesses a short and rounded transverse process. Neural canals of mid and posterior neural thoracics (**Th4-Th18**) have neural canals slitted at the top, in anterior view. Abbreviations: **C**, cervical; **Ca**, caudal; **Lr**, lumbar, **Th**, thoracic; **S**, sacral.

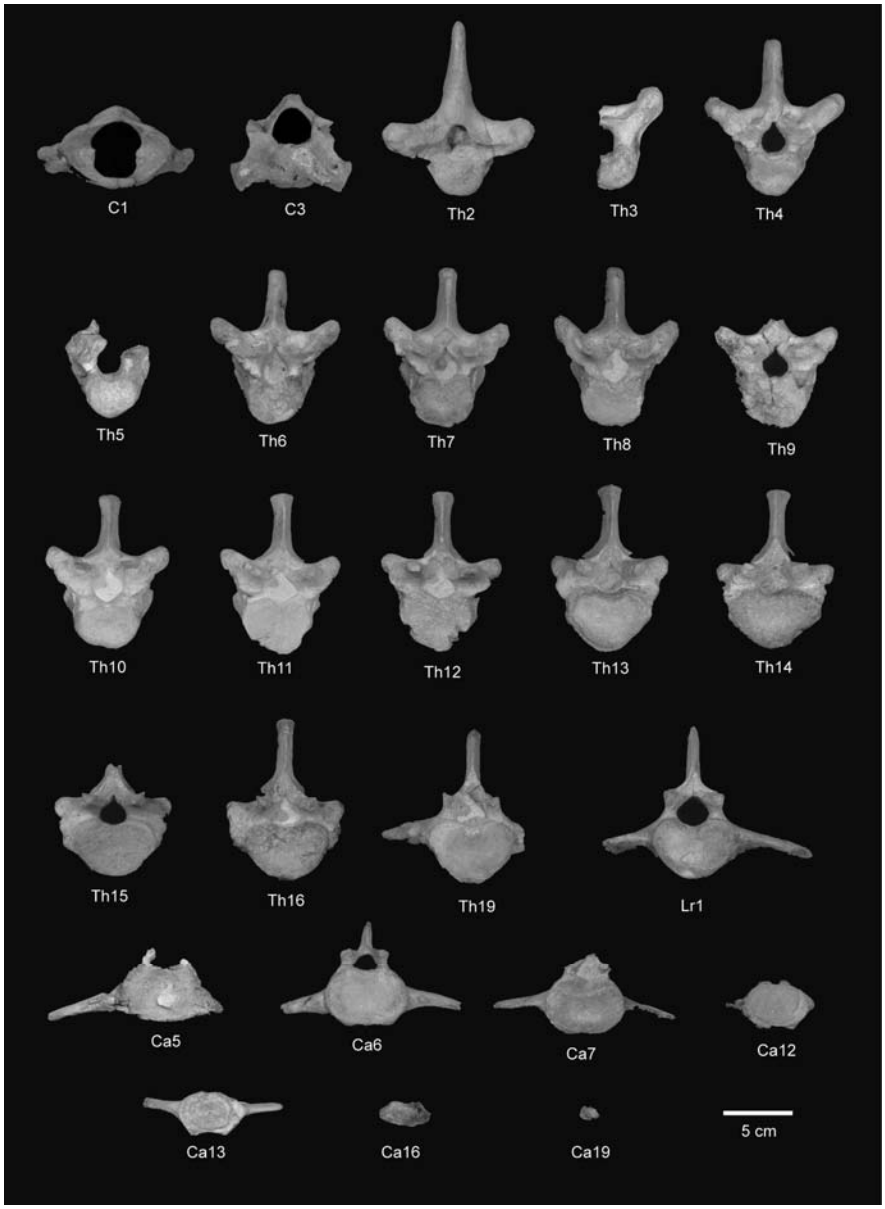

FIGURE 4.20. Dorsal view of cervical, thoracic, lumbar, caudal vertebrae of *Eotheroides sandersi* (UM 111558). Spacing between regional areas indicates missing vertebrae. Abbreviations: **C**, cervical; **Ca**, caudal; **Lr**, lumbar, **Th**, thoracic; **S**, sacral.

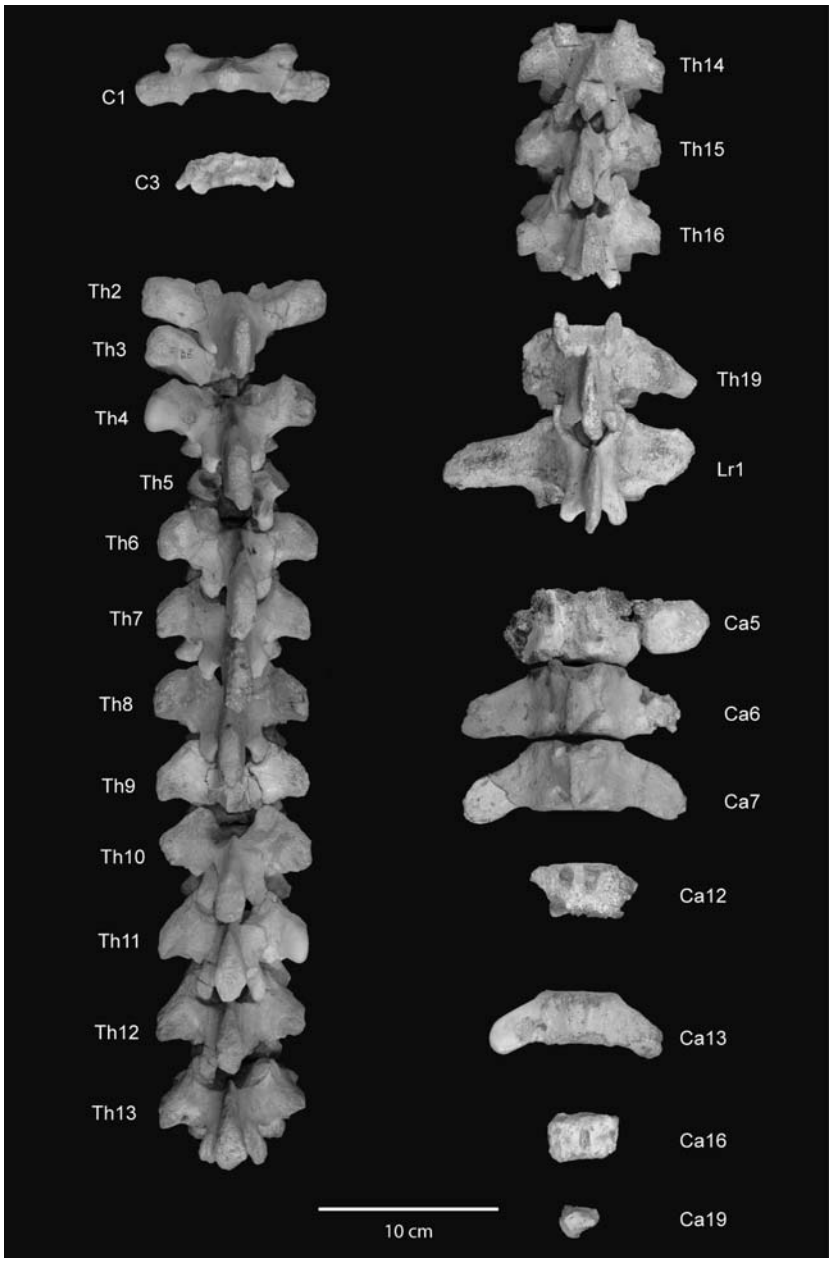

FIGURE 4.21. Lateral view of cervical, thoracic, lumbar, caudal vertebrae of *Eotheroides sandersi* (UM 111558). Abbreviations: **C**, cervical; **Ca**, caudal; **Lr**, lumbar, **Th**, thoracic; **S**, sacral.

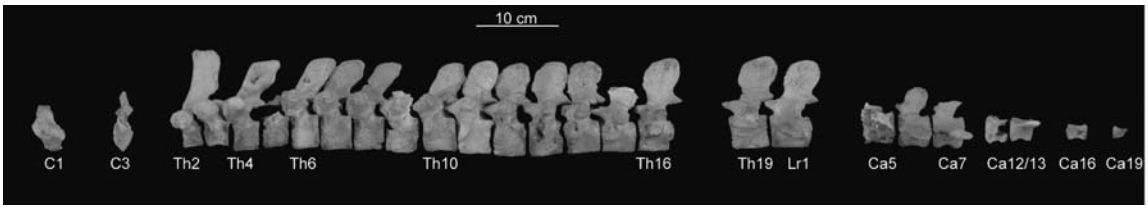

FIGURE 4.22. Dorsal view of thoracic vertebrae of *Eotheroides sandersi* (UM 97514). At least three thoracic should follow thoracic vertebra 16. Abbreviations: **Th**, thoracic.

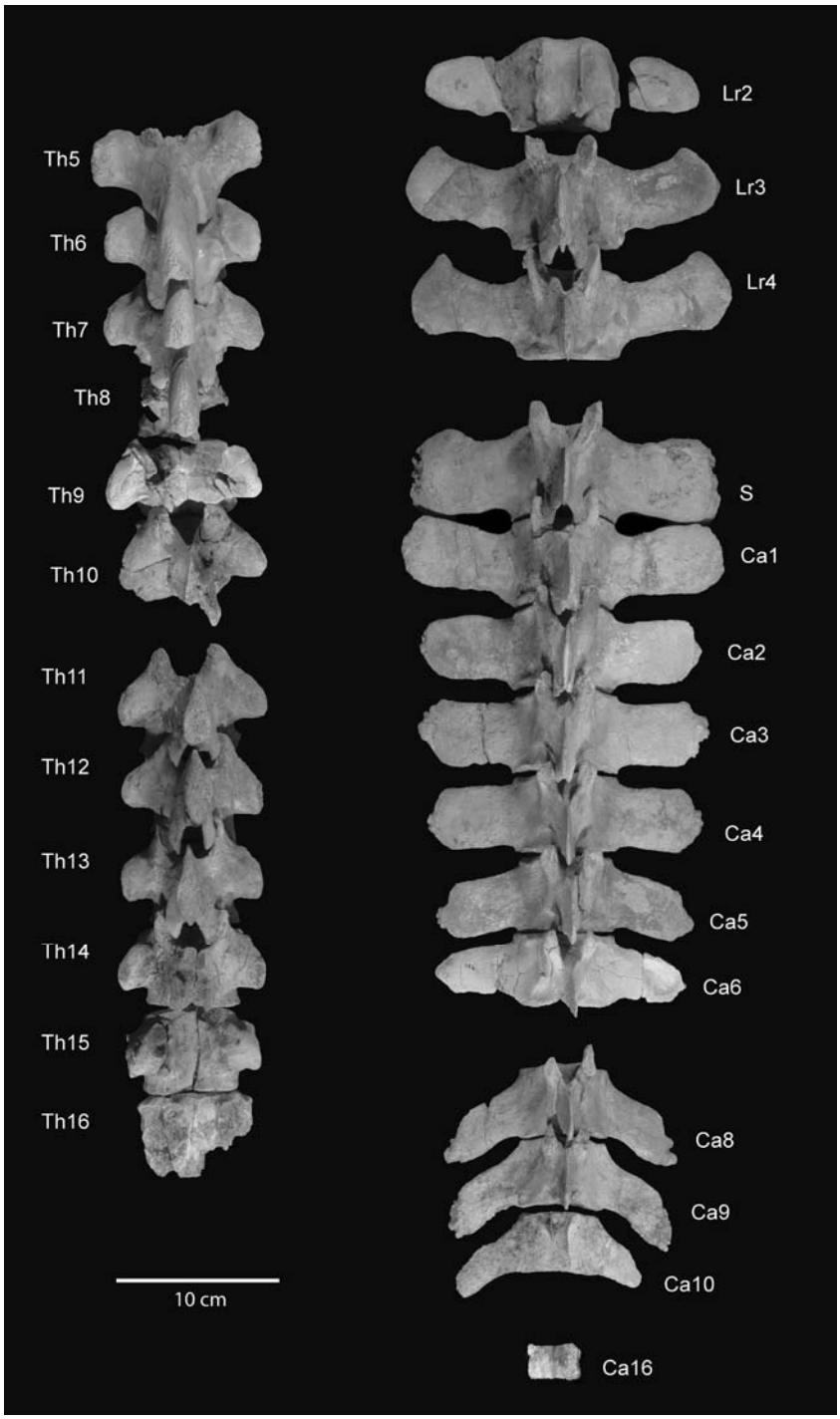

FIGURE 4.23. Cranial (anterior) view of thoracic vertebrae of *Eotheroides sandersi* (UM 97514). Abbreviations: **Th**, thoracic.

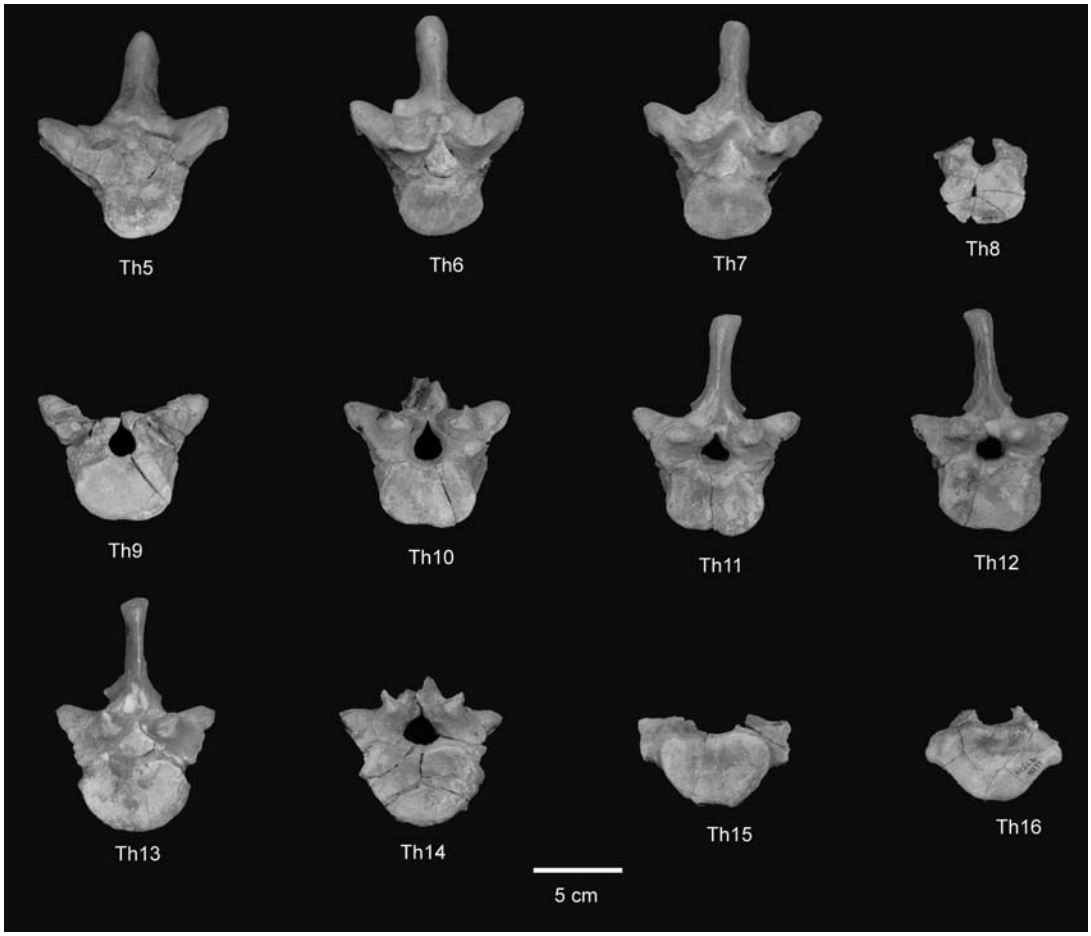

FIGURE 4.24. Cranial (anterior) view of lumbar, sacral, and caudal vertebrae of *Eotheroides sandersi* (UM 97514). Abbreviations: **Ca**, caudal; **Lr**, lumbar, **Th**, thoracic; **S**, sacral.

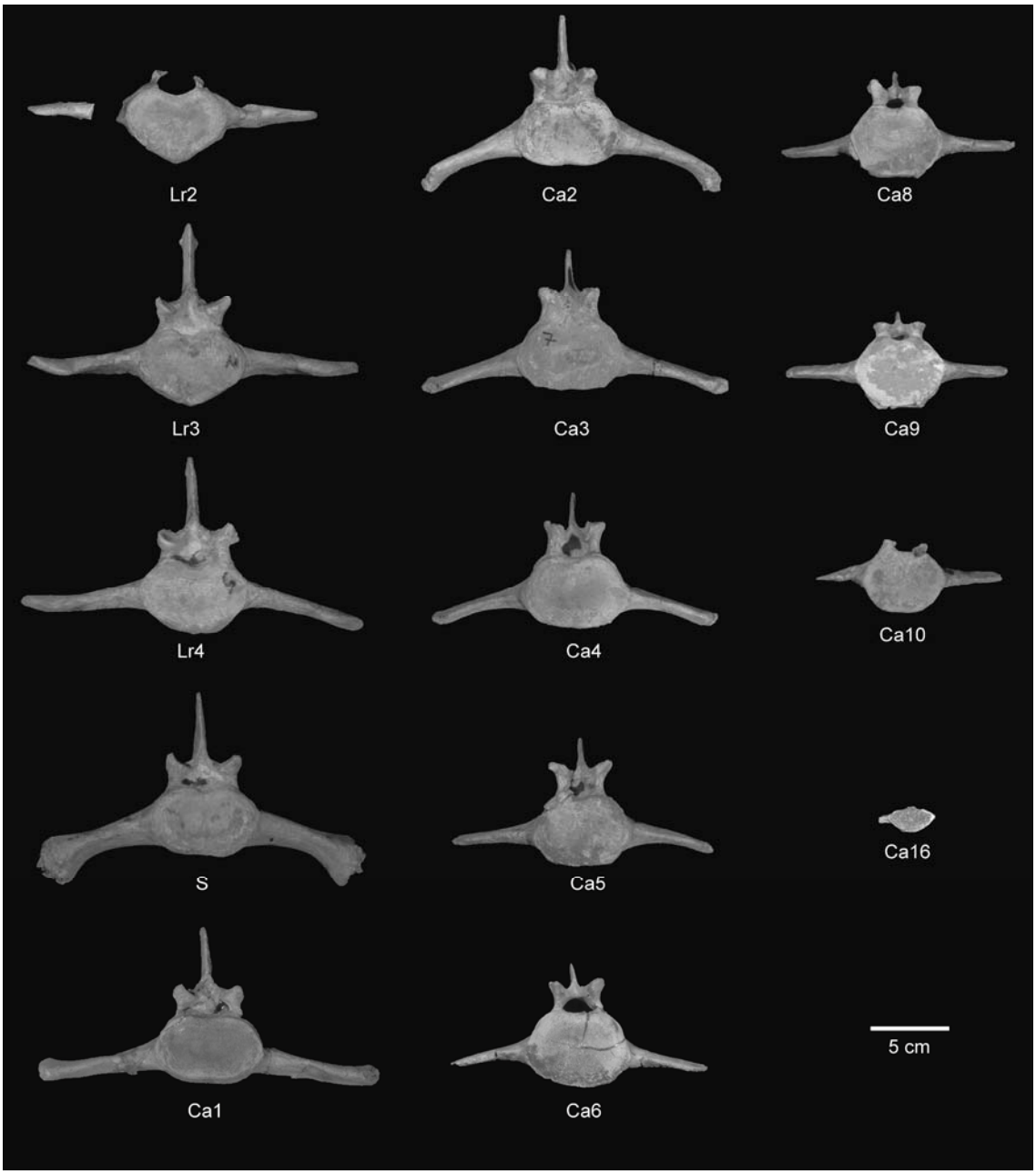

FIGURE 4.25. Lateral view of thoracic, lumbar, sacral, and caudal vertebrae of *Eotheroides sandersi* (UM 97514). Abbreviations: **C**, cervical; **Ca**, caudal; **Lr**, lumbar, **Th**, thoracic; **S**, sacral.

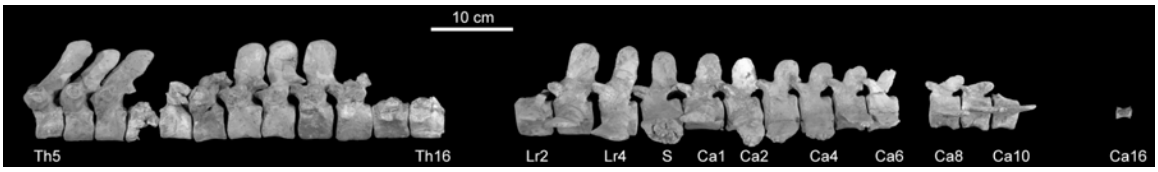

FIGURE 4.26. **A**: Cranial view of the ribs of *Eotheroides sandersi* sp. nov. CGM 42181 (holotype). The right side preserves rib 3 through rib 18; only the second rib from the left series survived natural sandblasting. Anterior ribs are pachyosteosclerotic and banana-like. **B**: Left and right ribs of *Eotheroides aegyptiacum* SMNS 43949 "st. XV (XIX)" collected from the Lutetian of the Mokattam Hills. The two symmetrical ribs in the middle of the photo are the left and right first rib showing the distally flattened and truncated ends. **C**: Ribs and vertebrae (***Wirbelkomplex***) of *Eotheroides aegyptiacum* SMNS 3543 " st. XVI (XX)" collected near below Masjid et Tingie from the lowest white bed of the Mokattam Hills; specimen is composed of one block. Note that in the pachyosteosclerotic ribs of the anterior and mid chest regions the gracile and slender ribs in the block to the right. The animal is mature, but smaller than *Eotheroides sandersi* and *Eotheroides clavigerum*. Abbreviations: **C**, cervical; **L**, left rib; **R**, right rib; **Th**, thoracic vertebra.

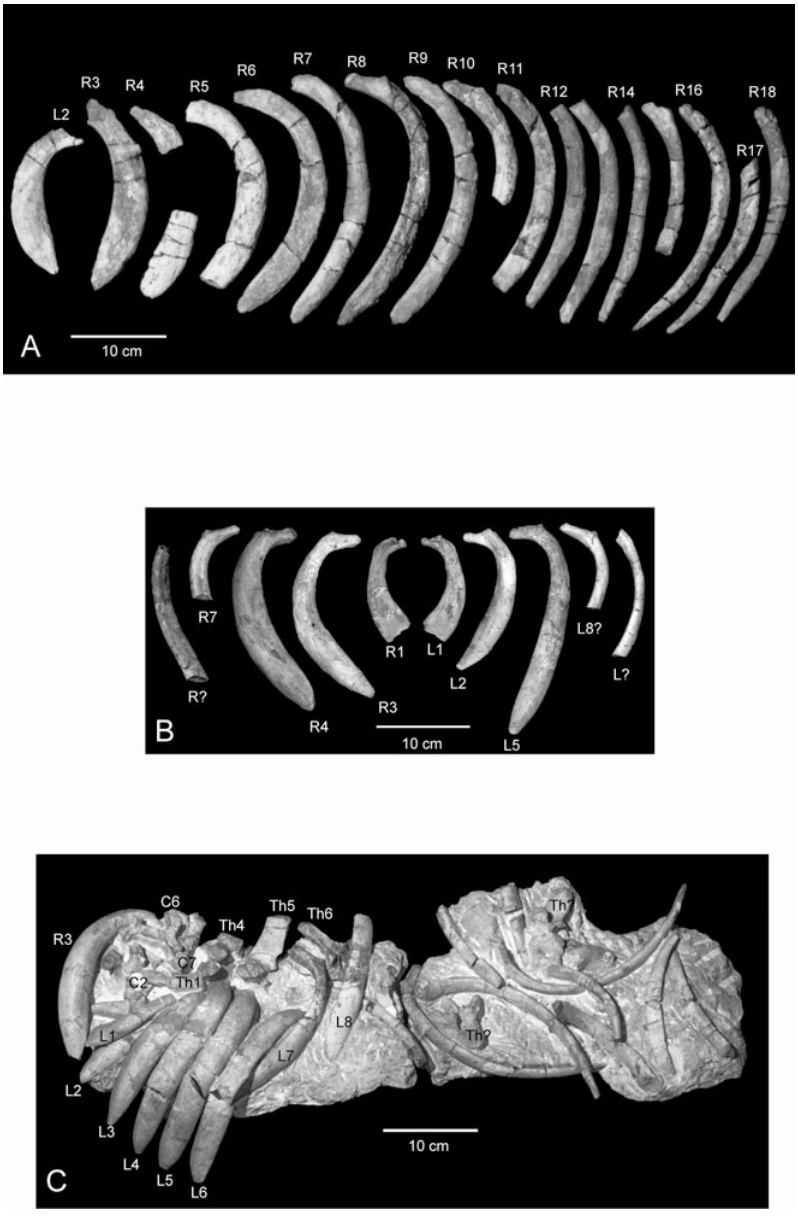

FIGURE 4.27. Cranial view of left and right ribs of *Eotheroides sandersi* (UM 111558) arranged by size and morphology. Note the heavy and swollen (pachyosteosclerotic) banana-like anterior ribs and thinner posterior ones. **R1** has a straight and truncated distal end; third rib (**R3**) is the most pachyosteosclerotic; and last rib in the preserved series (**R17**) shows a convoluted head. Abbreviations: **L**, left rib; **R**, right rib.

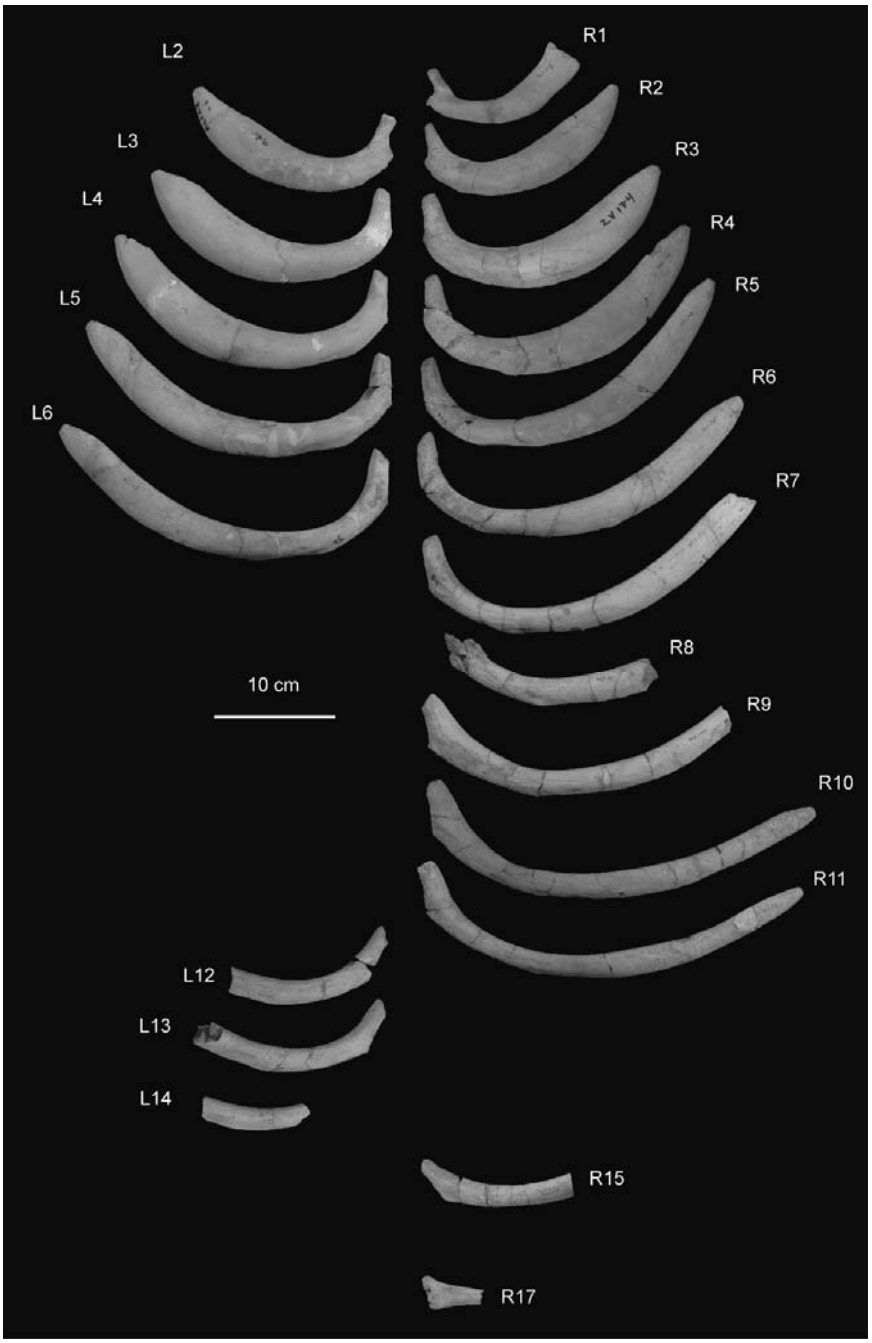

FIGURE 4.28. Cranial (anterior) view of left and right posterior ribs of *Eotheroides sandersi* (UM 97514) arranged according to their size and morphology. Abbreviations: **L**, left rib; **R**, right rib.

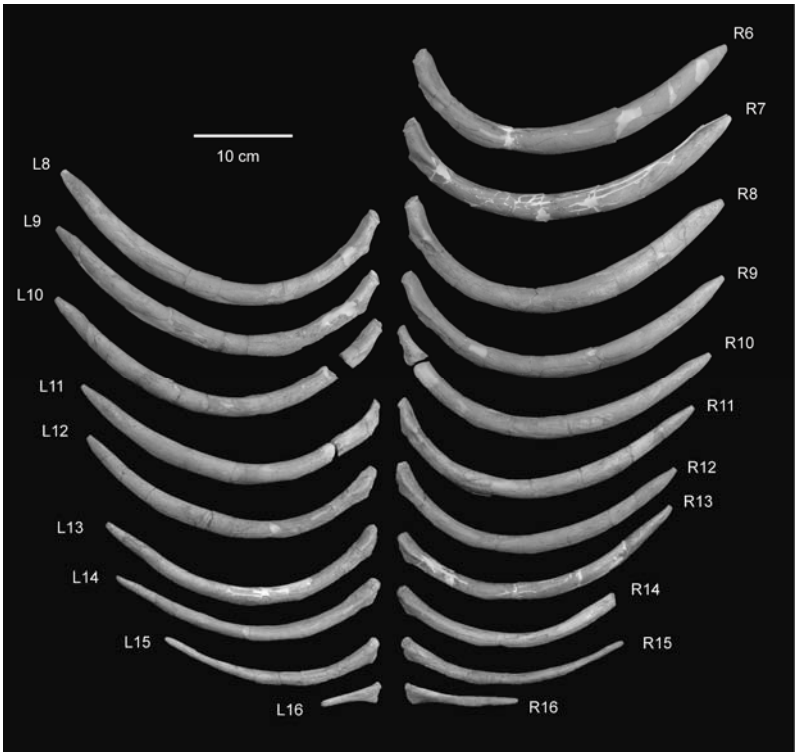

FIGURE 4.29. Ventral (**A**) and dorsal (**B**) views of the xiphisternum of *Eotheroides sandersi* (UM 111558). Notice the asymmetry, and the elliptical foramen posteriorly.

FIGURE 4.30. Scapular and humeral elements of *Eotheroides sandersi* CGM 42181 (holotype). **A**, Left scapula in lateral view. **B**, Left humerus in posterior view. **C**, Right humerus in posterior view. **D**, Right scapula in lateral view.

FIGURE 4.31. Forelimb elements of *Eotheroides sandersi* UM 111558. **A**, Left scapula, lateral view. **B**, Left humerus, anterior view. **C**, Right ulna, anterior view.

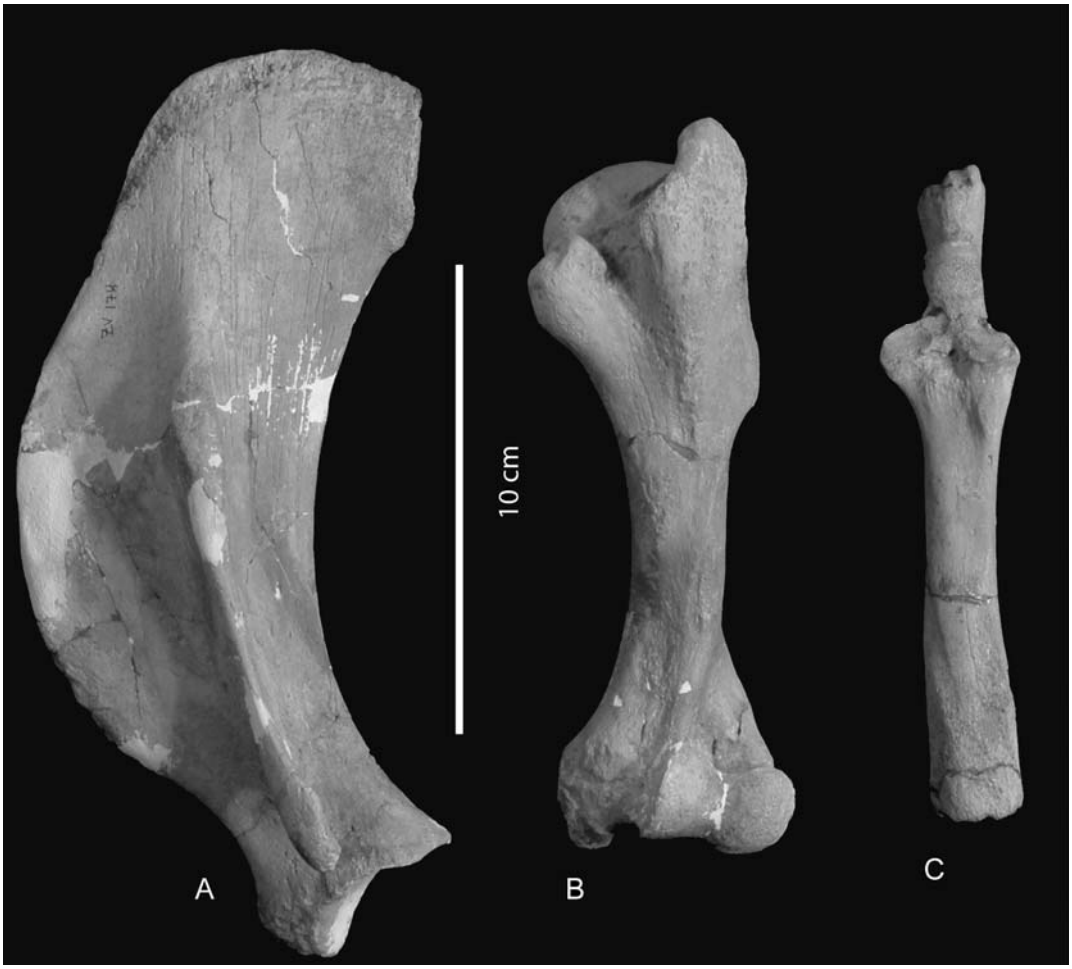

FIGURE 4.32. Left ulna of juvenile individual of *Eotheroides sandersi* UM 97515 missing its distal epiphysis, and it was not ankylosed with the radius. This is the smallest sirenian individual recovered form Wadi Al Hitan. **A**, Medial view; **B**, Anterior view; **C**, Lateral view.

FIGURE 4.33. Left metapodials and carpals of *Eotheroides sandersi* UM 111558. Metacarpal III, Met. III, is distinguished by a prolonged proximal articulation end directed medially. Metacarpal V is distinguished in having a blunt posterior edge.

FIGURE 4.34. Left and right innominate s and femora of *Eotheroides sandersi* CGM 42181 (holotype). **A**, Left innominate, lateral view. **B**, Left femur, anterior view. **C**, Right femur, anterior view. **D**, Right ilium, lateral view. Notice the swollen appears on the proximal end of the left ilium, and the reduced size of the femora.

FIGURE 4.35. Sacrum and left and right innominates of *Eotheroides sandersi* (UM 97514) from the Priabonian Birket Qarun Formation, Western Desert of Egypt. **A**, Left innominate lateral view. **B**, Right innominate lateral view. **C**, Right innominates in anterior view. **D**, Sacrum in cranial view. **E**, Left innominate in anterior view. F, Right innominates in median view. G, Left innominates in median view. Note the swollen-club-like proximal ilium; long, unfused pubis, and the reduced acetabulum and obturator foramen. Abbreviations: **act.,** acetabulum; **act. n.,** acetabular notch; **cre.**, cranial epiphysis; **dor. il. sp.** dorso iliac spine; **il.,** ilium; **isc.,** ischium; **isc. tub.,** ischiac tuberosity; **isc. shft.,** ischiac shaft; **n.c.**, nural canal; **n.sp.**, neural spine; **obt. f.,** obturator foramen; **pr. zph.**, prezygapophysis; **ps.,** pubis; **pub. symph.,** pubic symphysis; **pub. clft,** pubic cleft; **pub. ram. ant.,** anterior pubic ramus; **pub. ram. post.,** posterior pubic ramus; **sac. il. artic.**, sacroiliac articulation surface; **sac. il.,** sacral pleurapophyses**, t. pr.**, transverse process.

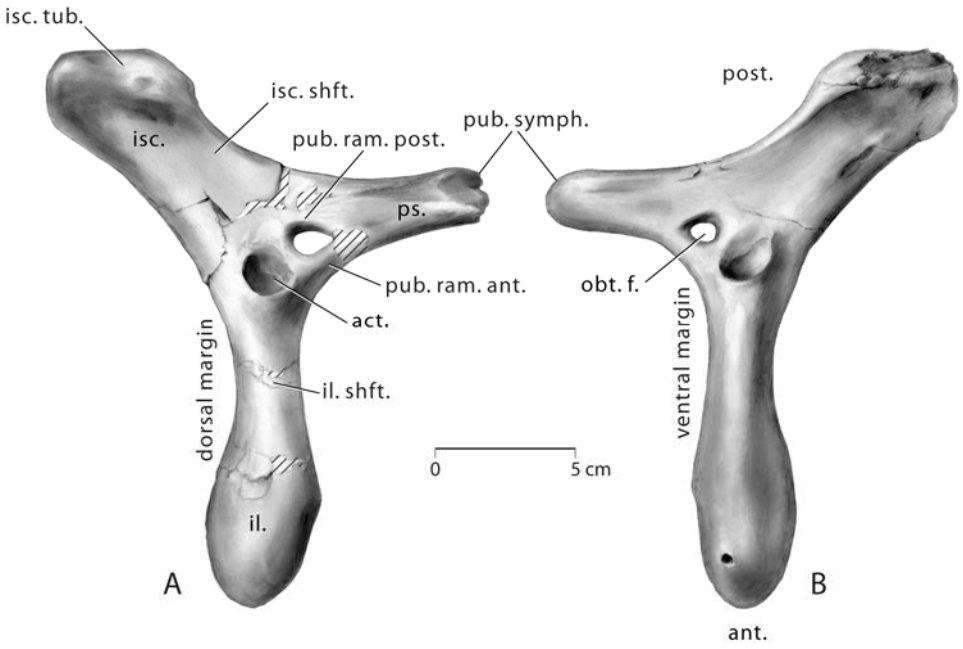

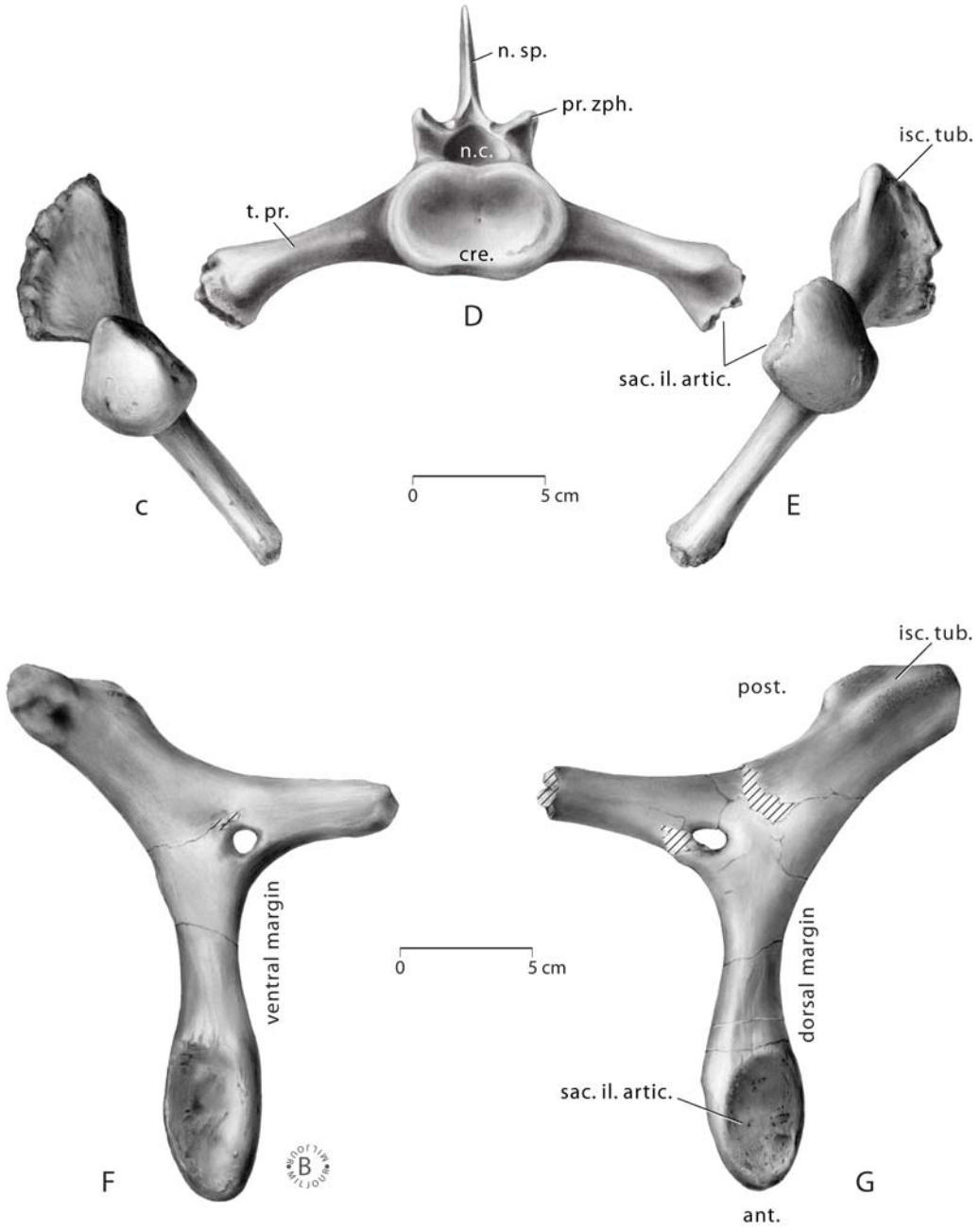
n. sp.
pr. zph.
n.c.
t. pr.
cre.
D
isc. tub.
sac. il. artic.
c
0
5 cm
E
isc. tub.
post.
ventral margin
dorsal margin
sac. il. artic.
F
G
ant.

FIGURE 4.36. Femora of *Eotheroides sandersi* (**A-D**) compared to that of *Eosiren* from the Qasr El Sagha Formation (**E** and **F**). **A** and **B**, Anterior and posterior views of the left femur of *Eotheroides sandersi* (UM 42181, holotype). **C** and **D**, Anterior and posterior views of the left femur of *Eotheroides sandersi* (UM 111558). **E** and **F**, Anterior and posterior views of the right femur of *Eosiren* sp. (UM 101226). The femur of UM 101226 is the only complete femur of *Eosiren* with proximal and distal ends. Morphology and length of these femora imply that there are no substantial lower limb or foot elements connected to them.

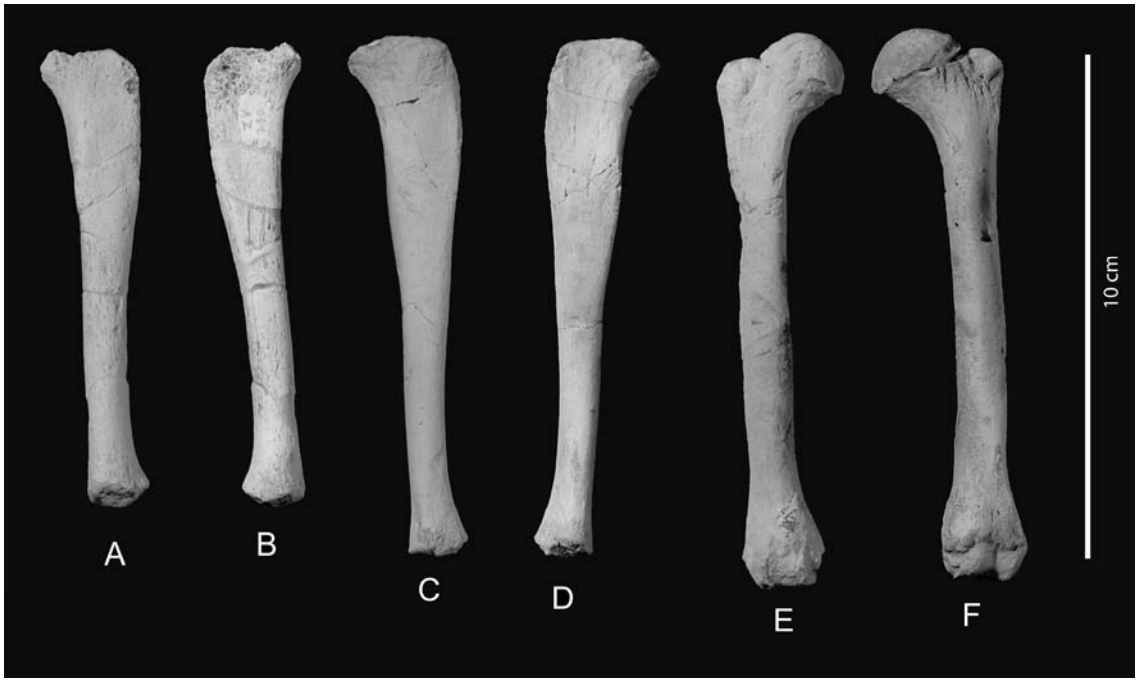

FIGURE 4.37. Femora, tibiae, and fibulae of Bartonian and Priabonian *Protosiren* from Egypt and Pakistan. **A** and **B**, Anterior view of the right femur, tibia, and fibula of the holotypic specimen *Protosiren smithae* (CGM 94810). **C**, Right tibia and fibula of *Protosiren smithae* (UM 101224). **D**, Left femur of *Protosiren sattaensis* (GSP-UM 3197) from the Bartonian of the Drazinda Formation of the Sulaiman range, Central Pakistan. Morphology and dimensions of the hindlimb elements of both taxa imply a functional distal leg that was used during swimming. Abbreviations: **Fb**., fibula; F**m.**, femur; **Tb.**, tibia.

FIGURE 4.38. Upper left cheek teeth of Paleogene sirenians from the Cairo and Fayum. **A**, *Protosiren fraasi* of middle Eocene of Mokattam Limestone near Cairo (cast, UM 22211, original specimen is in the Cairo Geological Museum). **B**, *Protosiren smithae* late Eocene, base of the Birket Qarun Formation (UM 94810, cast). **C**, *Eotheroides sandersi* from the late Eocene, middle part of the Birket Qarun Formation (UM 111558). **D**, *Eotheroides clavigerum* (UM 101219, holotype), late Eocene, base of the Birket Qarun Formation. **E**, *Eosiren* sp. (CGM 42180), late Eocene, the Qasr El Sagha Formation. **F**, *Eosiren stromeri* (UM 100137), late Eocene, Qasr El Sagha Formation. **G**, *Eosiren imenti* (CGM 40210), early Oligocene of the Jabal Qatrani Formation. Note that Protosirenidae has enlarged and robust molars bearing smooth enamel and a strong anterior cingulum and have a large and rounded metaloph in M^3; *Eotheroides* has quadratic first and second molars, with strong lingual cingula. *Eosiren stromeri* differs from *Eosiren libyca* in having a second molar significantly larger than M^3; *Eosiren imenti* is the largest of all Eocene and Oligocene dugongs seen in Egypt.

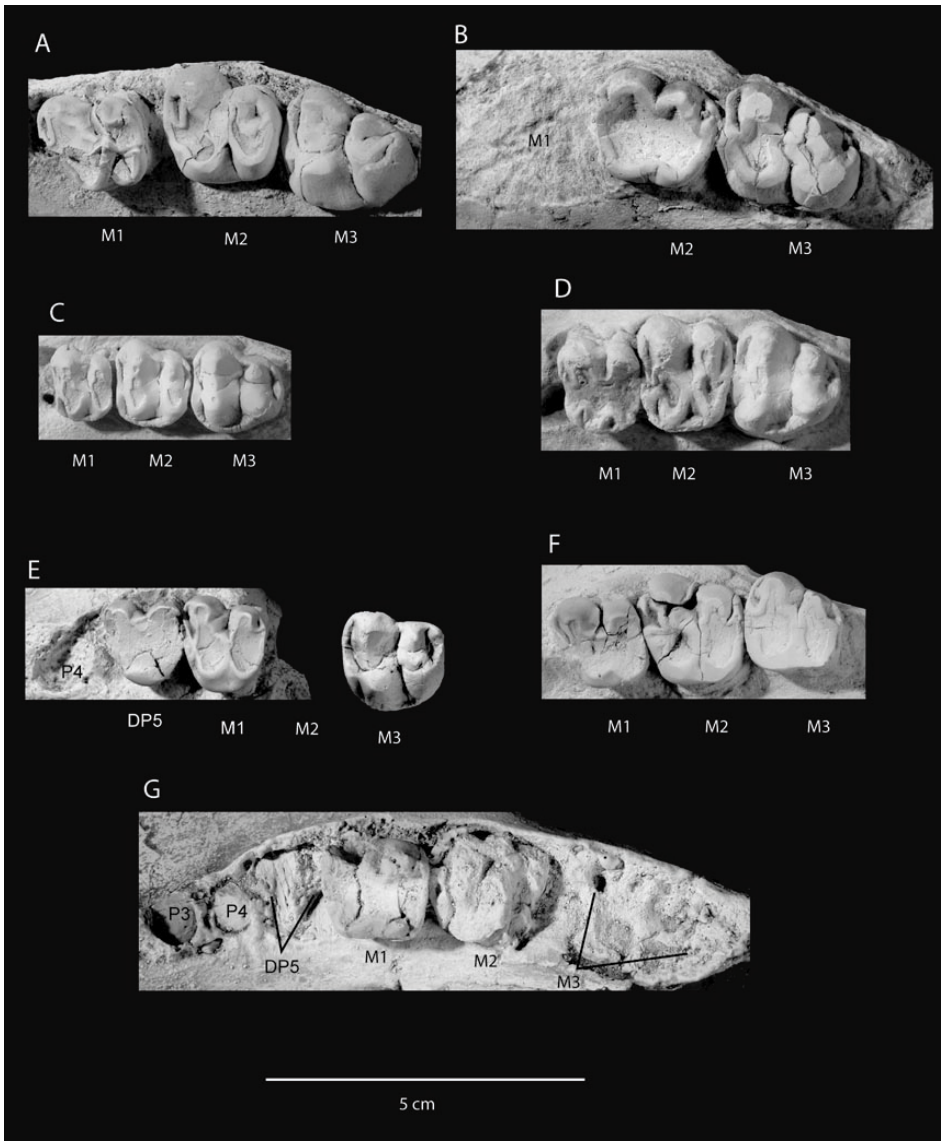

FIGURE 4.39. Mandibles of late Eocene Dugongidae (YPM 24851) collected from Wadi Al Hitan and described in Domning et al., 1982. **A**, Occlusal aspect; **B**, Lateral aspect. YPM 24851 is an immature individual as indicated by the erupting permanent teeth remodeling the remnants of the deciduous root alveolae. Abbreviations: **alv.dp$_x$**, alveoli of deciduous premolars; **c**, canine; **dp$_x$**, deciduous premolars; **p$_{1-X}$**, premolar; **m$_{1-x}$**, molars. The dental formula and number of teeth is based on the maximum number of teeth found in most primitive sirenians (3.1.5.3).

FIGURE 4.40. Mandibles of late Eocene *Eosiren stromeri* (UM 100137) collected from the Qasr El Sagha Formation at the northern exposure of Birket Qarun. **A**, Occlusal aspect; **B**, Lateral aspect. The anterior teeth are missing and their alveolae are broken. Robustness and widening on the anterior rostrum and its expanded masticating surface are characteristic of *Eosiren* mandibles. Abbreviations: $\mathbf{dp_x}$, deciduous premolars; $\mathbf{p_{1\text{-}x}}$, premolar; $\mathbf{m_{1\text{-}x}}$, molars. Dental formula and number of teeth is based on the maximum number of teeth found in most primitive sirenians, which is 3.1.5.3 (=3.1.4.dp_5.3).

FIGURE 4.41. Mandibles of late Eocene *Protosiren smithae* (UM 94810: cast of the holotype CGM 42292) described by Domning and Gingerich 1994. **A**, occlusal aspect; **B**, lateral aspect. *Protosiren smithae* has lost its fifth premolar in both upper and lower jaws. Abbreviations: **c**, canine; **dp_x**, deciduous premolars, **p_{1-X}**, premolar; **m_{1-x}**, molars. Dental formula of the lower jaw is 3.1.4.3.

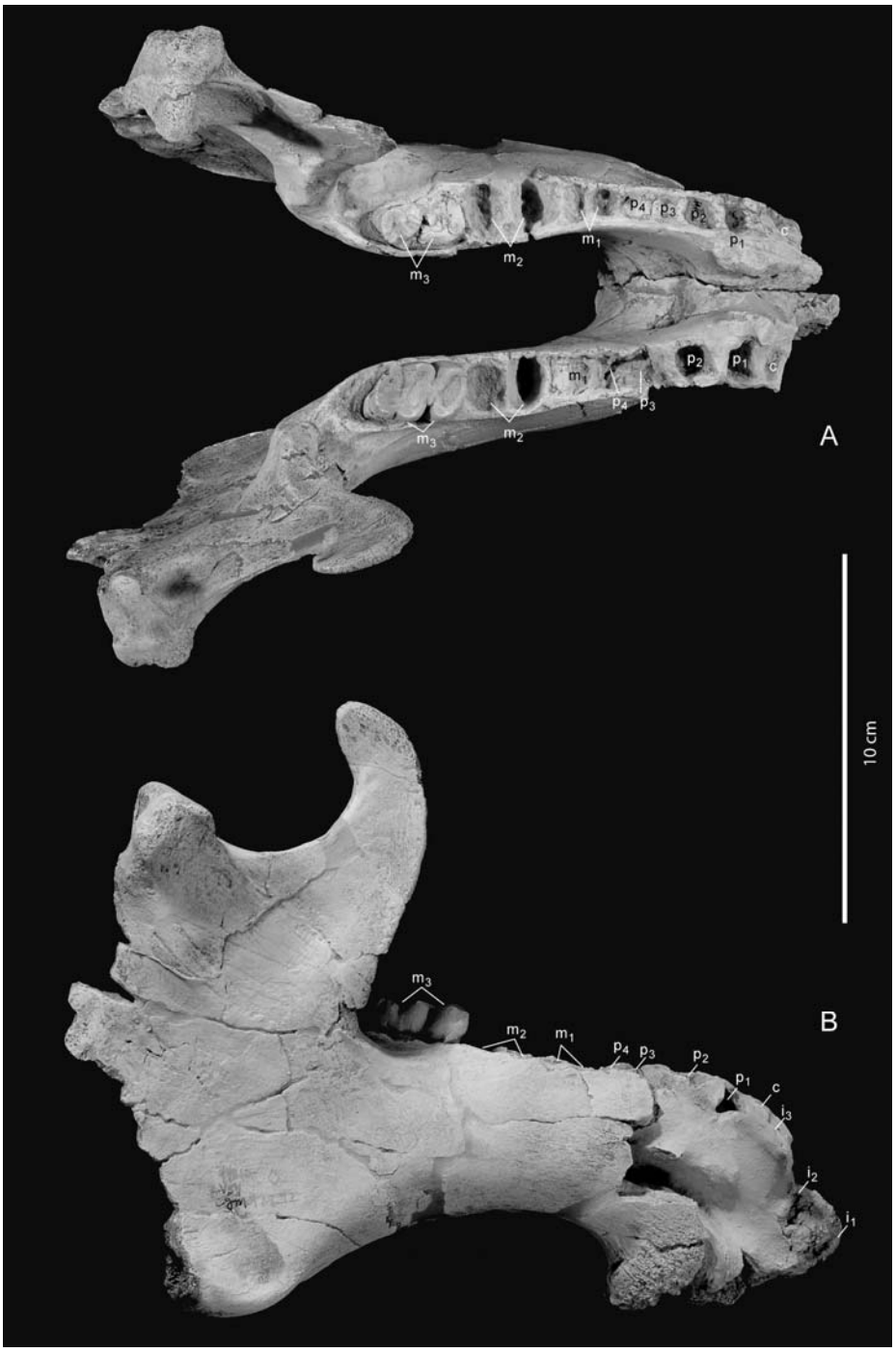

FIGURE 4.42. Mandibles of late Eocene *Eotheroides* sp. from North Carolina (USNM 214596). A, Occlusal aspect; B, Lateral aspect. The specimen was described as *Protosiren* sp. in Domning et al., 1982. However, postcranial associations indicate that this is an adult Eocene dugong instead. Dental formula of the lower jaw is 3.1.5.3. Note the narrowing of the tip of the masticating rostrum and the weak arching of the central surface of the mandible. Abbreviations: **c**, canine; **dp_x**, deciduous premolars, **p_{1-x}**, premolar; **m_{1-x}**, molars.

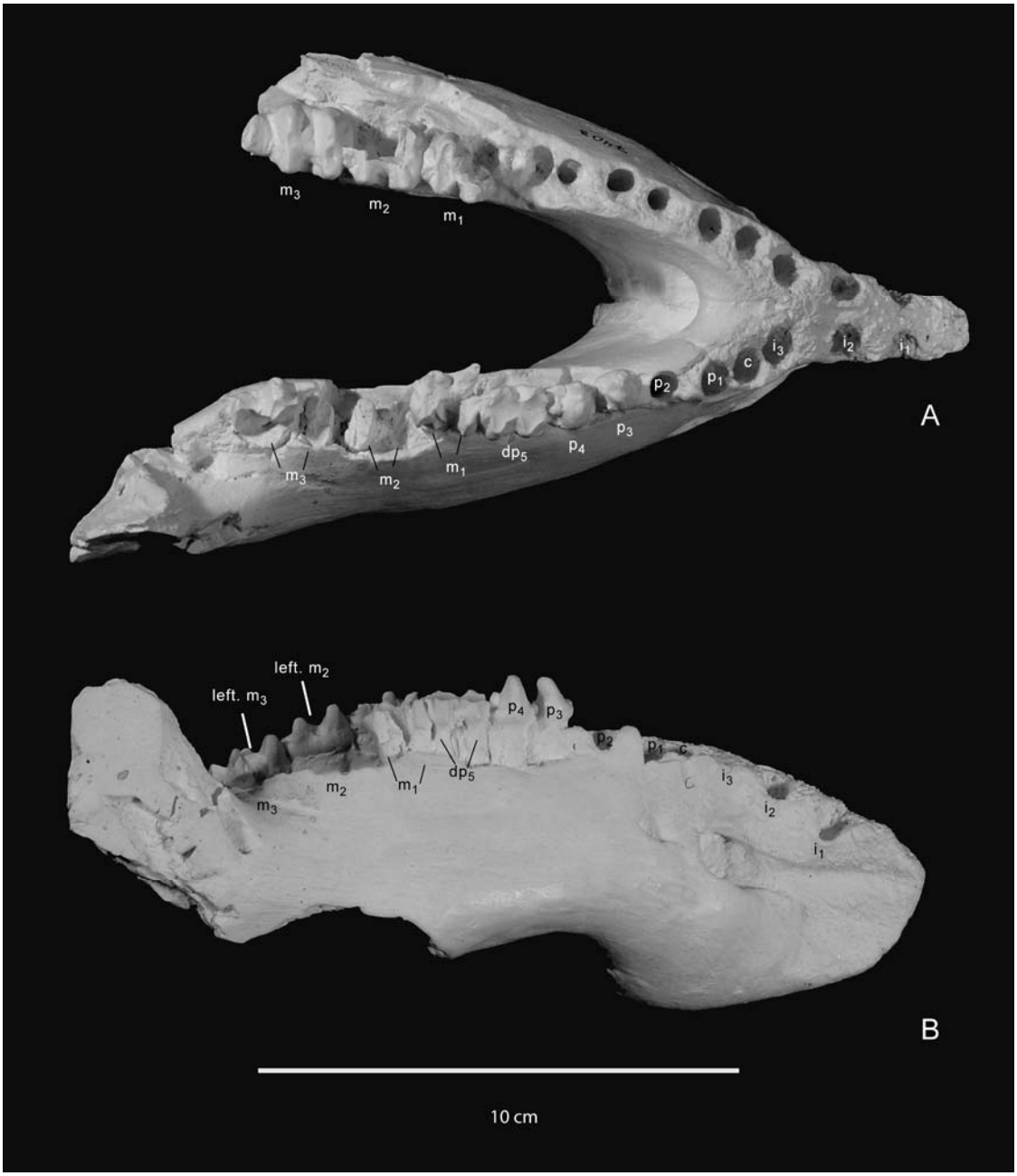

FIGURE 4.43. Right innominate bones of Paleogene African sirenians. A, *Protosiren fraasi* (SMNS 43976A, from Abel, 1904: pl. 7, fig. 1); B, *Protosiren smithae* (Domning and Gingerich, 1994, CGM 43392); C, *Eotheroides sandersi* (UM 97514); D, *Eotheroides clavigerum* (UM 101219); E, *Eosiren libyca* (UM 101226); F, *Eosiren libyca* (CGM 29774). Abbreviations: **act.,** acetabulum; **act. n.,** acetabular notch; **dor. il. sp.** dorso iliac spine; **il.,** ilium; **is.,** ischium; **obt. f.,** obturator foramen;; **ps.,** pubis; **ps. sym.,** pubic symphysis.

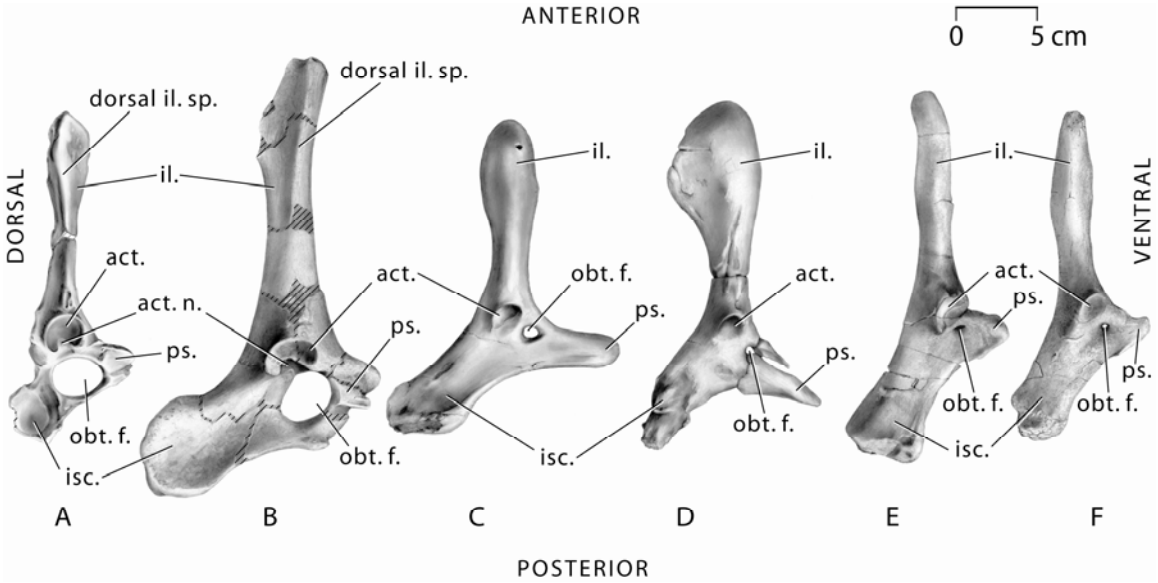

FIGURE 4.44. Lateral view of the vertebrae of late Eocene *Eosiren libyca* (UM 101226) from Qasr El Sagha Formation. Abbreviations: **C**, cervical; **Ca**, caudal; **Lr**, lumbar, **Th**, thoracic; **S**, sacral.

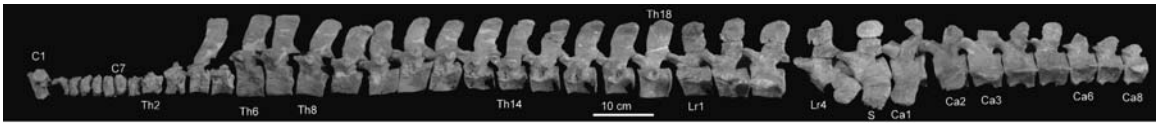

FIGURE 4.45. Cranial (anterior) view of the vertebrae of late Eocene *Eosiren libyca* (UM 101226) from the Qasr El Sagha Formation. Note that the thoracic vertebra bodies are close to heart-shape. C2 and S are in caudal view. Abbreviations: C, cervical; Ca, caudal; Lr, lumbar, Th, thoracic; S, sacral.

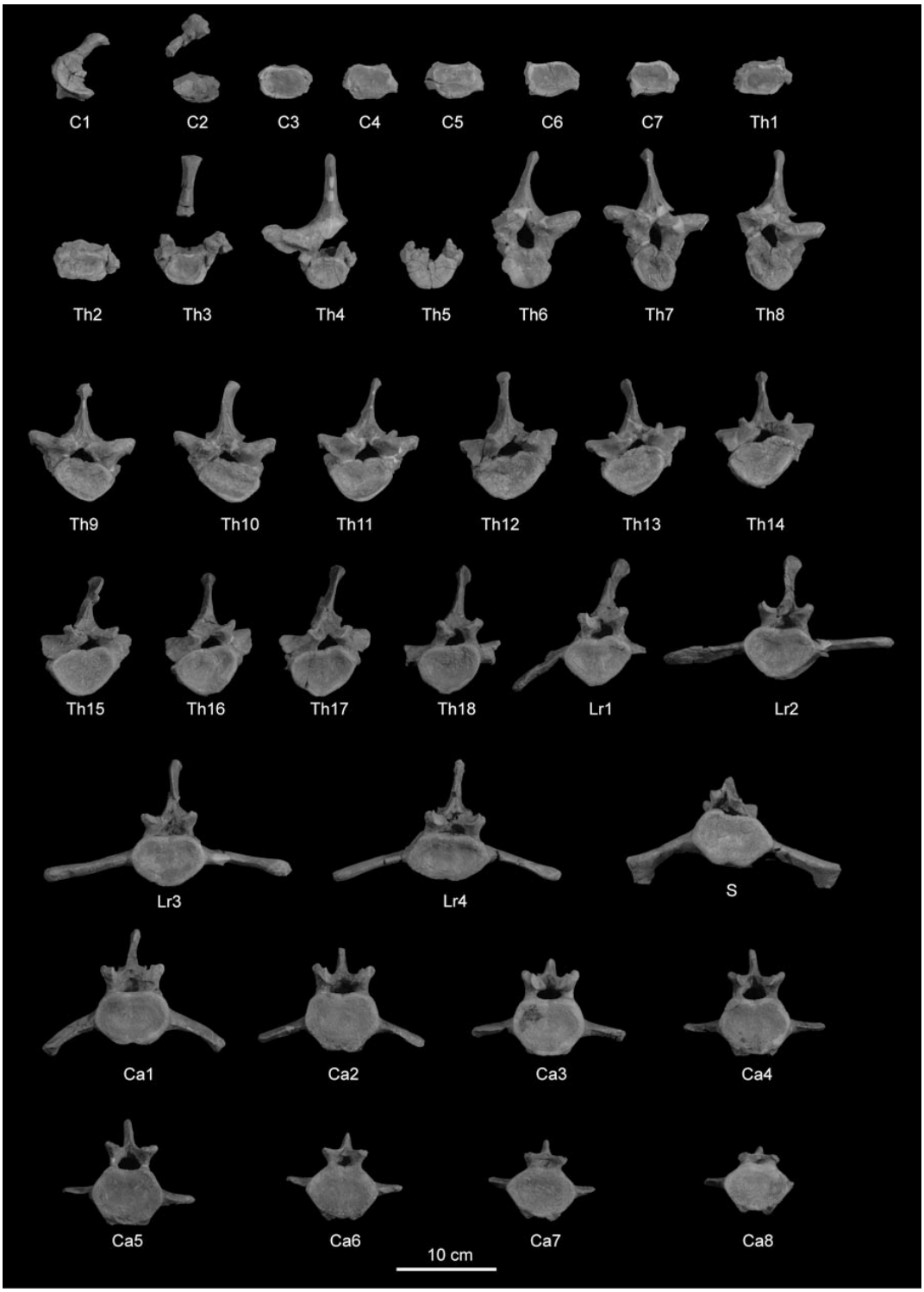

FIGURE 4.46. Cranial (anterior) view of cervical, thoracic, lumbar, sacral, and caudal vertebrae of late Eocene *Protosiren smithae* (UM 101224), collected from the base of the Birket Qarun Formation in Wadi Al Hitan. Keyhole-like neural foramen and long neural spines distinguish Protosirenidae from other Eocene sirenians. Abbreviations: **C**, cervical; **Ca**, caudal; **Lr**, lumbar, **Th**, thoracic; **S**, sacral.

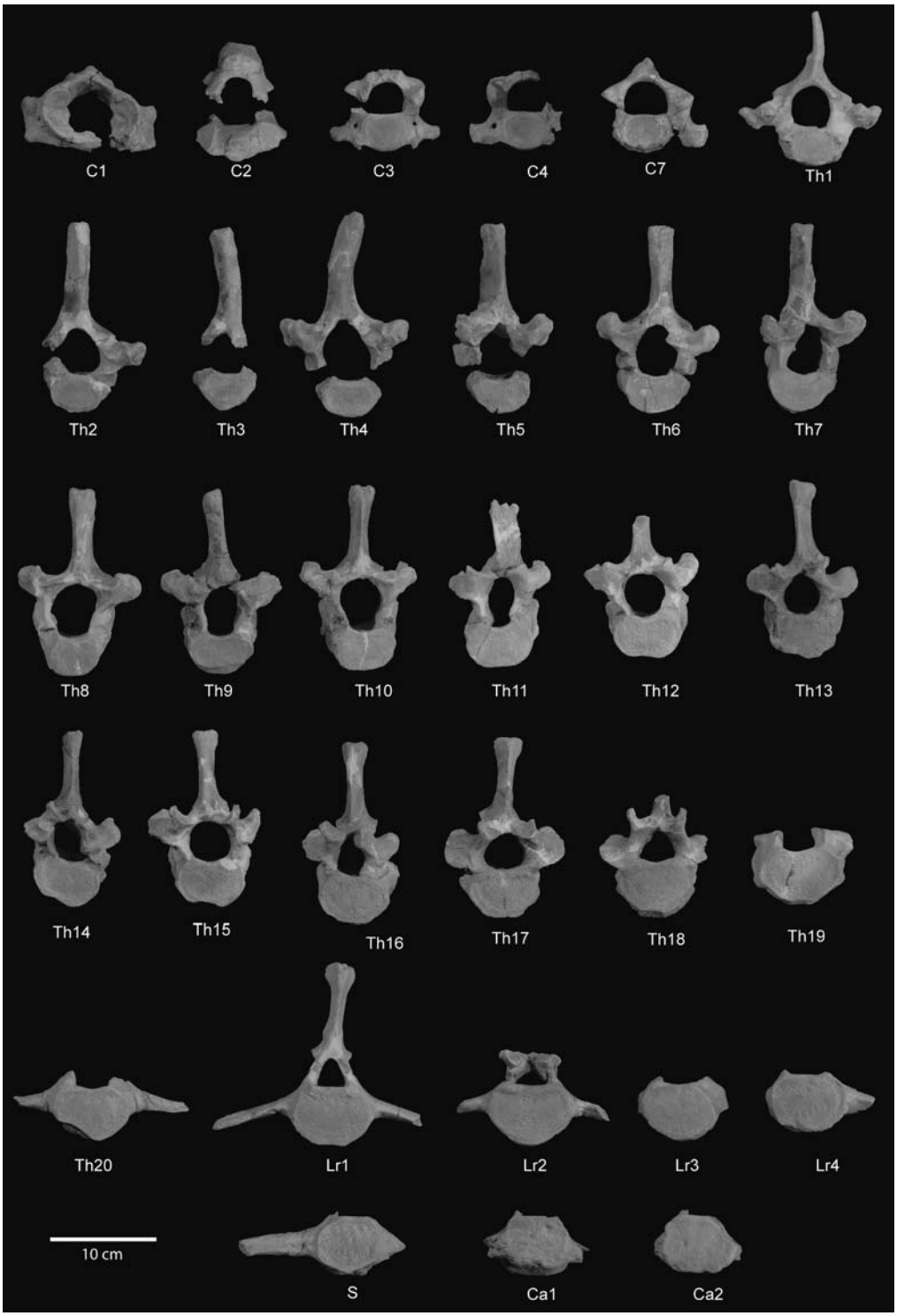

FIGURE 4.47. Lateral view of the vertebrae of late Eocene *Protosiren smithae* (UM 101224), collected from the base of the Birket Qarun Formation in Wadi Al Hitan. There are 20 thoracic, probably more than 4-6 lumbars, one sacral, and probably 20+ caudal vertebrae in this *Protosiren*. Abbreviations: **C**, cervical; **Ca**, caudal; **Lr**, lumbar, **Th**, thoracic; **S**, sacral.

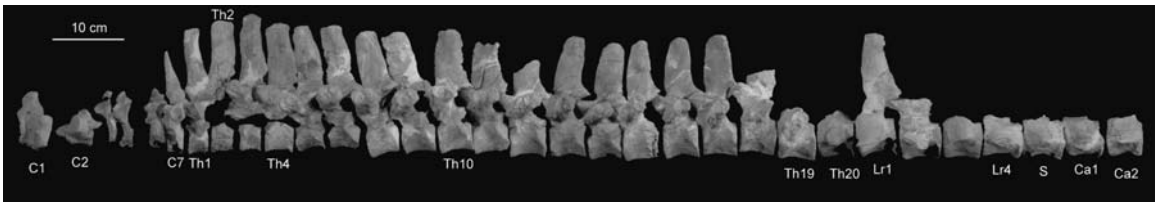

FIGURE 4.48. Cranial (anterior) view the right ribs of *Protosiren smithae* (UM 101224) from the base of the Birket Qarun Formation. The last rib on one side is short and fused with the last thoracic vertebra. Abbreviations: R, right rib.

FIGURE 4.49. Cranial (anterior) view the left ribs of *Eosiren libyca* (UM 101226) from the Qasr El Saga Formation. Note that the last rib is gracile and short. Abbreviations: **L**, left ribs.

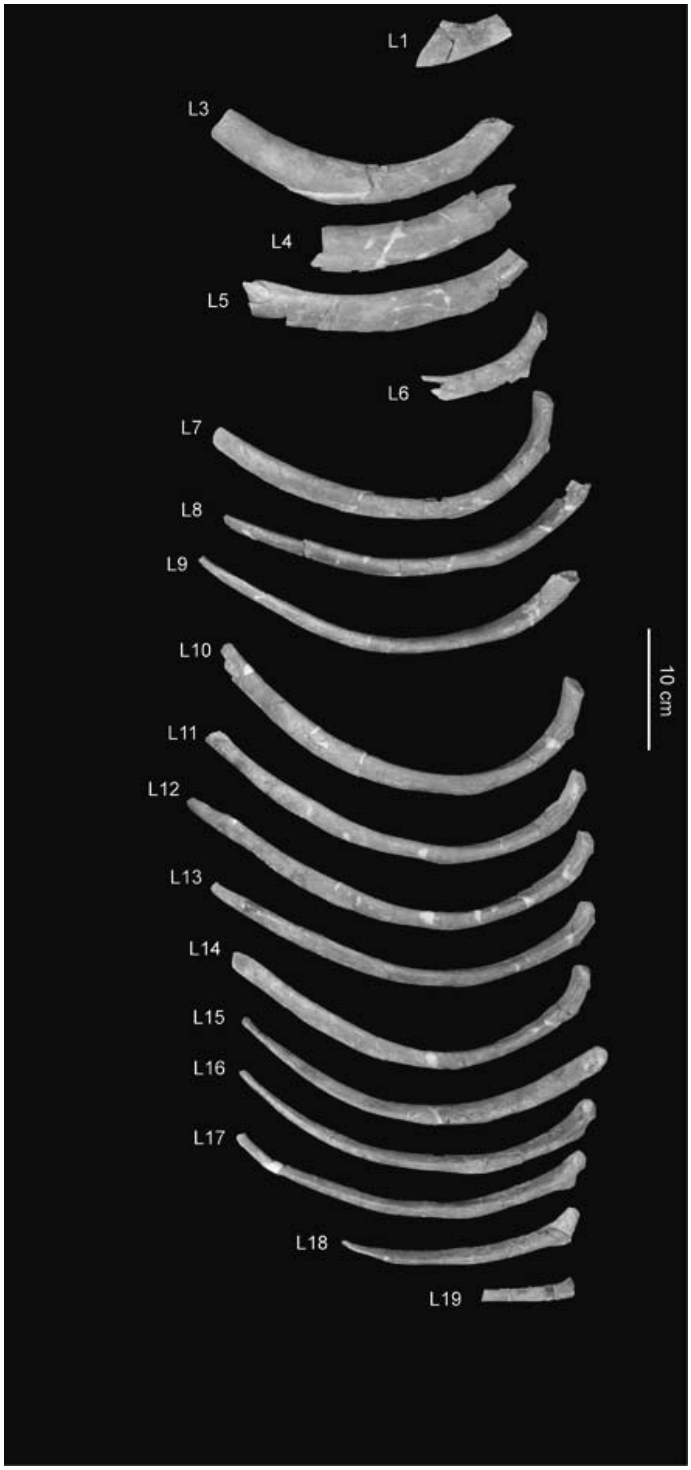

FIGURE 4.50. Sternal elements of *Protosiren*, *Eotheroides*, and *Eosiren* from the Fayum Province. **A**: Ventral view and **B**: Dorsal view of the manubrium of *Protosiren smithae* (UM 101224). **C:** Ventral view, and **D**: Dorsal view of the sternebrae of *Protosiren smithae* (UM 101224); the sternal elements of *Protosiren smithae* (UM 101224) resemble those of land mammals that are composed of a series of short, blocklike segments corresponding with the costal cartilages. **E**: Ventral view, and **F**: Dorsal view of the xiphisternum of *Eotheroides sandersi* (UM 111558), it is dorsoventrally flattened. **G**: Ventral view, and **H**: Dorsal view of the manubrium of *Eosiren libyca* (UM 101226) from the Qasr El Sagha Formation. **I**: Ventral view, and **J**: Dorsal view of the sternebrae of *Eosiren libyca* (UM 101226); both elements are dorsoventrally flattened. **K**: Ventral view, and **L**: Dorsal view of the xiphisternum *Eosiren libyca* (UM 97568).

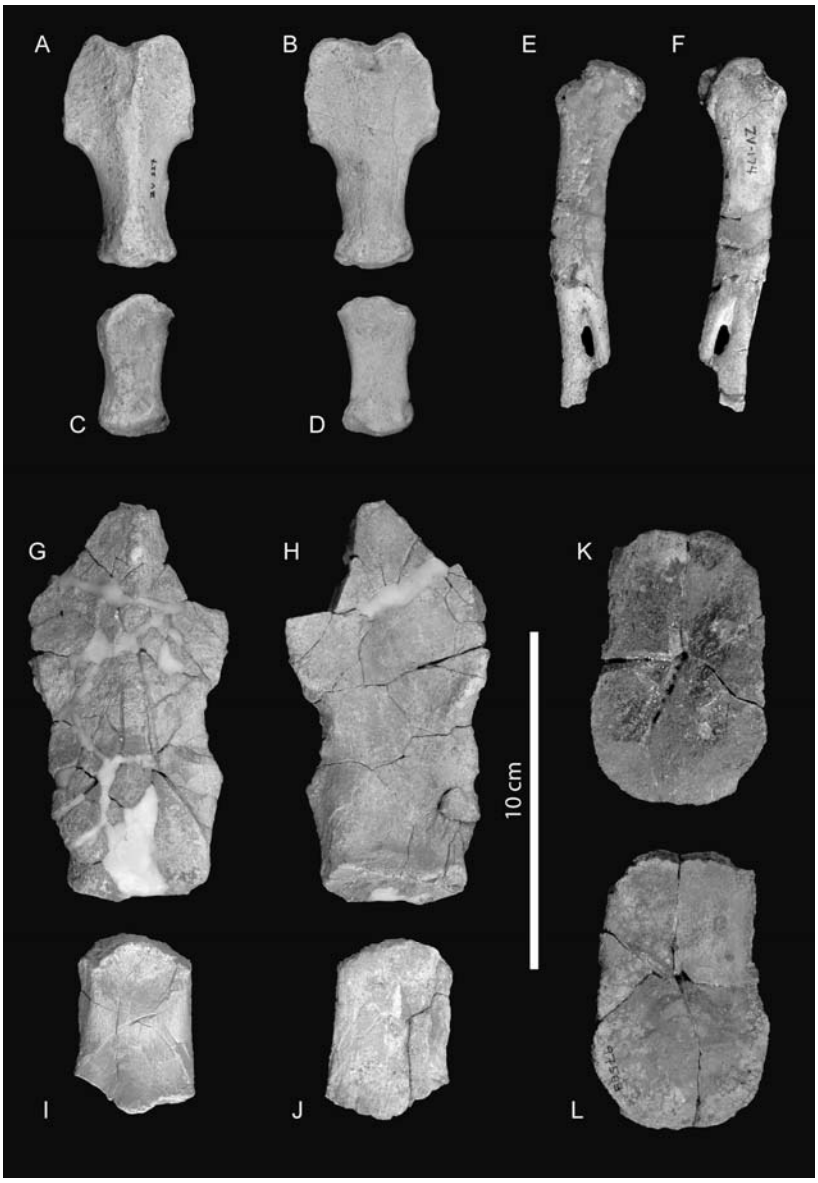

Literature Cited

ABEL, O. 1904. Die Sirenen der mediterranen Tertiärbildungen Österreichs. Abhandlungen der Kaiserlich-Königlichen Geologischen Reichsanstalt (Wien), 19:1-223.

ABEL, O. 1907. Die Stammesgeschichte der Meeressäugetiere. Meereskunde, 1:1-36.

ABEL, O. 1906. Die Milchmolaren der Sirenen. Neues Jahrbuch für Mineralogie, Geologie und Paläontologie, 2:50-60.

ABEL, O. 1912. Grundzüge der Palaeobiologie der Wirbeltiere. E. Schweizerbart, Stuttgart, 708 pp.

ABEL, O. 1913. Die eozänen Sirenen der Mittelmeerregion. Erster Teil: Der Schädel von *Eotherium aegyptiacum*. Paläontographica, 59:289-360 (title page bears date of 1912).

ABEL, O. 1919. Die Stämme der Wirbeltiere. Vereinigung Wissenschaftlicher Verleger, Walter de Gruyter & Co., Berlin and Leipzig, 914 pp.

ANDREWS, C. W. 1902. Preliminary note on some recently discovered extinct vertebrates from Egypt. (Part III.) Geological Magazine, 9:291-295.

ANDREWS, C. W. 1906. A Descriptive Catalogue of the Tertiary Vertebrata of the Fayum, Egypt. British Museum of Natural History, London, 324 pp.

BAJPAI, S., J. G. M. THEWISSEN, V. V. KAPUR, B. N. TIWARI, and A. SAHNI. 2006. Eocene and Oligocene sirenians (Mammalia) from Kachchh, India. Journal of Vertebrate Paleontology, 26:400-410.

BERTRAM, G. C. L., and C. K. R. BERTRAM. 1973. The modern Sirenia: their distribution and status. Biological Journal of the Linnean Society of London, 5:297-338.

BIZZOTTO, B. 1983. *Prototherium intermedium* n. sp. (Sirenia) dell'Eocene Superiore di Possagna e proposta di revisione sistematica del taxon *Eotheroides* Palmer 1899. . Memorie de Scienze Geologiche (Memorie dell'Instituto Geologico della R. Universita), Padua, 36:95-116.

BIZZOTTO, B. 2005. La struttura cranica di *Prototherium intermedium* (Mammalia: Sirenia) dell'Eocene superiore Veneto. Nuovi contributi alla sua anatomia e sistematica. Societa Veneziana di Scienze Naturali Lavori, 30:107-125.

BLAINVILLE, H. M. D. DE. 1840. Ostéographie, Livr. 7, Des Phoques (G. *Phoca*, L.). Paris, Arthus Bertrand.

BLAINVILLE, H. M. D. DE. 1844. Ostéographie, Livr. 15, Des Lamantins (Buffon), (*Manatus*, Scopoli), ou gravigrades aquatiques. Paris, Arthus Bertrand.

CARUS, J. V. 1868. Handbuch der Zoologie. 1ster band. Wirbelthiere, Mollusken und Molluscoiden. Wilhelm Engelmann, Leipzig, 894 pp.

DOMNING, D. P. 1994. A phylogenetic analysis of the Sirenia. Proceedings of San Diego Society of Natural History, 29:177-189.

DOMNING, D. P. 1996. Bibliography and Index of the Sirenia and Desmostylia. Smithsonian Contributions to Paleobiology, 80:iii + 611.

DOMNING, D. P. 2000. The readaptation of Eocene sirenians to life in water. In: J.-M. Mazin, V. de Buffrénil, and P. Vignaud (eds.), Secondary Adaptation of Tetrapods to Life in Water. Historical Biology (Special Issue), 14:115-119.

DOMNING, D. P. 2001a. Sirenians, seagrasses, and Cenozoic ecological change in the Caribbean. In: W. Miller III & S.E. Walker (eds.), Cenozoic Paleobiology: The Last 65 Million Years of Biotic Stasis and Change. Palaeogeography, Palaeoclimatology, Palaeoecology, 166:27-50.

DOMNING, D. P. 2001b. The earliest known fully quadrupedal sirenian. Nature, 413:625-627.

DOMNING, D. P., G. S. MORGAN, and C. E. RAY. 1982. North American Eocene sea cows (Mammalia: Sirenia). Smithsonian Contribution to Paleobiology 52:1-69.

DOMNING, D. P., and V. DE BUFFRÉNIL. 1991. Hydrostasis in the Sirenia: quantitative data and functional interpretations. Marine Mammal Science, 7:331-368.

DOMNING, D. P., and P. D. GINGERICH. 1994. *Protosiren smithae,* new species (Mammalia, Sirenia), from the late Middle Eocene of Wadi Hitan, Egypt. Contributions from the Museum of Paleontology. University of Michigan, 29:69-87.

DOMNING, D. P., P. D. GINGERICH, E. L. SIMONS, and F. A. ANKEL-SIMONS. 1994. A new early Oligocene dugongid (Mammalia, Sirenia) from Fayum Province, Egypt. Contributions from the Museum of Paleontology. University of Michigan, 29:89-108.

FITZINGER, L. J. 1842. Bericht über die in dem Sandlagern von Linz aufgefundenen fossilen Reste eines urweltlichen Säugers, (*Halitherium Cristolii*). Bericht ueber das Museum Francisco-Carolinum, 6:61-72.

GINGERICH, P. D. 1992. Marine mammals (Cetacea and Sirenia) form the Eocene of Jabal Mokattam and Fayum, Egypt: stratigraphy, age, and paleoenvironments. Contributions to the Museum of Paleontology, University of Michigan, 30:1–85.

GINGERICH, P. D., H. CAPPETTA, and M. TRAVERSE. 1992. Marine mammals (Cetacea and Sirenia) from the middle Eocene of Kpogamé- Hahotoé in Togo (abstract). Journal of Vertebrate Paleontology, 12 (3, supplement):29A-30A.

GINGERICH, P.D., D.P. DOMNING, C.E. BLANE, and M. UHEN. 1994. Cranial morphology of *Protosiren fraasi* (Mammalia, Sirenia) from the Middle Eocene of Egypt: a new study using computed tomography. Contributions from the Museum of Paleontology. University of Michigan, 29:41- 67.

GINGERICH, P. D., M. ARIF, M. A. BHATTI, H. A. RAZA, and S. M. RAZA. 1995. *Protosiren* and *Babiacetus* (Mammalia, Sirenia and Cetacea) from the middle Eocene Drazinda Formation, Sulaiman Range, Punjab (Pakistan). . Contributions from the Museum of Paleontology, University of Michigan, 29:331-357.

GRAY, J. E. 1821. On the natural arrangement of vertebrose animals. London Medical Repository, 15:296-310.

HEAL, 1973. Contributions to the study of sirenian evolution. Ph.D. thesis, University of Bristol, England (unpubl.).

ILLIGER, C. 1811. Prodromus systematis mammalium et avium additis terminis zoographicus utriusque classis, earumque versione Germanica. i-xviii, 1-302.

KAUP, J. J. 1838a. Über Zähnen von *Halytherium* und *Pugmeodon* aus Flonheim. Neues Jahrbuch für Geognosie, Geologie und Petrefactenkunde 1838:318-320.

KAUP, J. J. 1838b. Über Zähnen von *Halitherium* und Dugong. Neues Jahrbuch für Geognosie, Geologie und Petrefactenkunde, 1838:356.

KORDOS, L. 1981. Some complements to the knowledge of a Middle Eocene Sirenia, *Sirenavus hungaricus* Kretzoi, 1941. Fragmenta Mineralogica et Palaeontologica, 10:75-78.

KORDOS, L. 1977. A New Upper Eocene Sirenian *(Paralitherium tarkanyense* n.g.n.sp.) from Felsötrárkány, NE Hungary. Magyar Állami Földtani Intézet Évi Jelentése az 1975 Évröl, 1977:349-367.

KRETZOI, M.1941. *Sirenavus hungaricus* n.g. n. sp., ein neuer Prorastomide aus dem Mitteleozän (Lutetium) von Felsögalla in Ungarn. Annales Musei Nationalis Hungarici, Pars Mineralogica, Geologica et Palaeontologica, 34:146-156.

LEPSIUS, G. R.1882. *Halitherium Schinzi*, die fossile Sirene des Mainzer Beckens. Eine vergleichend-anatomische Studie. Abhandlungen des Mittelrheinischen Geologischen Vereins, 1:vi + 200 + viii.

LINK, H. F. 1795. Beyträge zur Naturgeschichte. Vol. 1, part 2. K. C. Stiller, Rostock and Leipzig, 126 pp.

LINNÆUS, C. 1758. Systema naturæ per regna tria naturæ, secundum classes, ordines, genera, species, cum characteribus, differentiis, synonymis, locis. decima Edition. Laurentius Salvius, Holmiæ, 824 pp.

MÜLLER, P. L. S. 1776. Des Ritters Carl von Linne' … vollständiges Natursystems Supplements- und Register-Band…. Nuremberg, Gabriel Nicolaus Raspe, 384 pp.

OWEN, R. 1855. On the fossil skull of a mammal (Prorastomus sirenoides Owen) from the island of Jamaica. Quarterly Journal of the Geological Society of London, 11:541-543.

OWEN, R. 1875. On fossil evidences of a sirenian mammal (*Eotherium aegyptiacum*, Owen) from the Nummulitic Eocene of the Mokattam Cliffs, near Cairo. Quarterly Journal of the Geological Society of London, 31:100-105.

PILLERI, G., J. BIOSCA, and L. VIA. 1989. The Tertiary Sirenia of Catalonia. Brain Anatomy Institute, University of Berne, Ostermundingen, 1-98 pp.

PALMER, T. S. 1899. Catalogus Mammalium tam viventium quam fossilium [Review of Dr. E. L. Trouessart's Catalogus Mammalium]. Science, 10:491-495.

SAGNE, C. 2001a. *Halitherium taulannense*, nouveau sirenien (Sirenia, Mammalia) de l'Eocene superieur provenant du domaine Nord-Tethysien (Alpes-de-Haute-Provence, France) Comptes Rendus de l'Academie des Sciences Serie II A Sciences de la Terre et des Planete, 333:471-476.

SAMONDS, K., ZALMOUT, I. S., and KRAUS, D. 2005. New sirenian fossils from the late Eocene of Madagascar. Journal of Vertebrate Paleontology, 25(3, supplement):108A.

SAVAGE, R. J. G. 1969. Early Tertiary mammal locality in southern Libya. Proceedings Geological Society of London, 1657:167-171.

SAVAGE, R. J. G. 1971. Review of the fossil mammals of Libya. In: Symposium on the Geology of Libya, University of Libya, pp. 215-225.

SAVAGE, R. J. G. 1977. Review of early Sirenia. Systematic Zoology 25:344–351.

SAVAGE, R.J.G., D.P. DOMNING, and J.G.M. THEWISSEN. 1994. Fossil Sirenia of the West Atlantic and Caribbean region. V. The most primitive known sirenian, *Prorastomus sirenoides* Owen, 1855. Journal of Vertebrate Paleontology, 14:427-449.

SICKENBERG O. 1934. Beiträge zur Kenntnis Tertiärer Sirenen. I. Die Eozänen Sirenen des Mittelmeergebietes; II. Die Sirenen des Belgischen Tertiärs. Mémoires du Museé Royal d'Histoire Naturelle de Belgique, 63:1–352.

SIEGFRIED, P. 1967. Das Femur von *Eotheroides libyca* (Owen) (Sirenia). Paläontologisches Zeitschrift, 41:165-172.

SPILLMANN, F. 1959. Die Sirenen aus dem Oligozän des Linzer Beckens (Oberösterreich), mit Ausführungen über "Osteoskelerose" und "Pachyostose". Österreichische Akademie der Wissenschaften, Mathematisch-Naturwissenschaftliche Klasse. Denkschriften, 110:1-68.

STROMER, E. 1921. Untersuchung der Hüftbeine und Hüftgelenke von Sirenia und Archaeoceti. Sitzungsber. Bayerische Akademie der Wissenschaften. Mathematisch-Physik Klasse, 1921:41-59.

WING, S. L., S. T. HASIOTIS, and T. M. BOWN. 1995. First ichnofossils of flank-buttressed trees (late Eocene), Fayum Depression, Egypt. Ichnos, 3:281-286.

ZIGNO, A. DE. 1875. Sireni fossili trovati nel Veneto. Memorie dell' Real Istituto Veneto di Scienze Lettere ed Arti, 18:427-456.

CHAPTER FIVE

SEXUAL DIMORPHISM IN EOCENE SIRENIA

Here I review elements of sexual dimorphism in living sirenians, and will focus on sexual dimorphism in the pelvic bones of Eocene and Recent sirenians.

Introduction

Sexes in mammals often differ in secondary characteristics not related to reproduction directly. Secondary sexual dimorphism can be expressed in many ways in mature males and females of the same species, such as overall body size, and the size and form of tusks, horns, and antlers. In extinct animals sexes can often be distinguished based on distinctive size distribution or morphological features.

In mammal orders, sexual dimorphism ranges from species in which females are larger than males to those in which males are much larger than females and possess profound secondary sexual characteristics that are absent in females (Bourlière, 1975; Ralls, 1977 and 1976).

Living members of the order Sirenia exhibit little or no sexual dimorphism in body size. Heinsohn (1972) examined 69 individuals of Australian dugongs, ranging from 1.09 to 3.05 m in body length, and found no significant sexual difference in size. Hartman (1971) suggested that female manatees may be larger than males.

Sexual dimorphism in dugongs may be inferred from the biometric analysis of the cranial elements by Spain and Heinsohn (1974), and then Spain et al. (1976) who ran an analysis of 26 variables obtained from 32 individuals with known sexes (16 males and 16 females). Sexual dimorphism was represented in a bivariate scatter plot of anterior snout width against snout length (Spain et al., 1976, pp. 494, fig. 1). In this case, a line separating the two sexes can be given by the expression: snout length = 10.306 + (1.485 x anterior snout width). However, these variables and equation are designed to sex living dugongs and seem not to distinguish males from females of Eocene fossil sirenians.

Another source of sexual dimorphism in the cranium of modern dugongs, not manatees, is in their tusks. Both sexes grow them but they erupt only in males and some older post-reproductive females (Marsh, 1980; Marsh et al., 1984a,b). A study of interspecific morphological variation in manatee skulls did not detect significant sexual dimorphism in any of the three living manatees (Domning and Hayek, 1986).

Postcranial elements are another locus of sexual dimorphism in sirenians. The main form of sexual dimorphism that is of interest in living and fossil Sirenia is the variability of their pelvic bone in both sexes. Pelvic bones of fossil and living sirenians have some landmarks and structures that are almost certainly related to sexual dimorphism. Krauss (1870: p. 613) suggested that the distal expansion and thickening of *Dugong* ischia (see Lorenz, 1904) might distinguish males from females. Similar morphologies were found in the Miocene hydrodamaline *Dusisiren jordani* (Domning, 1978), in Miocene *Metaxytherium serresii* (Domning and Thomas, 1987, p. 219), and in Miocene *Metaxytherium krahuletzi* (Domning and Pervesler, 2001, p. 37).

Since one of the ischium's principal functions is to provide attachment for the crura of the penis or clitoris, and since male genitals require larger surface attachment, it may be expected that this part of the innominate will be more enlarged in males than females. Muscle attachments on the distal edge of Recent dugong ischia are greatly variable in both sexes (Riha, 1911; Domning, 1977). Both males and females have the dorsal distal end of the ischium covered by the ischiococcygeus muscle that connects the ischium to the third chevron bone; in females the posterior edge (medially and laterally) is covered by the constrictor vestibuli muscle which holds the lateral walls of the vagina, while in males this portion of the ischium is covered partly by the bulbocavernosus muscle and enormously by the ischiocavernosus (see Riha, 1911: p. 420, figs. 14 and 15). The ischiocavernosus seems to be the main muscle responsible for enlargement and deflection of the ischium in adult males; this muscle is also responsible for causing the erectile tissues in male's penis to expand and enlarge.

Domning (1991) studied pelvic bones of 70 Australian dugongs with known sex and age which allowed him to produce a key to interpret these bones' variability (Domning, 1991, p. 314). The characters used by Domning (1991) in determining sexual dimorphism in mature Recent dugong innominate bones include presence of processes along the ventral border of the ischium; dorsoventral expansion of the posterior (distal) end of the bone; and flaring of the bone's posterior end away from the midline. Moreover, Domning noticed that the ischial distal end is thicker (>0.5 cm) in males than in females (≤0.5 cm). All of these characters tended to be more pronounced in adults than in immature animals and more in males than in females.

The pelvic vestiges of *Trichechus manatus* are sexually dimorphic as well. Krauss (1872) was first to report on sexual and ontogenetic variation in manatee pelvic bones in both sexes. Female pelvic bones are narrow proximally with distinct constriction at the middle of the ischium, while the males vestigial bones are broader and thicker than in females. The same conclusions were reached quantitatively by Fagone et al. (2000) for mature male and female pelvic bones of *Trichechus manatus latirostris*. Fagone et al. (2000) also found that sexual dimorphism in the pelvic bones of manatees is clearly developed and best demonstrated in males and females longer than 225 cm; and in all cases where males and females are longer than 225 cm, the weight of the pelvic bone of the males is always, exponentially with age and body length, greater.

Sexual dimorphism in Eocene Sirenia is almost certainly impossible to determine on the bases of body size, tusk size and eruption, or snout length/width relationship as documented in Recent dugongs (Spain et al., 1976, pp. 494, fig. 1). There are many reasons for this. First there are not so many complete individuals to represent one species. Second, almost all skulls preserve no tusks, and the sizes of tusk alveolae and cavities are very small in Eocene sirenians compared to those in *Dugong dugon*. However, the pelvic bones in both living and fossil sirenians (especially in the family Dugongidae) still display some other morphological indicators of sex.

Sexual Dimorphism in Eocene Sirenia

Well-preserved pelves of twelve or so Eocene sea cow specimens from Egypt and Pakistan (*Protosiren*, *Eotheroides*, and *Eosiren*) show variations in both form and size

that are interpretable as characteristic of males and females (Table 5.1). Expansion and narrowing, flaring and straightening, robustness and thinning, and smoothness and roughness were all noticed on the distal ends of well-preserved Eocene sirenian ischia from Egypt, and in all three Eocene genera represented: *Protosiren*, *Eotheroides*, and *Eosiren*. All of these innominates seem to represent mature individuals or subadults, because all three bones in the innominate (ilium, pubis, and ischium) are fused and suture lines have vanished. The ventral margin of the ischium is preserved in most of the studied specimens, including *Protosiren fraasi*, *Protosiren smithae*, *Protosiren sattaensis*, *Eotheroides sandersi*, *Eotheroides clavigerum*, and *Eosiren libyca*. The excellent preservation and preparation saved, in most cases, left and right pelves of the same individuals, and these were frequently found in skeletons of dentally mature animals. Having both innominates of the same individual allowed more comparisons, and detection of peculiar variations and landmarks of interest on both sides.

Observing the variability that is related to sexual dimorphism in Eocene sirenians requires finding features or processes that appear on the ventral or posterior margin of the ischium, similar to those found in Recent dugongs by Domning (1991). In all Eocene innominates from Egypt, ventral margins of the ischia are smooth and lack any prominences or processes; some ischia show narrowing and thinning of their distal ends; some ischia have their posterior portion expanded and developed into a thick protuberance expanded dorsoventrally with or without a rugose surface, and in most such cases the distal end is turned posterolaterally. Narrowing and thinning of the distal ends are characteristics of female ischia, and expansion and thickening of the posterior portion of the ischium are male characteristics (Domning, 1991). Dimensions of ischial distal

ends in the major Eocene groups are listed in Table 5.1 to show variations in size and morphology as a result of sexual dimorphism.

Pelvic morphology of Protosirenidae

In *Protosiren* species the pelves have long ilia, large obturator foramina, wide and deep acetabula, and long pubic symphyses. The ischia show more expansion and spatulation, but not extreme thickening mediolaterally at their distal ends; however, some inter- and intraspecific variations were found in *Protosiren* ischia.

A *Protosiren fraasi* pelvic bone (SMNS 43976: cast of a left pelvis [Figure 5.1A, B, C] from the Lutetian Mokattam Limestone of Cairo; Andrews, 1902; Abel, 1907) has the ventral margin of the ischium broken; the lateral wings of the ischium are slightly deflected and concave laterally to form a shallow basin, and the posterodorsal end is thin with no pronounced tuberosity. This could potentially be a female pelvis.

The holotype of *Protosiren sattaensis* (GSP-UM 3001, Figure 5.2) from the Bartonian Drazinda Formation of the Sulaiman Range of Pakistan preserves both innominate bones but the right side has better preservation of the ischium (Gingerich et al., 1995: p. 347, fig. 11). The ischium extends posteriorly from the center of the acetabulum for more than 90 mm and flares posteriorly with a thin tuberosity that is slightly deflected laterally. This could be interpreted as a female *Protosiren* as well, since the mediolateral thickness is almost the same as the thickness of the ramus (Table 5.1, Figure 5.2). The other specimen of *Protosiren sattaensis* with a pelvis (and a complete femur) is GSP-UM 3197 (Figure 5.2), found close to the locality of the

holotype mentioned earlier. This pelvis has an incomplete ventral ischial margin but seems to be narrower and thinner than that of the holotype, with a weak tuberosity at its posterior end; this is questionably interpreted as a female pelvis.

The pelvic bone of the type specimen of *Protosiren smithae* (CGM 42292) (Figure 5.1D, E, F) has a posterior border that is semicircular in outline, greatly thickened and somewhat rugose. The dorsal portion of this border bears a broad, more or less flat surface facing dorsally; the posterior extremity of the ischium is prolonged into a blunt protuberance whose roughened surface is directed posterolaterally; and the ventral part of the posterior border is much less thick but turns markedly outward, helping to form the concavity of the ischium's lateral surface. The overall aspect of this thickened and somewhat laterally curved termination of the ischium resembles that seen typically in males of modern *Dugong*, as opposed to females (Domning, 1991).

Pelvic morphology of Dugongidae

Eotheroides and *Eosiren* from the Eocene of Egypt preserve spectacular pelves along with detailed morphologies that allow close examination.

The ischium in the holotype of *Eotheroides clavigerum* (UM 101219) (Figure 5.3) from the Priabonian Birket Qarun Formation, which is best preserved on the left side, is long, thin, and narrow posterodorsally, curved medially, with a very weak tuberosity on the posteriormost edge and smooth internal and external sides. This probably represents a female. This animal is known from the skull and most of the skeleton of a dentally mature individual showing extensive dental wear, and small erupted tusks.

Eotheroides sandersi innominates are known from the holotype, CGM 42181 (Figure 5.4C, D), and from UM 97514 (Figure 5.4A, B). The pelves of CGM 42181 belong to a small or immature individual although the three bones of the pelvis seem to be fused; the ischium is flattened, narrow, and lacks any rugosity or tuberosity, which indicate this is a young female. The other individual of *Eotheroides sandersi* (UM 97514) has a broad, flat ischial ramus, the posterior end of the ischium is thickened and abruptly flares laterally below a line extending from the middle of its ventral edge to its posterodorsal corner. The entire margin of this flaring portion is 1-1.5 cm thick and rugose; also roughened somewhat are its posteromedial surface and the vertical medial surface of the bone's posterodorsal end. The latter two surfaces, both slightly concave, are separated by a broadly convex horizontal ridge. The degree of lateral flaring of the end of the ischium is comparable to or greater than that which today characterizes male *Dugong* (Domning, 1991).

Innominate bones of *Eosiren* (Figure 5.5) were collected from the Qasr El Sagha Formation, with many individuals and ontogenetic stages and intraspecific variations in the ischium represented. *Eosiren libyca* has a very advanced stage of reduction in its pelvis, in contrast with *Eotheroides* and *Protosiren*.

The best preserved pelves of *Eosiren libyca* include UM 101226, a completely preserved right innominate (Figure 5.5A,B,C) belonging to a skeleton of a large individual. The ilium is slender, straight, long, trihedral in cross section, showing a rugose concavity at the anterior end, and lacks the swelling seen in *Eotheroides*; the acetabulum is shallow and small, but relatively larger than in other described *Eosiren* individuals including those described by Andrews (1906, p. 214-215). The pubis is

triangular with a rough ventromedial end (possibly remains of the symphysal fibro-cartilage attachment). The obturator foramen is small and opens laterally to form a small basin. The ischium is long and similar to those found in male *Eotheroides sandersi*, but with less distal flaring and expansion. However, it shows considerable thickening and deflection of the end, and its mediodistal side is ornamented with rugosities and scars. The posteriormost end is occupied by two lateral concavities and one large medial depression for ligament attachments. All of these features indicate that this individual (UM 101226) was a male.

A cast of another pelvic bone of *Eosiren libyca* (CGM 29774) (Figure 5.5D, E, F) is very similar to that described in Andrews (1902). However, it is different from the pelvis of UM 101226 in having the distal end of its ischial thinner and narrower, but at the same time keeping an enlarged tuberosity with a pitted lenticular basin (8 mm wide) on its dorsal edge. This specimen could be a young male, as the tuberosity is not well developed yet the end of the tuberosity is already enlarged to twice the width of the ischial ramus.

The last specimen of *Eosiren libyca* to be discussed here (UM 101228) (Figure 5.5G, H, I) has a pair of poorly preserved pelves whose ischia are 12 mm thick mediolaterally and are conservative in thickness through the distal end. Its sex is a little ambiguous because of the moderate thickness of the ischium and presence of a narrow dorsoventral depression (on both pelves) at the terminal distal portion. Although lack of expansion and flaring may make it a good candidate for a female *Eosiren*, this specimen is an immature individual, as the caudal centra associated with it are not totally fused to the neural arches.

Discussion and Conclusions

Thickening of the distal end of the ischium in Protosirenidae and Dugongidae could be the best criterion to use in sexing Eocene sirenian innominates. Figures 5.6 and 5.7 and Table 5.1 present a summary of sexual dimorphism in the Eocene pelvic bones in hand. Figure 5.6 displays three ischial variables, two of which display significant sexual dimorphism in the pelvic bone. The difference between the mediolateral thickness of the ischial ramus and the mediolateral thickness of the distal end of the ischium is great in the following specimens: *Protosiren smithae* CGM 42292, *Eotheroides sandersi* UM 97514, *Eosiren libyca* CGM 29774, and *Eosiren libyca* UM 101226. It was small to negative in the following specimens: *Protosiren fraasi* SMNS 43976, *Protosiren sattaensis* GSP-UM 3001, *Protosiren sattaensis* GSP-UM 3197, *Eotheroides sandersi* CGM 42181, *Eotheroides clavigerum* UM 101219, and *Eosiren libyca* 101228.

In supposed male cases the ratio of the mediolateral thickness of the distal end of the ischium to the mediolateral thickness of the ischial ramus was between 1.8 and 2.3, while in putative females the ratio is between 0.8 and 1.0.

The only complete preserved pelvic bone of *Protosiren smithae* (CGM 42292) from Wadi Al Hitan shows a massive and robust distal end of the ischium, making it distinct from other Protosirenidae from the Lutetian of the Mokattam Hills (*Protosiren fraasi* SMNS 43976) and from the Bartonian of Central Pakistan (*Protosiren sattaensis* GSP-UM 3001and GSP-UM 3197). The pelvic bones of *Eotheroides* and *Eosiren* show extreme sexual dimorphism compared with other Eocene sirenians; this dimorphism is similar in form and degree to those in living dugongs.

Eocene pelvic bones may be the only elements usable for sexing these fossils. It is not clear if these animals were dimorphic in other features such as body size, or tusk size and morphology. Some Eocene sirenians grew a small tusk (35 mm long in *Eotheroides clavigerum* UM 101219), several times smaller than those of mature Recent dugongs (up to 200 mm long; Domning and Beatty, 2007), so these tusks are not well developed in early sirenians. Testing for sexual dimorphism in Eocene sirenian tusks would require a large sample for quantitative analysis in a population; such a sample is not available.

Gingerich et al. (1994: p. 62, fig. 7) showed that the type specimen of *Protosiren fraasi* (CGM 10171) has unusual features that are symmetrical on both sides of the midline. One of these features was interpreted as a well-developed rostral lacuna or sulcus "most probably for a proboscis" that is only found in the type specimen (CGM 10171), and is totally absent in SMNS 10576; this could be related to sexual dimorphism. As an analogy, in the Recent southern elephant seal, *Mirounga*, the males have a muscular proboscis that is lacking in females.

Pelvic bones of living and fossil dugongs have a pattern of sexual dimorphism similar to that of advanced whales and expected in the Eocene basilosaurine and dorudontine whales as well. An expansion of the ischium and thickening of the ilium seem to be the main sexual dimorphic features found in living whale's pelvic region (Struthers, 1893; Lönnberg, 1908; Kleinenberg et al., 1964, Berzin, 1972; Perrin, 1975; Rommel, 1990; Yoshida et al., 1994).

Being sexually dimorphic in both tusk and pelvic region, *Dugong dugon*'s males take advantage of the former accessories as strategic tools in mating and foraging. Preen (1989) reported that dugong males are more aggressive in physical competitions for

females than male manatees. Moreover, many scars and injuries appearing in dugongs presumably were made with mature male tusks by surface lunging while companioning for females. According to Anderson (1997, 2002), Australian dugongs in a cove of Shark Bay used the lekking strategy to secure a successful courtship. Lekking seems to be the main mating strategy in Australian dugongs, where the reproductive males have to establish two major conditions. One, is establishing display territories that are smaller than a normal home range where food resources are limited and there is apparent opportunity for mate choice by females. Two, maintaining strong sexual dimorphism and sexual bimaturism as expressed by males in ritualized display at the center of the mating area (Högland and Alatalo, 1995; Bradbury, 1977; Anderson, 2002).

Compared to recent dugongs, Eocene sirenians from Egypt have smaller body size, and small and unerupted tusks. These features made it difficult to draw a conclusion on what strategies had these marine mammals used in achieving successful mating. This leave us with only one option that Eocene dugongs may have used group mating strategy since there is, so far, no clear indication of male-male aggregation during mating. However, pattern and amount of sexual dimorphism in the pelvic region in the Eocene sirenians from Fayum is similar to that in Recent dugongs suggesting that this kind of sexual dimorphism existed in the early Tethyan ancestors and maintained appearance in the post Eocene simians.

TABLE 5.1. Dimensions of ischia of Eocene sirenians, showing variations in the thickness of the ischial ramus and tuberosity, and dorsoventral depth. All measurements are in mm. ♂: male, ♀: female.

Species	Maximum mediolateral thickness of the distal end of the ischium in mm	Mediolateral thickness of the ischium ramus in mm	Maximum dorsoventral thickness of the distal end of ischium in mm	Ln(Maximum mediolateral thickness of the distal end of the ischium in mm)	Ln(Maximum dorsoventral thickness of the distal end of ischium in mm)	Ln(Maximum dorsoventral thickness of the distal end of ischium in mm)	Difference between Ln(Maximum mediolateral thickness of the distal end of the ischium in mm) & Ln(Maximum dorsoventral thickness of the distal end of ischium in mm.)
Protosiren fraasi SMNS 43976 (♀)	8.3	8.1	43.0	2.119	2.094	3.761	0.024
Protosiren sattaensis GSP-UM 3001(♀)	12.9	10.9	38.0	2.560	2.385	3.638	0.174
Protosiren sattaensis GSP-UM 3197(♀)	10.8	13.5	50.0	2.381	2.600	3.912	-0.219
Protosiren smithae CGM 42292 (♂)	23.1	11.5	54.0	3.139	2.446	3.989	0.693
Eotheroides sandersi CGM 42181 (♀)	6.0	7.6	37.0	1.792	2.028	3.611	-0.236
Eotheroides sandersi UM 97514 (♂)	20.6	10.8	53.0	3.024	2.376	3.970	0.648
Eotheroides clavigerum UM 101219 (♀)	11.0	11.0	31.0	2.398	2.398	3.434	0.000
Eosiren libyca 101228 (♀)	11.0	11.3	28.0	2.398	2.425	3.332	-0.027
Eosiren libyca CGM 29774 (♂)	17.0	9.5	33.0	2.833	2.251	3.497	0.582
Eosiren libyca UM 101226 (♂)	27.8	12.3	47.0	3.324	2.507	3.850	0.817

FIGURE 5.1. Dorsal (A), lateral (B), and posterior views (C) of the left innominate of a possible female of *Protosiren fraasi* (SMNS 43976); the ischium is broad and thin, lacking a pronounced tuberosity; also the mediolateral thickness of the ischium does not change from the ramus to the distal end. D, E, and F, posterior, lateral and dorsal views, respectively, of the right innominate of a possible male of *Protosiren smithae* (CGM 42292); the dorsal view shows the extensive mediolateral thickening of the distal end (the tuberosity). Abbreviations: **act.,** acetabulum; **il.,** ilium; **isc.,** ischium; **isc.D,** ischium tuberosity depth; **isc.T,** ischium tuberosity thickness; **isc.R,** ischium ramus thickness; **isc. tub.,** ischiac tuberosity; **obt. f.**, obturator foramen; **ps.,** pubis; **sac. il. artic.**, sacroiliac articulation surface.

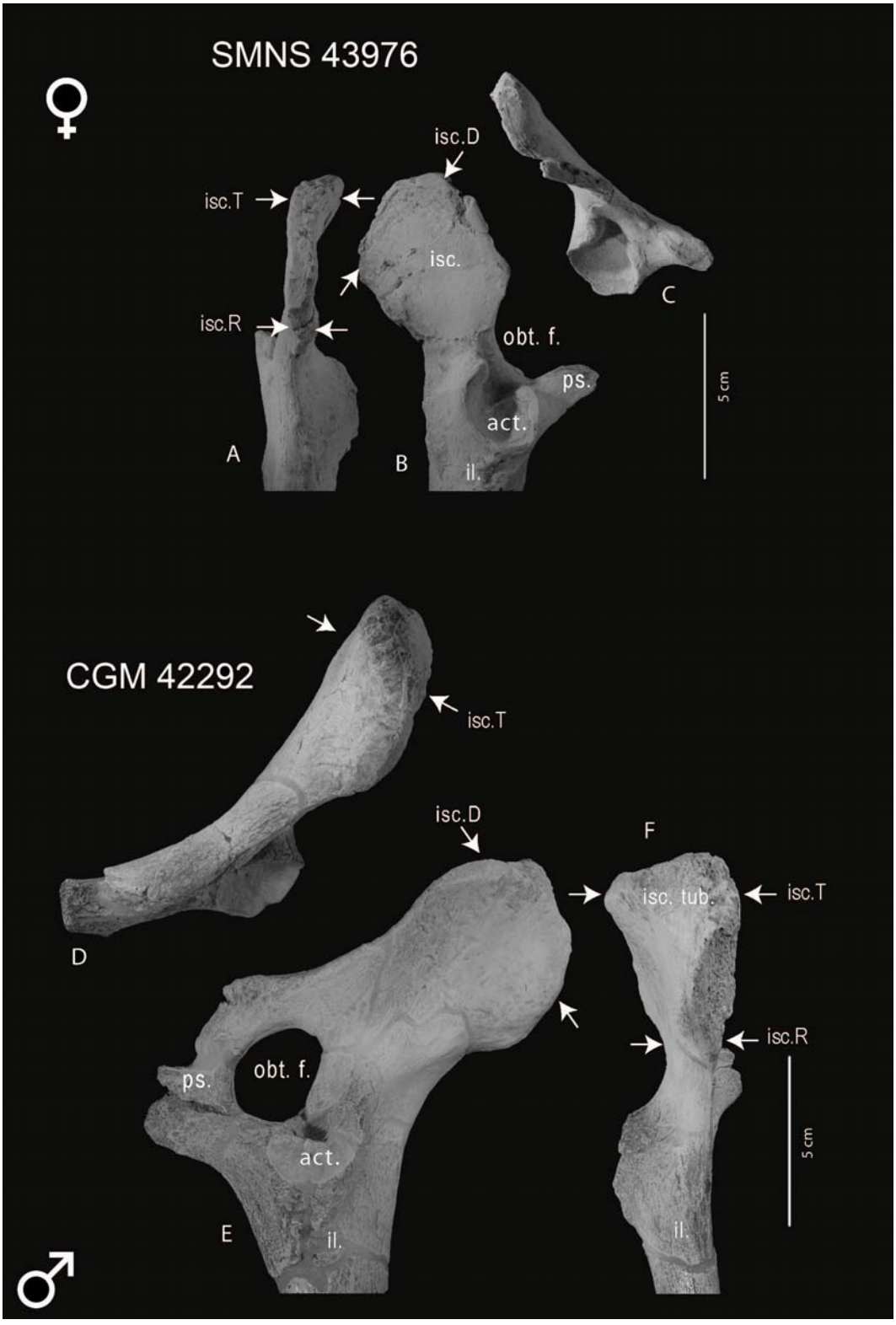
SMNS 43976
♀
isc.D
isc.T
isc.
isc.R
obt. f.
ps.
act.
il.
A
B
C
5 cm
CGM 42292
isc.T
isc.D
F
isc. tub.
isc.T
D
isc.R
ps.
obt. f.
act.
E
il.
il.
5 cm
♂

FIGURE 5.2. Posterior (A), lateral (B), and dorsal views (C) of the right innominate of a possible female of *Protosiren sattaensis* (GSP-UM 3001); the ischium is broad laterally, possessing a small tuberosity at its distal dorsal end with a slight lateral deflection; however, the mediolateral thickness of the ischium does not change significantly distally, suggesting that this individual was more likely a female (compare to CGM 42292). D and E, dorsal and lateral views, respectively, of the left innominate of a possible female of *Protosiren sattaensis* (GSP-UM 3197); the mediolateral thicknesses of the ischial distal end and the ramus are almost equal, suggesting that this pelvis is female. Abbreviations: **act.,** acetabulum; **il.,** ilium; **isc.,** ischium; **isc.D,** ischium tuberosity depth; **isc.T,** ischium tuberosity thickness; **isc.R,** ischium ramus thickness; **isc. tub.,** ischiac tuberosity; **obt. f.**, obturator foramen; **ps.,** pubis; **sac. il. artic.**, sacroiliac articulation surface.

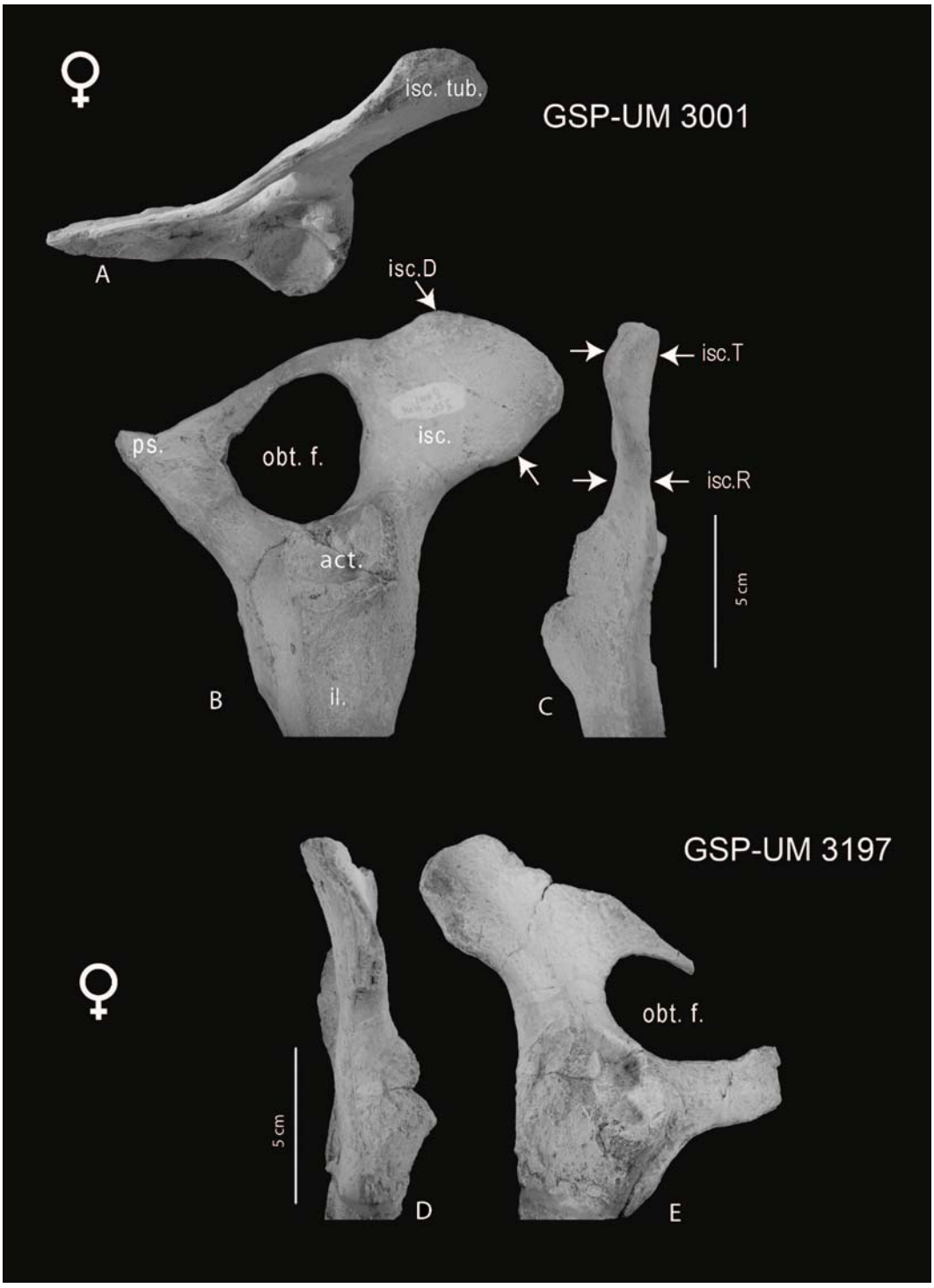
♀
isc. tub.
GSP-UM 3001
A
isc.D
isc.T
ps.
obt. f.
isc.
isc.R
act.
5 cm
B
il.
C
GSP-UM 3197
♀
obt. f.
5 cm
D
E

FIGURE 5.3. Posterior (A) and dorsal views (B) of the left innominate of a possible female of *Eotheroides clavigerum* (UM 101219); note the thinning and simplicity of the distal end of the ischium in both views and the small variation between the thickness of the ischial ramus and the bone's distal end (black arrows). Abbreviations: **act.,** acetabulum; **il.,** ilium; **isc.,** ischium; **isc.T,** ischium tuberosity thickness; **isc.R,** ischium ramus thickness; **isc. tub.,** ischiac tuberosity; **ps.,** pubis**; sac. il. artic.**, sacroiliac articulation surface.

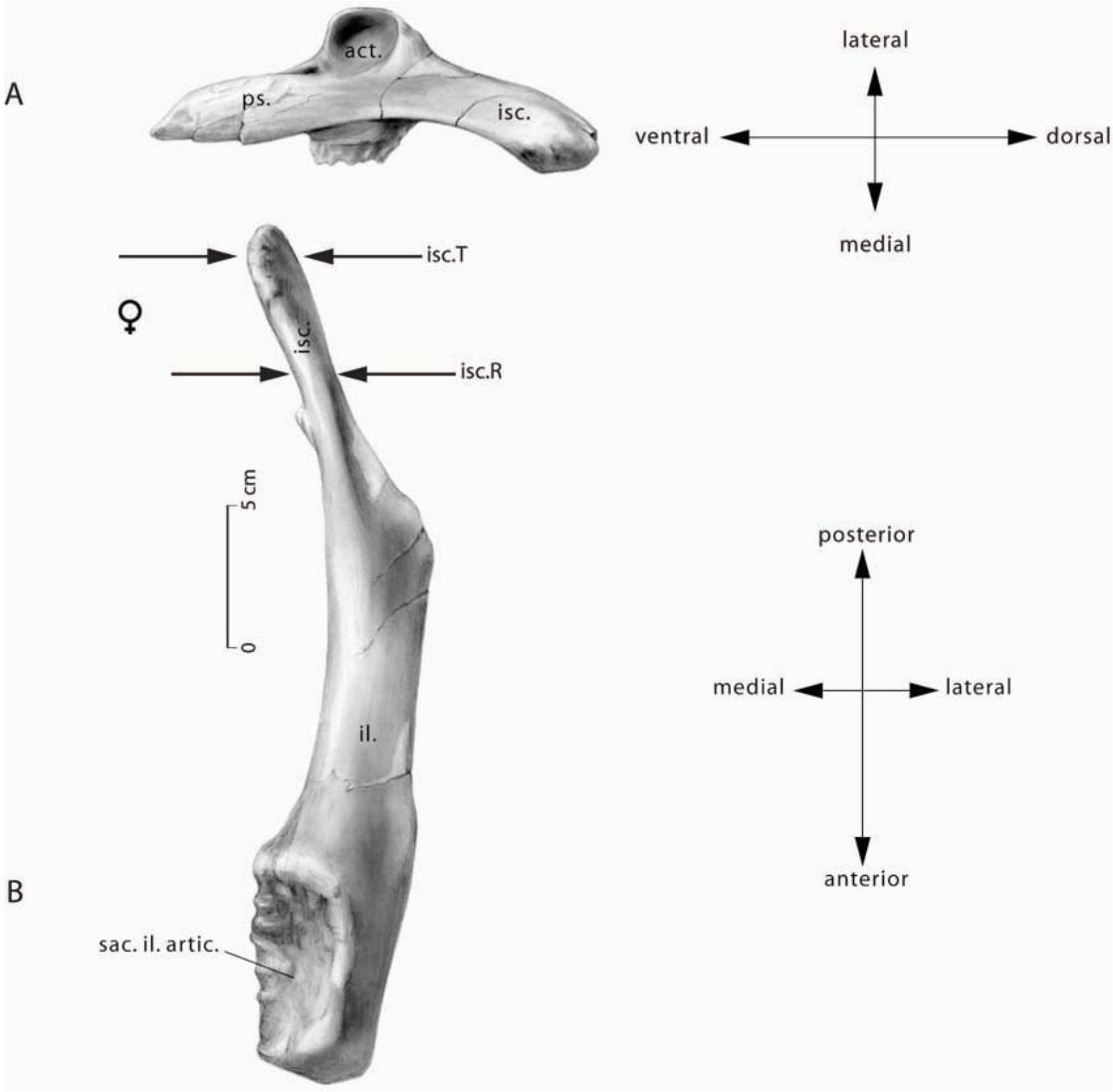

FIGURE 5.4. Posterior (A) and dorsal views (B) of the left innominate of a possible male of *Eotheroides sandersi* (UM 111558); note the expansion and thickening of the distal end. C and D, dorsal and lateral views, respectively, of the left pelvis of a possible female of *Eotheroides sandersi* (CGM 421981); the ischium here is thin and broad, lacking any tuberosity. Abbreviations: **act.,** acetabulum; **il.,** ilium; **isc.,** ischium; **isc.T,** ischium tuberosity thickness; **isc.R,** ischium ramus thickness; **isc. tub.,** ischiac tuberosity; **ps.,** pubis; **sac. il. artic.**, sacroiliac articulation surface.

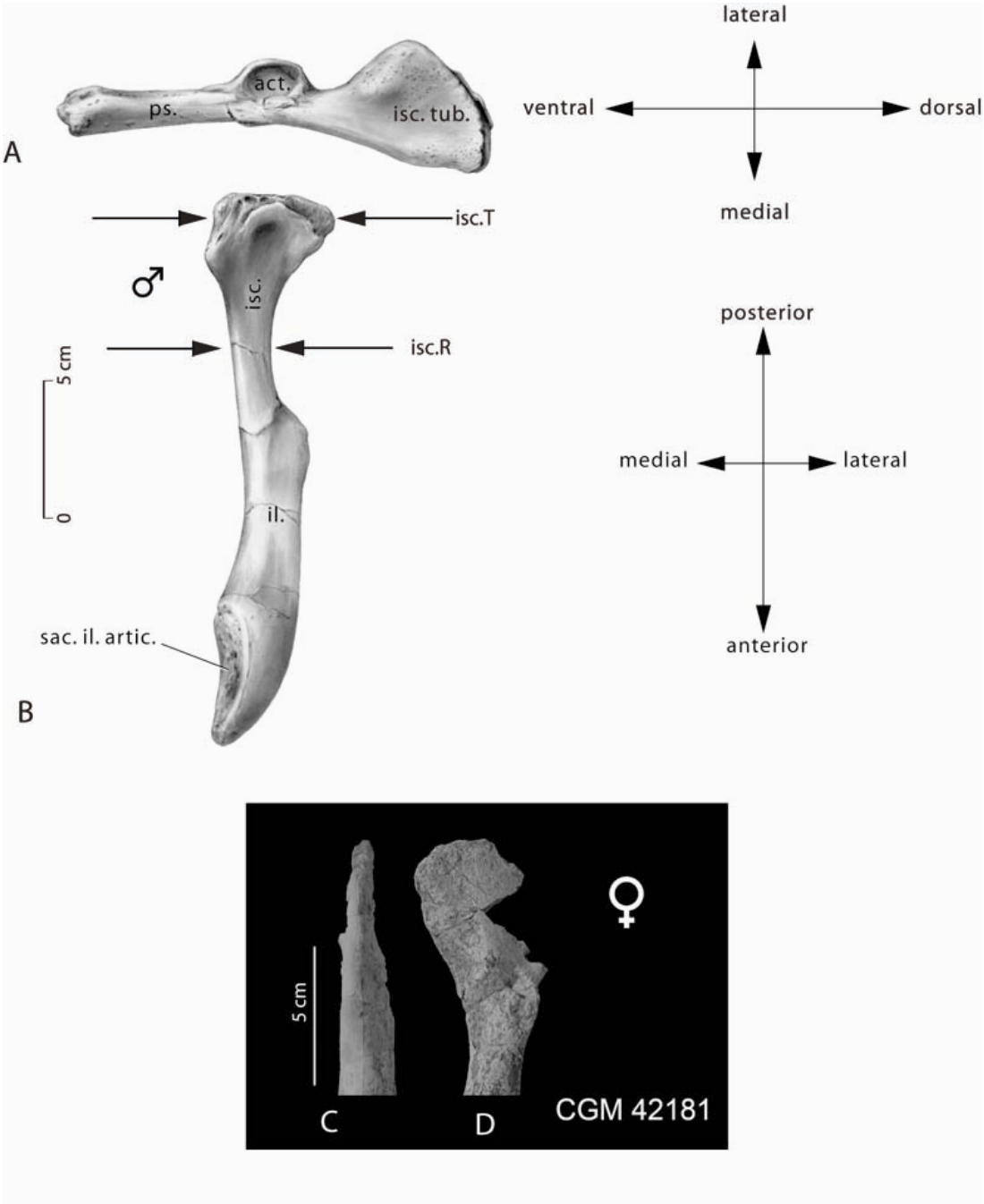

FIGURE 5.5. Posterior (A), lateral (B), and dorsal views (C) of the right innominate of a possible male of *Eosiren libyca* (UM 101226); note the expansion and thickening of the distal end. D, E, and F, posterior, lateral and dorsal views, respectively, of the right innominate of a possible young male of *Eosiren libyca* (CGM 29774); although the ischium is narrow dorsoventrally, it is thick mediolaterally. G, H, and I, dorsal, lateral and posterior views, respectively, of the left innominate of a possible female of *Eosiren libyca* (UM 101228); the ischium here is straight, rectangular, and conservative in mediolateral thickness from the ramus to its distal end. Abbreviations: **act.,** acetabulum; **il.,** ilium; **isc.,** ischium; **isc.D,** ischium tuberosity depth; **isc.T,** ischium tuberosity thickness; **isc.R,** ischium ramus thickness; **isc. tub.,** ischiac tuberosity; **obt. f.**, obturator foramen; **ps.,** pubis; **sac. il. artic.**, sacroiliac articulation surface.

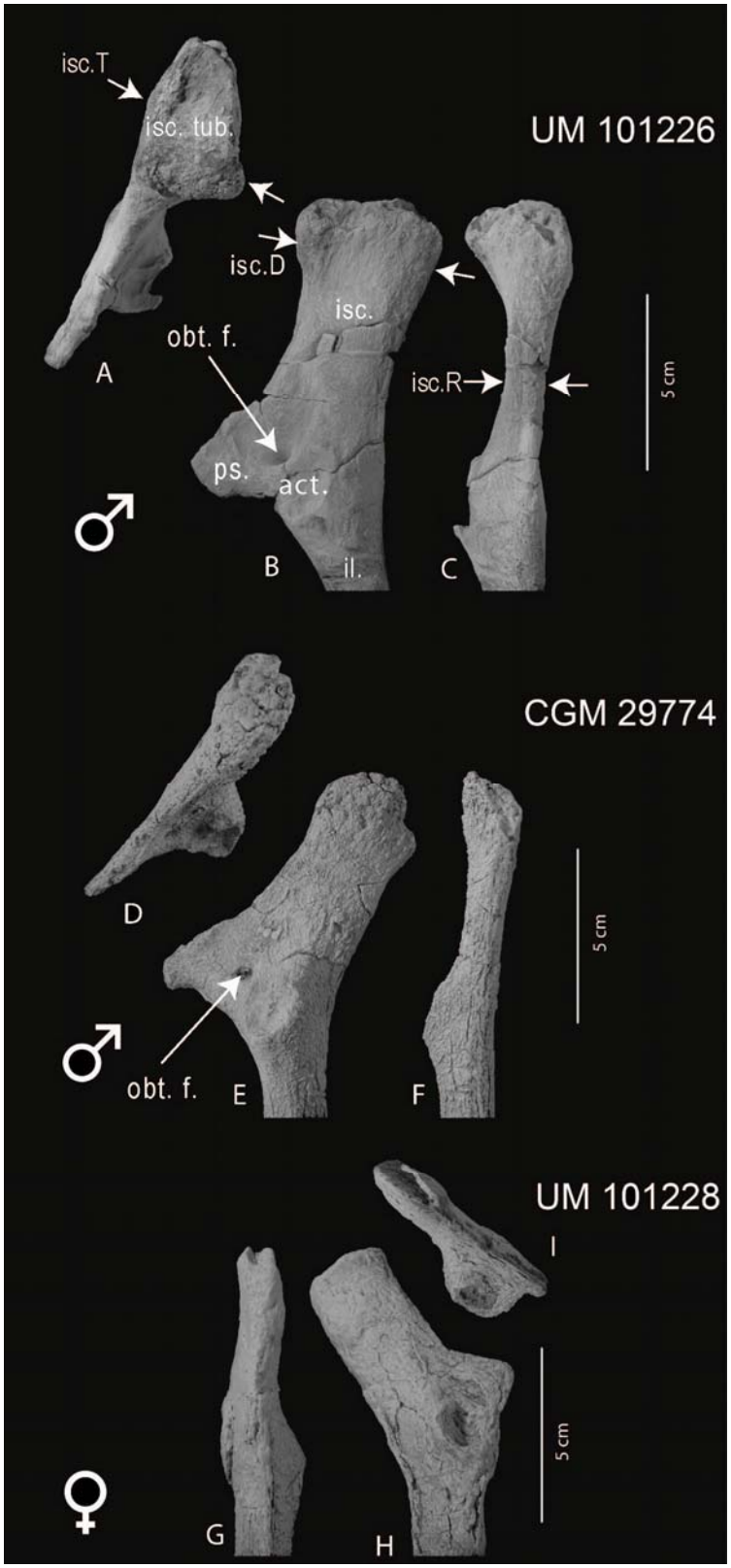
isc.T
isc. tub.
UM 101226
isc.D
isc.
obt. f.
A
isc.R
5 cm
ps.
act.
B
il.
C
CGM 29774
D
5 cm
obt. f.
E
F
UM 101228
I
5 cm
G
H

FIGURE 5.6. Sexual dimorphism in the pelvic bones of Eocene sirenians (*Protosiren, Eotheroides,* and *Eosiren*) presented here as interpreted from intraspecific variations between the mediolateral thickness of the ischial ramus (green squares) and its distal end (white diamonds). The difference between the thickness of the distal end of the ischium and the thickness of its ramus (red arrows) is significant in the putative males, while in females the difference is either small or zero. Sexual dimorphism is extreme in *Eotheroides sandersi* and *Eosiren libyca* as both males and females have clearly distinct ischial morphology in all studied pelves. Data are in Table 5.1.

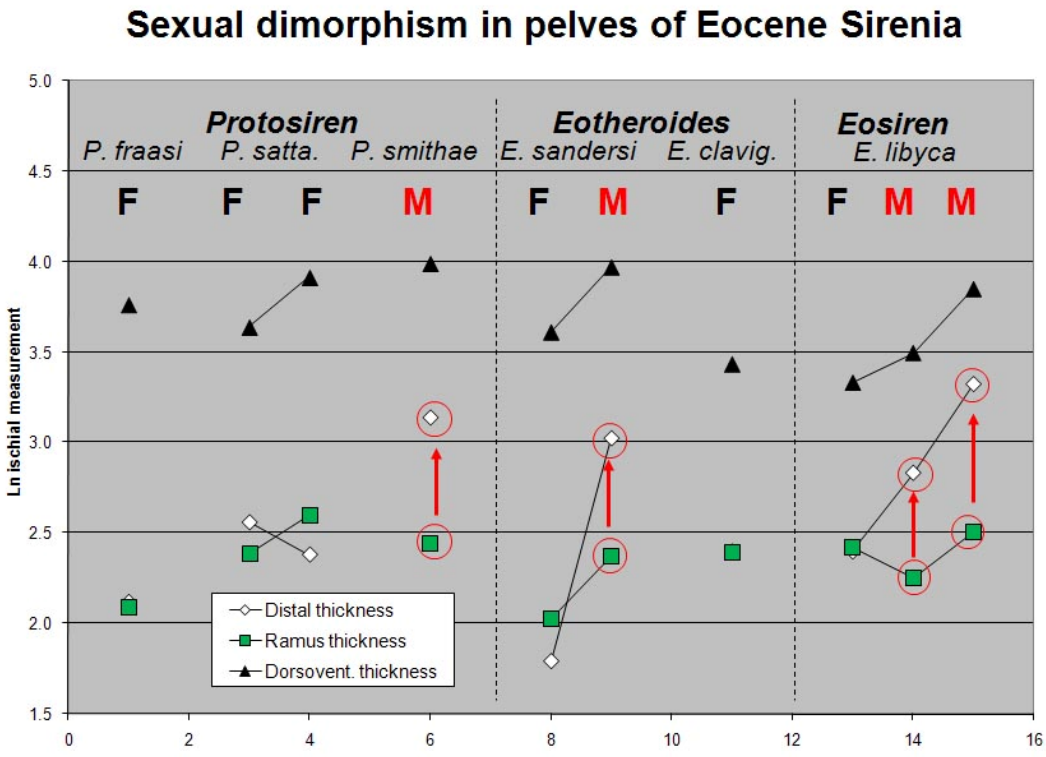

FIGURE 5.7. Sexual dimorphism in the pelvic bones of Eocene sirenians is presented as the ratio of the mediolateral thickness of the ischial ramus and its distal end. The general rule of thumb here is that the ratio of these numbers is about 2 in males and 1 or less in females.

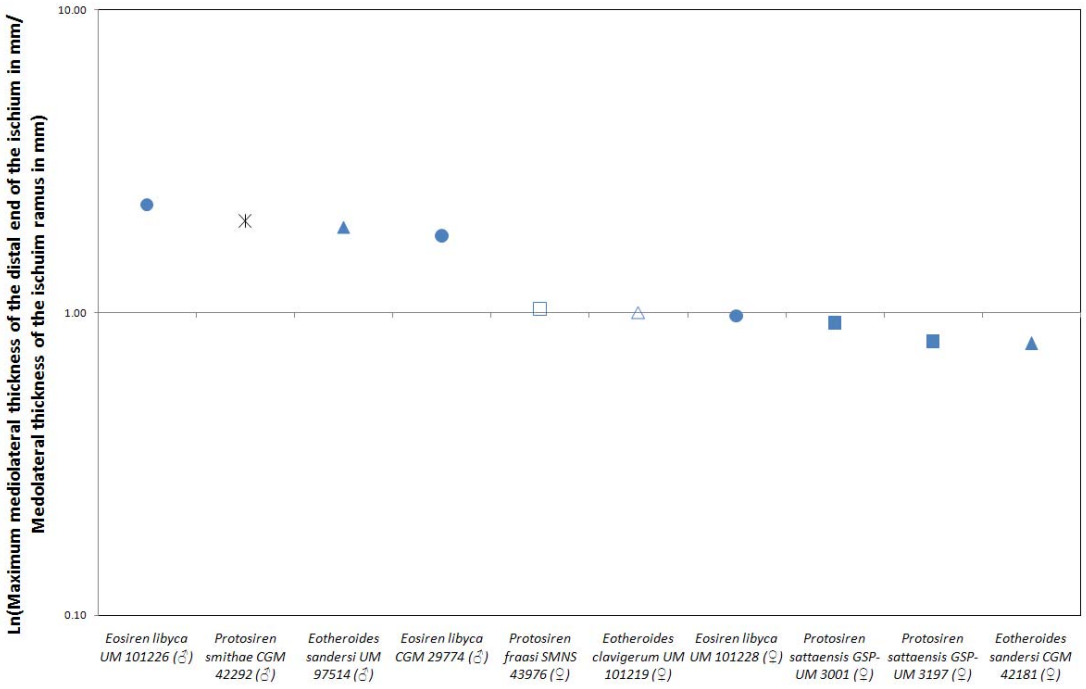

Literature Cited

ABEL, O. 1907. Die Stammesgeschichte der Meeressäugetiere. Meereskunde, 1:1-36.

ANDREWS, C. W. 1906. A Descriptive Catalogue of the Tertiary Vertebrata of the Fayum, Egypt. British Museum of Natural History, London, 324 pp.

ANDERSON, P. K. 2002. Habitat, niche, and evolution of sirenian mating systems. Journal of Mammalian Evolution, 9: 55-98.

ANDERSON, P. K. 1997. Shark Bay dugongs in summer I: A lek mating system. Behaviour, 134:443–462.

ANDREWS, C. W. 1902. Preliminary note on some recently discovered extinct vertebrates from Egypt. (Part III.) Geological Magazine, 9:291-295.

BERZIN, A. A. 1972. The Sperm Whale. (Translated from Russian). Israel Program of Scientific Translations, Jerusalem, 394 pp.

Bourlière, F. 1975. Mammals, small and large: the ecological implications of size. Pages 1-8 in F. H. Golley and K. Petrusewicz, eds. Small mammals: their productivity and population dynamics. Cambridge University Press, Cambridge.

BRADBURY, J. W 1977. Lek mating behavior in the hammerheaded bat. Zeitschrift für Tierpsychologie, 45:225-255.

DOMNING, D. P. 1977. Observations on the myology of *Dugong dugon* (Müller). Smithsonian Contribution to Zoology, 226:iii+57.

DOMNING, D. P. 1978. The myology of the Amazonian manatee, *Trichechus inunguis* (Natterer) (Mammalia: Sirenia). Acta Amazonica, 8(2), Supplement 1:1-81.

DOMNING, D. P. 1991. Sexual and ontogenetic variation in the pelvic bones of *Dugong dugon* (Sirenia). Marine Mammal Science 7:311-316.

DOMNING, D. P. and L. C. HAYEK. 1986. Interspecific and intraspecific morphological variation in manatees (Sirenia: *Trichechus*). Marine Mammal Science, 2: 87-144.

DOMNING, D. P., and H. THOMAS. 1987. *Metaxytherium serresii* (Mammalia: Sirenia) from the Early Pliocene of Libya and France: a reevaluation of its morphology, phyletic position, and biostratigraphic and paleoecological significance; pp. 205-232 in N. T. BOAZ, A. EL-ARNAUTI, A. W. GAZIRY, J. DE HEINZELIN, and D. D. BOAZ (eds.), Neogene paleontology and geology of Sahabi. Alan R. Liss, Inc, New York.

DOMNING, D. P., and P. D. GINGERICH. 1994. *Protosiren smithae*, new species (Mammalia, Sirenia), from the late Middle Eocene of Wadi Hitan, Egypt. Contributions from the Museum of Paleontology, University of Michigan, 29:69-87.

DOMNING, D. P., and P. PERVESLER. 2001. The osteology and relationships of *Metaxytherium krahuletzi* Deperet, 1895 (Mammalia: Sirenia) Abhandlungen der Senckenbergischen Naturforschenden Gesellschaft, 553:1-89.

DOMNING, D., and B. BEATTY. 2007. Use of tusks in feeding by dugongid sirenians: observation and tests of hypotheses. The Anatomical record, 290:523-538.

FAGONE, D. M., S. A. ROMMEL, and M. E. BOLEN. 2000. Sexual dimorphism in vestigial pelvic bones of Florida Manatees (*Trichechus manatus latirostris*). Florida Scientist, 63:177-181.

GINGERICH, P.D., D.P. DOMNING, C.E. BLANE, and M. UHEN. 1994. Cranial morphology of *Protosiren fraasi* (Mammalia, Sirenia) from the Middle Eocene of

Egypt: a new study using computed tomography. Contributions from the Museum of Paleontology, University of Michigan, 29:41- 67.

GINGERICH, P. D., M. ARIF, M. A. BHATTI, H. A. RAZA, and S. M. RAZA. 1995. *Protosiren* and *Babiacetus* (Mammalia, Sirenia and Cetacea) from the middle Eocene Drazinda Formation, Sulaiman Range, Punjab (Pakistan). Contributions from the Museum of Paleontology, University of Michigan, 29:331-357.

Hartman, D. S. 1971. Behavior and ecology of the Florida manatee, *Trichechus manatus latirostris* (Harlan), at Crystal River, Citrus County. Ph.D. Thesis, Cornell University, Ithaca, NY, 285 pp.

HÖGLUND, J. and R. V. ALATALO. 1995. Leks. Princeton University Press, Princeton, NJ, 248 pp.

KLEINENBERG, S. E., A. V. YABLOKOV, B. M. BELKOVICH, and M. N. TARASEVICH. 1964. Beluga (*Delphinapterus leucas*): Investigation of the species. Translated from Russian by Israel Program for Scientific Translations, Jerusalem, 1969. Akademii Nauk SSSR, Moscow, 376 pp.

KRAUSS, F. 1870. Beiträge zur Osteologie von *Halicore*. Archiv für Anatomie, Physiologie, und Wissenschaftliche Medecin, 1870:525-614.

KRAUSS, F. 1872. Die Beckenknochen des surinamischen *Manatus*. Archiv für Anatomie, Physiologie, und Wissenschaftliche Medecin, 1872:257-292.

LORENZ, L. V. 1904. Das Becken der Steller'schen Seekuh. Abhandlungen der Kaiserlich-Königlichen Geologischen Reichsanstalt (Wien), 19:1-11.

LÖNNBERG, E. 1910. The pelvic bones of some Cetacea. Arkiv für Zoologie, 7:1-15.

MARSH, H. 1980. Age determination of the dugong (*Dugong dugon* (Müller)) in northern Australia and its biological implications. Reports of the International Whaling Commission, (Special Issue 3):18 l-201.

MARSH, H., G. E. HEINSOHN, and T. D. GLOVER. 1984a. Changes in the ovaries and uterus of the dugong, *Dugong dugon* (Sirenia: Dugongidae) with age and reproductive activity. Australian Journal of Zoology, 32:743-747.

MARSH, H., G. E. HEINSOHN, and T. D. GLOVER. 1984b. Changes in the male reproductive organs of the dugong, *Dugong dugon* (Sirenia: Dugongidae) with age and reproductive activity. Australian Journal of Zoology, 32:721-742.

PERRIN, W. F. 1975. Variation of Spotted and Spinner Porpoise (genus *Stenella*) in the Eastern Pacific and Hawaii. Bulletin of the Scripps Institution of Oceanography, 21:1-206.

PREEN, A. 1989. Observations of mating behavior in dugongs (*Dugong dugon*). Marine Mammal Science, 5: 382-387.

RIHA, A. 1911. Das männliche Urogenitalsystem von *Halicore dugong* Erxl. Zeitschrift für Morphologie und Anthropologie, 13:395-422.

RALLS, K. 1976. Mammals in which females are larger than males. The Quarterly Review of Biology, 51:245-276.

RALLS, K. 1977. Sexual dimorphism in mammals: avian model and unanswered questions. The American Naturalist, 111:917-938.

ROMMEL, S. A. 1990. Osteology of the bottlenose dolphin; pp. 29-49 in R. R. REEVES and S. LEATHERWOOD (eds.), The Bottlenose Dolphin. Academic Press, San Diego.

SPAIN, A., and G. HEINSOHN. 1974. A biometric analysis of measurment data from a collection of North Queensland dugong skulls, *Dugong dugon* (Muller). Australian Journal of Zoology, 22: 249-257.

SPAIN, A., G. HEINSOHN, H. MARSH, and R. CORRELL. 1976. Sexual dimorphism and other sources of variation in a sample of dugong skulls from north Queensland. Australian Journal of Zoology, 24: 491-497.

STRUTHERS, J. 1893. On the Rudimentary Hind-limb of a Great Fin-Whale (*Balaenoptera musculus*) in Comparison with those of the Humpback Whale and the Greenland Right-Whale. Journal of Anatomy and Physiology, 27:291-335.

YOSHIDA, H., M. SHIRAKIHARA, A. TAKEMURA, and K. SHIRAKIHARA. 1994. Development, sexual dimorphism, and individual variation in the skeleton of the finless porpoise, *Neophocaena phocaenoides*, in the coastal waters of Western Kyushu, Japan. Marine Mammal Science, 10:266-282.

CHAPTER SIX

PALEOENVIRONMENTS AND PALEOECOLOGY

Paleoenvironments

Gingerich (1992) summarized the paleoenvironments of the Bartonian and Priabonian (middle and late Eocene) sedimentary formations in Wadi Al Hitan on the basis of sedimentological (sandstones and claystones intercalations and overlapping) and biological evidences (vertebrates and microvertebrate faunas).

Gingerich (1992) concluded that the Gehannam Formation was deposited in a shallow open marine shelf, and also clarified that the local exposure of the Gehannam Formation in Wadi Al Hitan is only a portion of a sedimentological belt that extends for several tens of kilometers roughly along the same latitude in northeast Africa (Egypt and Libya). Many fossil Marine mammal localities were found in the Gehannam Formation along the northern cliffs of the Fayum Basin (Beadnell, 1905; Gingerich, 1992). Each fossil locality produced along this formation is quantitatively and qualitatively distinct, implying that the deposition of the Gehannam Formation was along a diverse shallow environmental settings, especially in the transition zones to the Birket Qarun Formation.

New data coming form the lower part of the Gehannam Formation shows that abundant and diverse microfaunas, with significant proportions of planktonic foraminiferids (up to >60%), indicate outer neritic water depths and an open marine environment. Benthic foraminiferids are diverse and support this interpretation. At higher levels of this formation planktonic foraminiferids become rare, and benthic foraminiferids are less diverse, dominated by bolivinids and buliminids, suggesting shallowing and a somewhat restricted environment (*Chris King: personal communications 2008*).

Most of the sirenian fossils of Gehannam Formation are related to the family Protosirenidae and these were found in significant numbers in the middle part of this formation. Archaeocete whales are more abundant and diverse than sirenians, represented by a half dozen or so species ranging in size from 18 meters (*Basilosaurus isis*) to 4-5 meters (*Dorudon atrox*).

The Birket Qarun Formation in Wadi AL Hitan was investigated in detail by Gingerich (1992) as it produced most of the Priabonian vertebrate faunas found in northeast Africa. According to Gingerich (1992), variability in thickness, lithology, and distribution of the silisiclastic sediments of this formation gave it a distinctive geometry, with an outcrop belt exceeding 100 km stretching along a northeast-southwest axis and approximately 10-15 km wide along a southeast-northwest short axis. Gingerich also suggested that the thickness of the Birket Qarun Formation is on the order of 70 m at maximum near Wadi Al Hitan (see map in Figure 1.4), but thins rapidly perpendicular to the long axis of outcrop. This suggests that this formation was a part of an offshore sand barrier bar complex that was parallel to the shore line of ancient Tethys.

The rich marine mammal bearing beds of the Birket Qarun Formation include offshore sandstone bars resting on high sea stand deposits of fine sandstone with extensive bioturbation and trace fossil markers (Camp White Layer and its equivalents).

New information coming out of the Birket Qarun Formation indicates that most of the microfossils are decalcified, but samples collected from the upper part in a deep gulley in Minqar el Hut contain well-preserved microfaunas, with moderately diverse foraminiferids and ostracods. These indicate inner to mid-neritic water depths, and include planktonic foraminiferids. Associated fauna includes regular and irregular echinoids, bivalves and gastropods. These indicate normal salinity, well-oxygenated sea floor, moderate water depths and open marine connections not restricted or coastal (*Chris King: personal communications 2008*).

Sirenian fossils here are more diverse than in the Gehannam Formation as three species here found in the same formation. One of the very interesting sirenians found here is the heavy rib-cage *Eotheroides* that most probably survived in a water depth less than 10 meters.

The Qasr El Sagha Formation is extensively clastic with a strong terrestrial connection as indicated by the diverse terrestrial fauna in the quarries north of Birket Qarun (Lake Moeris). Vondra (1974) and Bown and Krause (1988) concluded that this formation was deposited in a deltaic and lagoonal setting as indicated by the large cross stratification sedimentary bodies and the low energy deep water muds and siltstones.

Paleoecology

Fayum marine mammals are found in several stratigraphic levels from the middle Lutetian to the end of the Priabonian, and sometimes at the base of the Oligocene. Patterns of abundance and preservation of these skeletons and partial skeletons are variable. The Lutetian Wadi El Rayan formations have a relatively poor fossil record from Fayum compared to the Bartonian and Priabonian marine mammal record of the Gehannam, Birket Qarun, and Qasr El Sagha formations in Wadi Al Hitan area where hundreds of skeletons of marine mammals are found. The reason why Wadi Al Hitan is unique and represents a vertebrate *Lagerstätte* is still not well understood. However, recognition of the sequence stratigraphy of this portion of the Eocene in Fayum and where it fits in the global stratigraphic framework is an essential task to establish a meaningful explanation for the abundance and preservation of the Wadi Al Hitan Marine mammal fauna (Peters et al., in press).

Eotheroides sandersi and *Eotheroides clavigerum* were found together at the base of the Birket Qarun along with *Protosiren smithae*; the middle and top part of the Birket Qarun produced *Eotheroides sandersi*. In Fayum, up to date, no *Eosiren* have been found in the Birket Qarun Formation as all *Eosiren* species are found either in the Qasr El Sagha Formation or the Lutetian of Mokattam Limestone; moreover, no *Protosiren* has been found above the lower third of the Birket Qarun Formation or in Qasr El Sagha Formation.

The coexistence of three species of sirenians (*Protosiren smithae*, *Eotheroides clavigerum*, and *Eotheroides sandersi*), that are morphologically and dentally different, in

the same biotope reflects the diversity of this group in the early Priabonian of the Fayum Basin.

This coexistence is similar to that which occurred in the Lutetian of the Mokattam Limestone where *Protosiren fraasi*, *Eotheroides aegyptiacum*, and probably ? *Eosiren abeli* overlapped in the same biotope. This trend in diversity is most probably achieved either by sharing niches and/or through food resource partitioning (for further discussion see Chapter Seven).

At any rate, sirenians from the Priabonian of Fayum (*Protosiren* and *Eotheroides*), along with Archaeocete whales (Gingerich, 1992), were found in fine siliciclastic sandstones and muds deposited along Tethyan shorefaces in a slightly restricted environment during a major highstand sea (Gingerich, 1992). This highstand lasted long enough for these marine mammals to flourish and interact with their paleocommunities in these shallow waters. Sediments of the Birket Qarun Formation contain many articulated and semi-articulated skeletons and partial skeletons of marine mammals. These sediments consist of an overall coarsening-upward succession of sands and muds that are themselves organized into a few meter-thick parasequences that generally coarsen upward into bioturbated fine sand and interfingered with muds and clays; this pattern and architecture of local environment is characteristics of lagoonal and estuarine environments (Gingerich, 1992).

Beside marine mammals (whales and seacows), the Wadi Al Hitan paleocommunities of invertebrates and vertebrates include: benthic and planktonic foraminiferas, mollusks (bivalves and gastropods), crabs, shrimps, and squids; selachian and bony fishes with a

wide range of sizes and with a diverse ecological and biological behaviors; snakes, sea turtles, crocodiles; and primitive elephants.

Of all the faunas associated with the marine mammals in Wadi Al Hitan, selachians (sharks and rays) are the most abundant and diverse group of fishes as their isolated teeth imply that there were at least three dozen of species living side by side with marine mammals.

The floral record is very rare from the Eocene of Wadi Al Hitan. Gingerich (1992), reported tree logs infected by *Teredo* shipworms, and some (?) mangrove root remains from the Camp White Layer and indicated that these are shallow or near shore in origin. Ichnofossils of flank-buttressed trees were reported from upper Eocene coastal deposits of the Qasr El Sagha Formation (Wing et al., 1995). These ichnofossils may represent terra-firma or mangrove forests that lived in a tropical climate and high water tables with low oxygen contents in the late Eocene (Wing et al., 1995, and Wing and Tiffeny, 1982).

The presence of seagrass remains is confirmed by blades of *Thalassodendron* sp. (Figure 6.1) that were found in the Birket Qarun Formation from above what is known as the Camp White Layer (CWL of Gingerich, 1992), and exactly from the same bed and locality of WH-074 (ZV-074) which produced *Basilosaurus isis* (UM 97507). The Qasr El Sagha Formation appears to be more diverse with its floral continents as it produced blades of *Thalassodendron* sp. and *Cymodocea* sp. (Figure 5.1) which were collected from the siltstones and mudstones associated with of the skeleton of *Eosiren libyca* (UM 101226), and possibly the same beds that produced the flank-buttressed trees of Wing et al. (1995). *Thalassodendron* sp. and *Cymodocea* sp. belong to the seagrass family Cymodoceacea which are flowering plants (see Phillips and Meñez, 1988; Green and

short, 2001) that appeared as early as the Late Cretaceous and were very common in the Tethyan Eocene (Ivany et al., 1990. This group of seagrass is significant as a water depth indicator because they are limited to water depths of less than 10 m where light and clarity are optimum for longevity and reproduction. This depth could be too shallow to consider as an ideal depth to support large marine vertebrates such as *Basilosaurus* and *Dorudon* who needed deeper water to swim in; however, this depth represent the lower margin at which nannoplanktons and benthic forams can exist.

Seagrasses recovered from the Eocene marine mammal bone beds of the Fayum Province addes another piece of information in reconstruction of the paleobiogeographic map of the Tethyan system and its connection with the Caribbean and North American shallow seas during the Eocene. Ivany et al. (1990) reported *Thalassodendron* and *Cymodocea* from the Eocene of Florida (Gulf of Mexico) from the same beds that produced sirenian remains; these seagrasses were colonized or partly encrusted with epiphytes and invertebrate larvae; this relationship between seagrass and microorganisms in the Eocene of North Africa has occurred in the red siltstone of the Qasr El Sagha Formation (Figure, 5.1). This may imply that these paleocommunities were more successful and widespread during the Eocene and may have been more dominant in shallow water than now due to the pattern of Tethys water circulation at that time.

FIGURE 6.1. Assorted Priabonian floral remains (potential sirenian diet) obtained while excavating marine mammal skeletons from Birket Qarun and Qasr El Sagha formation. **A,** *Thalassodendron* sp., seagrass blade found in a siltstone bed at locality WH-074 (ZV-74) where *Basilosaurus isis* (UM 97507) was excavated close to lower third of Birket Qarun and just above the Camp White Layer (CWL). **B,** *Thalassodendron* sp. and *Cymodocea* sp., seagrasses that were collected from sediments associated with *Eosiren libyca* skeleton (UM 101226) from Qasr El Sagha Formation, note that the long leaves of *Thalassodendron* sp. is encrusted by concentrations of epiphyte invertebrate (ep.ph.) microorganism and bryozoans. **C** and **D,** Leaf impression of aquatic plants (probable mangrove-like leaves) associated with Eosiren skeleton (UM 101226) from the Qasr El Sagha Formation.

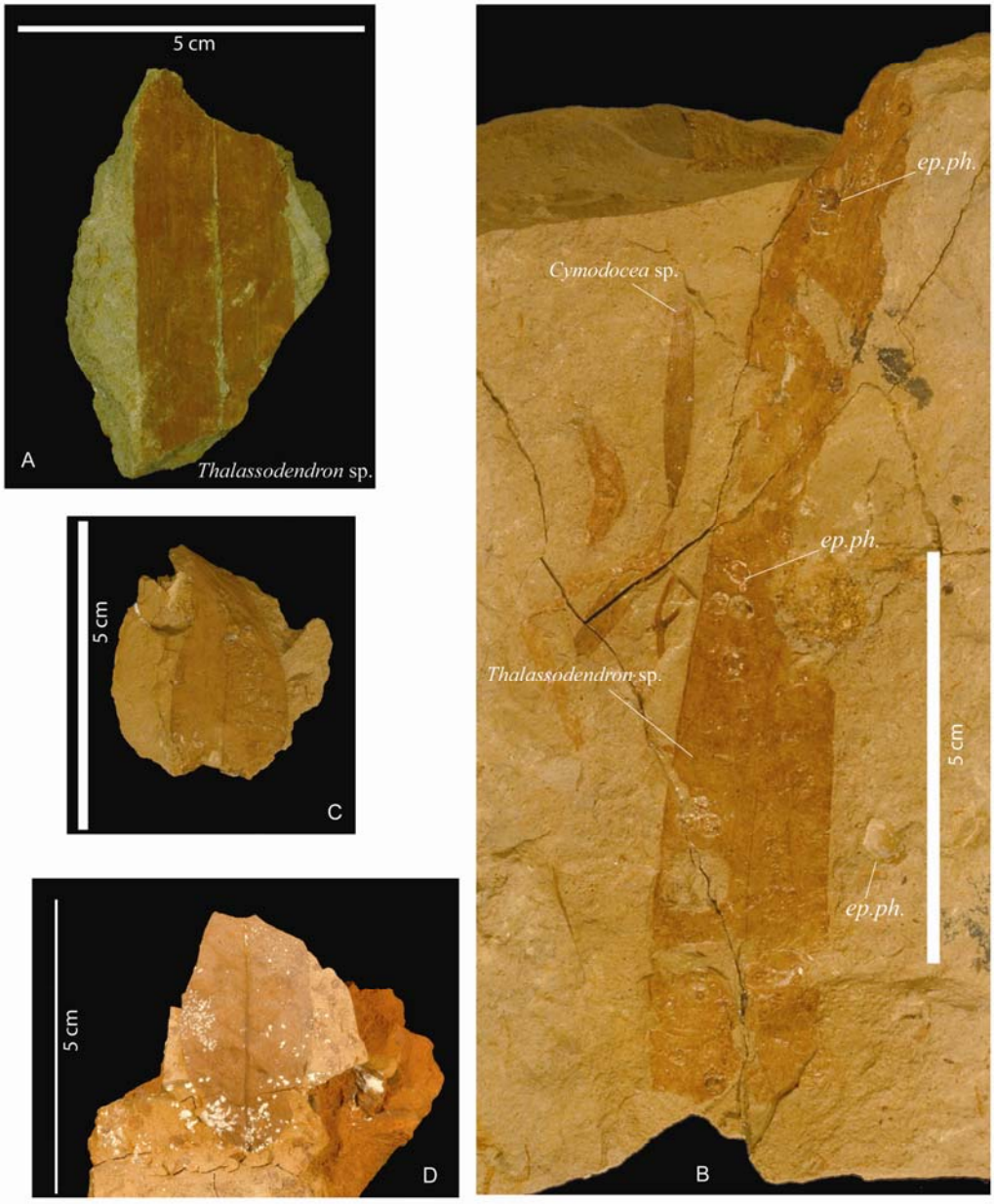
5 cm
A
Thalassodendron sp.
5 cm
C
5 cm
D
ep.ph.
Cymodocea sp.
ep.ph.
Thalassodendron sp.
5 cm
ep.ph.
B

Literature Cited

BEADNELL, H. J. L. 1905. The Topography and Geology of the Fayum Province of Egypt. Survey Department Egypt, Cairo, 101 pp.

BOWN, T. M., and M. J. KRAUS. 1988. Geology and paleoenvironment of the Oligocene Jebel Qatrani Formation and adjacent rocks, Fayum Depression, Egypt, United States Geological Survey Professional Paper, 1452:1-60.

GINGERICH, P. D. 1992. Marine mammals (Cetacea and Sirenia) from the Eocene of Gebel Mokattam and Fayum, Egypt: stratigraphy, age, and paleoenvironments. University of Michigan Papers on Paleontology, 30: 1-84.

GREEN, E. P., and F. T. SHORT. 2003. World Seagrass Atlas; in E. P. GREEN and F. T. SHORT (eds.). UNEP World Conservation Monitoring Centre, UCP, Berkely, 286 pp.

IVANY, L., R. W. PORTELL, and D. S. JONES. 1990. Animal-plant relationships and paleobiogeography of an Eocene seagrass community from Florida. Palaios, 5:244–258.

PHILLIPS, R. C., and E. G. MEÑEZ. 1988. Seagrasses. Smithsonian Contributions to the Marine Sciences, 34:104.

WING, S. L., and B. H. TIFFNEY. 1982. a paleotropical flora from the Oligocene Jebel Qatrani Formation of Northern Egypt: A preliminary report Miscellanous series of the Botanical Society of America, 162:67.

WING, S. L., S. T. HASIOTIS, and T. M. BOWN. 1995. First ichnofossils of flank-buttressed trees (late Eocene), Fayum Depression, Egypt. Ichnos, 3:281-286.

CHAPTER SEVEN

PALEOBIOLOGY OF THE EOCENE SIRENIA OF WADI AL HITAN

This chapter reveals the secondary features associated with adaptation to aquatic life in Wadi Al Hitan sirenians, and their swimming behavior and locomotion, and infers their feeding behaviors.

Secondary Adaptation to Life in Water

The fossil record of the earliest sirenian groups shows a gradual transition from more terrestrial ancestors with well developed hind limbs attached to a multi-sacral vertebrae to fully aquatic animals lacking hindlimbs, and bearing a single sacral vertebra and a tail modified to a fluke (Abel, 1907; Domning and Gingerich, 1994; Domning, 2001).

The extant sirenians are fully aquatic with morphologic and hydrostatic characteristics maintained as secondary adaptations to aquatic habitats. These morphological and skeletal characteristics include overall submarine or fusiform body shape, almost hairless and thick skin; large and mobile lips; short necks (short cervicals); forelimbs modified as flippers and hind limbs reduced to internal vestiges; and a tail modified into horizontal caudal fin for dorsoventral spinal undulation and paddling. Moreover, the body is stiffened by a subdermal connective-tissue sheath of helically wound fibers.

Cranially extant sirenians have deflected rostra, retracted nasal openings with nostrils always separated, and they lack paranasal air sinuses. The premaxillae are in contact with the frontals, the nasals are reduced in modern forms and sometimes fused with the frontals or totally absent, the supraorbital processes are heavy and prominent and lack postorbital bar, the skullcap is thick and heavy and made of the parietals that are fused into one piece with the supraoccipital. A sagittal crest is absent in almost all sirenians, however, a weak sagittal crest is present in *Pezosiren* (Doming, 2001b). The zygomatic process and the jugals are robust. To increase mastication abilities most sirenians posses strong deep pterygoids while early sirenians such as: *Prorastomus* and *Pezosiren* have small pterygoids. The infraorbital and mental foramina are large and directed anteriorly.

Sirenia is the only group of marine mammals that feeds extensively on coastal aquatic vegetation (seagrasses: angiosperms). The general dental formula of the most primitive forms of sirenians is 3:1:5:3 which is a synapomorphy for the order. The evolutionary history of their teeth indicates an increase in grinding capacity through heightened crowns (*Dugong*) or continuous replacement during forward migration of their functional teeth (*Trichechus*). Domning (2005: 86) stated that the presence of the large number of premolars with primitively long narrow rostrum and mandibular symphysis bearing parallel rows of incisors and canines suggests an early mechanism of intraoral food transport. However, in the latest Eocene or early Oligocene most forms (if not all) retained a broad rostrum and symphysis covered by horny pads, followed by loss of most of the anterior dentitions and permanent premolars except the first incisor that evolved into a tusk. The Miocene witnessed the first appearance of the large-bodied

Hydrodamalinae with edentulous jaws and keratinous rostral (masticating) pads that have interlocking ridges and grooves.

Sirenians has lost external ear pinnae, external auditory canal of the squamosal is very tiny and open ventrally, the tympanic is ring-shaped, and the ossicles are pachyosteosclerotic (thick and dense) and the largest and heaviest of any mammal. The tympanic sac (a membranous enclosure) is extended between the basicranium, pterygoid process, petrosal, and the well-ossified and drop-like ectotympanic ring. The external auditory meatus is a blind sac which is not connected to the tympanic membrane (Fischer and Tassy, 1993). Unlike *Prorastomus*, all other sirenians have their periotic unfused with the skull (Savage et al., 1994; Domning, 2001b).

Postcranial characteristics played a great factor in secondary adaptation and hydrostatic capabilities of this group in water: such characteristics include the compressed (or fused) cervical vertebrae. For instance *Trichechus* has six cervicals, while all other sirenians have seven cervicals like most mammals.

Sirenians have an elongate thorax and lungs with horizontal diaphragm (Domning 1977, 1978; Rommel and Reynoldas, 2000). There are fourteen to twenty-one thoracic vertebrae, followed by one to five lumbars, one to four sacrals (as in *Dugong* and *Prorastomus*, respectively), and eighteen to thirty-five caudal vertebrae. In quadrupedal forms (*Pezosiren*) there are four lumbars, and four fused sacrals, and about twenty caudals. *Protosiren* had nineteen thoracic vertebrae, one pre-lumbar, four lumbars, one sacral, and more than eighteen caudal vertebrae. *Dugong* has nineteen thoracic vertebrae, four lumbars, one sacral, and up to twenty-seven caudals. *Trichechus* has the most reduced number of vertebrae, the reduction in the cervicals is followed by a series of

reductions in the rest of the trunk: fourteen thoracics, two lumbars (the lowest of them is the sacrum, identified by the discrete ligament attached to the flat and reduced pelvis as seen in USNM 217259), and about twenty-three caudals. Manatees have a rounded tail, while *Dugong dugon* (the Indian Ocean and Australian sea pig), which differs from *Trichechus manatus* in being a faster swimmer and diver, has a strong fluke (Home, 1821). The muscle cutaneous trunci or the panniculus carnosus is greatly enlarged and partly inserts on the chevrons of the caudal vertebrae (Domning, 1978).

Sirenian ribs are of great interest because they constitute one of the key characters of the group. They show either osteosclerotic (dense and compact bone) or pachyosteosclerotic (thickened or swollen compact bones) (Kaiser 1966; Domning and De Buffrénil, 1991; and Rommel and Reynolds, 2000). *Dugong*, *Protosiren*, *Pezosiren,* *Prorastomus,* and *Eosiren* have osteosclerotic ribs, while *Trichechus*, *Eotheroides*, and to some degree *Prototherium* have pachyosteosclerotic ribs. The sternum is connected to two to five pairs of ribs. No sirenian taxon has a clavicle (Fischer and Tassy, 1993).

Scapulae of prorastomids are broad, not sickle-shaped as in Eocene Protosirenidae and Dugongidae. In *Dugong* and *Trichechus* the scapulae are thin, broad, and fan-shaped. Humeri are rounded and robust, radius and ulna have rounded cross section as well and sometimes are fused together. The manus is paddle-like, the carpals are arranged serially, the first digit is reduced and the fifth is enlarged and divergent (Domning, 1978, 2001, 2005).

The pelvic girdle of Prorastomidae and Protosirenidae was functional and was connected to either a multi-vertebrae sacrum (*Pezosiren*) or to a single sacral vertebra as in *Protosiren*. Dugongidae pelvic girdles (*Eotheroides*, *Eosiren*, *Prototherium*, and

Halitherium), are vestigial and connected to a single sacral vertebra. The pelvic girdle of the living *Dugong* is reduced to a slender hip bone attached to the sacral vertebra by a cartilaginous ligament. In manatees the sacrum is a small, triangular, flat bone attached to the lumbo-sacral region by a long ligament. It floats ventrolaterally in the abdomen. The sirenian femur in post-Eocene forms is very reduced and presumably functionless. *Pezosiren* and *Protosiren*, based on the size and form of their femora, had fully functional hindlimbs, either for carrying and supporting the body or for swimming and paddling. The femur in manatees is a small bone fused to the flat pelvis. Except for the Jamaican Eocene Sirenia, hands and feet of living and fossil sirenians are very similar; carpals metacarpals, tarsals and metatarsals are rounded; however, Domning (2001) showed that these elements in Prorastomidae are more flattened than in other Eocene relatives.

The Wadi Al Hitan sirenians are grouped into two major Families, Protosirenidae and Dugongidae. Morphological and dimensional characteristics of skeletal and cranial elements of both families show that they were fully aquatic mammals, and both were specialized in different swimming modes.

Protosirenidae, typified here by *Protosiren smithae*, shows the following secondary aquatic characters: osteosclerotic cranial and postcranial elements; slight rostral deflection; reduced nasals; short cervicals, increased length of the of thoracic-lumbar region; sacrum reduced into a single vertebra; increased robustness in proximal tail vertebrae with strong chevrons; widening of the neural canal in thoracic and lumbar vertebrae (key-hole shaped); unusually long spinous processes from the seventh cervical (C7) through the second caudal (Ca2) including the sacrum; ribs slender and lacking synovial joints and connected to the vertebrae through cartilage; forelimbs reduced and

form a flipper or hydrofoil; pelvic girdle composed of complete and functional hindlimb (including femur, tibia, fibula); pelvis with long symphysis; ilium long, rod-like with a triangular cros-ssection, obturator foramina still wide-open; femur with large head, lesser and greater trochanter, but third trochanter absent, and distal end of the femora with wide and developed (active and functional) condyles; tibia and fibula robust and rounded, not fused.

Dugongidae, as typified by *Eotheroides* from the Wadi Al Hitan and *Eosiren* from Qasr El Sagha, show variable degrees of osteosclerosis and pachyosteosclerotic cranial and postcranial elements; strong rostral deflection; nasals reduced but still elongate; short cervical; 17-19 (up to 20 in Protosirenidae) thoracic vertebrae and up to 4 lumbars (4-6 lumbars in Protosirinade); reduction of sacrum into single vertebra as in Protosirenidae; robust proximal tail vertebrae with strong chevrons; anterior ribs pachyosteosclerotic (extremely swollen in all *Eotheroides*), connected to vertebrae through real synovial joints; forelimbs reduced and flipper-like pelvis reduced; ilium varies from slender rod-like (ex., *Eosiren libyca*) to club-like (*Eotheroides*), and the obturator foramen diminutive or closed; tibia, fibula, and pes unknown.

In order to emphasize cranial and postcranial variations in Eocene sirenians of Egypt some representative measurements were selected to assess the dimensional characteristics of the functional regions in Dugongidae and Protosirenidae (Tables 7.1 through 7.14) (Figures 7.1 through 7.14).

Protosirenidae, when compared to Dugongidae, have the least deflect premaxillary rostrum (Figure 7.1); narrowest infraorbital foramen (Figure 7.2); the least width between both pterygoid processes (Figure 7.1); longest parietals along midline; the widest

masticating surface (Figure 7.1); widest mesorostral fossa (Figure 7.1); longest frontoparietal suture-contact (Figure 7.1), widest breadth across the supraorbital processes (Figure 7.1); heights neural spines (Figure 7.4); largest vertebral canals, largest and longest infraspinous fossa of scapula (Figures 7.8,9, and 10), deepest glenoid cavity (Figure 7.8); widest bicipital grove of humerus (Figure 7.9); shallowest olecranon and anconeal process (Figure 7.10); pelves (Figure 7.11) with longest iliae, largest acetabulae, largest obturator foramina, longest ischial processes; femora are the longest (Figure 7.12), widest anteriorly and posteriorly, midshaft wide mediolaterally, and have largest patellar articulation surface among sirenians; longest and widest fibulae and tibiae (Figure 7.13).

The Eocene dugongs of Egypt have largest rostral deflection (Figure 7.1); widest infraorbital foramina (Figure 7.1); longest nasal contacts along midline (Figure 7.1); longest jugals (Figure 7.1); infraspinous fossa lacks deflection (such deflection presents in all Protosirenidae scapulae); ulnae (Figure 7.10) with deepest olecranon and anconeal processes, and widest coronoid processes; pelves (Figure 7.11) short with reduced lengths of iliae and ischia associated with extreme reduction in pubis and pubic symphysis, acetabulum shallow and small, obturator foramen is very reduced; femora (Figure 7.12) shorter than Protosirenidae with small heads, proximal trochanters absent, narrow proximal and distal ends; tibia and fibula very reduced.

Locomotor Behavior

Cranial and skeletal modifications in *Protosiren* were of a great advantage to swimming and adaptation in water. Because a complete tail or elements from the posterior portion of the tail are unknown, the details of Protosirenidae swimming

behavior is still unclear; however recovery of complete cervical, thoracic, lumbar and sacral series (Figures 7.4 and 7.5) with complete spinous processes with well preserved landmarks, chevron bones, and complete anterior and posterior limbs were in contributing to reconstructing their possible swimming mode. Domning and Gingerich (1994) concluded that *Protosiren smithae* was an amphibious animal that supported itself by well developed fore- and hindlimbs and high neural arches of the anterior thoracic vertebrae. Moreover, they suggested that it was a divergently specialized form of early sirenian and less aquatic than contemporary primitive dugongs. *Protosiren* with its sacral morphology seems to be more aquatic and less primitive than *Prorastomus sirenoides* (described by Owen, 1855, and later by Savage et al., 1994) and *Pezosiren portelli* of Jamaica (Domning, 2000 and 2001). According to Thewissen and Domning (1992), Savage et al. (1994), Domning and Gingerich (1994), Domning (2000, and 2001), these Caribbean Eocene Prorastomidae may have been capable of walking and lifting their body off the ground. *Protosiren* had a pelvic girdle connected to a single sacral vertebra, and hindlimbs were probably functional in shallow waters. Although the acetabular joint for the femoral head is well developed, the morphology of the mono-vertebral sacrum as well as its transverse process connecting to the ilium imply that *Protosiren* was not a quadrupedal land animal, but may have walked on the bottom. However, the long spinous processes, and long lumbar vertebrae, prolongation of the zygapophyses, and the robustness of the anterior caudal vertebrae imply that *Protosiren* dorsoventrally undulated while swimming and was aided by alternation of hindlimbs, paddling and maybe fluke oscillation.

Ribs (Figure 7.7) and sternal elements in *P. smithae*, along with their unique morphology, were working as a unit that conducted the mechanisms of breathing and buoyancy in a manner different from those of sirenians that appeared in the post-Eocene. Ribs and sternal components of *Protosiren* lack pachyostosis, but at the same time retain osteosclerosis (Domning and de Buffrénil, 1991). Moreover, connections between rib heads and thoracic vertebrae are more controlled by ligamentous (cartilage) connective tissues rather than synovial articulations; and overall the narrow, block-like sternae are similar to those of terrestrial mammals. The characteristics of ribs and sternal elements of *Protosiren* were able to keep the ribcage articulation with the spinal column in more flexible mode and essentially mobile than those in *Eotheroides* and *Eosiren*. The ribcage (including the narrow sternum and the thoracic vertebrae) enabled a large excursion of air that maintained the constant differential pressure needed for changing water depth under.

The forelimbs of *P. smithae* probably functioned in a manner similar to any other sirenian. However, the extended olecranon process, which is unusual, and the convex posterior side of the ulna, imply that the forelimbs may have been engaged in more active work than digging roots of seagrasses - perhaps in lifting the front of the body and providing more thrust at take-off and during swimming.

In Eocene dugongs (*Eotheroides* and *Eosiren*), the structure of the vertebral column is not different from those of the living ones; they both have short cervicals, 17-19 thoracics, 4 lumbars, a single sacral, and 20-24 caudal vertebrae (Figures 7.3, 7.5, and 7.6). The lumbar region in both Eocene and Recent dugongs is longer than those in manatees and almost the same as in *Protosiren*. Moreover, pre- and post-zygapophyses of the lumbar and anterior caudal vertebrae are projected and extended beyond the

centrum borders; posterior caudal vertebrae are dorsoventrally compressed suggesting that Eocene dugongs retained a fluke at the end of their tail similar to those of recent forms (Figure 7.6). This vertebral arrangement and configuration suggests that dorsoventral undulation and associated caudal oscillation was the swimming mode of *Eotheroides and Eosiren*.

How fast were these animals compared to the recent dugong "*Dugong dugon*" is a relative question especially when it comes to *Eotheroides* with its pachyosteosclerotic ribs. While *Dugong* can cruise at 9 km/ h (Jarman, 1966) and can double or triple this speed at fleeing, manatees can swim only at 0.2-4 km/h (Kojeszewski and Fish, 2007), although they may be somewhat faster during migration (see Reid, 1996). *Protosiren* and *Eosiren*, with their osteosclerotic rib structure, probably swam as fast as *Dugong*, while *Eotheroides* may have been slower than *Dugong dugon* and other the Eocene forms because of the heavy weight placed in their anterior ribcages, suggesting uneven distribution of lungs inside their ribcage. However *Eotheroides* was almost certainly faster than manatee (*Trichechus manatus*), and did not follow the same swimming techniques that manatees use today. The advantage of pachyosteosclerosis in anterior thoracic ribs of *Eotheroides* may be in offsetting the excess weight produced in the anterior half of the body to adjust the center of gravity and maintain buoyancy while feeding and submerging in water with depths of less than 10 meters (Domning and de Buffrénil, 1991; Domning, 2000).

Feeding Behavior

Degree of rostral deflection, tooth morphology (Figure 7.14), pattern and form of dental wear, degree of pelvic and hindlimb reduction, are all different in the sirenian

species from both the Birket Qarun and Qasr El Sagha formations. This implies that these animals may have used different procedures in acquiring food and were adapted to different habitats (see Domning, 2001a, for a model based on the Cenozoic Caribbean Sirenia).

Protosiren has a weak to moderate rostral deflection within the range that is seen in living rostral *Trichechus*. Manatees consume a wide spectrum of submerged, emergent, floating, and shoreline vegetations; *Protosiren* probably was exposed to a wide spectrum of vegetations too and likely fed on bottom and surface float vegetations as they lived in a shallow marine environment. A broad dietary may be led to the development a larger tooth crown on both spacious the palate and the mandibles (Domning and Gingerich, 1994). Moreover, the bifid spinous processes of the posterior cervicals and anterior thoracic vertebrae in the holotype of *Protosiren smithae* (Domning and Gingerich, 1994, figs. 5 and 6) may have allowed more space for muscle attachment to support the back of the skull while feeding on the surface.

On the other hand *Eotheroides and Eosiren*, have a considerable rostral deflection that may reach more that 50°. This deflection may reach 70° in living dugongs according to (Domning, 1977; Domning et al., 1982). Also the Eocene dugongs retained two small tusks often with their tips worn out as seen in *Eotheroides clavigerum* (UM 101219). These Eocene dugongs most certainly grazed on seagrass meadows and mangrove leaves as both leaf types were found in the Birket Qarun and Qasr El Sagha formations, and from the same beds where these dugongs were collected.

In an attempt to document part of the aquatic behavior of the marine mammals in the Tethyan Eocene, Clementz et al.(2006) analyzed the dental enamel of three species found

in the Birket Qarun Formation for their oxygen and carbon isotopic signatures. Based on the oxygen isotope values, *Protosiren smithae* and *Eotheroides clavigerum* are typical of those animals that feed in estuary or marine ecosystems, while *Eotheroides sandersi* may represent a species that ventured into fresh water, which is a behavior that is noticed in today's *Dugong dugon*. The carbon isotope values extracted from the enamel of these sirenians indicates that they are at least 11% higher than of terrestrial mammals from the Qasr El Sagha and Jabal Qatrani formations; this high value of δC^{13} (between 0‰ and -2.8‰) is in the range of the δC^{13} of the Recent *Dugong dugon* (between -6‰ and 1.7‰, data from MacFadden et al., 2004), and implies that the only source of C4 involved in the sirenian diet is of marine source and most probably related to the available seagrass beds in both the Birket Qarun and Qasr El Sagha formations. Other aquatic herbivorous mammals (*Moeritherium* and *Barytherium*) that lived in the Fayum during the Priabonian and are found in the same formations that produced marine mammals, have low δC^{13} values as illustrated by Liu et al. (2008) and Clementz et al., (2008); these mammals were fresh water restricted mammals and mostly fed on river and deltaic vegetations.

Similar oxygen and carbon isotope analysis from different Eocene sirenian teeth from North America (MacFadden et al., 2004) shows that the δC^{13} of the North American *Protosiren* is very high (between 1.9‰ and 4.1‰) and it was interpreted as a strictly seagrass feeder.

Dental size and morphology of sirenian teeth (Figures 7.15, and Tables 7.14) show that Protosirenidae has almost uniform tooth size but with great variability in shape, (some individuals show different tooth size on left and right sides). which may be interpreted as irregularity in grazing or feeding behavior. In Dugongidae tooth size and

shape are variable at both the species and generic levels. *Eotheroides aegyptiacum* has the smallest tooth size among Egyptian sirenians, while *Eotheroides sandersi* and *Eotheroides clavigerum* have larger teeth that increase in size distally. Teeth of *Eosiren libyca* seem to have the same size and shape patterns of later *Eotheroides*, while *Eosiren stromeri* has larger tooth surfaces, most notably M^2 which is considerably larger than M^1 and M^3 (Figure 7.14).

TABLE 7.1A. Measurements of cranial elements the Egyptian Eocene sirenians known to date. All measurements are in mm, except RD was measured in degrees. Measurements follow after Domning (1978). See appendix for key to the measurements.

Measurements	Abb.
Condylobasal length	**AB**
Height of jugal below orbit	**ab**
Length of premaxillary symphysis	**AH**
Rear of occipital condyles to the anterior end of interfrontal suture	**BI**
Zygomatic breadth	**CC'**
Breadth across exoccipitals	**cc'**
Top of supraoccipital to ventral sides of occipital condyles	**de**
Length of frontals, level of tips of supraorbital processes of frontoparietal suture	**F**
Breadth across supraorbital processes	**FF'**
Breadth across occipital condyles	**ff'**
Breadth of cranium at frontoparietal suture	**GG'**
Width of foramen magnum	**gg'**
Length of mesorostral fossa	**HI**
Height of foramen magnum	**hi**
Width of mesorostral fossa	**JJ'**
Maximum height of rostrum	**KL**
Posterior breadth of rostral masticating surface	**MM'**
Anteroposterior length of zygomatic-orbital bridge of maxilla	**no**
Length of zygomatic process of squamosal	**OP**
Anterior tip of zygomatic process to rear edge of squamosal below mastoid foramen (length of the squamosal)	**OT**
Length of parietals, frontoparietal suture to rear of external occipital protuberance	**P**
Anteroposterior length of zygomatic process of squamosal	**QR**
Maximum width between labial edges of left and right alveoli across M^1	**rr'**
Length of cranial portion of squamosal	**ST**
Breadth across sigmoid ridges of squamosals	**ss'**
Dorsoventral thickness of zygomatic-orbital bridge	**T**
Anterior breadth of rostral masticating surface	**tt'**
Height of posterior part of cranial portion of squamosal	**UV**
Dorsoventral breadth of zygomatic process	**WX**
Maximum width between pterygoid processes	**yy'**
Length of jugal	**YZ**
Length of frontals in midline	**LFr**
Height of supraoccipital	**Hso**
Width of supraoccipital	**Wso**
Height of infraorbital foramen	**HIF**
Width of infraorbital foramen	**WIF**
Deflection of masticating surface of rostrum from occlusal plane (degrees)	**RD**

TABLE 7.1B. Measurements of cranial elements of *Eotheroides* and *Protosiren* species. All measurements are in mm; see appendix for key to the measurements.

Abb.	*Eotheroides clavigerum* UM 101219	*Eotheroides sandersi* UM 111.58	*Eotheroides aegyptiacum* SMNS St. III	*Protosiren fraasi* CGM 10171	*Protosiren fraasi* SMNS 10576 St. V	*Protosiren smithae* CGM 42292
AB	335	309		378	318	350
ab	37	37		46	47	55
AH	112	97		108	62	70
BI	182	194	180	186	196	224
CC'	187	142		172		185
cc'	104	95	72	132	108	136
de	103	92	79	105	89	114
F	126	120	85	104	105	106
FF'	107	82	89	92	112	139
ff'	73	65	54	83	59	80
GG'	44	50	49	58	58	92
gg'	32	32	26	37	26	39
HI	78	69		80	85	112
hi	25	25	26	23		44
JJ'	39	37		48	47	52
KL	65	56		45	48	53
MM'	43	42		57	51	77
no	65	53	52	60	52	55
OP	98	88		96		98
OT	120	117		126		132
P	62	56	78	110	86	100
QR	47	35	34	34	40	40
rr'	70	59	57	85	75	81
ST	78	57		73	77	76
ss'	147	126	106	136		136
T	18	12	15	13	13	14
tt'	28	25		37		38
UV	92	77	72	81	68	85
WX	38	34		32	38	43
yy'	38	41	29	21		21
YZ	177	133		131		140
LFr	123	88	57	72	54	87
Hso	53	50	41	55	42	57
Wso	69	68	55	77	85	94
HIF	27	30	20	14	10	15
WIF	19	20	11	10	7	10
RD	50	49		30	40	40

TABLE 7.1C. Abbreviations of measurements of cranial elements of *Eosiren* species. All measurements are in mm; see appendix for key to the measurements.

Abb.	*Eosiren stromeri* SMNS	*Eosiren stromeri* UM 100137	*Eosiren libyca* CGM. 10054	*Eosiren libyca* ST. XIX	*Eosiren libyca* MNHN 1913-22	*Eosiren libyca* BMNH M10910
AB		350	305			
ab		40		41	50	
AH	119	90	96	120	106	118
BI	217	240				
CC'		160		166	166	164
cc'	104	104	99			
de	104	101	111			
F	129	100		120	97	
FF'	124	118	89		108	105
ff'		66	74			
GG'	60	53	54	43	55	55
gg'	35	31	33			
HI			71	96	75	91
hi	35		23			
JJ'			31	45	41	42
KL	68	75	59	74	58	66
MM'	63	44	44	55	43	42
no		64	50	66	52	65
OP	110	112		100	96	104
OT		138			130	
P	71	96	65	82	96	82
QR		43		46	40	
rr'	88	58	40	61		
ST		82			75	
ss'	149	123				
T		12		17	11	
tt'	35			31	29	23
UV		87			86	
WX	49	37		38	37	45
yy'		24		51		
YZ					147	
LFr	107		89	105	89	95
Hso	43	51		46	55	
Wso	82	70	59	67	65	72
HIF			16	22	20	21
WIF			13	18	18	18
RD		55	51			44

TABLE 7.2A. Abbreviations used in measurements of Eocene sirenian mandibles. Measurements are followed after Domning (1978). All measurements are in mm; see appendix for key to the measurements.

Abb.	Measured dimension
AA	Total Length
AG	Anterior tip to front ascending ramus
AP	Anterior tip to rear of mental foramen
AQ	Anterior tip to front of mandibular foramen
AS	Length of symphysis
BG	Posterior extremity to front of ascending ramus
BQ	Posterior extremity to front of mandibular foramen
CD	Height of coronoid process
DF	Distance between anterior and posterior ventral extremities
DK	Height of mandibular notch
DL	Height of condyle
EF	Height at deflection point of horizontal ramus
EU	Deflection point to rear of alveolar row
GH	Minimum anteroposterior breadth of ascending ramus
GP	Front of ascending ramus to rear of mental foramen
IJ	Maximum anteroposterior breadth of dorsal part of ascending ramus
MN	Top of ventral curvature of horizontal ramus to line connecting ventral extremities
MO	Minimum dorsoventral breadth of horizontal ramus
RR'	Maximum breadth of masticating surface
SQ	Rear of symphysis to front of mandibular foramen
TU	Length of the alveolar row (M_{1-3})
VV'	Maximum width between labial edges of left and right alveoli across M_1
WW'	Minimum width between angles
XX'	Minimum width between condyles
MD	Deflection of symphysal surface from occlusal plane (degrees)

TABLE 7.2B. Measurements of Eocene sirenian mandibles, including those from North America. All measurements are in mm; MD in degrees; see appendix for key to the measurements.

Abb.	*Eotheroides clavigerum* UM 101219	*Eosiren stromeri* UM 100137	*Eosiren stromeri* UM 100137	*Eosiren libyca* ST.XIX	*Protosiren smithae* CGM 42292	*Eotheroides* sp. USNM 214596
AA	216	213	213	234	222	181
AG	150	170	170	173	154	147
AP	43	54	54		70	52
AQ	132	155	155	170	160	
AS	62	68	68	80	65	69
BG	64			70	74	
BQ	36	50	50	68	65	
CD	130				154	
DF	120	56	56	142	113	
DK	106			107	114	
DL	119			118	131	
EF	69	83	83	86	66	55
EU	77	105	105	88	86	87
GH	63			60	63	
GP	100	112	112		76	
IJ	65				76	
MN	32	37	37	35	26	18
MO	38	46	46	47	37	37
RR'	37	26	26	30	51	25
SQ	72	88	88	94	99	
TU	44	46	46		64	46
VV'	56	65	65	61	59	40
WW'	89	65	65	50	70	
XX'	99				100	
MD	50	43	43	52	58	37

TABLE 7.3A. Measurements of living sirenian centrum length. Data of *Dusisiren jordani* are from Domning (1978). All measurements are in mm; see appendix for key to the measurements.

Vert.	*Dugong dugon* USNM 197900 m	*Dugong dugon* USNM 257107 f	Vert.	*Dusisiren jordani* UCMP 77037	Vert.	*T. manatus* UMMZ 106206	*T. senegalensis* USNM 209007
C2	34		**C2**	85	**C2**	49	32
C3	11	9	**C3**	23	**C3**	16	12
C4	9	7	**C4**	19	**C4**	15	11
C5	7	7	**C5**	16	**C5**	15	12
C6	6	8	**C6**	20	**C6**	19	15
C7	7	13	**C7**	25	**Th1**	28	19
Th1	13	22	**Th1**	35	**Th2**	36	26
Th2	18	22	**Th2**	41	**Th3**	42	30
Th3	20	22	**Th3**	45	**Th4**	49	35
Th4	22	25	**Th4**	49	**Th5**	56	39
Th5	27	27	**Th5**	53	**Th6**	62	44
Th6	26	33	**Th6**	60	**Th7**	65	48
Th7	27	33	**Th7**	65	**Th8**	69	50
Th8	31	35	**Th8**	67	**Th9**	66	54
Th9	33	36	**Th9**	69	**Th10**	72	53
Th10	32	36	**Th10**	71	**Th11**	74	51
Th11	34	37	**Th11**	74	**Th12**	74	51
Th12	35	37	**Th12**	74	**Th13**	71	51
Th13	36	37	**Th13**	74	**Th14**	70	60
Th14	36	37	**Th14**	79	**Th15**	68	47
Th15	36	37	**Th15**	77	**Th16**	69	44
Th16	36	35	**Th16**	75	**Th17**	61	45
Th17	35	35	**Th17**	76	**Lr1**	63	43
Th18	35	39	**Th18**	75	**Lr2**	59	40
Th19	36	40	**Th19**	72	**Ca1**	54	38
Lr1	39	40	**Th20**	74	**Ca2**	54	40
Lr2	37	42	**Th21**	77	**Ca3**	54	38
Lr3	38	46	**Lr1**	74	**Ca4**	54	39
Lr4	40	44	**Lr2**	81	**Ca5**	54	39
S	39	43	**Lr3**	78	**Ca6**	53	40
Ca1	33	45	**S**	76	**Ca7**	53	36
Ca2	38	42	**Ca1**	73	**Ca8**	51	35
Ca3	35	40	**Ca2**	70	**Ca9**	48	32
Ca4	38	39	**Ca3**	70	**Ca10**	46	32
Ca5	36	32	**Ca4**	70	**Ca11**	41	29
Ca6	35	38	**Ca5**	67	**Ca12**	41	27
Ca7	32	38	**Ca6**	67	**Ca13**	38	25
Ca8	31	35	**Ca7**	69	**Ca14**	34	25
Ca9	30	32	**Ca8**	66	**Ca15**	32	22
Ca10	25	30	**Ca9**	64	**Ca16**	30	19
Ca11	23	28	**Ca10**	59	**Ca17**	30	18
Ca12	19	23	**Ca11**	59	**Ca18**	27	19
Ca13	18	20	**Ca12**	56	**Ca19**	26	17
Ca14	17	17	**Ca13**	50	**Ca20**	25	17
Ca15	15	16	**Ca14**	46	**Ca21**	24	16
Ca16	13	15	**Ca15**	42	**Ca22**	24	13
Ca17	12	14	**Ca16**	40	**Ca23**	23	
Ca18	12	13	**Ca17**	39			
Ca19	13	12	**Ca18**	33			
Ca20	11	10	**Ca19**	31			
Ca21	11	9	**Ca20**	29			
Ca22	9	9	**Ca21**	26			
Ca23	7	7	**Ca22**	24			
Ca24	7	8	**Ca23**	21			
			Ca24	19			
			Ca25	17			
			Ca26	17			
			Ca27	16			
			Ca28	15			
			Ca29	15			
			Ca30	14			

TABLE 7.3B. Measurements of Fossil Eocene Centrum length. All measurements are in mm; see appendix for key to the measurements.

Vert.	*Eotheroides sandersi* UM 97514	*Eotheroides sandersi* UM 111558	*Eotheroides clavigerum* UM 101219	*Eosiren libyca* UM 101226	*Eosiren stromeri* UM 100137	*Eosiren libyca* UM 101228	*Protosiren smithae* UM 101224
C2			44		41		54
C3			14	17	46		17
C4				18			13
C5		15	15	15			
C6				16			
C7			18	19			17
Th1			28	22	42		22
Th2		25	31	31	39	36	27
Th3		26	35	30	36		30
Th4		30	38	34	41		34
Th5	31	33	40	32	54		38
Th6	35	33	42	43	56		37
Th7	36	36	47	45	49		42
Th8	35	36	45	45	57		44
Th9	37	37	45	58	58		46
Th10	38	39	47	46	63	52	46
Th11	38	39	47	47	58		45
Th12	38	39	41	48	58		46
Th13	40	40	49	49			46
Th14	40	41		45			47
Th15	41	40	50	49	52		46
Th16		41	48	47			45
Th17	40			48			46
Th18		45		48			47
Th19/20							50
Lr1	41	44		48			51
Lr2	42			48			52
Lr3	43			49			50
Lr4				49			51
S	42		36	52			48
Ca1	42			51			53
Ca2	40		41	50			50
Ca3	40			48		59	46
Ca4	38			48		58	
Ca5	38	39		45		57	
Ca6	39	36		38		55	
Ca7		35		37		53	
Ca8	37			34		53	
Ca9	35					52	
Ca10	28					50	
Ca11							
Ca12		27					
Ca13		27					
Ca14							
Ca15							
Ca16	17	23	24				
Ca17							
Ca18							
Ca19		18	17				

TABLE 7.4A. Measurements of maximum vertebral height in living and Miocene sirenians. Data of *Dusisiren jordani* are from Domning (1978). All measurements are in mm; see appendix for key to the measurements.

Vert.	*Dusisiren jordani* UCMP 77037	Vert.	*Dugong dugon* USNM 257107 f	*Dugong dugon* USNM 197900 m	Vert.	*Trichechus manatus* UMMZ 106206
C1	124	**C1**		86	**C1**	93
C2	119	**C2**		75	**C2**	86
C3	110	**C3**	61	60	**C3**	69
C4	103	**C4**	61	58	**C4**	71
C5	118	**C5**	67	67	**C5**	71
C6	124	**C6**	65	63	**C6**	73
C7	133	**C7**	69	64	**Th1**	107
Th1	155	**Th1**	77	74	**Th2**	125
Th2	175	**Th2**	94	91	**Th3**	137
Th3	196	**Th3**	102	103	**Th4**	127
Th4	226	**Th4**	115	113	**Th5**	129
Th5	241	**Th5**	127	108	**Th6**	144
Th6	243	**Th6**	127	107	**Th7**	146
Th7	240	**Th7**	126	107	**Th8**	147
Th8	234	**Th8**	127	109	**Th9**	151
Th9	238	**Th9**	125	109	**Th10**	163
Th10	241	**Th10**	125	108	**Th11**	164
Th11	271	**Th11**	124	112	**Th12**	163
Th12	282	**Th12**	127	109	**Th13**	159
Th13	280	**Th13**	130	120	**Th14**	156
Th14	305	**Th14**	131	118	**Th15**	157
Th15	302	**Th15**	133	121	**Th16**	153
Th16	276	**Th16**	126	113	**Th17**	127
Th17	260	**Th17**	124	114	**Lr1**	106
Th18	256	**Th18**	103	112	**Lr2**	109
Th19	253	**Th19**	107	108	**Ca1**	106
Th20	248	**Lr1**	114	107	**Ca2**	100
Th21	252	**Lr2**	114	109	**Ca3**	96
Lr1	254	**Lr3**	110	98	**Ca4**	92
Lr2	252	**Lr4**	110	95	**Ca5**	85
Lr3	250	**S**	112	95	**Ca6**	78
S	251	**Ca1**	112	92	**Ca7**	75
Ca1	242	**Ca2**	111	97	**Ca8**	66
Ca2	232	**Ca3**	108	88	**Ca9**	62
Ca3	221	**Ca4**	101	90	**Ca10**	50
Ca4	219	**Ca5**	96	88	**Ca11**	43
Ca5	214	**Ca6**	95	87	**Ca12**	38
Ca6	203	**Ca7**	88	84	**Ca13**	35
Ca7	195	**Ca8**	85	75	**Ca14**	30
Ca8	183	**Ca9**	79	74	**Ca15**	28
Ca9	175	**Ca10**	71	66	**Ca16**	27
Ca10	161	**Ca11**	65	58	**Ca17**	25
Ca11	152	**Ca12**	56	48	**Ca18**	21
Ca12	137	**Ca13**	49	41	**Ca19**	18
Ca13	116	**Ca14**	42	36	**Ca20**	16
Ca14	99	**Ca15**	34	28	**Ca21**	15
Ca15	88	**Ca16**	27	17	**Ca22**	12
Ca16	73	**Ca17**	24	16	**Ca23**	11
Ca17	64	**Ca18**	20	16	**Ca24**	9
Ca18	57	**Ca19**	17	13		
Ca19	54	**Ca20**	12	12		
Ca20	43	**Ca21**	9	9		
Ca21	36	**Ca22**	10	8		
Ca22	31	**Ca23**	8	6		
Ca23	25	**Ca24**	6	7		
Ca24	20	**Ca25**	6			
Ca25	17					
Ca26-29	16,14,12,12					
Ca30-32	11,12,10					

TABLE 7.4B. Measurements of maximum vertebral height in Fossil Eocene sirenian of Egypt. All measurements are in mm; see appendix for key to the measurements.

Vert.	*Eotheroides clavigerum* UM 101219	*Eotheroides sandersi* UM 97514	*Eotheroides sandersi* UM 111558	*Eosiren libyca* UM 101226	*Protosiren smithae* UM 101224
C1	68		57	66	85
C2	73				96
C3					77
C4					75
C5	84		65		
C6					
C7					88
Th1	123				145
Th2	120				171
Th3	116		113		173
Th4	122	120	103		180
Th5	121	116		126	165
Th6		109	103	130	168
Th7		111	103	134	165
Th8	123		99	128	168
Th9	120			114	169
Th10			101	117	166
Th11		111	109	120	
Th12	118	116	108	112	
Th13		119	110	116	163
Th14			105	115	159
Th15	126			124	159
Th16			108	122	163
Th17				123	160
Th18			105	127	
Th19/20					
Lr1			104	124	163
Lr2				128	161
Lr3		112		124	
Lr4		106		118	
S		98		110	
Ca1		94		110	
Ca2	78	89		102	
Ca3		83		109	
Ca4		81			
Ca5		76	66	102	
Ca6		74		82	
Ca7				73	
Ca8		65		64	
Ca9		58			
Ca10		43			
Ca11					
Ca12					
Ca13					
Ca14					
Ca15					
Ca16	27	14	20		
Ca17					
Ca18					
Ca19	12				

TABLE 7.5A. Measurements of maximum vertebral breadth in living and Miocene sirenian. Data of *Dusisiren jordani* are from Domning (1978). All measurements are in mm; see appendix for key to the measurements.

Vert.	*Dusisiren jordani* UCMP 77037	Vert.	*Dugong dugon* USNM 257107 f	*Dugong dugon* USNM 197900 m	Vert.	*Trichechus manatus* UMMZ 106206	*Trichechus senegalensis* USNM 209007
C1	203	**C1**		111	**C1**	132	104
C2	125	**C2**		70	**C2**	78	71
C3	156	**C3**	89	86	**C3**	94	82
C4	168	**C4**	90	86	**C4**	100	93
C5	196	**C5**	97	85	**C5**	118	104
C6	207	**C6**	109	96	**C6**	151	10
C7	270	**C7**	106	108	**T1**	135	110
T1	240	**Th1**	126	105	**T2**	131	112
T2	249	**Th2**	125	107	**T3**	130	110
T3	248	**Th3**	109	118	**T4**	127	116
T4	244	**Th4**	114	111	**T5**	129	110
T5	235	**Th5**	113	103	**T6**	126	106
T6	230	**Th6**	112	99	**T7**	127	104
T7	221	**Th7**	114	95	**T8**	128	97
T8	217	**Th8**	113	93	**T9**	123	95
T9	209	**Th9**	108	94	**T10**	124	95
T10	201	**Th10**	109	97	**T11**	107	95
T11	183	**Th11**	105	97	**T12**	104	95
T12	194	**Th12**	100	98	**T13**	111	94
T13	184	**Th13**	99	98	**T14**	103	95
T14	187	**Th14**	99	95	**T15**	98	88
T15	187	**Th15**	97	94	**T16**	99	85
T16	191	**Th16**	99	91	**T17**	99	208
T17	185	**Th17**	95	87	**L1**	289	245
T18	189	**Th18**	92	82	**L2**	410	238
T19	190	**Th19**	81	82	**S**	395	226
T20	197	**Lr1**	265	61	**Ca1**	367	222
T21	200	**Lr2**	264	67	**Ca2**	337	203
L1	506	**Lr3**	237	62	**Ca3**	320	188
L2	582	**Lr4**	262	60	**Ca4**	310	180
L3	606	**S**	215	59	**Ca5**	285	158
S	617	**Ca1**	188	56	**Ca6**	276	147
Ca1	508	**Ca2**	170	55	**Ca7**	256	129
Ca2	424	**Ca3**	154	53	**Ca8**	235	112
Ca3	366	**Ca4**	136	140	**Ca9**	218	97
Ca4	324	**Ca5**	125	110	**Ca10**	184	82
Ca5	295	**Ca6**	109	97	**Ca11**	154	7
Ca6	260	**Ca7**	96	84	**Ca12**	133	63
Ca7	222	**Ca8**	84	73	**Ca13**	108	55
Ca8	203	**Ca9**	78	68	**Ca14**	88	47
Ca9	185	**Ca10**	75	68	**Ca15**	69	39
Ca10	170	**Ca11**	72	70	**Ca16**	54	32
Ca11	164	**Ca12**	70	68	**Ca17**	83	24
Ca12	163	**Ca13**	69	71	**Ca18**	38	19
Ca13	171	**Ca14**	65	71	**Ca19**	29	16
Ca14	178	**Ca15**	66	70	**Ca20**	29	12
Ca15	186	**Ca16**	33	70	**Ca21**	21	8
Ca16	187	**Ca17**	61	67	**Ca22**	18	
Ca17	183	**Ca18**	58	67	**Ca23**	9	
Ca18	170	**Ca19**	53	62			
Ca19	166	**Ca20**	51	58			
Ca20	159	**Ca21**	48	19			
Ca21	153	**Ca22**	44	17			
Ca22	144	**Ca23**	38	12			
Ca23	133	**Ca24**	33	15			
Ca24-26	120,106,94	**Ca25**	28				
Ca27-29	79,67,55						
Ca30-31	43-23						

TABLE 7.5B. Measurements of maximum vertebral breadth in Eocene sirenian. All measurements are in mm; see appendix for key to the measurements.

Vert.	*Eosiren libyca* UM 101226	*Eotheroides clavigerum* UM 101219	*Eotheroides sandersi* UM 97514	*Eotheroides sandersi* UM 111558	*Eosiren stromeri* UM 100137	*Eosiren libyca* UM 101228	*Protosiren smithae* CGM 42292	*Protosiren smithae* UM 101224
C1	105	116		106			126	134
C2		70					83	93
C3							90	104
C4							90	99
C5		107		84				
C6							104	
C7							110	115
Th1		108			119		118	132
Th2		100			126		121	123
Th3		100		101	118			105
Th4	134	94		93	107			99
Th5		90	99					89
Th6	108	93	91	86	95			111
Th7	102	86	93	82	94			112
Th8	106	87		81				112
Th9	104	87	89	81				111
Th10	98	86	87	98		81		106
Th11	98	85	88	79				90
Th12	99	91	83	80				105
Th13	98	79	81	78				98
Th14	94		86	79				96
Th15	88		79	77				107
Th16	86			78				88
Th17	83	82	70					105
Th18	92							111
Th19/20				118				
Lr1	196			168				213
Lr2	229							
Lr3	236		190					
Lr4	228		188					
S	210		191				201	107
Ca1	181		192					
Ca2	164		175				181	113
Ca3	141		177					
Ca4	152	182	168					
Ca5	133		156			153		
Ca6	116			144		119		
Ca7	106			120		106		
Ca8	104		143			97		
Ca9			136			93		
Ca10			114			90		
Ca11						88		
Ca12						87		
Ca13				95				
Ca14								
Ca15				40				
Ca16		67	33					
Ca17								
Ca18								
Ca19		23						

TABLE 7.6A. Ratios of centrum widths to centrum length in living and Miocene sirenian. Data of *Dusisiren jordani* are from Domning (1978). All measurements are in mm; see appendix for key to the measurements.

Vert.	*Dusisiren jordani* UCMP 77037	Vert.	*D. dugon* USNM 197900 m	*D. dugon* USNM 257107 f	Vert.	*T. manatus* UMMZ 106206	*T. senegalensis* USNM 209007
C2	1.04	**C2**	1.13		**C2**	1.09	0.58
C3	3.91	**C3**	3.48	4.71	**C3**	3.42	3.66
C4	4.95	**C4**	4.22	5.82	**C4**	3.55	3.94
C5	6.06	**C5**	6.00	5.79	**C5**	3.03	3.55
C6	5.00	**C6**	7.31	5.33	**C6**	2.24	2.62
C7	4.64	**C7**	6.97	3.88	**Th1**	1.56	2.18
Th1	2.91	**Th1**	3.35	2.13	**Th2**	1.19	1.53
Th2	2.34	**Th2**	2.15	1.83	**Th3**	1.13	1.42
Th3	2.16	**Th3**	2.07	1.70	**Th4**	1.05	1.32
Th4	2.08	**Th4**	1.70	1.67	**Th5**	1.04	1.24
Th5	2.09	**Th5**	1.49	1.65	**Th6**	0.95	1.21
Th6	1.90	**Th6**	1.54	1.33	**Th7**	1.01	1.20
Th7	1.85	**Th7**	1.46	1.44	**Th8**	0.98	1.21
Th8	1.94	**Th8**	1.32	1.44	**Th9**	1.14	1.13
Th9	1.96	**Th9**	1.26	1.53	**Th10**	1.03	1.16
Th10	1.97	**Th10**	1.53	1.60	**Th11**	1.05	1.21
Th11	2.01	**Th11**	1.51	1.51	**Th12**	1.00	1.23
Th12		**Th12**	1.45	1.56	**Th13**	1.03	1.31
Th13		**Th13**	1.45	1.66	**Th14**	0.97	1.08
Th14		**Th14**	1.42	1.68	**Th15**	0.98	1.37
Th15	1.78	**Th15**	1.61	1.60	**Th16**	0.96	1.51
Th16	1.92	**Th16**	1.57	1.69	**Th17**	1.04	1.54
Th17	2.00	**Th17**	1.68	1.78	**Lr1**	1.25	1.58
Th18	2.01	**Th18**	1.65	1.58	**Lr2**	1.26	1.61
Th19	2.15	**Th19**	1.53	1.55	**Ca1**	1.36	1.67
Th20	2.08	**Lr1**	1.59	1.18	**Ca2**	1.33	1.57
Th21	2.04	**Lr2**	1.82	1.76	**Ca3**	1.31	1.59
Lr1	2.15	**Lr3**	1.62	1.50	**Ca4**	1.26	1.57
Lr2	2.02	**Lr4**	1.53	1.63	**Ca5**	1.24	1.51
Lr3	2.09	**S**	1.50	1.54	**Ca6**	1.27	1.47
s	2.20	**Ca1**	1.68	1.47	**Ca7**	1.18	1.52
Ca1	2.15	**Ca2**	1.46	1.46	**Ca8**	1.24	1.52
Ca2	2.11	**Ca3**	1.52	1.48	**Ca9**	1.23	1.57
Ca3	2.07	**Ca4**	1.44	1.58	**Ca10**	1.24	1.49
Ca4	2.06	**Ca5**	1.47	1.83	**Ca11**	1.38	1.57
Ca5	2.04	**Ca6**	1.46	1.52	**Ca12**	1.23	1.57
Ca6	2.01	**Ca7**	1.59	1.58	**Ca13**	1.15	1.67
Ca7	1.80	**Ca8**	1.52	1.64	**Ca14**	1.18	1.37
Ca8	1.95	**Ca9**	1.52	1.74	**Ca15**	1.16	1.56
Ca9	1.91	**Ca10**	1.77	1.76	**Ca16**	1.07	1.63
Ca10	1.97	**Ca11**	1.80	1.74	**Ca17**	0.96	1.56
Ca11	1.86	**Ca12**	2.01	1.96	**Ca18**	0.99	1.27
Ca12	1.89	**Ca13**	1.91	2.63	**Ca19**	0.88	1.10
Ca13	2.02	**Ca14**	2.11	2.23	**Ca20**	0.80	0.93
Ca14	2.11	**Ca15**	2.10	2.23	**Ca21**	0.69	0.77
Ca15	2.17	**Ca16**	2.20	2.22	**Ca22**	0.52	0.64
Ca16	2.05	**Ca17**	2.42	2.21	**Ca23**	0.35	
Ca17	1.97	**Ca18**	2.33	2.49			
Ca18	2.12	**Ca19**	2.02	2.21			
Ca19	2.16	**Ca20**	1.89	2.41			
Ca20	2.17	**Ca21**	1.78	2.53			
Ca21	2.23	**Ca22**	1.95	2.36			
Ca22	2.33	**Ca23**	1.67	2.59			
Ca23	2.52	**Ca24**	2.13	2.54			
Ca24	2.68	**Ca25**		2.09			
Ca25	2.76						
Ca26	2.65						
Ca27	2.44						
Ca28	2.07						
Ca29	2.13						
Ca30-31	2.07, 1.31						

TABLE 7.6B. Ratios of centrum widths to centrum length in Eocene sirenian from the Fayum region. All measurements are in mm; see appendix for key to the measurements.

Vert.	*Eotheroides sandersi* UM 97514	*Eotheroides sandersi* UM 111558	*Eotheroides clavigerum* UM 101219	*Protosiren smithae* UM 101224	*Eosiren libyca* UM 101226	*Eosiren libyca* UM 101228
C1						
C2			0.84	0.85		
C3			2.76	2.75	2.88	
C4				3.16	2.72	
C5		2.48	1.91		2.93	
C6					2.81	
C7			2.28	2.70	2.32	
Th1			1.21	2.06	1.68	
Th2			1.18	2.00	1.42	0.75
Th3		1.25	1.20	1.71	1.43	
Th4		1.15	1.12	1.49	1.35	
Th5	1.29	1.01	1.15	1.46	1.28	
Th6	1.26	1.10	0.99	1.58	1.09	
Th7	1.31	1.10	1.05	1.49	1.04	
Th8	1.31	1.04	0.80	1.26	1.20	
Th9	1.43	1.12	1.14	1.31	0.78	
Th10	1.42	1.10	1.13	1.27	1.26	0.81
Th11	1.32	1.15	1.20	1.47	1.30	
Th12	1.37	1.19	1.16	1.44	1.25	
Th13	1.43	1.26	1.19	1.50	1.37	
Th14	1.43	1.33		1.34	1.42	
Th15	1.39	1.40	1.18	1.34	1.29	
Th16		1.31	1.17	1.38	1.26	
Th17	1.43			1.57	1.23	
Th18		1.17		1.42	1.29	
Th19/20				1.41		
Lr1		1.19		1.41	1.46	
Lr2	1.46			1.47	1.00	
Lr3	1.50			1.31	1.51	
Lr4	1.44			1.23	1.59	
S	1.45		1.86	1.37	1.46	
Ca1	1.43			1.33	1.41	
Ca2	1.53		1.53	1.43	1.40	
Ca3	1.55			1.53	1.44	1.44
Ca4	1.66				1.44	1.41
Ca5	1.47	1.30			1.51	1.58
Ca6	1.56	1.41			1.82	1.38
Ca7		1.42			1.84	1.56
Ca8	1.43				1.85	1.51
Ca9	1.51					1.58
Ca10	1.71					1.52
Ca11						
Ca12		1.24				
Ca13		1.11				
Ca14						
Ca15						
Ca16	1.53	1.74	1.52			
Ca17						
Ca18						
Ca19		1.22	1.03			

TABLE 7.7. Cross-sectional area of midshafts of Eocene and living sirenians. All measurements are in mm^2; see appendix for key to the measurements.

Rib	*Protosiren smithae* UM 101224	*Eotheroides sandersi* UM 111558	*Eotheroides sandersi* UM 97514	*Eotheroides sandersi* CGM 42181	*Eotheroides clavigerum* UM 101219	*Eosiren libyca* UM 101226	*Trichechus manatus* UMMZ 106206
R1	275	608			1258		770
R2	464	967		1026	1833		858
R3	638	1398		1312	2279		1656
R4	693	1208			2279		1716
R5	840	839		1080	1890		1872
R6	884	819	980	896	2208	840	1980
R7	825	708	891	850	1540	648	2065
R8	748	713	1080	840	1518	627	2304
R9	816	546	660	736	1472	527	2442
R10	806	572	667		1333	480	2546
R11	792	544	609	704	1230	480	2516
R12	714	522	475	651	1102	448	2376
R13	713	522	475	588	1090	400	2275
R14	713		330	486	1053	384	2142
R15	600	450	198	336	828	345	2145
R16	570		156	345	782	330	1276
R17	567	192		286	693	294	506
R18	400			330	625	228	
R19	360						

TABLE 7.8. Scapular dimensions of Eocene Sirenia from Egypt; notice that *Eotheroides clavigerum* and *Protosiren* have the longest blades and spines, and widest breadths. All measurements are in mm; see appendix for key to the measurements.

Key	Measurements	*Eotheroides clavigerum* UM 101219	*Eotheroides clavigerum* UM 94806	*Eotheroides sandersi* UM 111558	*Eotheroides sandersi* CGM 42181	*Protosiren smithae* UM 101224
1	Scapular length along the spine	226	218	192	196	230
2	Spine length	137	118	106	103	144
3	Scapular breadth	76		65	61	78
4	Infraspinous fossa breadth	51	57	46	43	60
5	Neck breadth	46	40	34	36	44
6	Neck height	19	19	15	17	27
7	Distance from median glenoid cavity to acromion	30	36	29	38	31
8	Glenoid process breadth	51	52	43	47	56
9	Glenoid cavity breadth	38	43	34	36	43
10	Glenoid cavity height	29	30	26	25	34
11	Breadth of the acromion			6		11
12	Spine height from dorsal surface			21		34
13	Spine height from ventral surface	54	48	39		64
14	Distance between anterior tip of glenoid process and anterodorsal edge of blade	142		123	123	153
15	Distance between posterior tip of the glenoid process and first posterior edge of blade	99		85	93	89
16	Circumference of the blade	565		475	490	583

TABLE 7.9. Humeral measurements of Fayum Eocene sirenians. All measurements are in mm; see appendix for key to the measurements.

key	Measurements	*Eotheroides clavigerum* UM 101219	*Eotheroides clavigerum* UM 94806	*Eotheroides sandersi* UM 111558	*Eotheroides sandersi* CGM 42181	*Protosiren smithae* CGM 42292
1	Length (greater tubercle to distal end)	169	179	155	137	158
2	Length from the head to the distal end	159	164	142	137	155
3	Proximal end maximum breadth	59	56	51	43	57
4	Head height	16	18	17	17	26
5	Head length	42	43	36	35	45
6	Head width	36	39	31	33	37
7	Bicipital groove width	13	12	9	13	18
8	Maximum width of the midshaft	37	29	23	26	23
9	Minimum width of the shaft in the middle	25	18	19	18	21
10	Minimum circumference of the shaft	97	76	70	71	70
11	Distal end maximum breadth	50	39	42	46	54
12	Trochlea breadth	34	27	31	32	31
13	Trochlea height	29	19	24	21	25
14	Trochlea height n the middle	18	11	18	15	16
15	Olecranial fossa width	18	23	20	20	21
16	Olecranial fossa height	20	21	28	16	23
17	Olecranial fossa depth	13	15	8	12	10

TABLE 7.10. Ulnar measurements of Eocene sirenians of Egypt. All measurements are in mm; see appendix for key to the measurements.

key	Measurements	*Eotheroides clavigerum* UM 101219	*Eotheroides sandersi* UM 111558	*Eotheroides aegyptiacum* SMNS St.XXX	*Protosiren smithae* CGM 42292
1	Greatest length	146	136		138
2	Length of the olecranon	30	21	22	34
3	Smallest depth of olecranon	32	24	15	24
4	Greatest depth at the anconeal process	35	26	13	29
5	Height of the trochlear notch	26	22	21	24
6	Breadth across the coronoid process	35	30	25	23
7	Height from the coronoid process to the distal epiphysis	110	98		94
8	Circumference of midshaft	61	50		56
9	Width of the distal epiphysis	21	16		16
10	Length of the distal epiphysis	29	24		28

TABLE 7.11. Pelvic measurements of Eocene sirenians of Egypt. All measurements are in mm; see appendix for key to the measurements.

Key	Measurements	*Eotheroides clavigerum* UM 101219	*Eotheroides sandersi* CGM 42181	*Eotheroides sandersi* UM 97514	*Eosiren libyca* UM 101226	*Protosiren smithae* CGM 42292
1	Total length	215	153	186	197	250
2	Ilium length from center of acetabulum to proximal end	145	107	107	119	165
3	Ilium dorsoventral diameter at midshaft	23	17	21	17	27
4	Ilium mediolateral diameter of at midshaft	24	19	20	18	18
5	Ilium circumference at midshaft	76	60	65	49	81
6	Symphysis length	2		18	12	35
7	Pubic line length from center acetabulum to pubic symphysis	70		75	29	56
8	Pubic ramus thickness in front of the obturator foramen	13	7	12	13	19
9	Pubic Ramus thickness behind the obturator foramen	16	7	21	22	16
10	Acetabulum diameter	19	16	17	20	24
11	Acetabulum external diameter	24	18	23	24	30
12	Acetabulum depth	11	5	10	10	11
13	Obturator foramen length	5	5	8	5	28
14	Obturator foramen height	5	5	13	4	22
15	Ischium length from center of the acetabulum to distal end	89	48	91	105	105
16	Ischiac ramus thickness dorsoventral	34	30	34	32	48
17	Ischiac ramus thickness mediolaterally	9	6	11	12	10
18	Maximum dorsoventral length of the distal end of the ischium	28	27	52	47	54
19	Maximum mediolateral thickness of the distal end of the ischium	9	6	16	28	22
20	Distance between the inner posterior edge of the obturator foramen and the ischiac tuberosity	86	47	94	86	73
21	Length of the sacral articulation surface with the sacrum (anteroposterior length of the oval articulation)	53	31	45	12	26
22	Height of the sacral articulation surface with the sacrum (dorsoventral height of the oval articulation)	41	16	33	16	14
23	Maximum height of the proximal end of the ilium dorsoventrally	47	27	33	17	40
24	Maximum width of the proximal end of the ilium mediolaterally	43	23	28	15	21

TABLE 7.12. Femur bone measurements of Eocene sirenians of Egypt, and Jamaica (Domning, 2001). All measurements are in mm; see appendix for key to the measurements.

Key	Measurements	*Eotheroides sandersi* *CGM 42181*	*Eotheroides sandersi* *UM 111558*	*Eosiren libyca* *UM 101226*	*Protosiren smithae* *CGM 42292*	*Pezosiren portelli* *USNM 517465*
1	Greatest length			108	144	162
2	Total length from the femoral head			108	138	162
3	Head height			9	13	23
4	Head length anteroposteriorly			13	20	21
5	Head width mediolaterally			20	27	49
6	Greatest proximal width	19	20	26	48	49
7	Length of the femoral body	91	102	98	122	150
8	Width across the second trochanter	14	15	18	30	48
9	Minimum width of the diaphysis	9	7	11	19	11
10	Minimum circumference of diaphysis	28	25	14	52	
11	Minimum width of the distal end	12	11	16	21	15
12	Greatest width of the distal end	12	12	13	35	45
13	Width between the external ends of the distal lateral condyles			6	26	
14	Internal distance between the lateral condyles				5	17

TABLE 7.13. Tibial and fibular measurements of Eocene sirenians from Egypt and Jamaica (Domning, 2001). All measurements are in mm; see appendix for key to the measurements.

Key.	Measurements	*Protosiren smithae* CGM 42292	*Protosiren smithae* UM 101224	*Pezosiren portelli* USNM 517466
1	Greatest length of the tibia	109	110	130
2	Greatest length of the tibia including the epiphyses	121	116	
3	Greatest width of the proximal end	24	32	35
4	Greatest length of the proximal end	22	22	17
5	Greatest proximal width including the fibula	38	41	35
6	Median width of the tibial shaft (minimum)	12	16	18
7	Median length of the tibial shaft (minimum)	22	16	13
8	Smallest circumference of the tibial diaphysis	48	51	
9	Maximum distal tibial end length	22	16	
10	Maximum distal width		24	
11	Total fibular length	108	103	
12	Width of the fibular proximal end	11	17	
13	Length of the proximal fibular end	14	11	
14	Median shaft length	9	9	
15	Median fibular width	9	7	
16	Circumference of the fibular median shaft	31	34	

TABLE 7.14. Upper cheek tooth width and length ratio showing the morphology of molar teeth of the same species and compared to other Eocene contemporaneous sirenians of Egypt. Original dimensions are in mm; see appendix for key to the measurements.

Taxon	M^1 (Width/Length)	M^2 (Width/Length)	M^3 (Width/Length)
***P. fraasi* CGM C. 10171 (right maxilla)**	0.93	0.92	0.81
***P. fraasi* SMNS 10576 St. V (right maxilla)**	1.07	0.98	0.80
***P. fraasi* Senck. M3742 St. XXXVIII (right maxilla)**	0.96	1.02	
P. smithae CGM 42292 (right maxilla)		0.89	0.79
***Eotheroides sandersi* UM 111558 (left maxilla)**	1.14	1.15	0.88
***Eotheroides clavigerum* UM 101219 (left maxilla)**	1.18	1.15	0.90
***Eotheroides aegyptiacum* (SMNS St.XI (XIV)) (left maxilla)**	1.06	0.96	0.81
***Eotheroides aegyptiacum* (SMNS St.III) (left maxilla)**	1.09	1.08	0.94
***Eosiren libyca* SMNS St. XVIII (right maxilla)**	1.25	1.14	0.99
***Eosiren libyca* SMNS St. XIX (right maxilla)**		0.99	0.91
***Eosiren stromeri* UM 100137 (left maxilla)**	1.07	0.98	0.91
***Eosiren stromeri* SMNS St. I (left maxilla)**	1.44	1.19	0.97

TABLE 7.15. Upper cheek tooth total area in Eocene sirenians of Egypt. All measurements are in mm. Of all Eocene Egyptian sirenians *Eosiren stromeri* has its M^2 larger than M^1 and M^3. Original dimensions are in mm; see appendix for key to the measurements.

Taxon	M1 (length X Width) in mm^2	M2 (length X Width) in mm^2	M3 (length X Width) in mm^2
***Protosiren fraasi* CGM C. 10171**	243.8	300.5	300.1
***P. fraasi* SMNS 10576 St. V**	224.8	227.2	223.8
***P. fraasi* Senck. M3742 St. XXXVIII**	175.5	186.3	
***Protosiren smithae* CGM 42292**		341.44	388.5
***Eotheroides sandersi* UM 111558**	106.2	141.0	178.8
***Eotheroides clavigerum* UM 101219**	187.4	225.0	247.1
***Eotheroides aegyptiacum* SMNS St.XI (XIV)**	101.9	138.0	130.8
***Eotheroides aegyptiacum* SMNS St.III**	111.6	128.1	130.4
***Eosiren libyca* SMNS St. XVIII**	270.5	348.3	403.0
***Eosiren libyca* SMNS St. XIX**		276.4	307.3
***Eosiren stromeri* UM 100137**	215.8	300.1	222.3
***Eosiren stromeri* SMNS St. I**	243.8	407.0	280.5

FIGURE 7.1. Proportional scatter plot of linear dimensions of cranial elements of several species of Eocene Sirenia from the Bartonian and Priabonian of Egypt. Measured landmarks and abbreviations are after Domning (1978). Data and abbreviations are in Table 7.1.

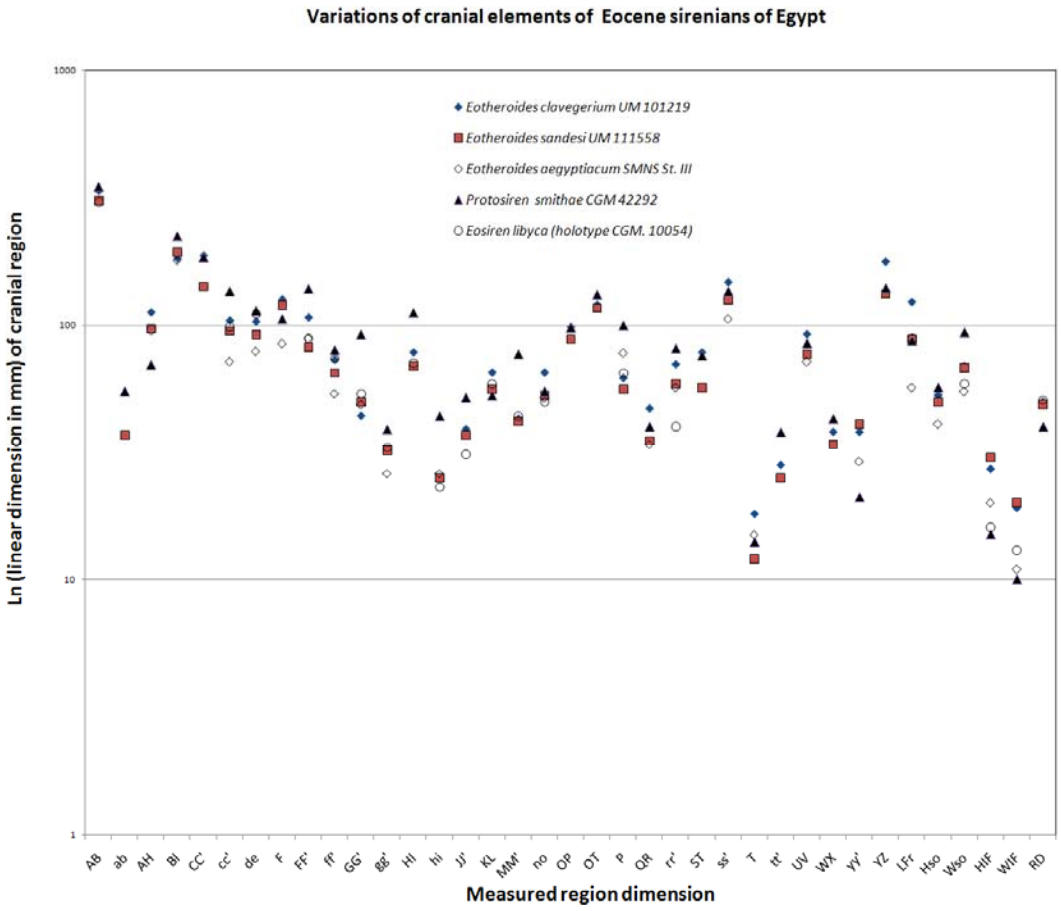

FIGURE 7.2. Proportional scatter plot of linear dimensions of mandibular elements of several species of Eocene Sirenia from the Bartonian and Priabonian of Egypt. Measured landmarks and abbreviations are after Domning (1978). Data and abbreviations are in Table 7.2.

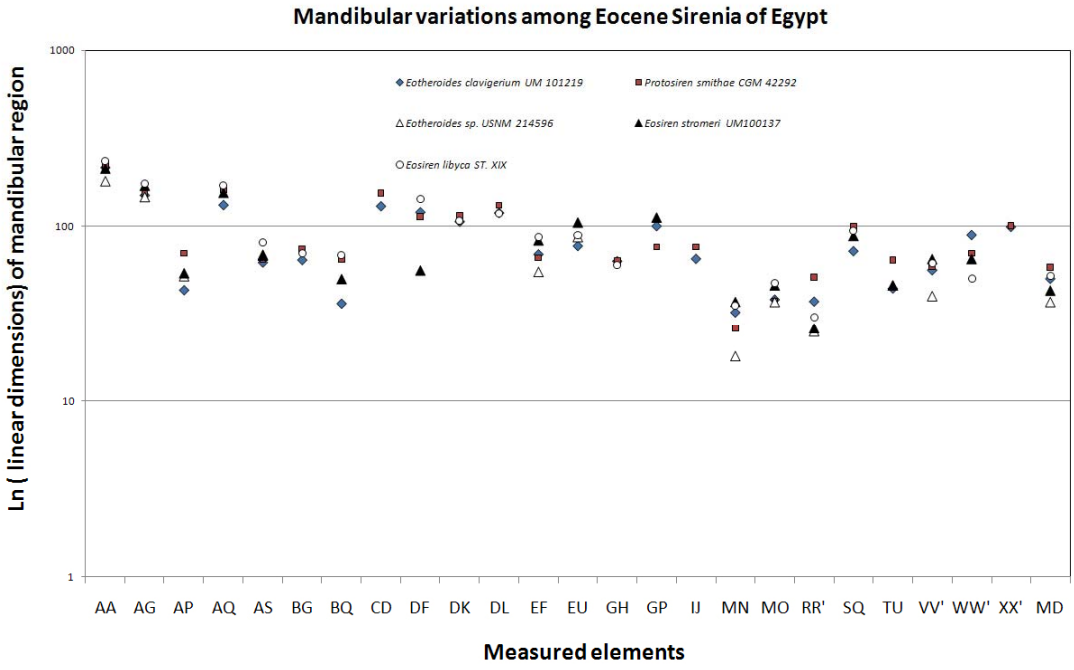

FIGURE 7.3. Vertebrae **length** profiles of living (A) and fossil (B) Sirenia showing regional variations in centra lengths along the vertebral column. All sirenians show short cervicals, increased number of thoracics and lumbars, single sacral and long tail; however, Trichechidae has a different configuration in the vertebral column than that of Protosirenidae and Dugongidae. Increasing in centrum lengths and number of thoracic and lumbar vertebrae has an implication of increasing in the dorsoventral undulation in sirenians, and increase in the length of the lungs with equal weight along the thoracic region. *Dusisiren jordani* included here to show the maximum limit to which size Dugongidae can reach. Data are in Table 7.3. Abbreviations: **C**, cervical; **Ca**, caudal; **Lr**, lumbar, **Th**, thoracic; **S**, sacral.

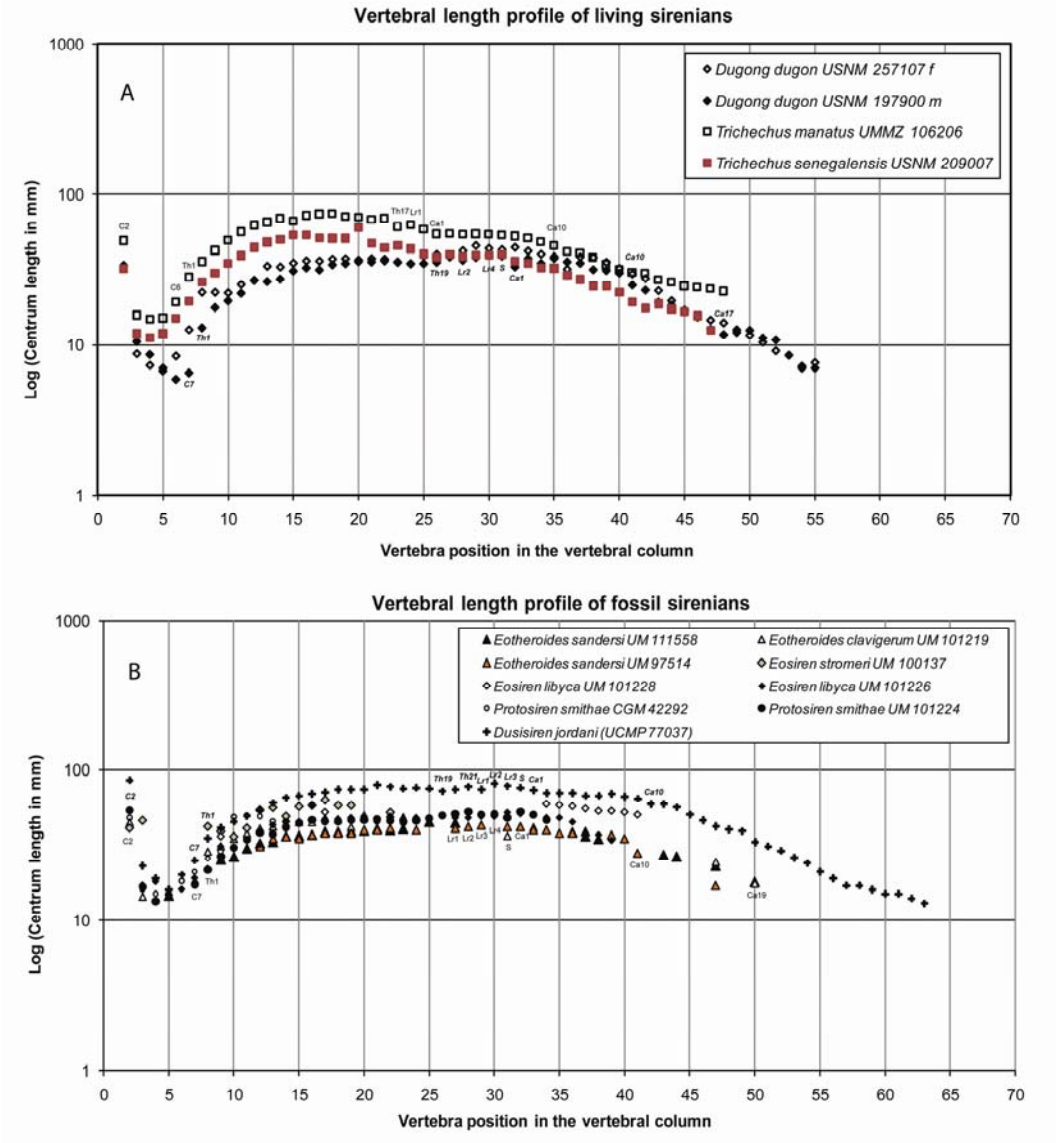

FIGURE 7.4. Maximum vertebral **height** profiles of living (A) and Eocene (B) sirenian vertebral columns (including lengths of neural arches); the long neural arches in anterior and middle thoracic vertebrae may indicate more muscular support and/or and function in the anterior limbs; and the longer the neural arches in posterior lumbar and caudal vertebrae has a greater effect on dorsoventral undulation. *Protosiren smithae*, *Dusisiren jordani* (a Hydrodamalinae dugong from the Miocene of West Coast of North America, Domning 1978), and *Trichechus manatus* that has a longer anterior vertebral spines. All living and fossil dugongs seem to have longer posterior spines than *Trichechus*. This may explain why the dugongs are adapted to deeper and more open marine environments than manatees. Data are in Table 7.4. Abbreviations: **C**, cervical; **Ca**, caudal; **Lr**, lumbar, **Th**, thoracic; **S**, sacral.

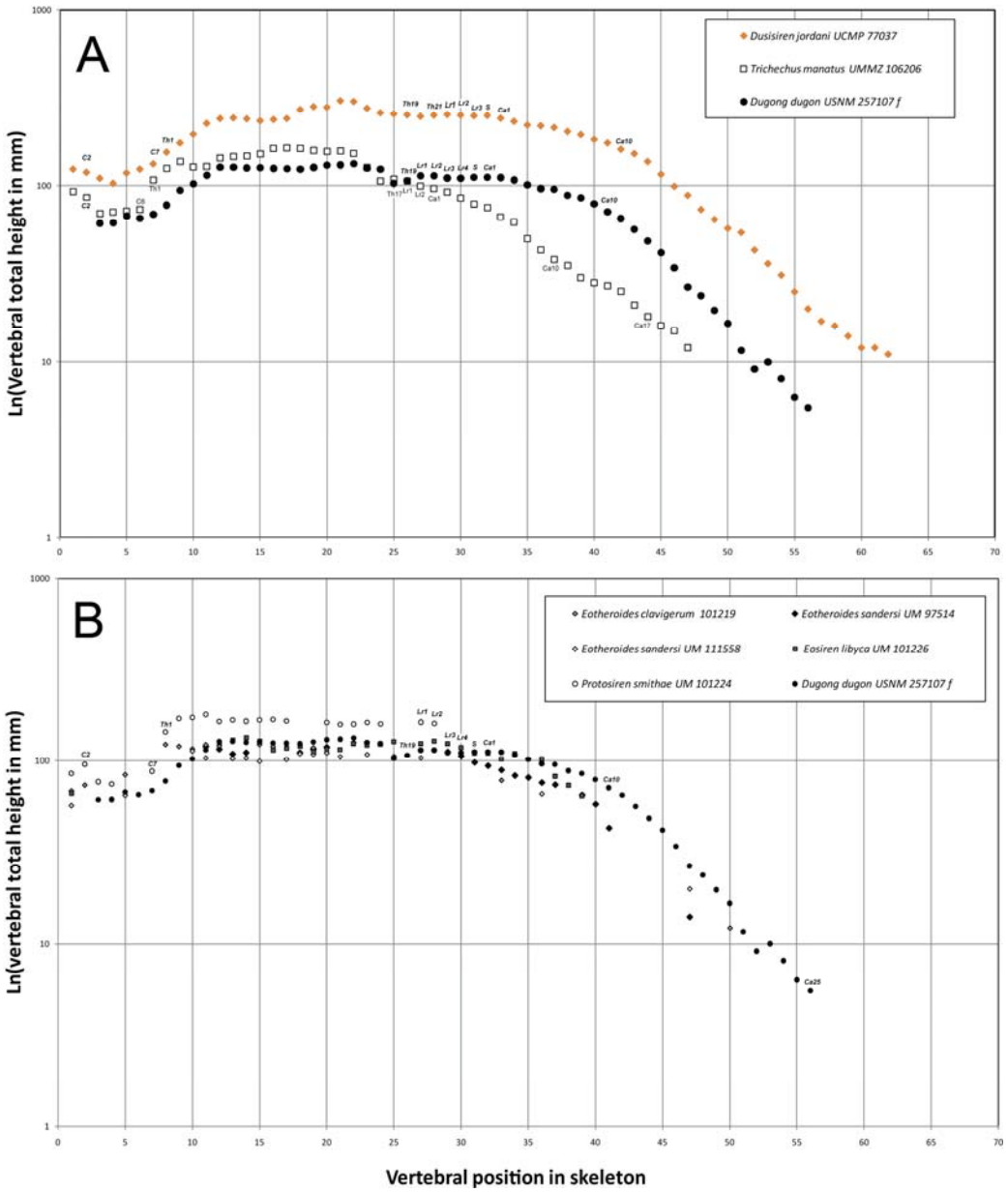

FIGURE 7.5. Maximum vertebral **breadth** profiles of living (A) and Eocene (B) sirenian vertebral columns. The greater the breadth of the transverse processes the more buoyant the animal is; lumbar and anterior caudal vertebrae of *Dusisiren jordani* and *Trichechus manatus* have reached a great vertebral breadth which aids in buoyancy; however in *Trichechus* manatus and *Trichechus senegalensis* the breadth decreases after the first lumbar vertebra and the tail tapers posteriorly. All Eocene sirenians seems to follow *Dugong dugon* profile or close to it where the lumber and anterior caudal vertebrae decrease in breadth gently after the second or third lumbar to the midway point of the tail, after that they keep increasing their breadth slightly, and then gently taper posteriorly. Data are in Table 7.5A and B. Abbreviations: **C**, cervical; **Ca**, caudal; **Lr**, lumbar, **Th**, thoracic; **S**, sacral.

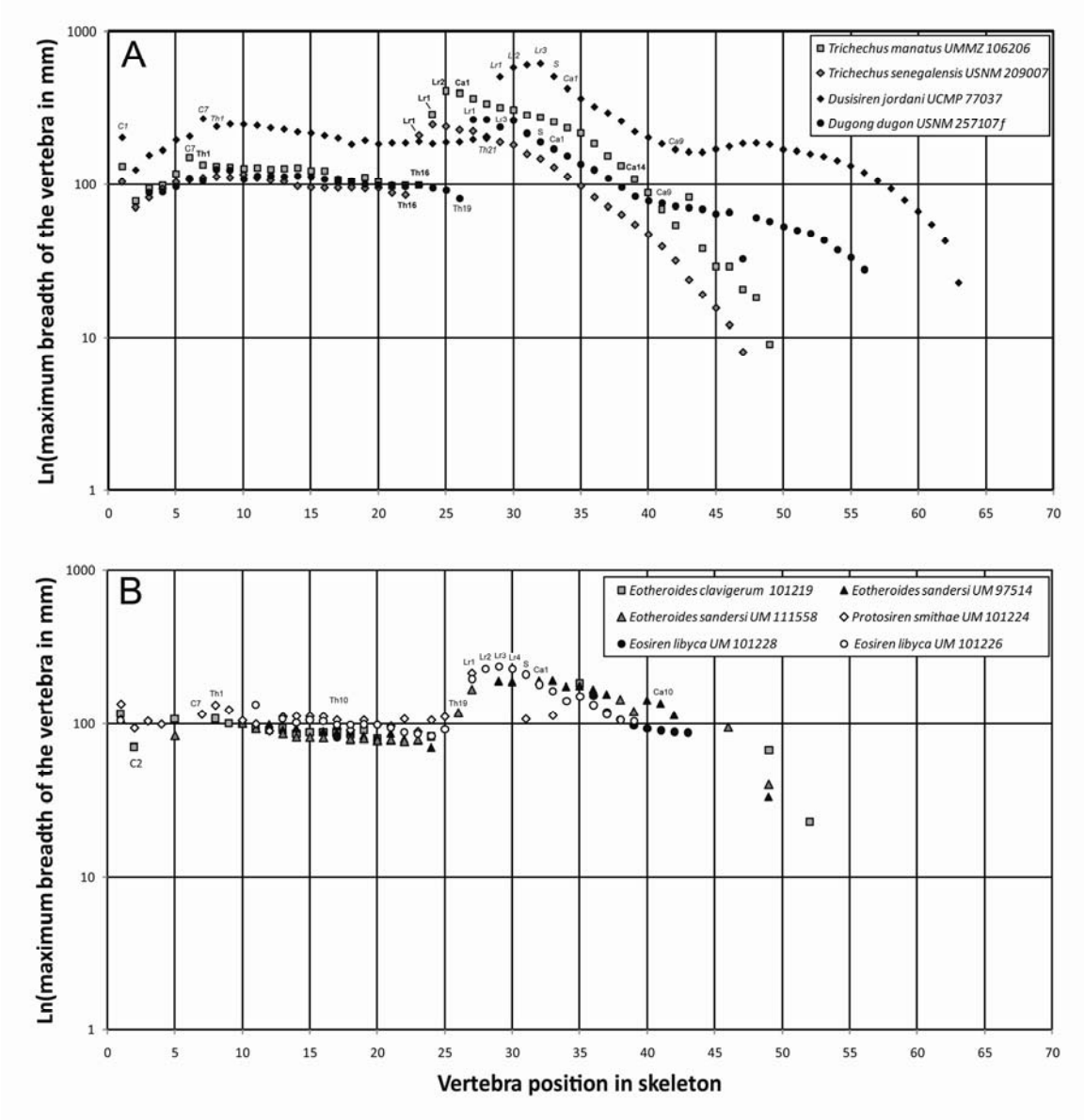

FIGURE 7.6 (A and B). Plots of total width/ total length ratios of vertebral centra in living and Eocene sirenian vertebral columns showing different patterns in lumbar and caudal morphologies along these profiles. The end of each profile, depending on the quality and completeness of the vertebral columns, may indicate whether a fluke was present or not based on comparison with *Dugong dugon* which has a fluke, or *Trichechus manatus* and *Trichechus senegalensis* which have a rounded tail. Dugong posterior caudal vertebrae have centra widths larger than anteroposterior lengths, in manatees the posterior caudal vertebrae tend to be long and narrow towards the tip of the tail. The trend in dugongs profiles (living and fossil) begins separating from the manatee's around Ca2 (Ca11 in manatees); after this the dugong vertebrae continue to be wider than longe with an abrupt change in the ratios as an indication of an active fluke present; in manatees the posterior caudal vertebrae are conservative in tapering towards the tip of the tail as no indication of fluke is present. Number of vertebrae and their regional distribution are different in Recent dugongs and manatees; manatees (dark closed triangles, abbreviations are below the triangles) have 6 cervicals, 16-17 thoracics, 2 lumbars, and 23 caudals; while dugongs (gray circles with abbreviations at the top) have 7 cervicals, 19 thoracic, 5-6 lumbars (including the sacrum), and 22-32 caudals. Abbreviations: **C**, cervical; **Ca**, caudal; **Lr**, lumbar, **Th**, thoracic; **S**, sacral. Data are in Table 7-6A and B; key to measurements are in the appendix of measurement.

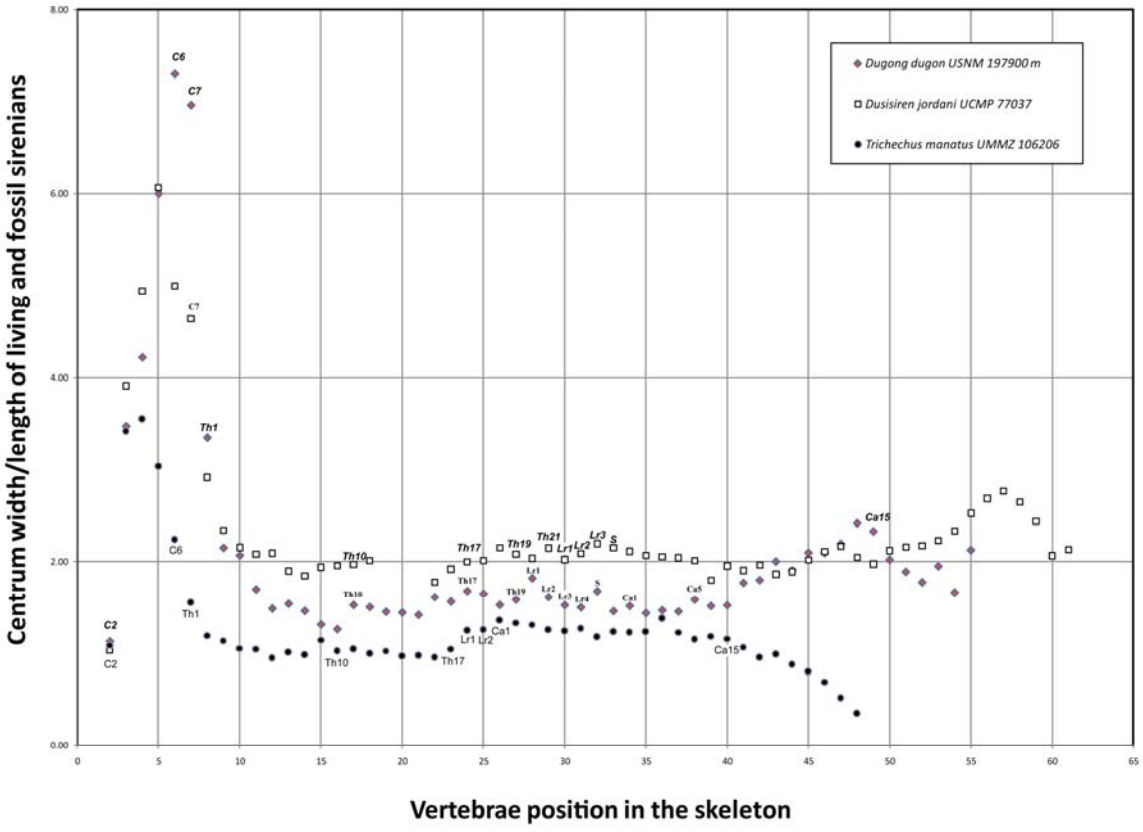
Centrum width/length of living and fossil sirenians
Vertebrae position in the skeleton
Dugong dugon USNM 197900 m
Dusisiren jordani UCMP 77037
Trichechus manatus UMMZ 106206
C6
C7
Th1
C2
Th10
Th17
Th19
Th21
Lr1
Lr2
Lr3
S
Ca1
Ca5
Ca15

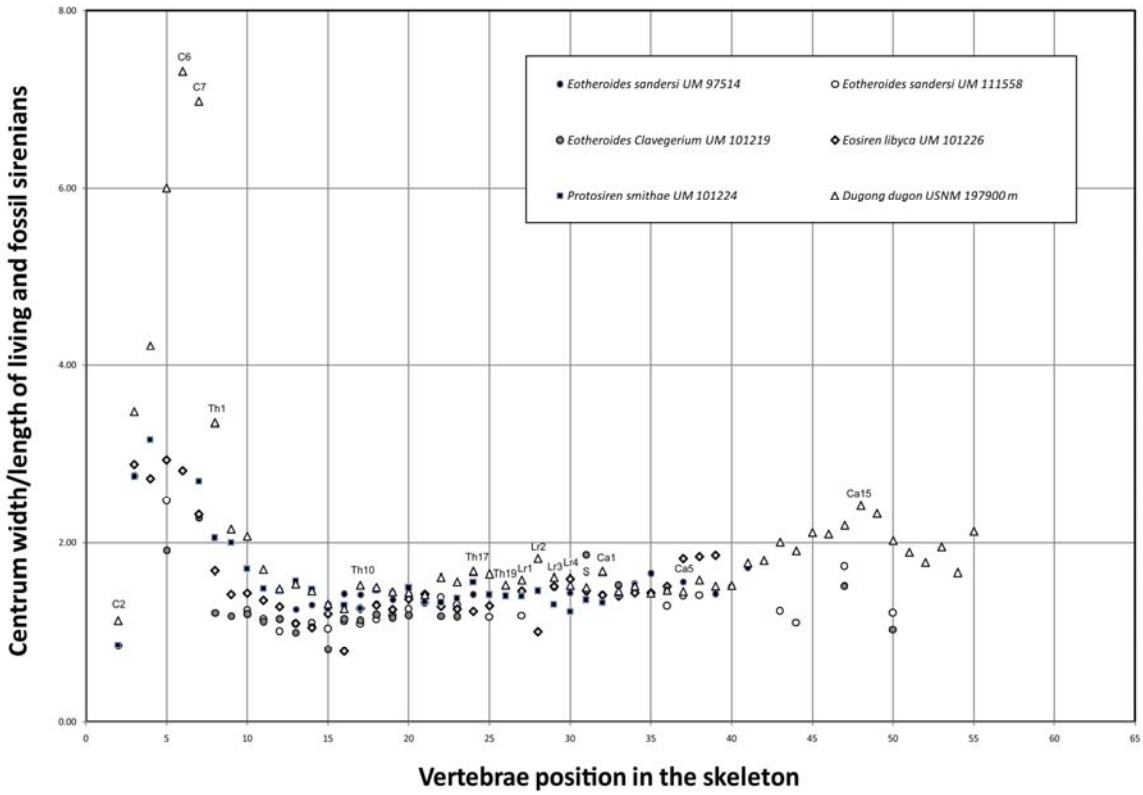
Centrum width/length of living and fossil sirenians
Vertebrae position in the skeleton
Eotheroides sandersi UM 97514
Eotheroides sandersi UM 111558
Eotheroides Clavegerium UM 101219
Eosiren libyca UM 101226
Protosiren smithae UM 101224
Dugong dugon USNM 197900 m
C6
C7
Th1
C2
Th10
Th17
Th19
Lr1
Lr2
Lr3
Lr4
S
Ca1
Ca5
Ca15

FIGURE 7.7. Cross-sectional variations in rib midshaft of Eocene sirenians compared to those of recent manatees. Notice the high expansion of cross-section of the anterior ribs in *Eotheroides* species compared to contemporaneous species and a living manatees. Data are in Table 7.7.

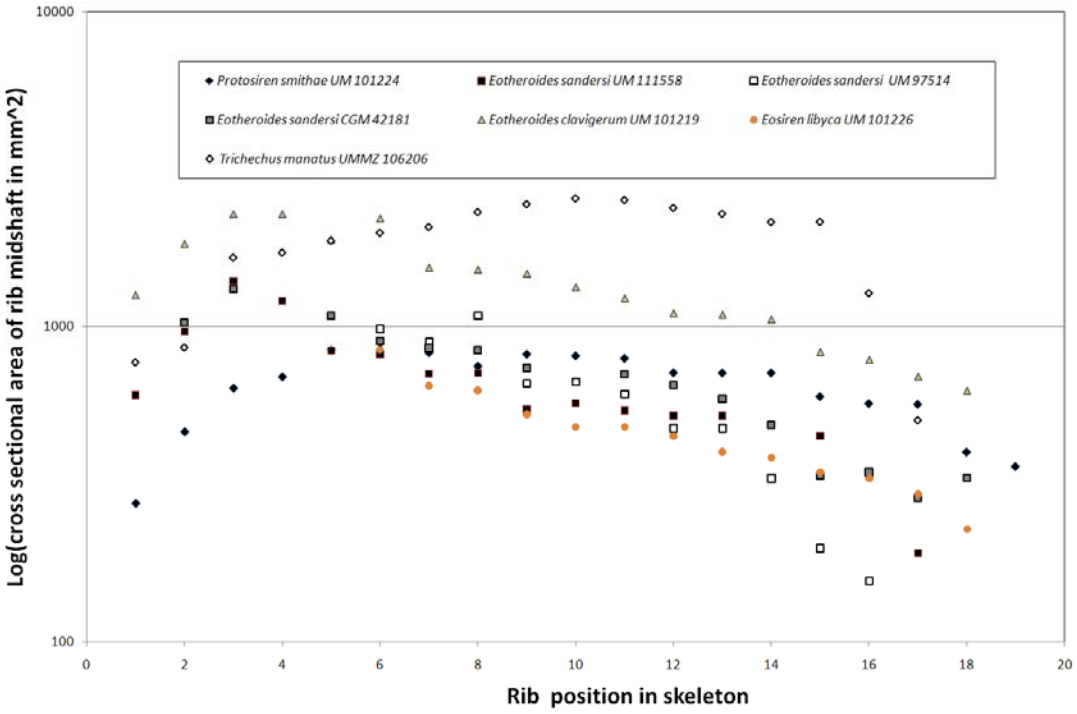

FIGURE 7.8. Proportional scatter plot of linear dimensions of scapula of several species of Eocene Sirenia from Egypt. Measured landmarks and abbreviations are after Domning (1978). Data are in Table 7.8; key is in the appendix of measurements.

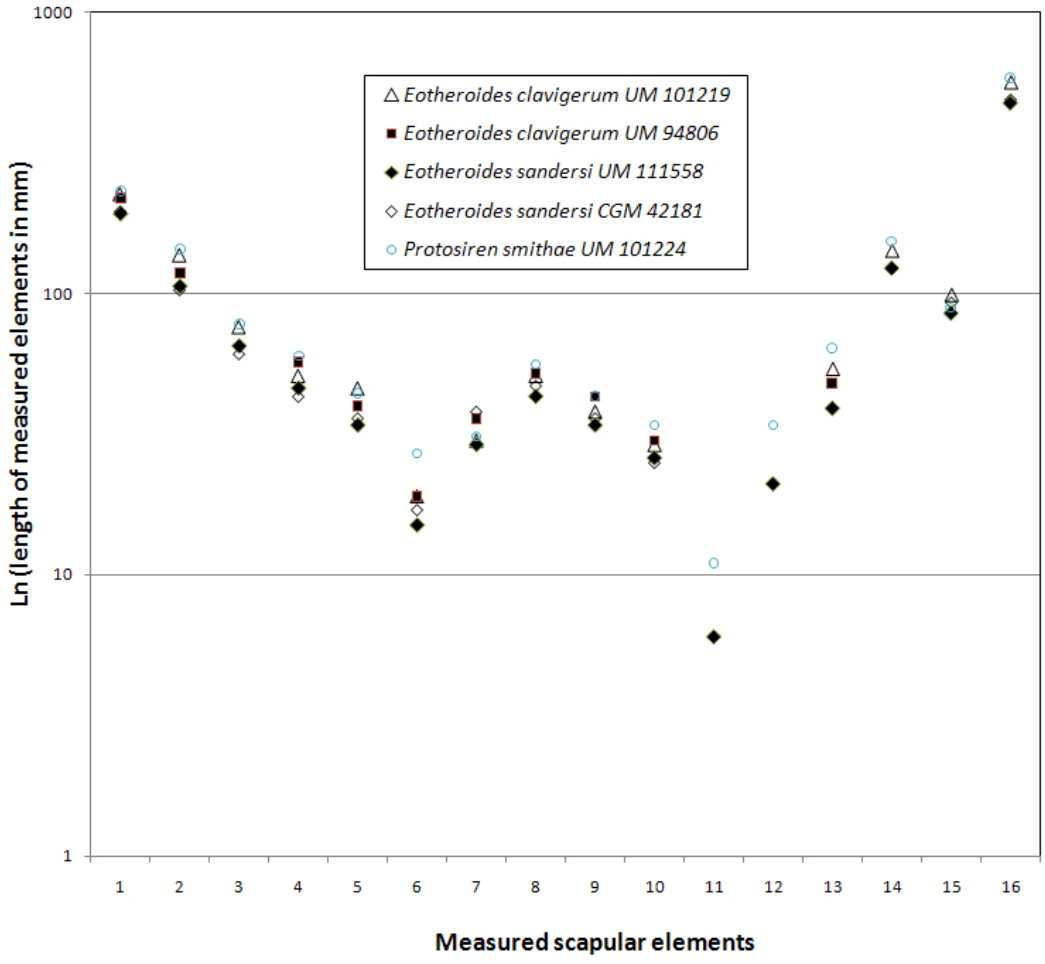

FIGURE 7.9. Proportional scatter plot of linear dimensions of humerus of several species of Eocene Sirenia from Egypt Data are in Table 9; key is in the appendix of measurements.

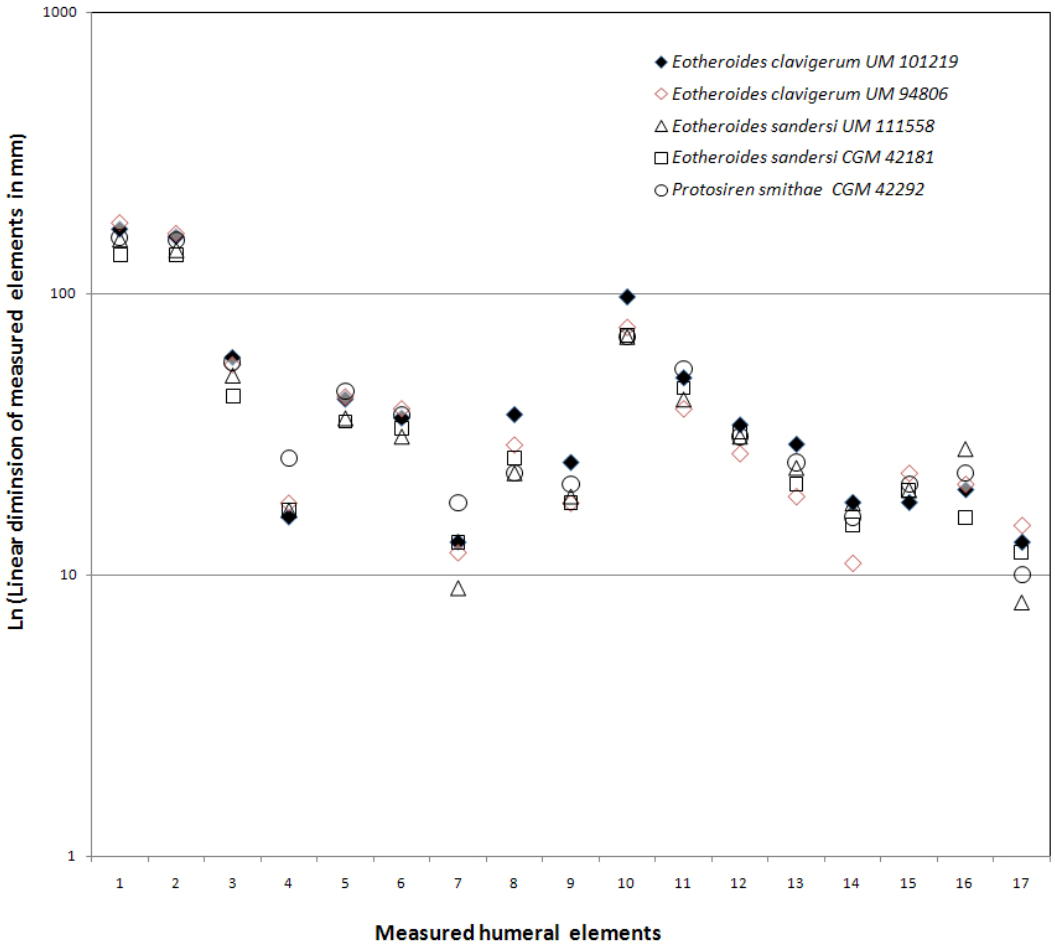

FIGURE 7.10. Proportional scatter plot of linear dimensions of ulna of several species of Eocene Sirenia from Egypt. Data are in Table 10; key is in the appendix of measurements.

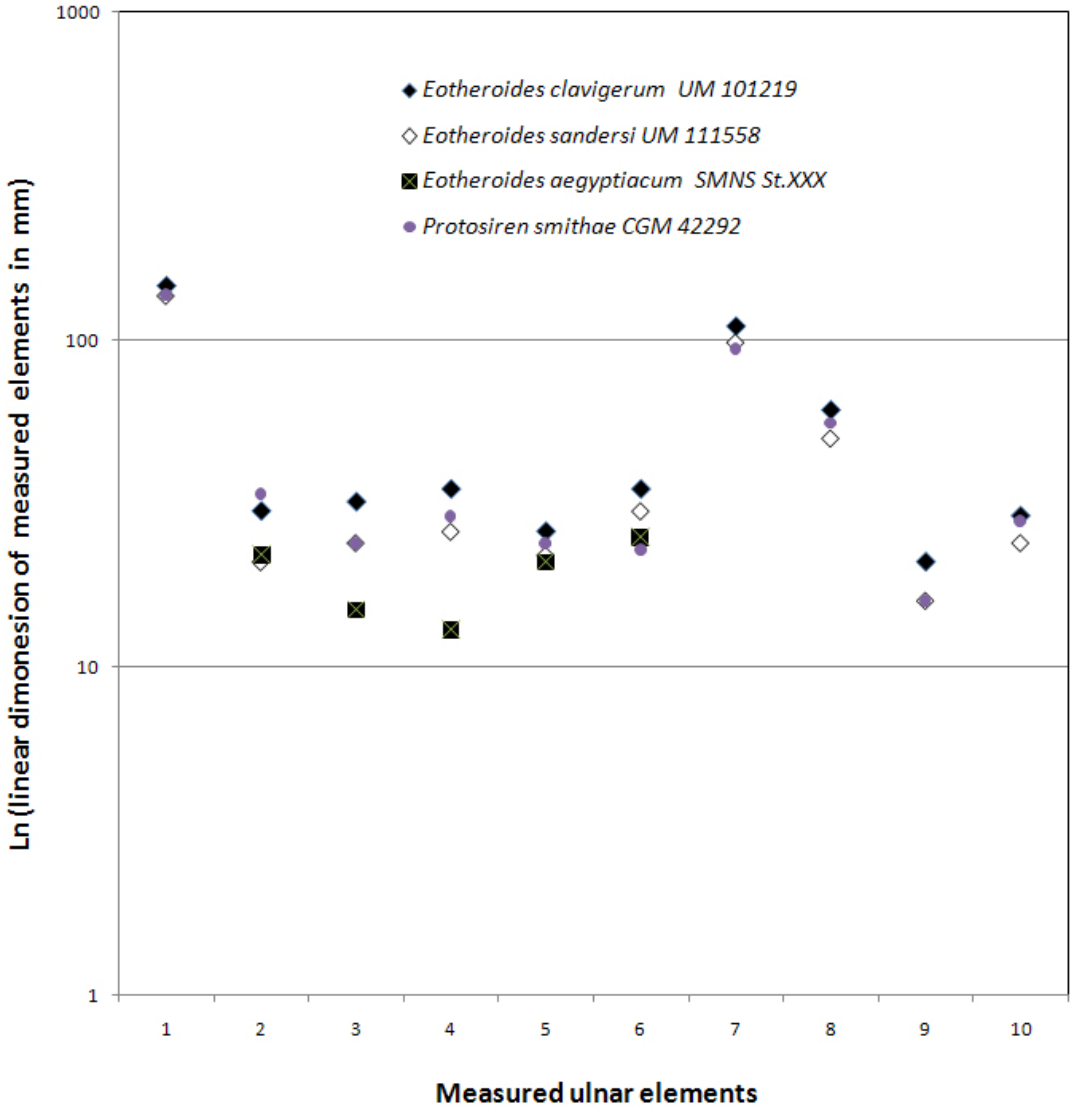

FIGURE 7.11. Proportional scatter plot of linear dimensions of innominate of several species of Eocene Sirenia from Egypt. Data are in Table 7.11; key is in the appendix of measurements.

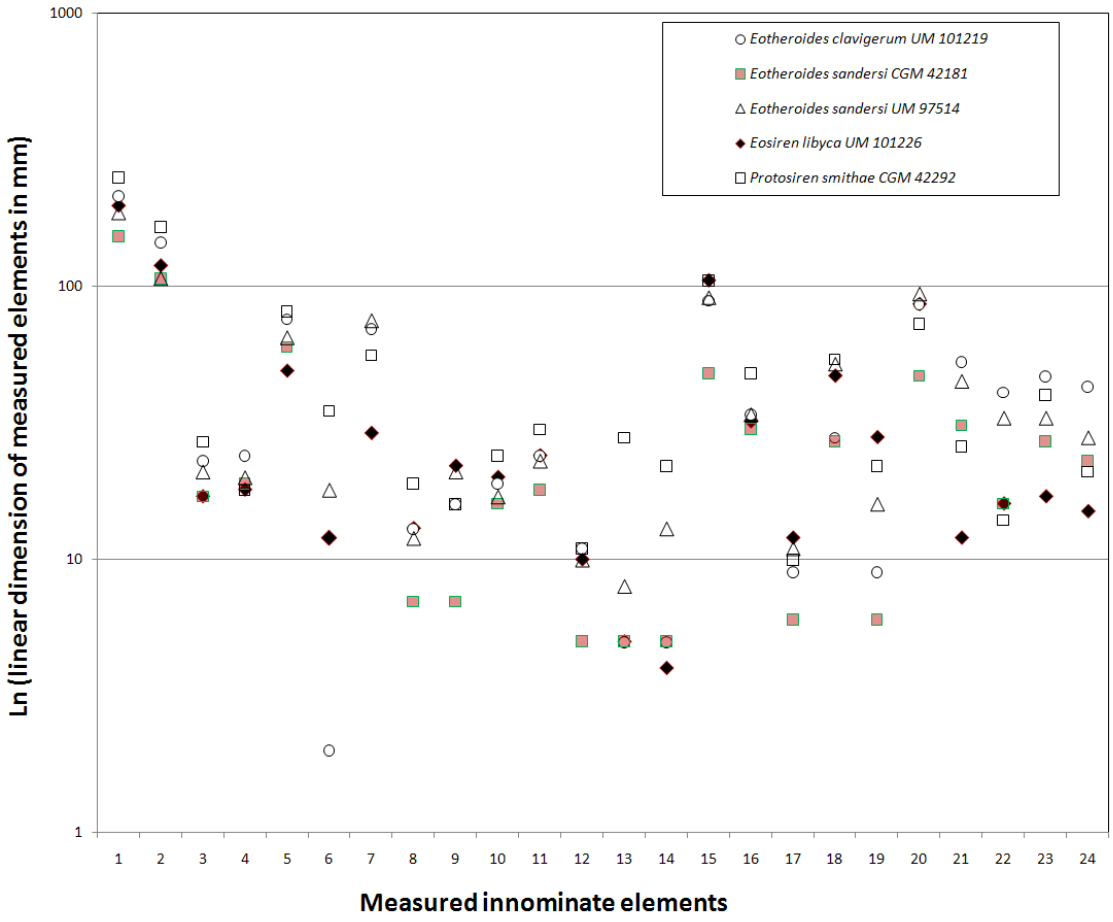

FIGURE 7.12. Proportional scatter plot of linear dimensions of femur of several Eocene species including those from the Eocene of Jamaica (Data of Daryl Domning, in preparation). *Pezosiren* (the Eocene semiaquatic Sirenia from Jamaica) and *Protosiren* have the largest femora with functional proximal and distal ends. Data are in Table 7.12; key is in the appendix of measurements.

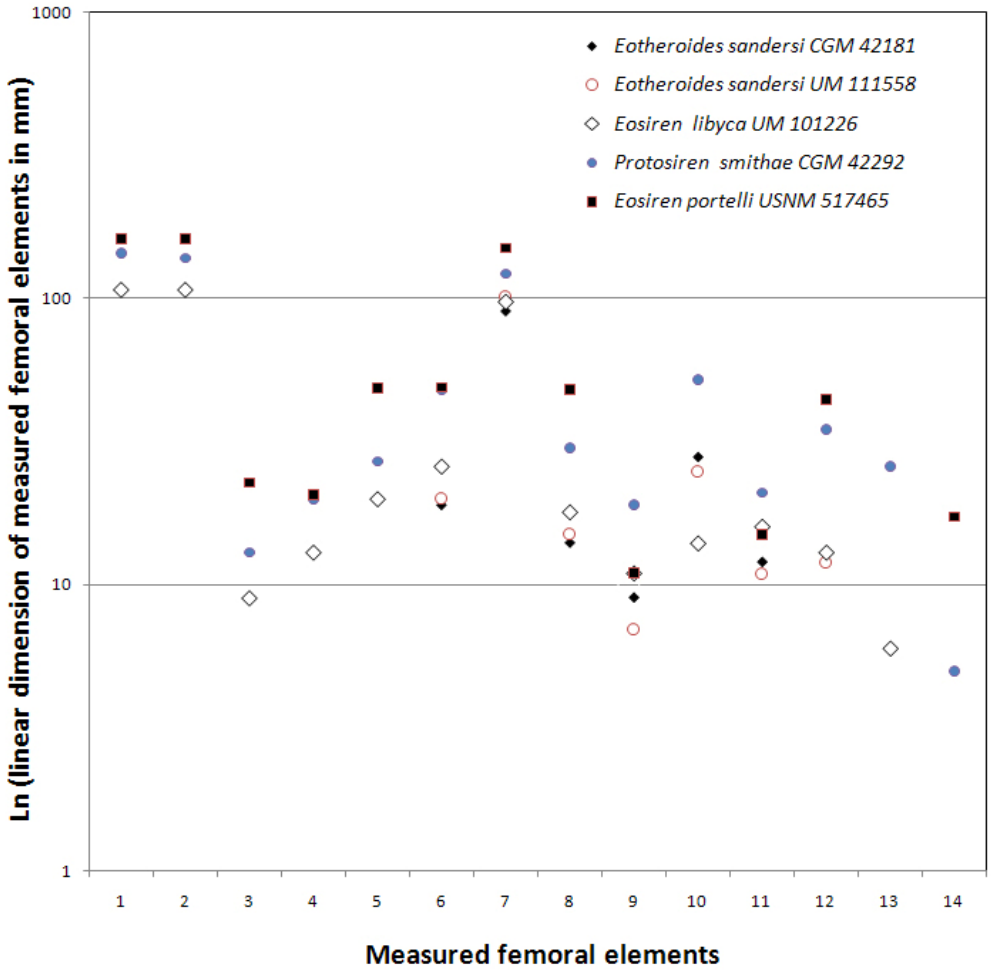

FIGURE 7.13. Proportional scatter plot of linear dimensions of tibia and fibula of Protosirenidae and Prorastomidae, no tibiae or fibulae of dugongs are known. Data are in Table 7.13; key is in the appendix of measurements.

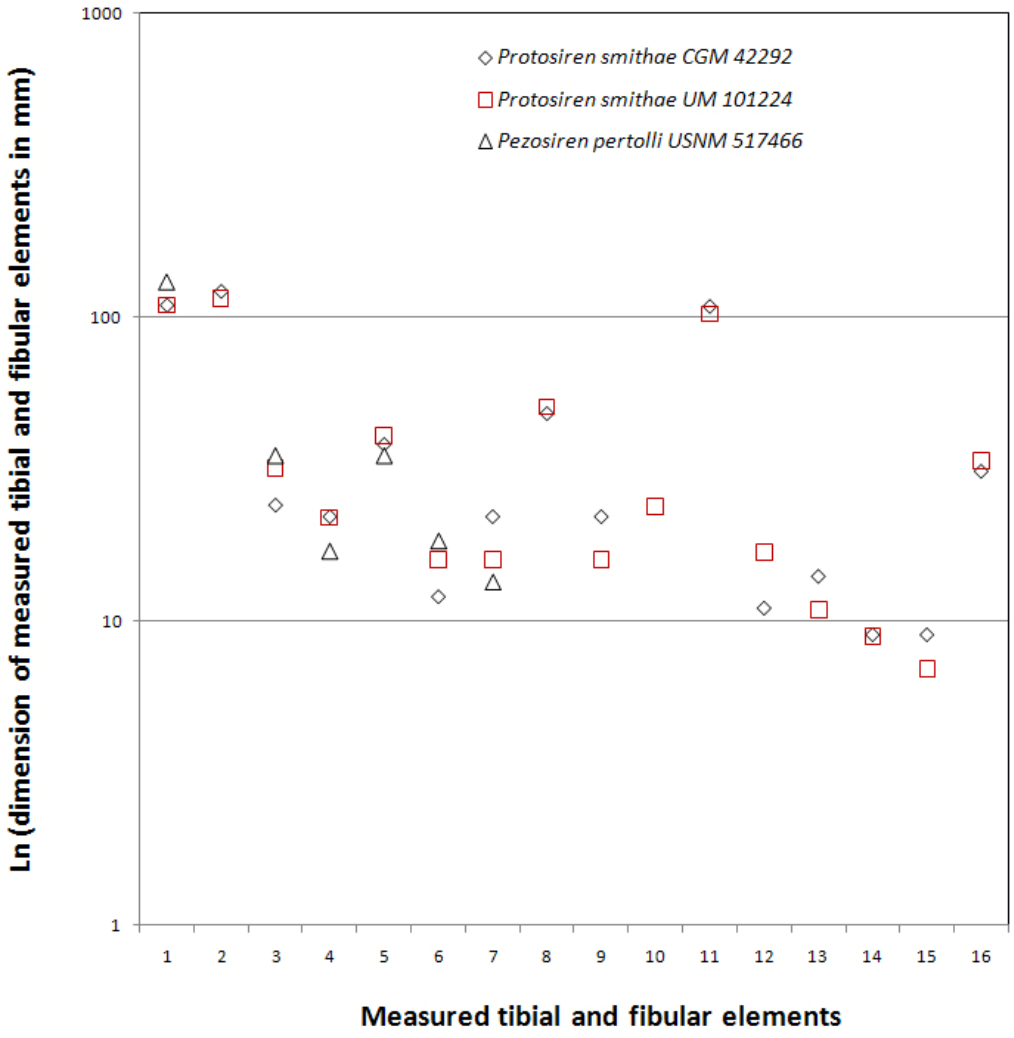

FIGURE 7.14. Variation of dental morphology and size in various Eocene Sirenia from Egypt including those from the Mokattam Hills. Data are in Tables 7.14 and 5.15; key is in the appendix of measurements.

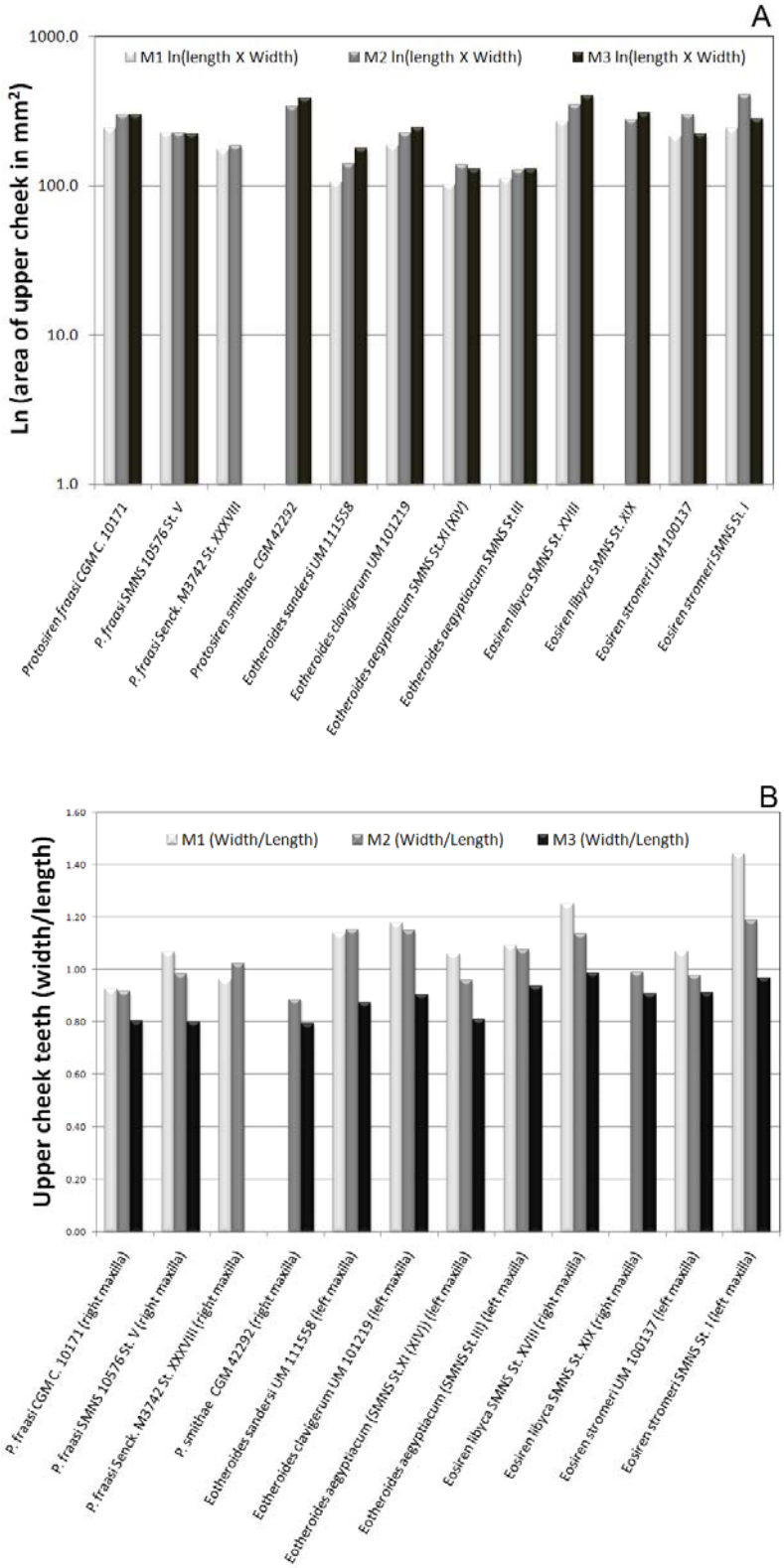

Literature Cited

ABEL, O. 1907. Die Stammesgeschichte der Meeressäugetiere. Meereskunde, 1:1-36.

ANDREWS, C. W. 1906. A Descriptive Catalogue of the Tertiary Vertebrata of the Fayum, Egypt. British Museum of Natural History, London, 324 pp.

ANDREWS, C. W. 1902. Preliminary note on some recently discovered extinct vertebrates from Egypt. (Part III.) Geological Magazine, 9:291-295.

CLEMENTZ, M. T., A. GOSWAMI, P. D. GINGERICH, and P. L. KOCH. 2006. Isotopic records from early whales and sea cows: contrasting patterns of ecological transition. Journal of Vertebrate Paleontology, 26:355-370.

CLEMENTZ, M. T., P. A. HOLROYD, and P. L. KOCH. Identifying aquatic habits of herbivorous mammals through stable isotopes analysis. Palaios, 23:574-585.

DOMNING, D. P. 1977. Observations on the myology of *Dugong dugon* (Müller). Smithsonian Contribution to Zoology, 226:iii+57.

DOMNING, D. P. 1978. The myology of the Amazonian manatee, *Trichechus inunguis* (Natterer) (Mammalia: Sirenia). Acta Amazonica, 8:1-81.

DOMNING, D. P. 1994. A phylogenetic analysis of the Sirenia. Proceedings of San Diego Society of Natural History, 29:177-189.

DOMNING, D. P. 2000. The readaptation of Eocene sirenians to life in water. In: J.-M. Mazin, V. de Buffrénil, and P. Vignaud (eds.), Secondary Adaptation of Tetrapods to Life in Water. Historical Biology (Special Issue), 14:115-119.

DOMNING, D. P. 2001a. Sirenians, seagrasses, and Cenozoic ecological change in the Caribbean. In: W. Miller III & S.E. Walker (eds.), Cenozoic Paleobiology: The

Last 65 Million Years of Biotic Stasis and Change. Palaeogeography, Palaeoclimatology, Palaeoecology, 166:27-50.

DOMNING, D. P. 2001b. The earliest known fully quadrupedal sirenian. Nature, 413:625-627.

DOMNING, D. P., G. S. MORGAN, and C. E. RAY. 1982. North American Eocene sea cows (Mammalia: Sirenia). Smithsonian Contribution to Paleobiology 52:1-69.

DOMNING, D. P., and H. THOMAS. 1987. *Metaxytherium serresii* (Mammalia: Sirenia) from the Early Pliocene of Libya and France: a reevaluation of its morphology, phyletic position, and biostratigraphic and paleoecological significance; pp. 205-232 in N. T. BOAZ, A. EL-ARNAUTI, A. W. GAZIRY, J. DE HEINZELIN, and D. D. BOAZ (eds.), Neogene paleontology and geology of Sahabi. Alan R. Liss, Inc, New York.

DOMNING, D. P., and V. DE BUFFRÉNIL. 1991. Hydrostasis in the Sirenia: quantitative data and functional interpretations. Marine Mammal Science, 7:331-368.

DOMNING, D. P., and P. D. GINGERICH. 1994. *Protosiren smithae*, new species (Mammalia, Sirenia), from the late Middle Eocene of Wadi Hitan, Egypt. Contributions from the Museum of Paleontology. University of Michigan, 29:69-87.

DOMNING, D. P., and P. PERVESLER. 2001. The osteology and relationships of *Metaxytherium krahuletzi* Deperet, 1895 (Mammalia: Sirenia) Abhandlungen der Senckenbergischen Naturforschenden Gesellschaft, 553:1-89.

DOMNING, D., and B. BEATTY. 2007. Use of tusks in feeding by dugongid sirenians: observation and tests of hypotheses. The Anatomical record, 290:523-538.

FRAAS, E. 1904. Neue Zeuglodonten aus dem unteren Mitteleocän vom Mokattam bei Cairo. Geologische und Paläontologische Abhandlungen, Jena, 6:197-220.

GINGERICH, P.D., D.P. DOMNING, C.E. BLANE, and M. UHEN. 1994. Cranial morphology of *Protosiren fraasi* (Mammalia, Sirenia) from the Middle Eocene of Egypt: a new study using computed tomography. Contributions from the Museum of Paleontology. University of Michigan, 29:41- 67.

GINGERICH, P. D., M. ARIF, M. A. BHATTI, H. A. RAZA, and S. M. RAZA. 1995. *Protosiren* and *Babiacetus* (Mammalia, Sirenia and Cetacea) from the middle Eocene Drazinda Formation, Sulaiman Range, Punjab (Pakistan). . Contributions from the Museum of Paleontology, University of Michigan, 29:331-357.

GREEN, E. P., and F. T. SHORT. 2003. World Seagrass Atlas; in E. P. GREEN and F. T. SHORT (eds.). UNEP World Conservation Monitoring Centre, UCP, Berkely, 286 pp.

HARTMAN, D. 1979. Ecology and behavior of the manatee (*Trichechus manatus*) in Florida, Volume Special Publication No. 5. The American Society of Mammalogists, vii+153 pp pp.

JARMAN, P. J. 1966. The status of the dugong (*Dugong dugon* Müller) in Kenya. East African Wildlife Journal, 4:82-88.

KOJESZEWSKI, T., and F. E. FISH. 2007. Swimming kinematics of the Florida manatee (*Trichechus manatus latirostris*): Hydrodynamic analysis of an undulatory mammalian swimmer. Journal of Experimental Biology, 210:2411-2418.

LIU, A. G. S. C., E. R. SEIFFERT, and E. L. SIMONS. 2008. Stable isotope evidence for an amphibious phase in early proboscidean evolution. Proceedings of the The National Academy of Sciences of the United States of America, 105:5786–5791.

MACFADDEN, B. J., P. HIGGINS, M. T. CLEMENTZ, and D. S. JONES. 2004. Diets, habitat preferences, and niche differentiation of Cenozoic sirenians from Florida: Evidence from stable isotopes. Paleobiology, 30:297-324.

OWEN, R. 1855. On the fossil skull of a mammal (Prorastomus sirenoides Owen) from the island of Jamaica. Quarterly Journal of the Geological Society of London, 11:541-543.

PREEN, A. 1995. Diet of dugongs: are they omnivores? Journal of Mammalogy, 76:163-171.

REID, J. P. 1996. Chessie the manatee: from Florida to Rhode Island. Argos Newsletter, 15:13.

SAVAGE, R.J.G., D.P. DOMNING, and J.G.M. THEWISSEN. 1994. Fossil Sirenia of the West Atlantic and Caribbean region. V. The most primitive known sirenian, *Prorastomus sirenoides* Owen, 1855. Journal of Vertebrate Paleontology, 14:427-449.

THEWISSEN, J. G. M., and D. P. DOMNING. 1992. The role of phenacodontids in the origin of the modern orders of ungulate mammals. Journal of Vertebrate Paleontology, 12:494-504.

CHAPTER EIGHT

SUMMARY

The purpose of this study was to report, describe, and interpret morphologies and adaptations of new sea cow fossils from the late Eocene of the Fayum Basin, Egypt. Chapters one and two present a review of the geology, stratigraphy, and sirenian faunal contents including the new material of the Wadi Al Hitan UNISCO World Heritage Site. Chapter three reviews the systematics, temporal and spatial distribution of Cenozoic African sea cows. Chapter four includes detailed diagnosis, description, affinities and relationships of the new fossil seacows from Wadi Al Hitan. Chapter five details morphological variations in the pelvic bone of Eocene sea cows and explores the possibility of sexual dimorphism. Chapter six reviews the paleoenvironment and paleoecology of marine mammal bearing beds in Egypt. Chapter seven summarizes morphological variations in Egyptian Eocene sea cow skeletal and dental elements.

Some of the facts and conclusions about Wadi Al Hitan sea cows can be summarized as fellows:

1) The richly fossiliferous marine mammal bone-bearing beds of middle and late Eocene sediments of the Wadi Al Hitan in the Western Desert of Egypt are important for understanding the morphology and evolution of Eocene sirenians in Africa. *Protosiren*, *Eotheroides*, and *Eosiren* are all known from Wadi Al Hitan and the Fayum Basin, and all are represented by exceptionally complete skulls and axial skeletons with pectoral and pelvic girdles.

2) Preservation and articulation patterns in Wadi Al Hitan were mostly governed by physical factors rather than biological. The Birket Qarun and most of Qasr El Sagha formations were deposited in a quiet and restricted environment, close to the shoreface. Repetition of thick fine sandstone, shale, and clays, and their lateral variations and shifting from one facies to another in a shallowing upward sequence, as in the Wadi Al Hitan, is diagnostic of a lagoonal or estuarine environment. These lagoons and estuaries were greatly controlled by tectonically active NE Africa and eustacy. Lutetian and Bartonian carbonate rocks of the Wadi Al Rayan Series were mostly nummulitic with slightly siliciclastic and glauconitic components, and were deposited in a deeper environment than those of the Birket Qarun and Qasr El Sagha formations.
3) The skeletal remains of *Protosiren* and *Eotheroides* of the Birket Qarun Formation are of special interest because they represent an intermediate stage of evolution and an intermediate stage of secondary adaptation to life in water.
4) *Protosiren smithae* of Domning and Gingerich (1994) is a direct descendant of *Protosiren fraasi*, and these species differ from contemporary sirenians (*Eotheroides*) in being larger; having slight rostral deflection; having osteosclerotic postcranial elements lacking pachyostosis; having thoracic through lumber vertebrae with spinous processes higher than those of any other sirenian, having thoracic vertebrae with a keyhole-shaped vertebral canal; and having rib heads with a cartilaginous, rather than fully-ossified, articular surface. *Protosiren* retained larger hind limbs than contemporaneous sirenians, although these were

highly reduced compared to hind limbs of land mammals and they were incapable of supporting the weight of the body on land.

5) *Eotheroides clavigerum* sp. nov. and *Eotheroides sandersi* sp. nov. are most similar to *Eotheroides aegyptiacum* (Owen, 1875) from the Lutetian nummulitic limestone beds of Cairo as they share the following derived characteristics: prominent falx cerebri and bony tentorium in the roof of the braincase; nasals long and in contact along the midline; palate broad with its posterior border posterior to the toothrow; and anterior ribs pachyosteosclerotic. Wadi Al Hitan *Eotheroides* were medium to large dugongs, ranging in length from 1.5 to 2.5 m; the skull is robust and heavy; the rostrum is deflected and bears medium to diminutive tusks; the trunk is widest between the ninth and eleventh thoracics; the end of the tail was fluked; the pelvis is greatly reduced with a shallow acetabulum, but retains an expanded, club-like ilium, and the femur is short and slender. There cannot have been any substantial lower leg or foot. Of all cranial and postcranial elements, extensively pachyosteosclerotic anterior ribs and club-like ilia are central in diagnosis of the genus and its species. *Eotheroides*, like *Eosiren*, had more reduced hind limbs compared to those of *Protosiren* and both were fully aquatic.

6) *Eosiren libyca* Andrews (1902) and *Eosiren stromeri* (Sickenberg, 1934) are limited to the Qasr el Sagha Formation and neither of these species have been found in older units. Both species of *Eosiren* are similar to species of *Eotheroides*. However, in *Eosiren* the ribs are gracile and osteosclerotic but not pachyostotic,

and the ilium is narrow and rod-like. In *Eosiren stromeri* the M^2 is always larger than M^3, a consistent difference from *Eosiren libyca*.

7) Seagrass preserved as leaf impressions in Priabonian marine mammal beds is a direct indicator of the shallowness of Tethyan waters in the Fayum Basin. This corner of Africa was a special environment that supported sirenian faunas for more than 13 million years (middle to late Eocene) and sea cows survived here through the early Oligocene. The coexistence of *Protosiren smithae*, *Eotheroides clavigerum*, and *Eotheroides sandersi* in the same biotope reflects the diversity of this group in early Priabonian Tethys. The morphological diversity reflects dietary and environmental specialization and niche partitioning. The presence of associated seagrass fossils in both the Birket Qarun and Qasr El Sagha Formations implies that they were deposited in settings that are less than 10 meters deep.
8) Protosirenidae, Dugongidae and Trichechidae (including: *Anomotherium* of Siegfried 1965 and *Miosiren* of Dollo 1889) are the only sirenian families that are known to have lived in the nearshore habitats of the African continent, although it is not unlikely that Prorastomidae were once represented there as well. Dugongidae account for more than 85% of Africa's sirenian fossil record. No trichechid fossils have been found in Africa, but the living West African manatee probably arrived there from the New World in the late Pliocene or Pleistocene.
9) The most important skeletal elements for the diagnosis of *Eotheroides* species are the anteriorly extensively pachyosteosclerotic ribs, and the innominates with their club-like ilia. The morphology of the skeletal elements of Lutetian and Priabonian *Eotheroides* are characteristic of fully aquatic marine mammals.

These large marine herbivores spent their life in water either grazing on seagrass meadows in the tidal zone or consuming planktonic algae and floats from the surface. Distal thickening of the ischium can be used as sexing criterion in Eocene sirenian innominates. In all supposed males the ratio of the mediolateral thickness of the distal end to the mediolateral thickness of the ischiatic ramus is between 1.8 and 2.3, while in putative females the ratio is between 0.8 and 1.0.

APPENDIX

Key to landmarks for cranial element measurements used in the study based on Domning (1978). A, lateral view; B, dorsal view; D, palatal view; C, ventral view of *Protosiren fraasi* maxilla showing dental measurements used in the study.

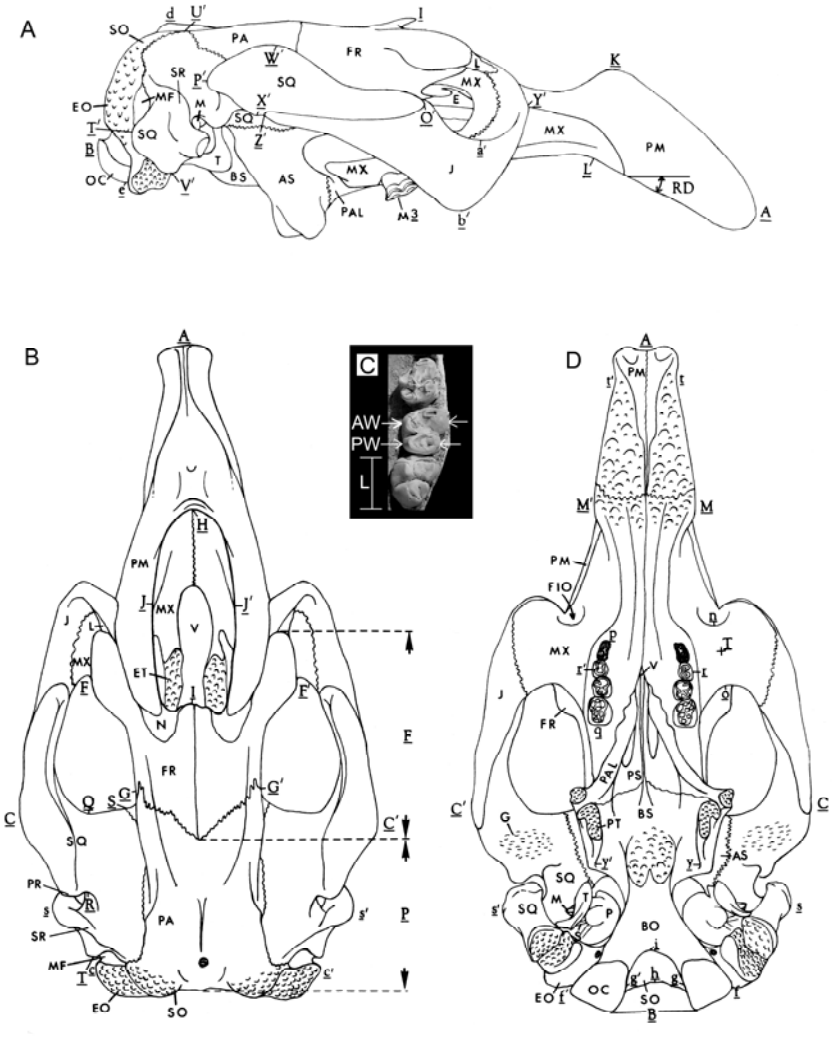

Key to landmarks for mandibular measurements used in the study based on Domning (1978). A, dorsal view; B, lateral view.

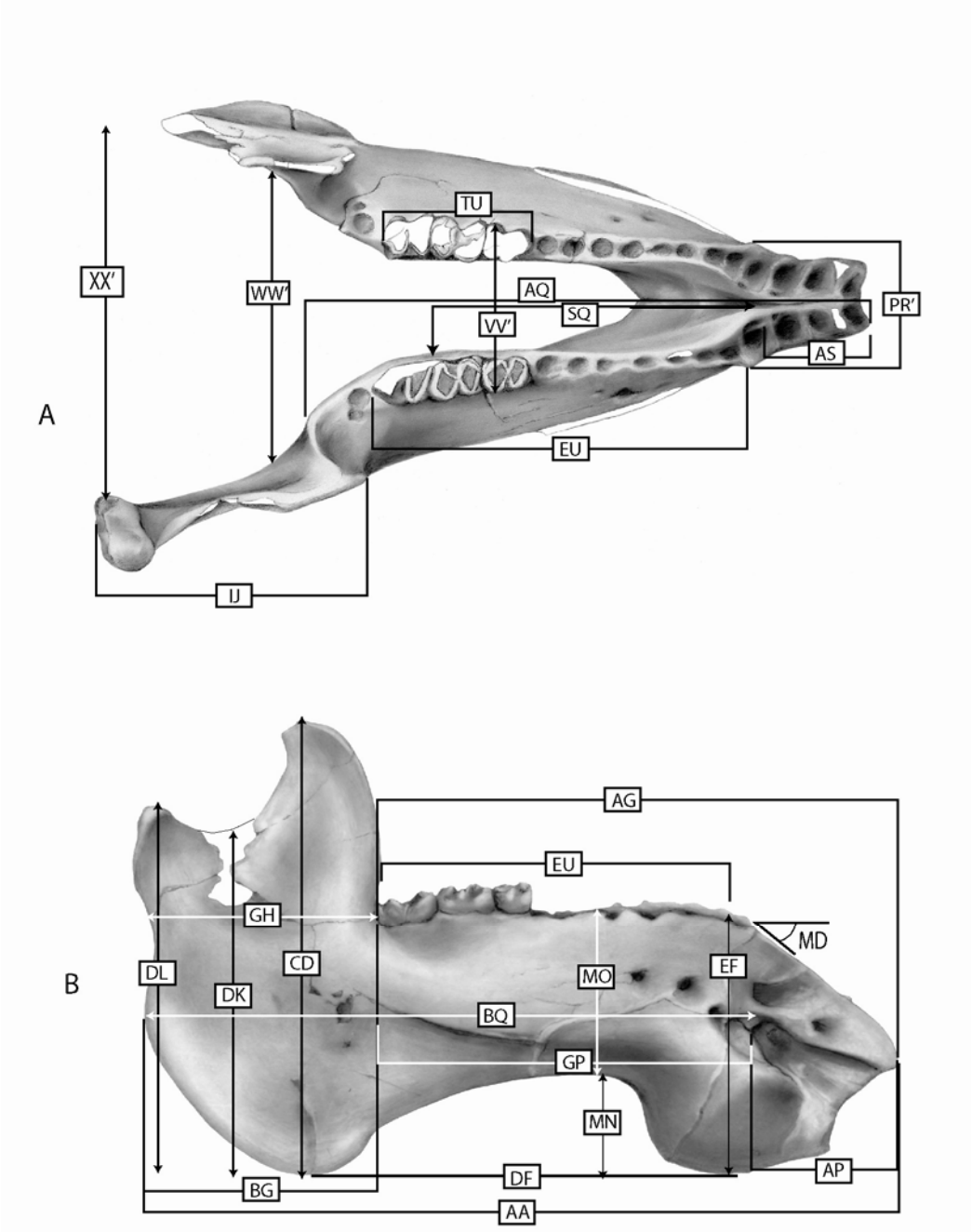

Key to landmarks for vertebral measurements used in the study. A, cranial view; B, lateral view.

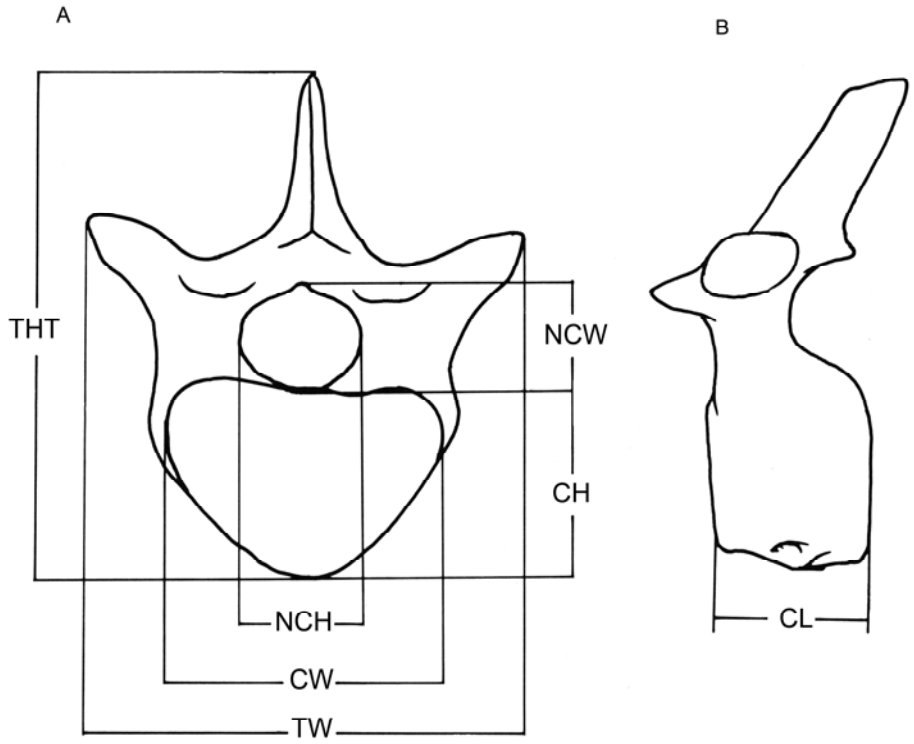

Key to landmarks for rib measurements used in the study. Rib is in cranial view.

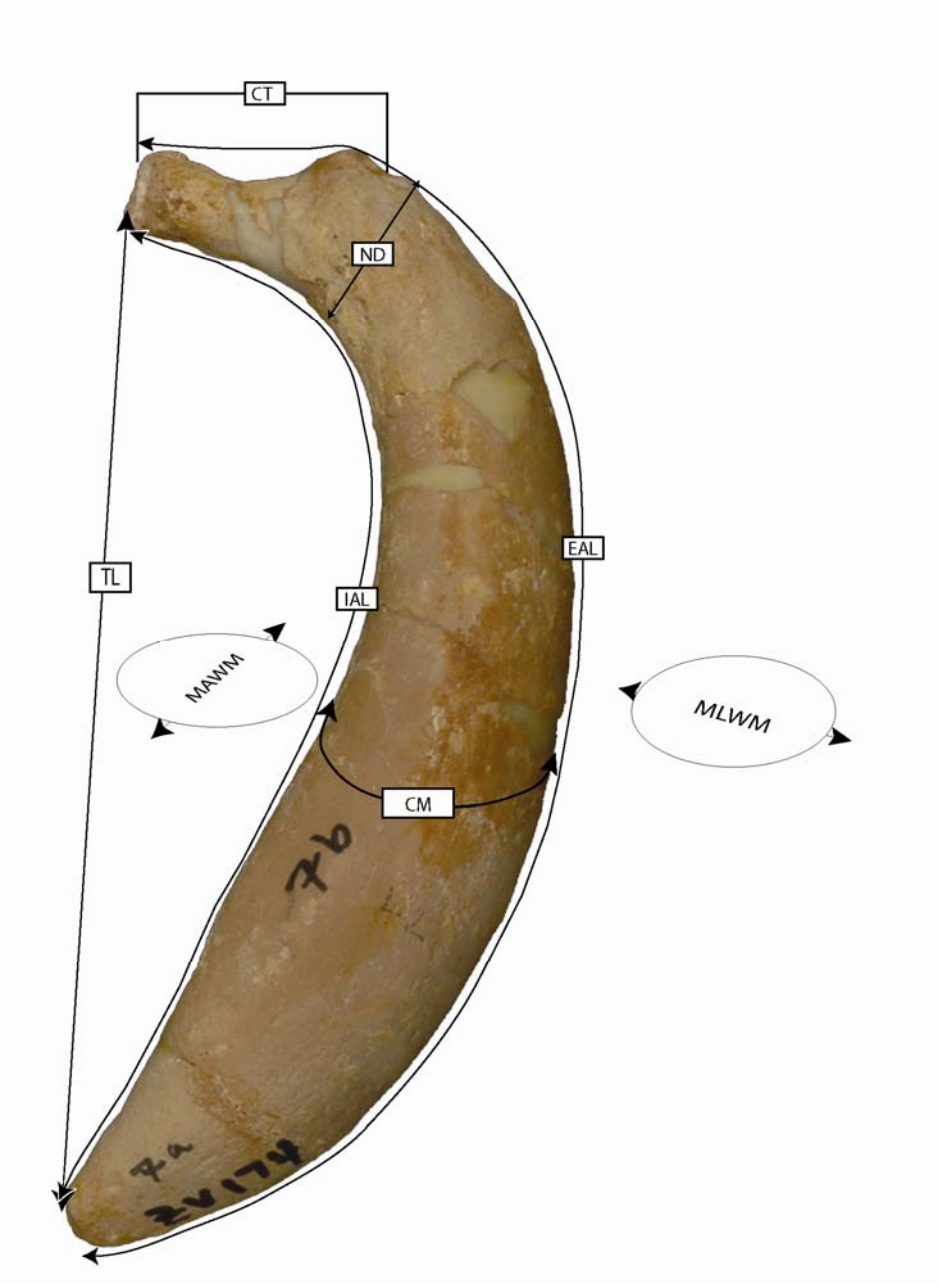

Key to landmarks for scapular measurements used in the study. A, lateral view; B, posterior view.

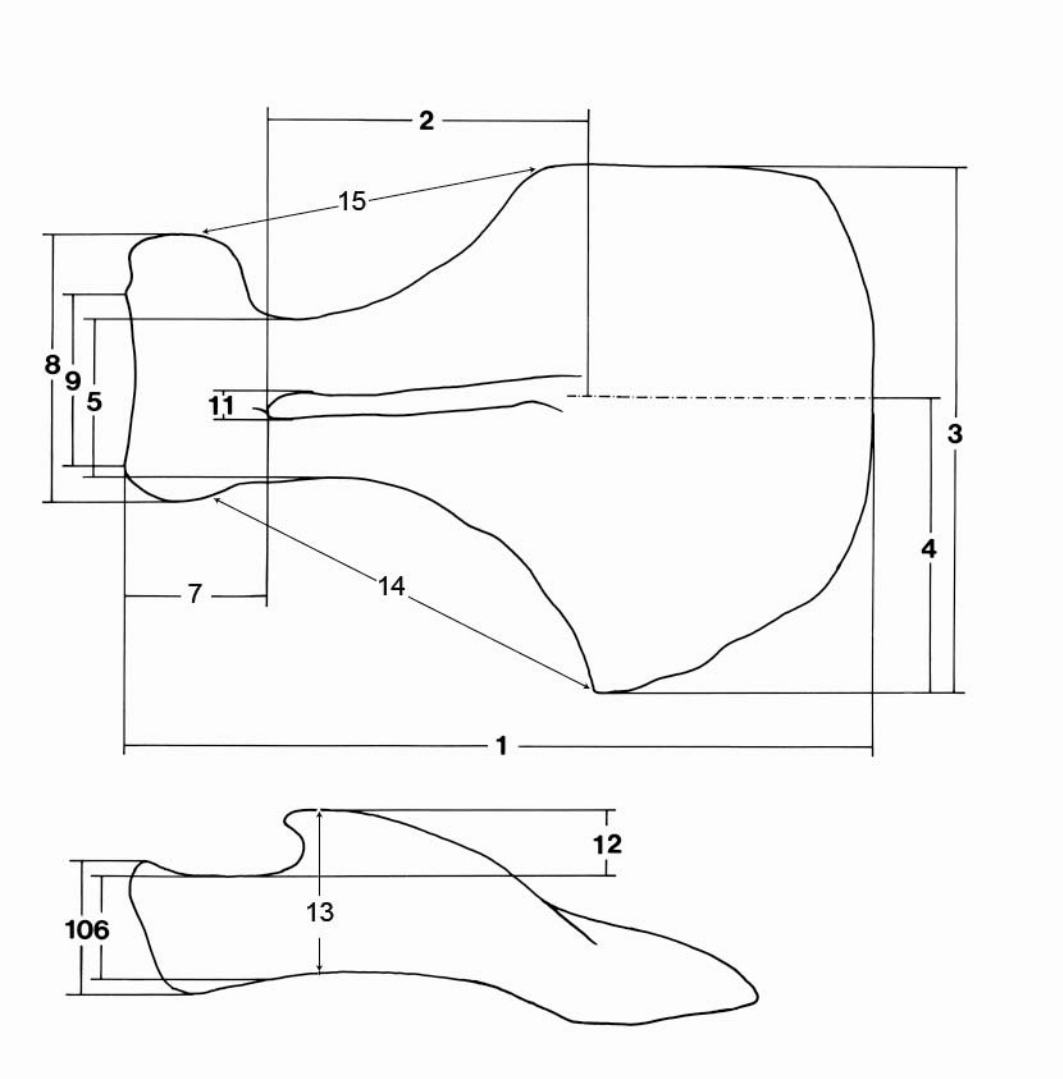

Key to landmarks for humeral measurements used in the study. A, anterior view; B, posterior view; C, medial view; D, proximal view; E; distal view.

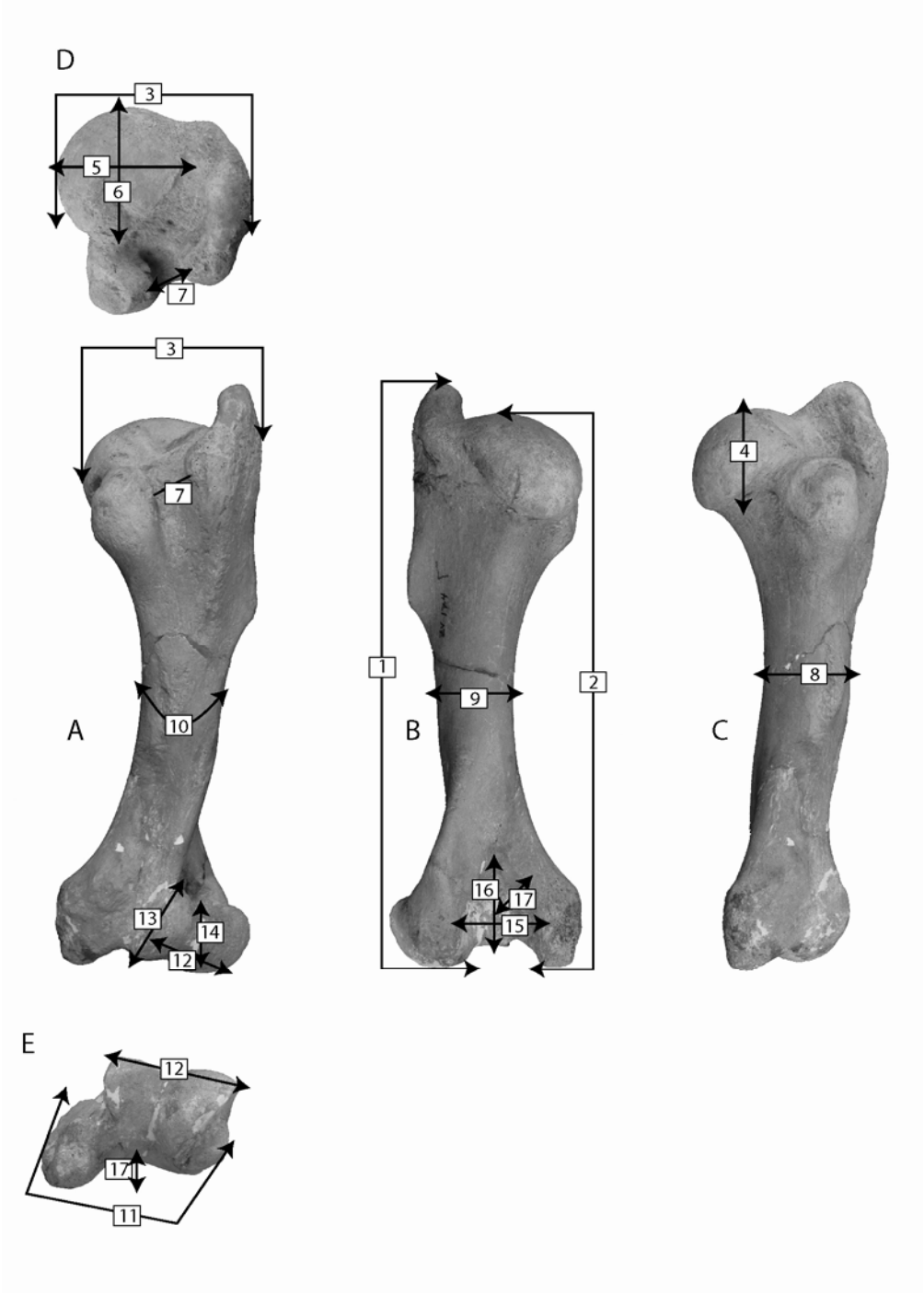

Key to landmarks for ulnar measurements used in the study. A, medial view; B, lateral view; C, anterior view; D, proximal view; E; distal view.

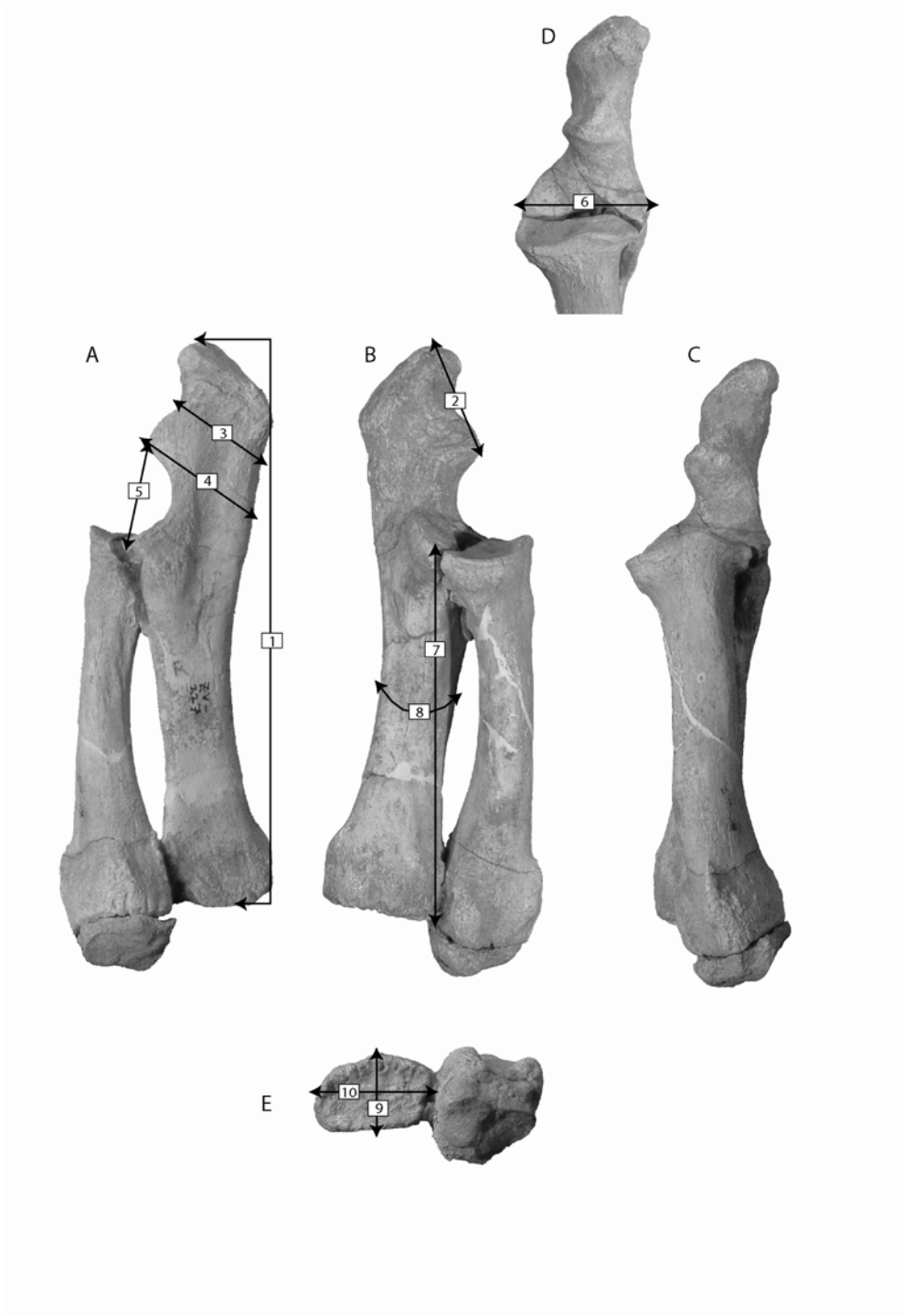

Key to landmarks for radial measurements used in the study. A, medial view; B, lateral view; C, anterior view; D, proximal view; E; distal view.

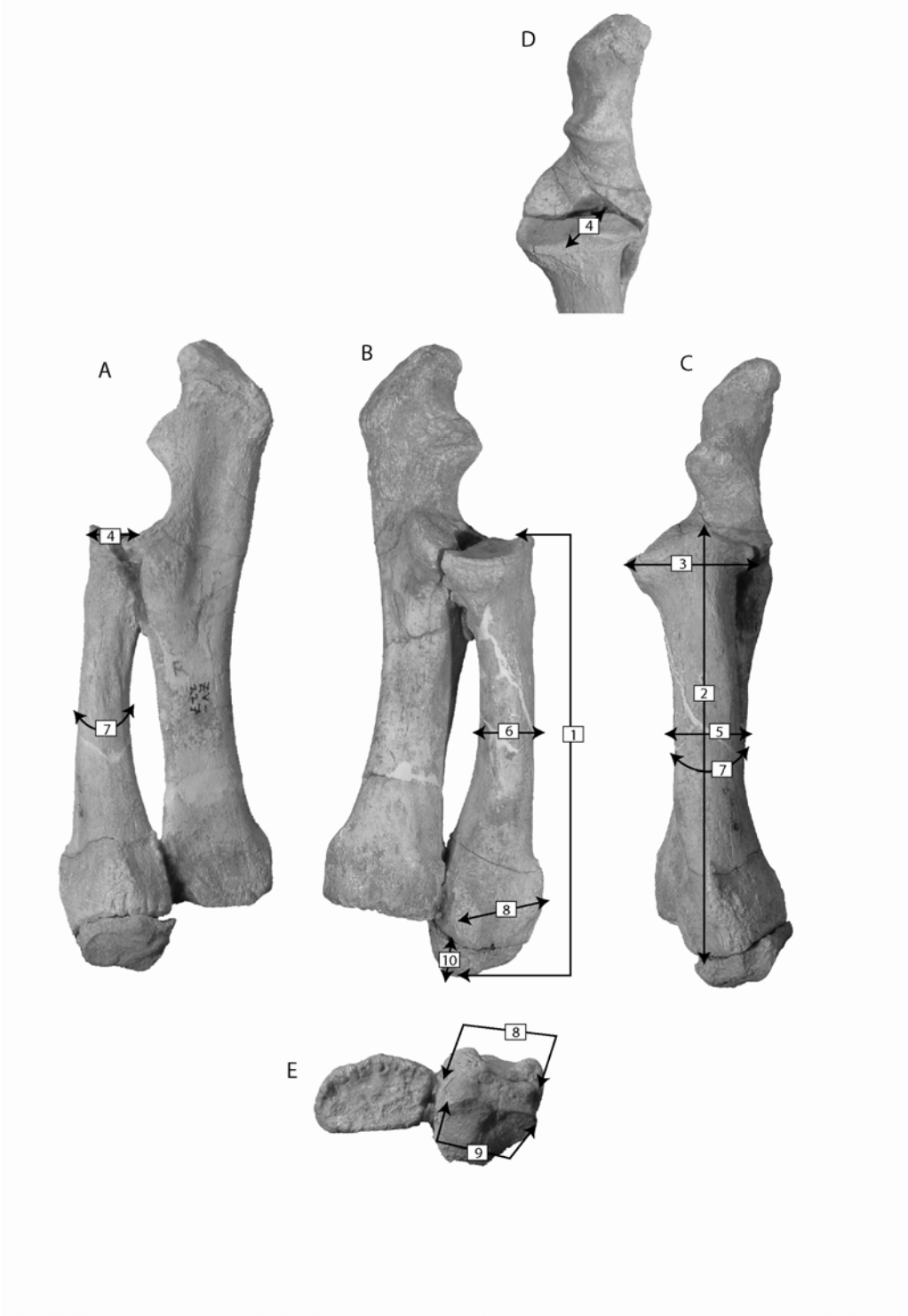

Key to landmarks for pelvic bone measurements used in the study. A, Lateral view; B, medial view; C, dorsal view; D, posterior view.

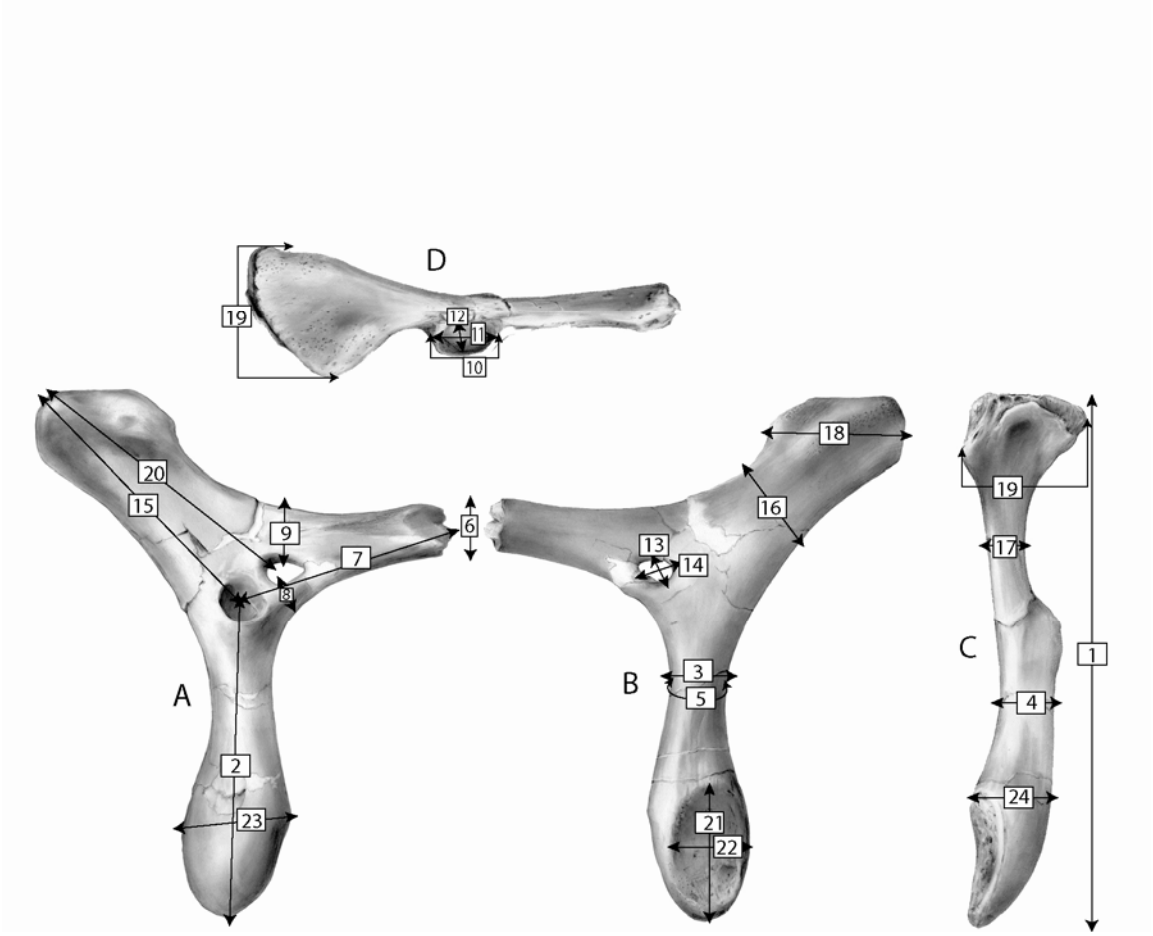

Key to landmarks for femoral measurements used in the study. A, medial view; B, anterior view; C, posterior view; D, proximal view; E; distal view.

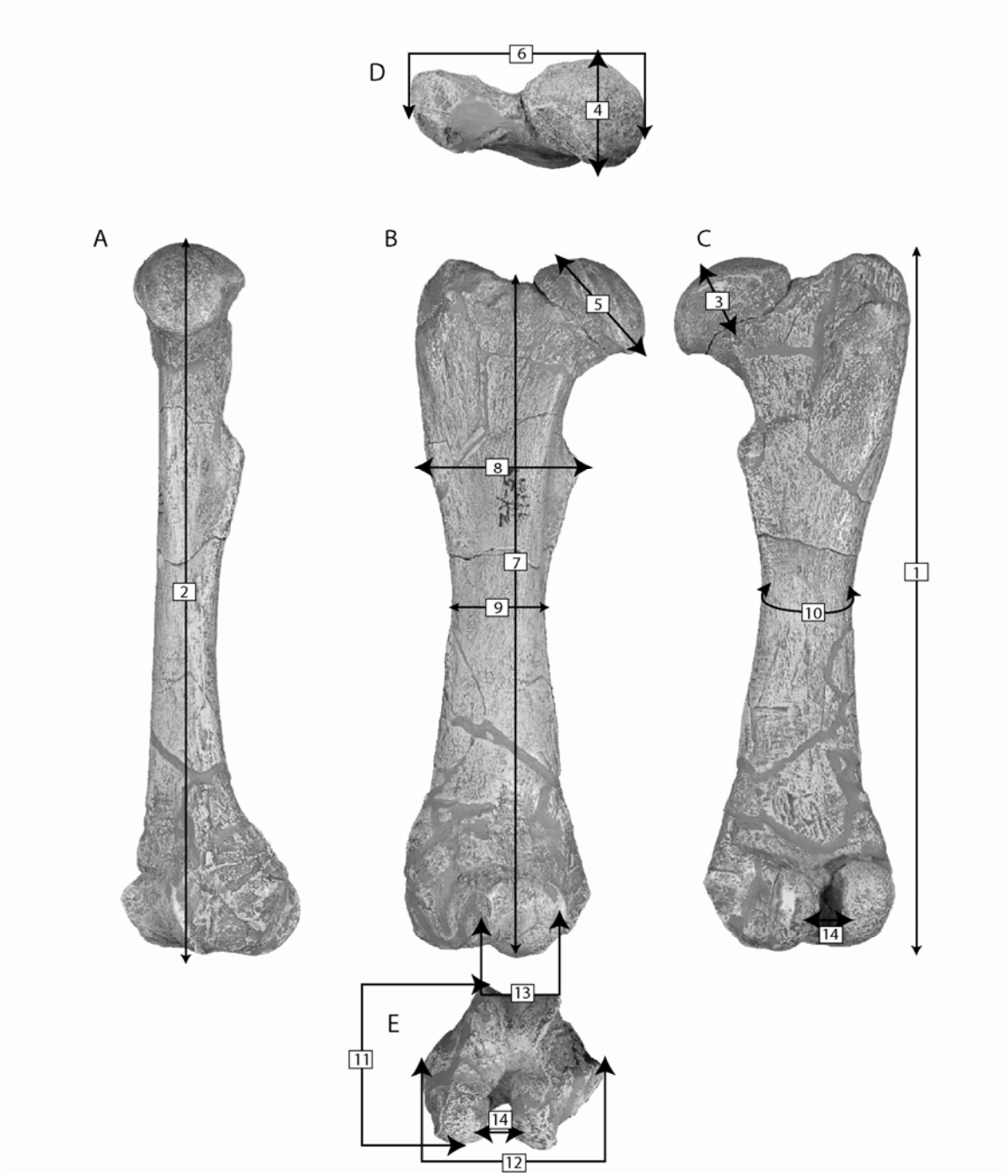

Key to landmarks for tibial and fibular measurements used in the study. A, anterior view; B, posterior view; C, proximal view; D, distal view.